





Diploma Thesis

Economic integration potential of industrial heat pumps into the European market based on the example of the rotation heat pump

carried out for the purpose of obtaining the degree of Dipl.-Ing., submitted at TU Wien, Faculty of Mechanical and Industrial Engineering, by

Matthias Herneth

Mat.Nr.: 11812344

under the supervision of

Ao. Univ. Prof. Dipl.-Ing. Dr. techn. Ponweiser Karl

Vienna, September 2023





Task of the diploma thesis

Mr. Herneth, 11812344 is given the following task:

The generation of thermal energy accounts for one third of the final energy consumption in Europe. In industry, around 60% of the final energy consumption is process heat, which is majorly provided by fossil fuels. Therefore, cutting greenhouse gas emissions through providing thermal energy is essential to achieving climate targets.

The heat pump is a technology that can raise low temperature levels to higher temperatures through a left-handed thermodynamic cycle. Industrial heat pumps can reach temperatures > 100 °C, which can address industrial processes. Therefore, fossil heating can be partly replaced by heat pumps leading to significant lower greenhouse gas emissions.

Based on these fundamentals, integration possibilities of heat pumps in the European industry are investigated and concepts for shifting waste heat into district heating networks by heat pumps are planned. In the development of the integration concepts, a special focus is placed on future technologies like waste heat utilization of green hydrogen production and the combination with other renewable energy sources (solar thermal, geothermal, biomass CHP, ...).

The coefficient of performance and economic feasibility calculations refers to the industrial heat pump of an Austrian manufacturer. Finally, a market analysis will be carried out to determine the potential of the investigated concepts in Europe.

Duration: 02/2023 – 09/2023	
Matthías Herneth	
Matthias Herneth	Supervising Professor



This work was supported by ecop Technology GmbH.

I confirm, that going to press of this thesis needs the confirmation of the examination committee.

Affidavit

I declare in lieu of oath, that I wrote this thesis and performed the associated research myself, using only literature cited in this volume. If text passages from sources are used literally, they are marked as such.

I confirm that this work is original and has not been submitted elsewhere for any examination, nor is it currently under consideration for a thesis elsewhere.

I acknowledge that the submitted work will be checked electronically-technically using suitable and state-of-the-art means (plagiarism detection software). On the one hand, this ensures that the submitted work was prepared according to the high-quality standards within the applicable rules to ensure good scientific practice "Code of Conduct" at the TU Wien. On the other hand, a comparison with other student theses avoids violations of my personal copyright.

Vienna, 31.08.2023

Matthías Herneth Matthias Herneth

Acknowledgments

I would like to express my sincerest gratitude to all employee of ecop technology GmbH the whole Group is acknowledged for their friendship and support in many difficult ways.

Especially I want to thank Dipl. Ing. Andreas Längauer for his assistance by daily technical questions and the excellent TEAM-work.

I would like to especially thank my thesis adviser Ao. Univ. Prof. Dipl.-Ing. Dr. techn. Ponweiser Karl for his guidance, help and quick support during the whole research work.

Appreciation is also extended to all members of the Technische Universität Wien, who gave me the during the last five years all the knowledge I needed to write this thesis.

A big thank you is also due to my friends and study colleagues for the great time.

Finally, I also want to say thank you to my family who continuously support me and have my back. Without you, none of this would have been possible.

"Energy transition is not a choice, but an imperative for a sustainable future." - Ban Ki-moon

I Table of Contents

II .	Abstract.		VIII
Ш	List of fig	jures	IX
IV	List of ta	bles	XXVIII
V	List of Ab	breviations and Symbols	XXI
1	Introdu	ıction	1
2	Funda	mentals of heat pumps	2
	2.1 Ind	lustrial heat pump manufacturer	6
	2.1.1	Kobelco	8
	2.1.2	Hybrid Energy AS	9
	2.1.3	Combitherm	10
	2.1.4	Mayekawa	10
	2.1.5	Sustainable Process heat GmbH (SPH)	11
	2.1.6	Ochsner	11
	2.1.7	eNGie – thermeeco2	12
	2.1.8	Ecop Technology GmbH	12
	2.2 Re	ference HP - ecop Rotation heat pump	13
	2.2.1	General	13
	2.2.2	Thermodynamic process of the RHP	13
	2.2.3	Demonstration plant	17
	2.2.4	Advantages and Disadvantages of the RHP	17
3	Econo	mic Analysis	18
	3.1 Inv	restment decisions with Total Cost of Ownership	18
	3.1.1	The factor time in a TCO	19
	3.1.2	Discounted payback period	20
	3.2 Ele	ectricity to gas price ratio	23
	3.2.1	Electricity price	24
	3.2.2	Gas price	28
	3.2.3	Electricity to gas price ratio	31
	3.3 CA	PEX and subsidies of a HP	34

	3.4	4	Car	bon pricing in Europe	.36
		3.4	.2	Carbon price trend and influence on the power to gas ratio	.41
	3.	5	Sur	mmary economic parameters	.45
	3.6	6	Cor	ntracting model	.46
	3.	7	Def	inition of market potential	.46
4		Ма	rket	segments and potential	.47
	4.	1	Geo	othermal energy	.63
		4.1	.1	Geothermal energy general	.63
		4.1	.2	Geothermal energy in Europe	.64
		4.1	.3	Geothermal applications for heat pumps	.66
		4.1	.4	Economic efficiency for the geothermal use cases	.72
		4.1	.5	Market potential geothermal systems	.75
	4.2	2	Нус	drogen Electrolysis	.78
		4.2	.1	Production of green hydrogen	.79
		4.2	.2	Stack-cooling (Use case H ₂ -1)	.81
		4.2	.3	Gas drying of hydrogen (Use case H ₂ -2)	.87
		4.2	.4	Hydrogen compression (Use case H ₂ -3)	.90
		4.2	.5	Economic efficiency for the H ₂ use cases	.96
		4.2	.6	Market potential green hydrogen	.96
	4.3	3	Sol	ar thermal energy	.99
		4.3	.1	Solar district heating (Use case Solar-1)	103
		4.3	.2	Solar heat for industrial processes (Use case Solar-2)	116
		4.3	.3	Economic efficiency of SDH and SHIP systems	125
		4.3	.4	Market potential SDH and SHIP systems	130
	4.4	4	Flue	e gas utilization	136
		4.4	.1	Steam generator feed preheating with IHP add on	136
		4.4	.2	Flue gas condensation (Use case Flue-3)	143
	4.	5	Ste	am generation	152
5		Sur	nma	ary	174
	5.	1	Ind	ustrial heat pumps	174
	5.2	2	Ecc	onomic analysis and commodity prices	175

5.3	Mai	rket potential Europe	.177
5.3	3.1	Geothermal energy	.182
5.3	3.2	Hydrogen electrolysis	184
5.3	3.3	Solar thermal energy	.187
5.3	3.4	Flue gas utilization	190
5.3	3.5	Steam generation	192
5.4	Sur	nmary heat pump COP and EU market potential	.195
5.5	Out	llook	.199

II Abstract

Thermal energy accounts for 55% of the energy required in industry and is responsible for 10% of global CO₂ emissions. Around the world, industry is undergoing major changes to limit its emissions and avert a climate catastrophe. The EU's requirement for climate neutrality by 2050 poses major challenges for industry, but at the same time creates significant new economic sectors. Around 32% of the thermal energy required in industry is < 200 °C. At the same time, there are often waste heat streams in a similar temperature level emitted by the same industry. Heat pumps are a technology to use such waste heat flows in a thermodynamic cycle as source to heat a sink very efficiently. While conventional heat pumps have already made a name for themselves in domestic and low temperature applications, industrial heat pumps are being used in industries and higher temperature applications.

This work has been concerned with analyzing areas of application for industrial heat pumps in the European market and assessing their potential and economic viability. The focus was not on a detailed technical description, but much more on achievable coefficients of performance and the availability of heat sources. The coefficient of performance calculated in this paper are based on the high temperature rotation heat pump of the Austrian manufacturer ecop Technology GmbH.

Previous studies have mostly limited the potential of industrial heat pumps to most suitable industries for heat pumps (food and beverages, chemical, paper, refinery), as they have a simultaneous thermal energy source and sink. This work also investigates the combination of heat pumps with renewable heat sources and storages, if no simultaneous source and sink is available. Exemplary heat pump combinations with geothermal and solar thermal energy were developed. Furthermore, future developments in the energy market are included. For example, the largest identified potential is the stack cooling of hydrogen electrolysers. Hydrogen production is currently of little importance, but will grow by a factor of 300 - 1000 till 2030. Another focus was the production of steam with heat pumps. Large parts of the thermal energy demand of industrial processes are based on steam as an energy carrier. In all areas, promising concepts with great potential were identified. The identified marketpotential of industrial heat pumps in Europe resulted in 51,1 - 73,9 GW thermal capacity.

For the economic analysis, a comprehensive analysis of the most sensitive parameters (natural gas prices, electricity prices, CO2 certificate prices) was carried out. The coefficient of performance was simulated based on the rotation heat pump of the company ecop Technology GmbH for concept typical temperatures. From an economic point of view, all investigated concepts can hold their own against fossil reference scenarios. However, it should be emphasized at this point that dynamic payback periods are mostly above industry standard payback periods of 1 - 3 years.

III List of figures

Figure 1 Efficiency of different electrified heating technologies; in this figure . (dot) is used
in difference to , (comma) [5]2
Figure 2 Projected worldwide thermal energy supply for the light industry to meet IEA
goals [8]2
Figure 3 Simplified visualization of a HP with possible sources, sinks and process
mediums [6]3
Figure 4 Energy flow diagram of traditional process heating (left) and process heating
with HP (right) [9]4
Figure 5 Total waste heat supply and LT process heat demand in four selected European
industries; in this figure . (dot) is used in difference to , (comma) [8]5
Figure 6 Simplified decision map if a HP is feasible for a given process [8]5
Figure 7 Survey among 27 experts about market barriers of IHP [10]6
Figure 8 Concept and typical COP of operating temperatures of the Kobelco HP; in this
figure . (dot) is used in difference to , (comma) [12], [14]9
Figure 9 Simplified flow diagram of the hybrid energy HP [15]10
Figure 10 Possible use cases of SPH HP [18]11
Figure 11 Overview of Ochsner HT-HP; ; in this figure . (dot) is used in difference to ,
(comma) [13]
Figure 12 Cycle process of a conventional HP (left) and the Joule Process of the ecop
RHP (right) [23]14
Figure 13 T,s diagrams which show the conventional HP typical Carnot process (left),
Joule Process (right) [23]
Figure 14 ecop RHP rotor with the three fluid circuits (sink, source and working fluid), the
colors imply temperature levels (red hot > yellow > green > blue); e.g.: exempli gratia
(exemplary) [22]
Figure 15 Cycle process (Joule process) of the ecop RHP divided in some steps in a T,s-
diagram; in this figure . (dot) is used in difference to , (comma) [23]
Figure 16 Relevant sections of the Joule process in the working fluid section; in this figure
. (dot) is used in difference to , (comma) [23]
Figure 17 Schema of the rotation heat pump in a biomass CHP [22]17
Figure 18 maximal reachable COP of the Carnot process (left) and the Joule process
(right); in this figure . (dot) is used in difference to , (comma) [23]18
Figure 19 TCO investment decision-making processes [27]19
Figure 20 Visualization of discounting and compounding [30]20
Figure 21 Sensitivity analysis of the PP according to their variation in the range of 50 $-$
$150\ \%$ of the current calue; in this figure . (dot) is used in difference to , (comma) $\ [10]$
22

Figure 22 Cost parity of HP and gas boiler systems in accordance to the temperature lift
and power to gas ratio; prices are based on 2016; in this figure . (dot) is used in difference
to , (comma) [10]22
Figure 23 Electricity to gas price ratio of European countries for a small-scale industrial
end-user (2 - 20 GWh/yr electricity; 3 to 28 GWh/yr gas); in this figure . (dot) is used in
difference to , (comma) [4]23
Figure 24 Electricity prices for private and industrial customers in Austria [33]24
Figure 25 Electricity marketplaces in Europe [33]24
Figure 26 Electricity prices of the different plants based on the merit order model [36].25
Figure 27 Simplified Diagram to visualize the electricity price based on the Merit Order
principle [35]
Figure 28 Long-term average power price in selected European countries for four
scenarios [34]27
Figure 29 Increasing volatile power prices due to seasonal fluctuations in Europe [34] 28
Figure 30 Long-term development of commodity prices, European Allowances (EUA):
carbon pricing see 3.4 [34]29
Figure 31 Historical electricity to gas price ratio of selected European countries between
2008 and 2022 [38]31
Figure 32 Power to gas ratio in EU-27 based on different sources and scenarios [32], [34],
[37]32
Figure 33 Influence of the power and NG taxation on the electricity to gas price ratio [1]
33
Figure 34 Electricity and gas prices in Europe and the USA in 2021 and 2022 [1], [39] 33
Figure 35 Specific investment costs of industrial HP according to different sources; in this
figure . (dot) is used in difference to , (comma) [10]36
Figure 36 History of the total cap and the CO _{2-ev} emissions in Europe [42]37
Figure 37 History of the CO₂-certificate prices between 2008 and 2023 in € / ton CO₂-ev
[45]38
Figure 38 Visualization of Scope 1,2 and 3 Emissions [47]39
Figure 39 CO ₂ prices of EU countries in 2021 and the beginning year of CO ₂ taxation [45]
40
Figure 40 Composition of non-household electricity and gas prices in selected European
countries in 2022 [38]43
Figure 41 Future trend of the EU-ETS price in the Energy Brainpool scenario [34]44
Figure 42 EU-ETS price trend in a hydrogen scenario [2]
Figure 43 Exemplary OPEX sales model for thermal energy [22]46
Figure 44 Different kinds of potential and what they include [40]47
Figure 45 The share of the industrial thermal energy demand in the global energy demand
and the primary energy sources, 1 Btoe = 1,163 * 10 ⁴ TWh [1]48

Figure 46 Breakdown of the total thermal energy demand in Europe (RES = renewable energy sources), "a" means anno and stands for year [4]49
Figure 47 Market potential of IHP in EU28 based on industries and temperature levels [11]51
Figure 48 Cumulative waste (top) and process (bottom) heat below 200 °C in the four investigated sectors in the EU28 [9]
Figure 49 Specification of the 4 174 heat pump units in the EU28: (left) by power and sink/source temperature, (right) by calculated COP; in this figure . (dot) is used as decimal point instead of a , (comma) [9]
Figure 51 Industrial gas and process heat demand by temperature level and HP replacement potential in Europe 2019, 1 bcm = 10 TWh [7]
Figure 54 Two ways to integrate HP into DH networks a) parallel b) serial [57]60 Figure 55 Heat sources for DH in Europe in 2021 [58]61 Figure 56 Large heat pump stock for DHC in selected European countries and their
thermal energy supply in 2021; in this figure . (dot) is used in difference to , (comma) [58]
Figure 57 Overview hydrothermal, petrothermal systems; open and closed systems; EGS: enhanced geothermal system, GSHP: ground source heat pump [61]
Figure 60 temperature levels of the commercialized geothermal areas in Europe [65] 67 Figure 61 District heating concepts for geothermal systems direct (left) serial (right) [66]
Figure 62 Doubled use of the geothermal energy based on [67]
based on [67]
Figure 66 Use case Geo-3 with a direct use of low temperature geothermal energy based on [67]71
Figure 67 Example of the ecop RHP in use case Geo-3 [68]72

Figure 68 Visualization of the levelized costs of heating for use case Geo-1 [70]73
Figure 69 Visualization of the levelized costs of heating for use case Geo-2 [70]74
Figure 70 Visualization of the levelized costs of heating for use case Geo-3 [70]75
Figure 71 Number of GeoDH plants in Europe in operation and under development [65]
Figure 72 Existing GeoDH project in Neustadt Glewe (Germany) based on [71], [72], [73], [74]77
Figure 73 Total geothermal technical, economic, and market potential for the integration
of a HP into geothermal systems by using use case Geo-1-3 [71], [72], [73], [74]78
Figure 74 Overview of the current state of the art electrolyser technologies [76]79
Figure 75 Cross section and chemical reaction equations of the PEM electrolyser [57]80
Figure 76 Scheme of a AEL cell and the related chemical reaction equations [57]81
Figure 77 Simplified scheme of an electrolysis stack and the cooling circuit including the ecop RHP modified by [22], [81]82
Figure 78 RHP simulation for electrolyser stack cooling use case H ₂ -1 [68]83
Figure 79 Market share of electrolyser technologies and predicted full load hours; in this
figure , (comma) are used as thousand-digit-draw [82]83
Figure 80 Waste heat utilization of an electrolyser reference facility in Sweden [57]84
Figure 81 Cooling circuit and DH connection of the stack cooling in Lulea [57]85
Figure 82 Sensitivity analysis of the reference scenario cooling system [57]86
Figure 83 Specification of the ecop RHP for the Lulea DH application [68]87
Figure 84 Relative humidity of hydrogen depending on the pressure and temperature [80]
88
Figure 85 Simplified scheme of waste heat recovery of the hydrogen drying process [57],
[70]89
Figure 86 RHP simulation for gas drying use case H ₂ -2 [68]90
Figure 87 Specific energy consumption for the compression of hydrogen [80]91
Figure 88 Specific compressor work for an isothermal, isentropic and intercooled
compression [80]91
Figure 89 Exemplary intercooled compressors in series [85]92
Figure 90 Compressibility factor (left) and real isentropic exponent (right) of hydrogen as
a function of pressure and temperature [85]93
Figure 91 Resulting temperature of an isentropic compression of hydrogen starting at 10
°C and 50 bar [85]93
Figure 92 Simplified visualization of energy flows during compression and possible
thermal energy extraction [70]94
Figure 93 Integration of the RHP in the interstage cooling of the hydrogen compression
[70]95
Figure 94 RHP for utilization of hydrogen compression waste heat H2-3 [68]96

Figure 95 Electrolysis capacity extension from 2022 till 2030 in selected countries; in this figure . (dot) are used as thousand-digit-draw [83]97
Figure 96 Expected waste heat potential from PEM and AEL electrolysers in the
EU27+UK and the rest of the world in 2030 and 2040; in this figure . (dot) is used as
- , ,
thousand-digit-draw [91]
Figure 97 Comparison between electrolyser waste heat potential and DH heating demand in 2040 in selected European countries; for a explanation of the country shortcuts follow
the Link Microsoft Word - Country_Abbreviations.doc (gesis.org), in this figure . (dot) is
used as thousand-digit-draw [91]
Figure 98 Potential of ecop RHP for the waste heat utilization of green hydrogen
production [70]
Figure 99 Parallel combination of STE, HP, and TES [97]
Figure 100 Serial combination of STE, HP and TES; a) top: preheating STE and HP
reheat (source for HP waste heat or environment); b) middle: preheating HP and STE
reheat (source for HP waste heat or environment); c) bottom: preheating STE and HP
reheat (source for HP is the TES return flow) [97]
Figure 101 Solar contribution for heating in accordance with the storage availability [98]
Figure 102 Types of sensible thermal energy long-term storages [99]
Figure 103 Typical integration of a HP in a SDH system [100]104
Figure 104 Possible set up of a SDH system with several renewable energy sources [101]
Figure 105 Sensitivity analysis of the SDH feed and return flow temperature on the solar
yield [102]
Figure 106 Simplified layout of the SDH network in Dronninglund, pumps indicate the flow
direction [3]
Figure 107 Thermal energy demand and solar yield over the year in the Dronninglund-
SDH [3]107
Figure 108 ecop RHP for Dronninglund [68]108
Figure 109 FPC arrays (left) and PTES (right) in Dronninglund [3]108
Figure 110 ecop RHP for providing high temperatures for conventional DH networks [68]
Figure 111 1/2 ecop RHP switch in series for providing high temperatures for conventional
DH networks with high COP [68]109
Figure 112 2/2 ecop RHP switch in series for providing high temperatures for conventional
DH networks with high COP [68]110
Figure 113 Simplified visualization of the thermal energy supply in a typical summer
operation: direct solar usage and charging of daily buffer storage [104]111
Figure 114 Simplified visualization of the thermal energy supply in a typical summer
operation: direct solar usage and charging of PTES [104]

Figure 115 Simplified visualization of the thermal energy supply in a typical autumn operation: discharging PTES directly via HEX into DH network [104]
Figure 118 Simplified visualization of the thermal energy supply in a typical winter operation: using STE as source for RHP, RHP is used for heating the DH return flow [104]
Figure 119 Simplified visualization of the thermal energy supply using PTES via HEX for DH return preheating and afterwards as source for RHP for DH end heating (top) Specifications of the ecop RHP in this operation point (bottom) [68], [70]
Figure 128 Electricity supply of the PVT and PV system and the electricity demand of the RHP and other consumers, COP of the RHP is assumed to be constant [105]

Figure 132 Resulting prices of combinations between solar collector aperture area and
storage capacity; green mean cost effective, red bad ratio for cost effectiveness; in this
figure . (dot) are used as thousand-digit-draw [112]129
Figure 133 Summary of Danish SDH achievements [3]130
Figure 134 Newly installed large-scale STE capacity between 2010 and 2016 in the
countries Denmark, China, Germany and Austria [3]131
Figure 135 Promotion schemes for solar based systems and boundary conditions in the
countries Denmark, China, Germany and Austria along nine axes [3]133
Figure 136 Potential for solar thermal energy in Europe depending on the LCOH and the
SF [108]134
Figure 137 Solar heat potential depending on the LCOH for some European countires
[108]
Figure 138 STE potential in several European countries in TWh per year and as fraction
of the total industrial thermal energy demand [32]136
Figure 139 Set up of a conventional gas boiler (top) and its simplified visualization
(bottom) based on [70], [115]137
Figure 140 Simplified visualization of the RHP integration for the freshwater feed
preheating in the gas boiler circuit [70]138
Figure 141 Simulation of the ecop RHP in the gas boiler add on setup (Use case Flue-1)
[68]
Figure 142 ecop RHP dynamic payback period according to the gas boiler inlet
temperature (= Eco outlet temperature) [70]140
Figure 143 Set up of the steam boiler without external freshwater preheating based on
[70] , [115]140
Figure 144 Simplified visualization of the RHP integration in the gas boiler circuit without
external freshwater preheating [70], [115]141
Figure 145 ecop RHP dynamic payback period according to the gas boiler inlet
temperature (= Eco 1 outlet temperature) [70]142
Figure 146 European steam boiler market shares by primary energy (2022) based on
[118]142
Figure 147 Heat pump integration in comparison to a gas boiler; in this figure . (dot) is
used in difference to , (comma) [119], [120]143
Figure 148 Extractable energy depending on the fuel and the water content [122]146
Figure 149 Flue gas treatment in a biomass CHP [123]147
Figure 150 Relation between the cooling circuit temperature and den condensate mass
flow [124]
Figure 151 Flue gas condensation used for air preheating [121], [124]148
Figure 152 (top) Exemplary visualization of the parallel integration of the ecop RHP in a
condensing HEX and (bottom) exemplary simulation of ecop RHP in this setup (Flue-3)
based on [68], [123]149

Figure 153 (top) Exemplary visualization of the serial integration of the ecop RHP in a
condensing HEX and (bottom) exemplary simulation of ecop RHP in this setup (Flue-3)
based on [68], [123]
Figure 154 Comparison between conventional combustion-based steam generation and
HP driven processes; in this figure . (dot) is used as decimal point instead of a , (comma)
[8]
Figure 155 Required energy for steam generation visualized in a p-h diagram, A: 0,1 MPa,
20°C; B: 0,2 MPa, 125 °C; in this figure . (dot) is used in difference to , (comma) as
decimal point [125]154
Figure 156 Multiple processes in the p-h diagram to achieve steam generation (getting
from point A to B), a) direct path, b) three different paths based on relaxation, heating an
compression; in this figure . (dot) is used in difference to , (comma) [125]155
Figure 157 T-Q diagram of the different paths to evaluate the exegetic losses, area I to III
symbolize the exergy losses [125]
Figure 158 Closed-loop steam generating units; (top) with flash tank, (bottom) with steam
generator [8], [126]
Figure 159 Open-loop steam generating units with MVC [8], [126]157
Figure 160 Combined steam generating unit steam generator + MVC [8], [126], [127]
Figure 161 (top) Integration of a HP in a flash drum system, (bottom) T-s diagram of the
flash cycle compared to a typical evaporation in a thermal boiler [70], [128]159
Figure 162 Simulation of the ecop RHP for a flash tank use case (Steam-1) at low
temperature [68]
Figure 163 Simulation of the ecop RHP for a flash tank use case (Steam-1) at higher
temperatures [68]
Figure 164 Combination of a HP and a steam generator [70], [120]162
Figure 165 Simulation of the ecop RHP for a steam generator use case [68]163
Figure 166 (left) Recompression via MVR of the vapor in the process, (right) MVC
Compression of generated low-pressure steam [129]
Figure 167 Industrial example of an MVR system integrated in a drying process [129]
Figure 168 Example for flash tank with MVC driven steam supply; logarithmic mean
temperature difference (LMTD), heat exchanger (HX); in this figure . (dot) is used as
Figure 171 Combination between geothermal heat and a HP for steam generation, (left)
HP uses geothermal heat as source for evaporation of feedwater in a steam generator,
decimal point instead of a , (comma) [130]
THE USOS GOULDENTIAL HEAL AS SOULCE FOL EVAPOLATION OF IECUWARD HEA STEAM GENERALDI,

(right) geothermal heat is used directly in a steam generator for evaporation and an MVR
is used for increasing the pressure [127]
Figure 172 Waste heat utilization for steam generation in a steel plant [8]168
Figure 173 SWOT analysis of the steam generating HP into the steel plant [8]169
Figure 174 Important points that must be considered if the pressure is being reduced in
an existing steam supply [132]
Figure 175 Total costs for steam production (CAPEX + OPEX) for a HP with (top) flash
tank, (bottom) steam generator and a reference scenario [70]
Figure 176 Stock of fossil boilers in European countries; in this figure ' (apostrophe) are
used as thousand-digit-draw [120]173
Figure 177 Market potential of IHP in Europe based on industries and temperature levels
[11]179
Figure 178 Fraction of heat pump for process heat < 200 °C; in this figure . (dot) is used
as decimal point instead of a , (comma) [6]180
Figure 179 Heat sources for district heating in Europe (2021) [58]181
Figure 180 Overview of the geothermal sources in Europe [63]182
Figure 181 Doubled use of the geothermal energy based on [67]183
Figure 182 Simplified scheme of an electrolyser stack cooling with a heat pump and
further hydrogen processing steps (purification and compression) until storage by [22]
[81]185
Figure 183 Solar district heating network in Dronninglund (Denmark), the pumps indicate the flow direction [3]
Figure 184 Simplified visualization of a high temperature heat pump integration for the
freshwater feed preheating in the gas boiler circuit [70]190
Figure 185 ecop RHP dynamic payback period according to the gas boiler inle
temperature (= economizer outlet temperature) [70]191
Figure 186 T-s diagram of the flash cycle compared to a typical evaporation in a therma
boiler [70], [128]192
Figure 187 Combination of ecop rotation heat pump and a steam generator, exemplary
temperature levels are shown in the figure [70], [120]193
Figure 188 (left) mechanical vapor recompression, (right) mechanical vapor compression
of generated low-pressure steam [129]194

IV List of tables

difference to , (comma) [11], [12]7
Table 2 Technical specification of the ecop RHP [23]13
Table 3 Summary of the European power prices between 2025 and 2050 by scenarios [34]28
Table 4 Long-term price trends of commodities by Aarlborg University, conversion factor to €/MWh is 3,6 GJ/MWh; in this table . (dot) is used in difference to , (comma) [32]29 Table 5 Conversion factor from USD/MBtu to €/MWh is factor 3 considering 1,15 €/USD; in this table . (dot) is used in difference to , (comma) [37]
scenarios [32], [34], [37]32
Table 8 Summary of CAPEX and OPEX subsidies in European countries for large heat pumps [41]
Table 9 CO _{2-ev} emissions of different fuels according to the generation of 1 kWh of thermal energy [49], [50]
Table 10 CO₂ tax trend of Austria, Anm. 1.: for 2023 taxes of 32,5 € where applied [51]41
Table 11 Comparison between national CO ₂ prices (example Germany) and the EU ETS System [45], [51]41
Table 12 Carbon price for certificates in selected areas based on different scenarios [37]
Table 13 Summary of gas boiler and HP parameters for later economic calculations [2],
[32], [34], [37], [40]45
Table 14 Process and space heat / cooling demand in the EU28+3 countries in TWh/yr;
Table 14 Process and space heat / cooling demand in the EU28+3 countries in TWh/yr;
Table 14 Process and space heat / cooling demand in the EU28+3 countries in TWh/yr (in this table . (dot) is used in difference to , (comma)) [8], [9], [52]
Table 14 Process and space heat / cooling demand in the EU28+3 countries in TWh/yr (in this table . (dot) is used in difference to , (comma)) [8], [9], [52]
Table 14 Process and space heat / cooling demand in the EU28+3 countries in TWh/yr (in this table . (dot) is used in difference to , (comma)) [8], [9], [52]
Table 14 Process and space heat / cooling demand in the EU28+3 countries in TWh/yr; (in this table . (dot) is used in difference to , (comma)) [8], [9], [52]

Table 21 Specifications and waste heat potential of a 100 MW electrolyser (left) PEM or
(right) AEL; in this table . (dot) is used in difference to , (comma) [57]85
Table 22 HP specifications of the Lulea project, COP is reffered to the ambient
temperature by; in this table . (dot) is used in difference to , (comma) [57]86
Table 23 Parameters of the different storage facilities and thermal energy generation
during compression *calculated according to Equation (9), parameter estimated by Figure
92 [80], [89], [90]
Table 24 Specifications of the SDH system in Dronninglund; in this table . (dot) is used in
difference to , (comma) [3]106
Table 25 Set up for renewable thermal energy supply [70]
Table 26 Processes in the textile industry and their temperature level [105]120
Table 27 Renewable energy concept components [105]122
Table 28 Parameters for the economic efficiency analysis based on ÖNORM M7140 [105]
124
Table 29 LCOH (in €/kWh) and dynamic amortization period of the project based on [105]
125
Table 30 Cost structure for a small and large scale SDH system; in this table . (dot) is
used as decimal point and , (comma) as thousand-digit-draw [32]127
Table 31 CAPEX structure of the BIG Solar Graz project; in this table . (dot) are used as
thousand-digit-draw [63]
Table 32 SDH trends in four different countries (Denmark, China, Germany, Austria); in
this table . (dot) is used as decimal point and , (comma) as thousand-digit-draw [3]132
Table 33 Market data of large-scale SDH systems in Europa (2018); in this table . (dot)
are used as thousand-digit-draw [114]134
Table 34 Research studies of SGHP over the world; in this table . (dot) is used as decimal
point instead of a , (comma) [120]153
Table 35 Summary of different MVC/R compression units, PD blowers = positive
displacement blowers; in this figure . (dot) is used as decimal point instead of a , (comma)
[130]
Table 36 Parameters for economic efficiency analysis [70]170
Table 37 Summary the most relevant gas boiler and HP parameters for later economic
calculations [2], [32], [34], [37], [40]177
Table 38 Needed investment to realize the IHP demand in the four mentioned sectors
with unit costs between 200 - 500 €/kW; in this table . (dot) is used as decimal point
instead of a , (comma) [9]180
Table 39 Heat generation during compression to different end pressures depending on
the storage facilities *calculated according to Equation (9), parameter estimated by Figure
92 [80], [89], [90]
Table 40 Summary of the ecop rotation heat pump COP calculations of the different use
cases

Table 41 Summary of the market potential (EU28) of the investigated market	segments;
decimal places are not pictured in this table; District heating = DH	197
Table 42 Summary of different studies aiming on identifying the industrial I	heat pump
potential in EU28 [40]	199

V List of Abbreviations and Symbols

Abbreviations

AEL alkaline electrolysis

AHEAD advanced heat pump demonstrator

ATES aquifer thermal energy storage

Bundesminesterium für Wirtschaft und Ausfuhrkontrolle **BAFA**

BTES borehole thermal energy storage

CAPEX capital expenditures

CBAM carbon border adjust mechanism

CHP combined heat and power COP coefficient of performance CO_{2-ev} carbon dioxide equivalent

DH district heating

DHC district heating and cooling

DHW domestic hot water

Eco economizer

EEX European energy exchange

EGS enhanced geothermal system

exempli gratia (exemplary) e.g.

EPEX European power exchange

ETC evacuated tube collectors

etc. et cetera

EUA European allowances

EU-ETS European Union – emissions trading system

EU27 European Union with 27 members

EU28+3 European Union with 28 members and Switzerland, Norway, and

Luxembourg

ev equivalent

FLH full load hour

FPC flat plate collectors

GeoDH geothermal district heating

GSHP ground source heat pump

GWP global warming potential h enthalpy

HEX heat exchanger

HFKWs hydrofluorocarbons

HFOs hydrofluorolefines

HP heat pump

HT high temperature

HT-HP high temperature heat pump

HX heat exchanger

IEA-SHC international energy agency-solar heating and cooling

IHP industrial heat pump

in intlet

LCC life cycle costs

LCOE levelized cost of electricity

LCOH levelized cost of heat

LMTC logarithmic mean temperature difference

LNG liquified natural gas

LT low temperature

LUVO air preheater

max. maximum

MVC mechanical vapor compression

MVR mechanical vapor recompression

NG natural gas

O&M operation and maintenance

OTC over the counter

out outlet

p pressure

PD blowers positive displacement blowers

PET polyethylenterephthalat

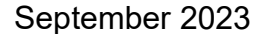
PFAS per- and polyfluorinated

pH pondus hydrogenii

PTC parabolic through collectors

PTES pit thermal energy storage

PVT photovoltaic/thermal collector



quarter q

Q heat load

RES renewable energy sources

RHP rotation heat pump

rotations per minute rpm

saturated sat.

SDH solar district heating

SF solar fraction

SGHP steam generating heat pump

SHIP solar heat for industrial processes

SN serial number

SOEL solid oxide electrolyser cell

ST solar thermal

STE solar thermal energy

Τ temperature

TCO total costs of ownership

Temp. temperature

TES thermal energy storage

TRL technical readiness level

TSA temperature swing absorption

TTES tank thermal energy storage

pieces pcs.

PEC primary energy consumption

PEF primary energy factor

PEFe primary energy factor for electricity

PEF_h primary energy factor for heat

PEM polymer electrolyte membrane

PΝ nominal pressure stage

PSA pressure swing absorption

PV photovoltaic

UK United Kingdom

USA United States of America

VAT value added taxes

September 2023

September 2023

Formula symbols

-		
Α	cross-sectional area	m^2
A_{cell}	cell surface	cm²
$A_{payback}$	payback period	yr
$\dot{B}_{flue~gas}$	flue gas mass flow	kg/s
CAPEX	capital expenditures	€
C_{CO2}	EU-ETS price for Carbon emissions	€/t
$C_{electricity}$	electricity price	€/kWh
$ar{\mathcal{C}}_{H_2}$	mean specific heat capacity of hydrogen	kJ/(kg K)
C_{NG}	NG price	€/kWh
COP	COP of HP for given scenario	-
$ar{c}_{p,flue\ gas}$	mean specific heat capacity of flue gas	kJ/(kg K)
$c_{p,T_{1,\mathrm{sat.}}}$	specific heat of the saturated liquid at the higher pressure	kJ/(kg K)
DPP	discounted payback period	yr
FLH	yearly full load hours	h/a
f_{NG}	scope 1 CO ₂ emission factor of NG	gCO _{2-ev} /kWh
H_i	caloric value	kJ/kg
H_s	heating value	kJ/kg
H_1	enthalpy of saturated liquid at the higher pressure	kJ/kg
H_2	enthalpy of saturated liquid at the lower pressure	kJ/kg
H_4	enthalpy of water vapor at the lower pressure	kJ/kg
$\Delta H_{v, T_2}$	heat of vaporization of saturated liquid at the lower pressure	kJ/kg
I	current density	A/cm²
i	discount rate	%
$K_{condensing\ HEX}$	cost of the condensing HEX	€
K_{heat}	revenue for extracted thermal energy	€/kWh
K-n	cash value	€
K_0	present value	€
$LCOH_{Geo-1}$	levelized cost of heat for use case Geo-1	€/MWh
$\dot{m}_{H_2,production}$	mass flow of hydrogen	kg/s

n	observation period	yr
n_{C}	number of cells	-
$\mathit{OPEX}_{\mathit{gas\ boiler}}$	operational expenditures of a gas boiler	€
$OPEX_{HP}$	operational expenditures of a HP	€
$OPEX_{savings}$	savings of the operational expenditures	€
P _{cool, gas drying}	cooling power for gas drying	kW
PP	static payback period	yr
$\frac{p_2}{p_1}$	compression ratio	-
$\dot{Q}_{condensing\ HEX}$	extracted thermal power in the condensing HEX	kW
Q_{demand}	thermal energy demand	kWh
\dot{Q}_{gen}	generated thermal power in electrolyser	W
q -n	discounting factor	-
$T_{in,flue\ gas}$	condensing HEX flue gas inlet temperature	K
$T_{out,flue\ gas}$	condensing HEX flue gas outlet temperature	K
$\Delta T_{H_2,cooling}$	cooling circuit temperature difference	K
T_1	initial temperature	K
T_2	final temperature	K
$T_{1,\text{sat.}}$	temperature of the saturated liquid at the higher pressure	K
$T_{2,\text{sat.}}$	temperature of the saturated liquid at the lower pressure	K
V_{cell}	cell voltage	V
V_{tn}	thermoneutral voltage	V
X_{steam}	weight ratio of vaporized liquid / total liquid mass	-
Z_i	compressibility factor	-
α	condensation factor	-
$\kappa_{p,v}$	real isentropic exponent	-
$\zeta_{gas\ boiler}$	combustion efficiency of gas boiler	-

Physical quantities

Α Ampere year а

bar bar

bcm billion cubic meters

billion tonnes of oil equivalent **Btoe**

centimeter cm

gram g

GW Gigawatt

GWh Gigawatt hour

Hz Hertz J Joule K Kelvin

kilograms kg kJ kilojoule kW kilowatt

 kW_p kilowatt peak

L liter m meter

millimeter mm Mt Megaton MW Megawatt

 Nm^3 norm cubic meters

TWh Terawatt hour

Τ tone ٧ Volt W Watt yr year $^{\circ}C$ Celsius

€ Euro

k€ kilo € (thousand €)

inch

chemical elements and molecules

CH₄ methane

 CO_2 carbon dioxide

September 2023

H_2	(account) budroach
Па	toaseous i nvorogen
1 • Z	(gaseous) hydrogen

 H_20_{liq} (liquid) water

 NH_3 Ammonia

02 (gaseous) oxygen

Introduction

Around half of the global final energy consumption used in the residential and industrial sector attributes to thermal energy. Today, three quarters of the industrial thermal energy demand is produced by burning fossil fuels being responsible for 40 % of the global energy related Carbon dioxide equivalent (CO_{2-ev}) emissions. 10 % of the global CO₂ is emitted to provide thermal energy for the industry. Therefore, arises the necessity to substitute fossil thermal energy supply by more sustainable solutions [1], [2], [3], [4].

Depending on the temperature level different sustainable heating technologies can be used. It is distinguished between direct and indirect conversion. An example for indirect conversion is the generation of green hydrogen by electrolysis. Hydrogen offers the possibility to generate high temperatures, while being storable and transportable, but it comes with several conversion losses. Direct conversion use electricity directly to generate thermal energy such as electric boilers, metallic resistance, plasma torches, electromagnetic heating (induction, infrared, microwave, radio wave) or heat pumps. Each of these technologies is best in a specific temperature level, why there is not a single technology for all applications. In this thesis it is focused on the temperature level of < 100 °C and 100 – 200 °C. One technology to provide these temperatures in an efficient and sustainable way are heat pumps (HP) [1], [2], [3], [4].

Figure 1 (in this figure . (dot) is used in difference to , (comma)) show three ways (hydrogen boiler, electric heater and HP) to electrify the thermal energy supply and their efficiencies. Efficiency is in this table incorrectly stated as coefficient of performance (COP) for all technology, whereas thermodynamically a COP can only be defined for circular processes. COP in this sense means the amount of thermal energy output per electrical energy input. The COP is highest for a HP and minimal for a hydrogen boiler, however hydrogen boiler or electric heater can reach significant higher temperature levels [5].

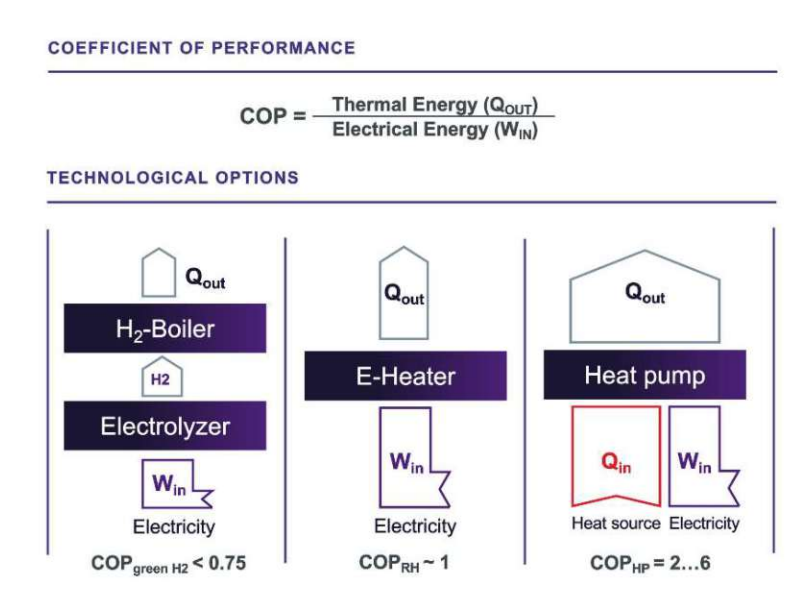


Figure 1 Efficiency of different electrified heating technologies; in this figure . (dot) is used in difference to , (comma) [5]

Figure 2 shows the necessary transition of heating technologies for low temperature (LT), medium and high temperature (HT) heat supply between 2020 and 2050 for the global light industry (sub-sectors mentioned in the figure) to meet the international energy agency (IEA) net zero goals by 2050. All the technologies mentioned above will have an important role in this transition. To meet the global HP role in 2050, 500 MW thermal HP power must be installed every month for the next 30 years [6], [7], [8].

Projected Worldwide Heat Supply for the Light Industry to Meet **IEA Goals**

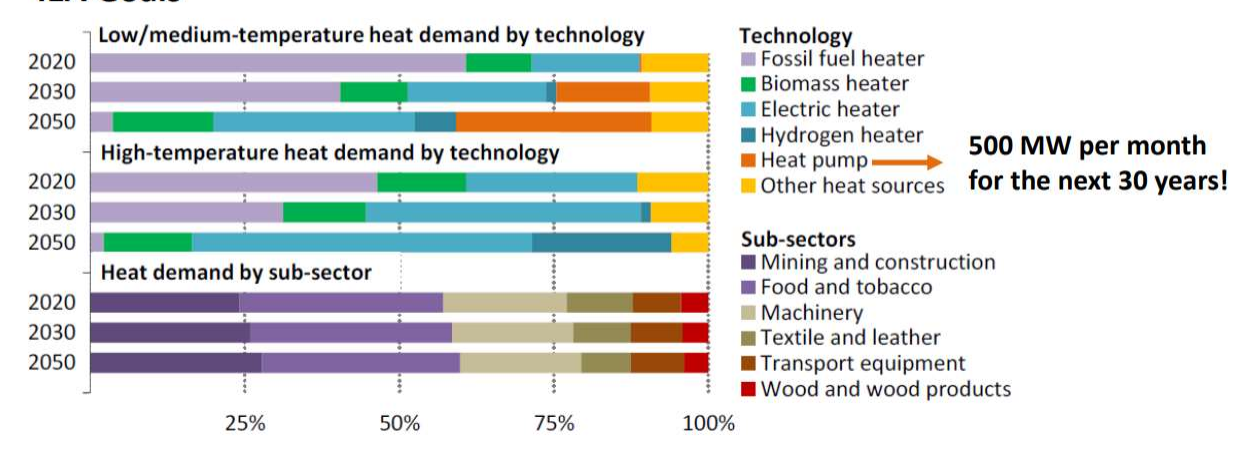


Figure 2 Projected worldwide thermal energy supply for the light industry to meet IEA goals [8]

Fundamentals of heat pumps

Heat pumps use a left-handed thermodynamic cycle to absorb thermal energy from a source a low temperatures to provide thermal energy at higher temperatures on the sink side. Figure 3 shows simplified the left-handed process of a HP and possible thermal energy sources and sinks. The thermodynamic cycle is used to evaporate, compress, condense and expand an refrigerant driven by electricity. Thermal energy

sources may be air, water, ground or waste heat and typical end-users are households (buildings), district heating or the industry. Process medium on the sink side may be air, water, steam, or other heated material [6].

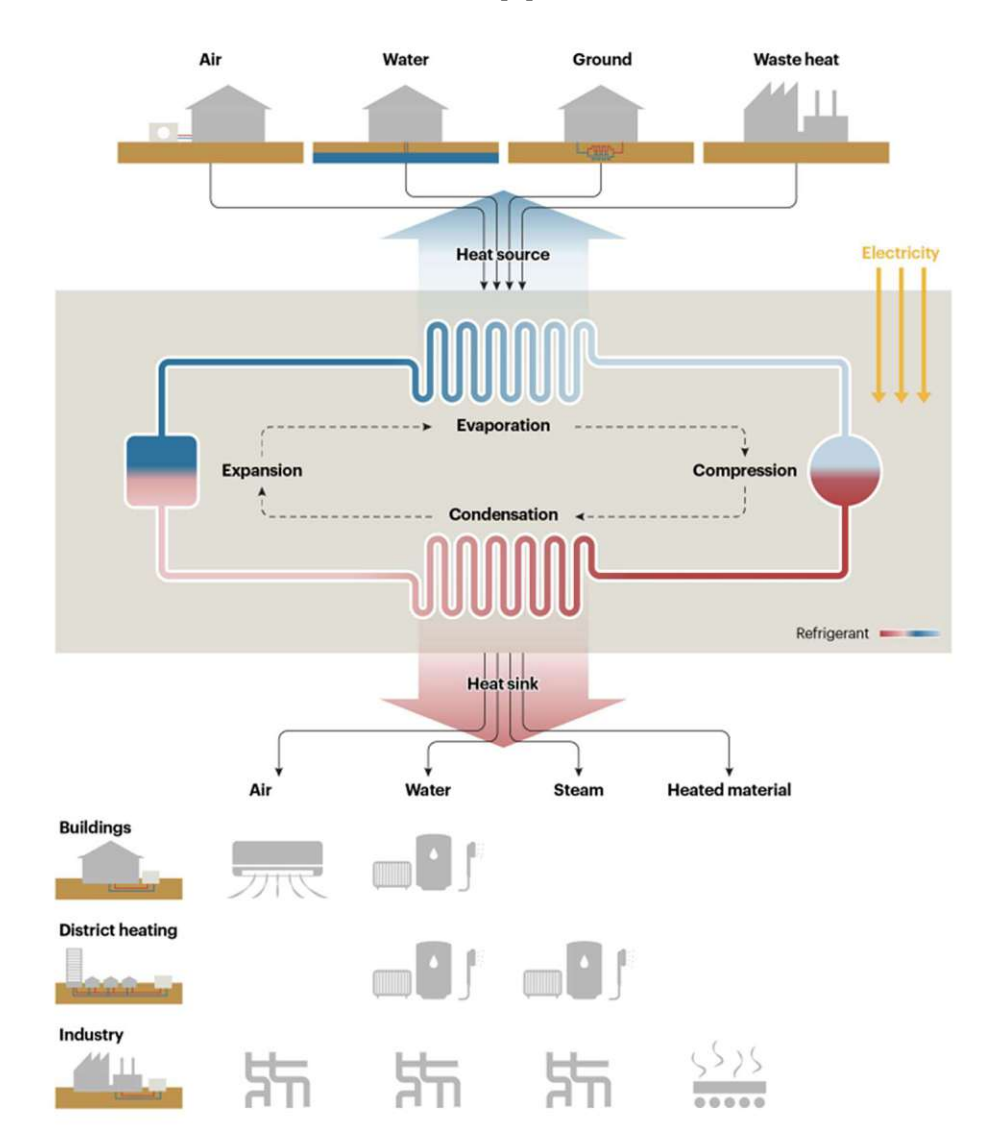


Figure 3 Simplified visualization of a HP with possible sources, sinks and process mediums [6]

Conventional heat pumps are a very efficient way to generate thermal energy up to 100 °C. This temperature level can address the residential heating requirements (space heating (SP) and domestic hot water (DHW)) as well as 11 % of the industrial thermal energy demand. Industrial heat pumps (IHP) can reach temperatures up to 200 °C filling the gap of the 100 – 200 °C temperature level. This temperature level accounts for 20 % of the industrial thermal energy demand. Old district heating systems also operate at temperatures greater than 100 °C [1].

Figure 4 shows a comparison of an energy flow diagram of traditional process heating and process heating with a HP. Traditional process heating uses a primary energy source like gas, oil or biomass and convert it directly with some conversion losses in process heat. HP need electricity as primary energy. The HP uses electricity to transfer thermal energy from a low temperature source (like waste heat or environmental heat) to a higher temperature sink. The COP for heat pumps is typically between three and seven. This means that three to seven units thermal energy are produced with a single unit of electricity. The primary energy factor (PEF) for electricity (PEFe) defines the ratio between the primary energy consumption (PEC) and the end-user consumption of electricity. The PEF for thermal energy (PEF_h) defines the ratio between the PEC and the thermal energy used by the end-consumer [9].

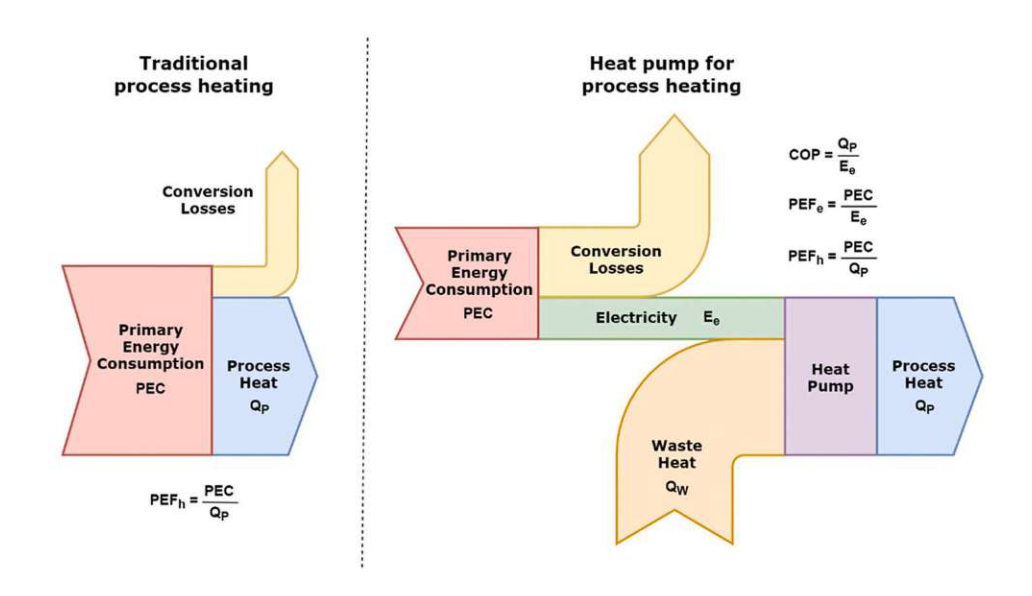


Figure 4 Energy flow diagram of traditional process heating (left) and process heating with HP (right) [9]

HP require a thermal energy source, which is typical LT waste heat or environmental heat. Therefore, the possibility to use HP for process heating is limited to the availability of a thermal energy source. Study [9] investigated the waste heat and process heat potential in four European industries (food, paper, chemical, refinery) shown in Figure 5 (in this figure . (dot) is used in difference to , (comma)). The waste heat potential is highest at lower temperatures and lower at higher temperatures. The heat demand is highest at high temperatures. Therefore, the HP should be able to provide with a low temperature source a high temperature sink. The difference between the source inlet (in) and the sink outlet (out) temperature is called temperature swing. In general increasing temperature lifts lead to lower COP. In Figure 5 an example for a temperature lift of 80 K (60 to 140 °C) reaching a COP of 2,4 is visualized [8].

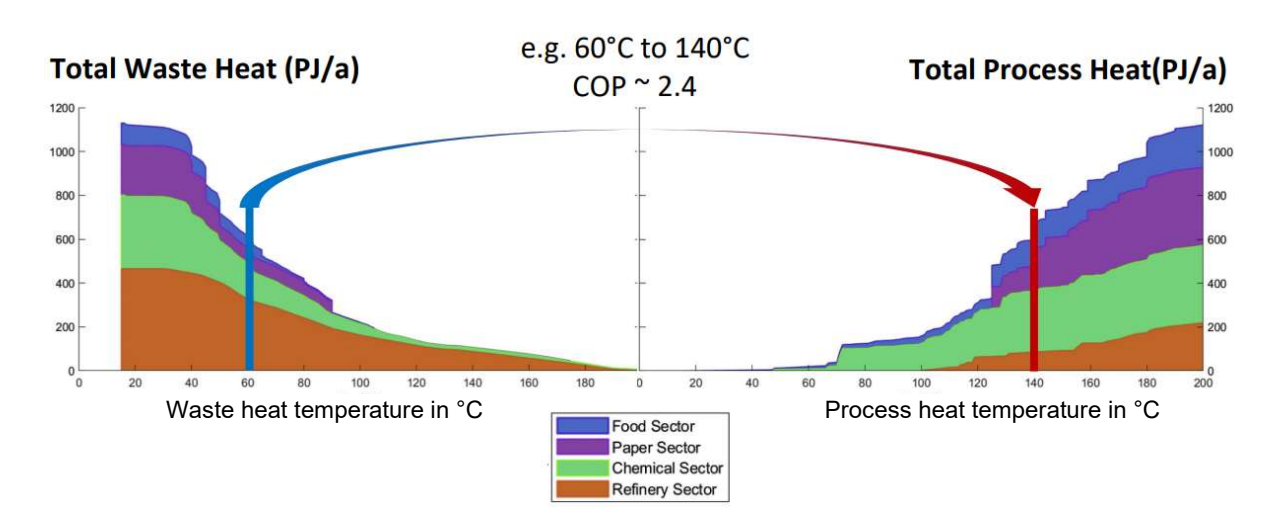


Figure 5 Total waste heat supply and LT process heat demand in four selected European industries; in this figure . (dot) is used in difference to , (comma) [8]

Figure 6 shows a very simplified decision map, if a HP is suited for the given problem or not. First a process should be optimized, and internal heat recovery should be implemented. If there is still enough waste heat, the simultaneity of the waste heat supply and the process heat demand or the feasibility of a buffer storage must be checked. In the next step the temperature levels and the reachable COP of a HP can be determined. With these information's and the knowledge of expected full load hours (FLH) the profitability of a HP can be checked [8].

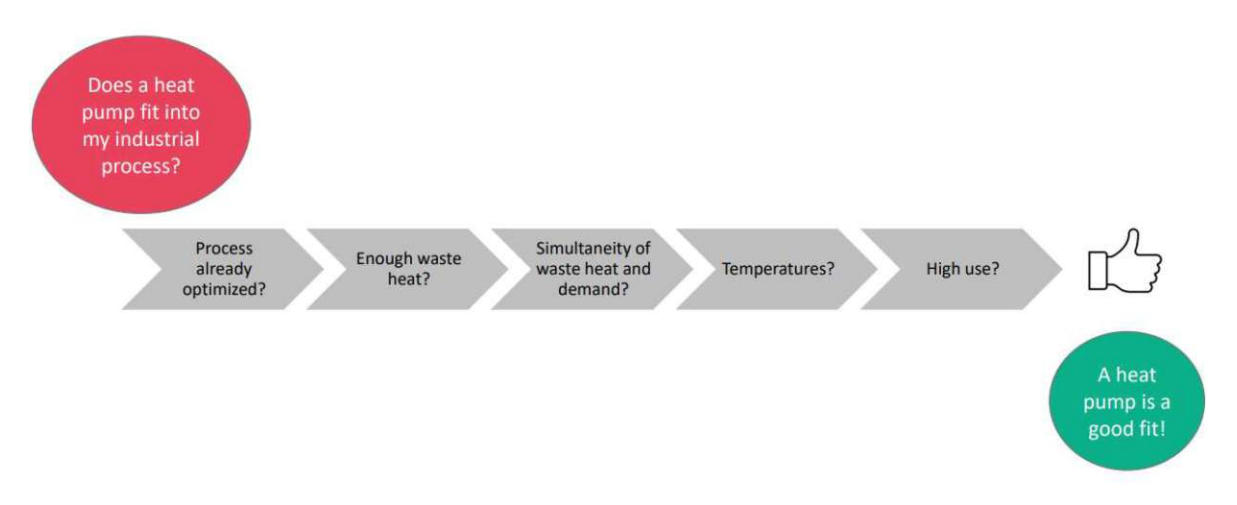


Figure 6 Simplified decision map if a HP is feasible for a given process [8]

With the given assumptions the implementation of a HP can lead to [8]:

- Lower operational expenditures (OPEX)
- Valorization of waste heat
- Increase energy efficiency
- Reduce CO_{2-ev} emissions

Figure 7 gives a summary of market barriers of IHP of different stakeholders. On the side of the industrial customers, the product acceptance ("no, one fits all solution"), complexity of systems and the knowledge of different technologies is a problem. Furthermore, the capital expenditures (CAPEX) of HP solutions are typical higher than for fossil solutions and traditional payback periods of 1-3 years are not feasible. The competitiveness in terms of life cycle costs (LCC) is strongly dependent on fuel prices (electricity, gas, ...), which are difficult to predict for an investment horizon of > 20 years (yr). The temperature level of HP is limited and the COP is weaker for greater temperature swings and higher temperature levels [10].

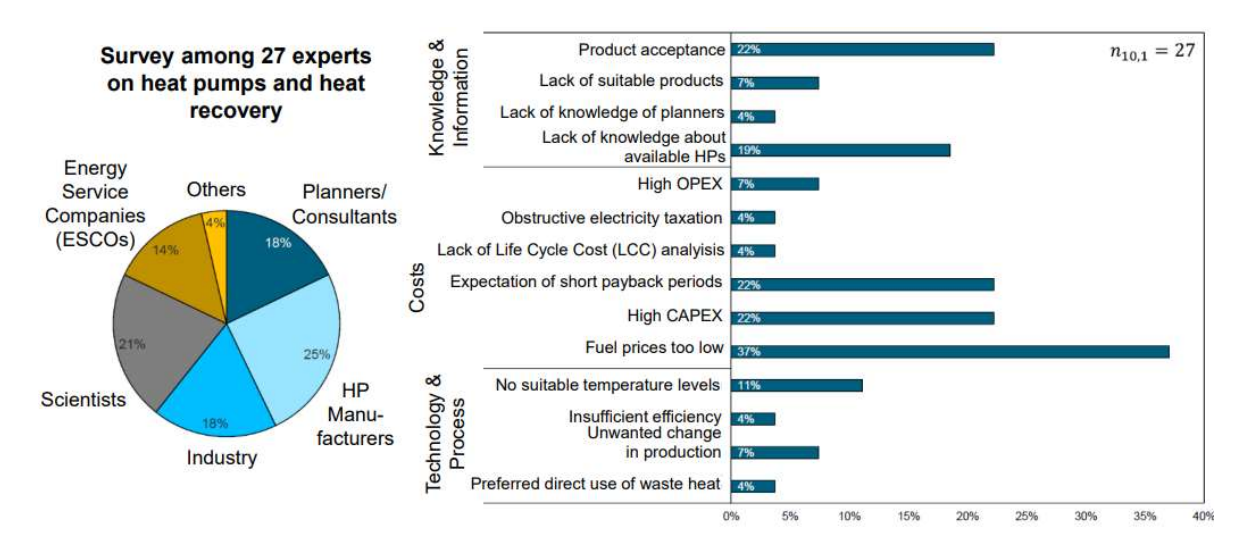


Figure 7 Survey among 27 experts about market barriers of IHP [10]

In the following thesis areas of interest for the implementation of a HP are analyzed and their cost effectiveness and potential within these areas is investigated.

2.1 Industrial heat pump manufacturer

The following Table 1 (in this table . (dot) is used in difference to , (comma)) gives an overview of global high temperature heat pump (HT-HP) manufacturer and their technical readiness level (TRL). There is a wide variety of compressor types and working fluids, whereas some are already commercially available, and others are in a research state. Temperatures higher than 165 °C can only be reached by a mechanical compression of steam [11], [12], [13].

Table 1 Overview of development of HT-HP manufacturer; in this table . (dot) is used in difference to, (comma) [11], [12]

Supplier	Compressor type	Working fluid	Capacity	T _{max supply}	TRL
Fuji Electric	Reciprocating	R-245fa	0.03 MW	120 °C	9
Emerson	Scroll and EVI Scroll	R-245fa, R410a, R-718	0.03 MW	120 °C	6
Mayekawa (EcoSirocco)	Reciproating	R-744	0.1 MW	120 °C	8-9
Mayekawa (EcoCircuit)	Reciprocating	R-1234ze(E)	0.1 MW	120 °C	8-9
Skala Fabrikk	Piston	R-290, R-600	0.3 MW	115 °C	7
Kobelco Compressors Corp. (SGH165)	Twin-screw	R-245fa/R-134a, R-718	0.4 MW	175 °C	9
Kobelco Compressors Corp. (SGH120)	Twin-screw	R-245fa	0.4 MW	120 °C	9
Mitsubishi Heavy Industries	Two-stage centifugal	R-134a	0.6 MW	130 °C	9
есор	Centrifugal	ecop fluid 1	0.7 MW	150 °C	6-7
Mayekawa Europe (HS Comp)	Piston	R-600	0.8 MW	120 °C	7
Kobelco Compressors Corp. (MSRC160L)	Twin-screw	R-718	0.8 MW	175 °C	9
Enertime Centrifugal		R-1336mzz(Z), R-1224yd(Z), R-1233zd(E)	2.0-10.0 MW	160 °C	4-8
Spilling	Piston	R-718	1.0-15.0 MW	280 °C	9
Epcon	HP centrifugal fan	R-718	0.5-30.0 MW	150 °C	9
Turboden	Turbon	Application specific	3.0-30.0 MW	200 °C	7-9
MAN Energy Solutions	Centrifugal turbo with expander	R-744	10.0-50.0 MW	150 °C	7-8
Piller	Turbo	R-718	1.0-70.0 MW	212 °C	8-9
Siemens Energy	Turbo (Geared / single-shaft)	R-1233zd(E) / R-1234ze(E)	8.0-70.0 MW	160 °C	9 (to 90 °C)
Qpinch	Chemical adsorption heat transformer	R-718, H3PO4 and derivatives	>2.0 MW	230 °C	9

Mayekawa Europe (FC Comp)	Screw	R-601	1.0 MW	145 °C	5
GEA	Semi-hermetic piston	R-744	0.1-1.2 MW	130 °C	8
Fenagy	Reciprocating	R-744	0.3-1.8 MW	120 °C	5-6
Rank	Screw	R245fa, R-1336mzz(Z), R-1233zd(E)	0.12-2.0 MW	160 °C	7
SRM	Screw	R-718	0.25-2.0 MW	165 °C	5
Combitherm	Semi-hermetic screw	R-1233zd(E)	0.3-3.3 MW	120 °C	9
Sustainable Process Heat	Piston	HFOs	0.3-5.0 MW	165 °C	6-8
Hybrid Energy	Piston, Screw	R-717, R-718	0.5-5.0 MW	120 °C	9
Johnson Controls	Reciprocating	R-717, R-600 (cascade)	0.5-5.0 MW	120 °C	7-8
ToCircle	Rotary vane	R-717, R-718	1.0-5.0 MW	188 °C	6-7
Weel & Sandvig	Turbo	R-718	1.0-5.0 MW	160 °C	4-9
Olvondo	Piston (double acting)	R-704	5.0 MW	200 °C	9
Heaten	Reciprocating, custom design	HFOs	1.0-6.0 MW	165 °C	7-9
Enerin	Piston	R-704	0.3-10.0 MW	250 °C	6
Ohmia Industry	Centrifugal / Piston	R-717, R-718	1.2-10.0 MW	150 °C	7-8

In the following sections some HT-HP manufacturer are analyzed in more detail. Further information about the different manufacturer and their technology can be found in [11].

2.1.1 Kobelco

The Japanese company Kobelco offers a special HP concept with a thermal energy supply capacity of 624 kW to generate saturated steam with 135 - 175 °C. In the evaporator the working fluid is heated up and vaporized by the source and is being compressed to higher temperatures. In the condenser thermal energy is transferred to pressurized circulating water at 115 °C, which is being decompressed to 0,1 MPa in a flash tank. Flash steam with 110 °C is generated and compressed to 0,8 MPa and 175 °C. In Figure 8 (in this figure . (dot) is used in difference to , (comma)) you can see a technical diagram of the machine with typical COP depending on the temperature level [12], [14].

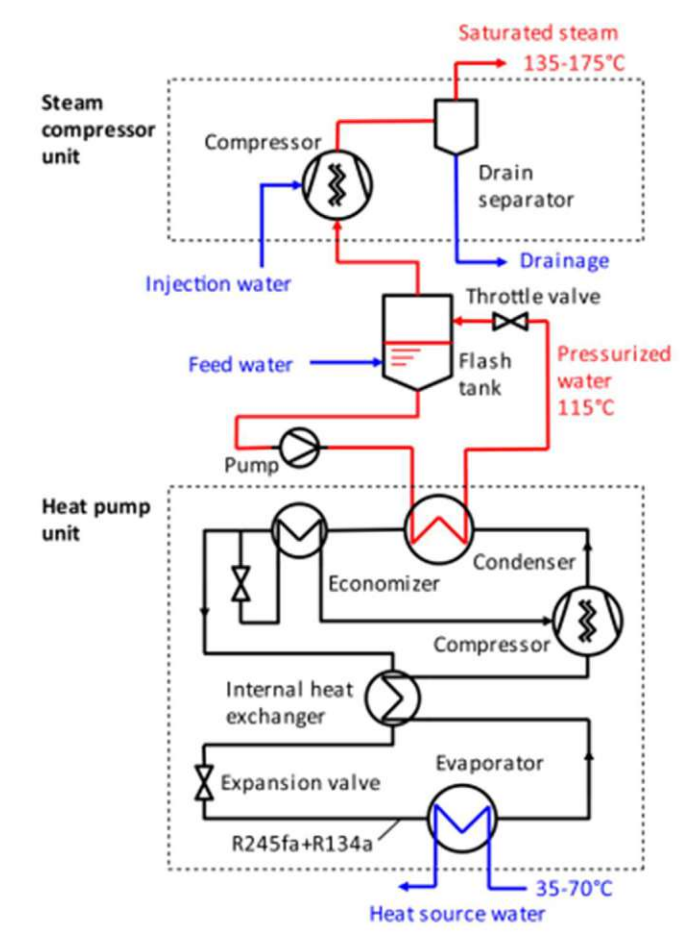


Figure 2: System configuration

Table 1: Performance

T _{source,in}	T _{source,out}	T _{sink,in}	T _{sink,out}	COPheating
[*C]	[°C]	[°C]	[*C]	[-]
70	65	20	165	2.5
70	65	20	135	3.0
50	45	20	165	1.9
50	45	20	135	2.2

Figure 8 Concept and typical COP of operating temperatures of the Kobelco HP; in this figure . (dot) is used in difference to , (comma) [12], [14]

2.1.2 Hybrid Energy AS

Hybrid Energy is a Norwegian company offering a hybrid HP with a mixture of ammonia and water as working fluid. Temperature levels of up to 120 °C can be reached. A simplified flow diagram of the hybrid HP is shown in Figure 9. Hybrid Energy has three different models depending on the thermal energy output (1 – 5 MW) and temperature level (90 - 120 °C) [15].

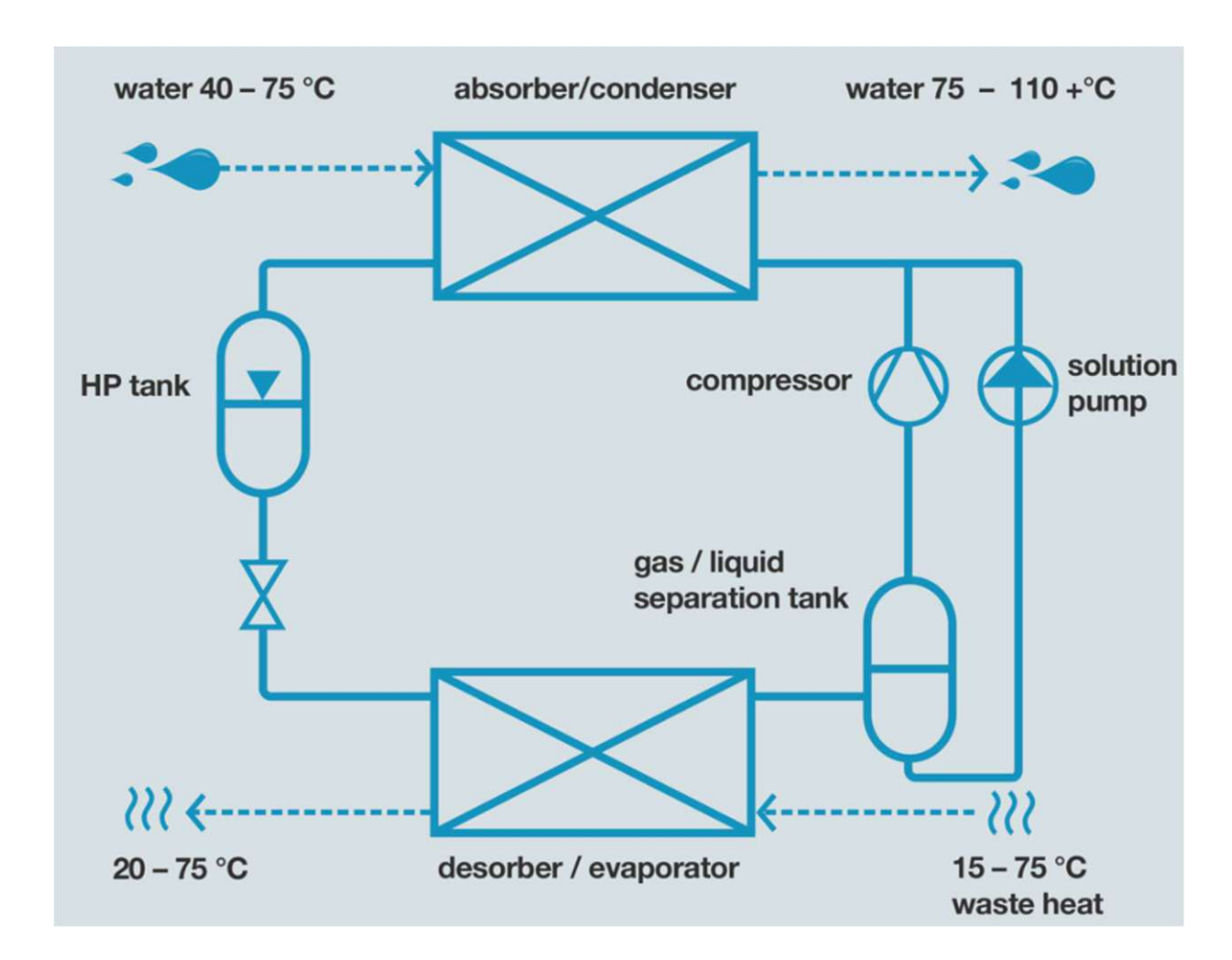


Figure 9 Simplified flow diagram of the hybrid energy HP [15]

There are several HP of Hybrid Energy (most of them in Scandinavia) in operation. Their HP is used in dairies, food processing, wastewater & sewage treatment, and for district heating (DH) [15].

2.1.3 Combitherm

The german company Combitherm offers a HP series with a thermal energy output between 20 – 1000 kW and temperatures up top 120 °C. The working fluids are HFOs (hydrofluorocarbons), HFKWs (hydrofluorolefines) and natural working fluids. The compression is done with screw or reciprocating piston compressors. A reference project of Combitherm is a fish factory in Norway, where waste heat of a drying process is reheated via a HP and feed back into the process [16].

2.1.4 Mayekawa

Mayekawa is a Japanese company offering different kinds of HP. Their portfolio include ammonia-, mobile-, snow melting- and CO₂ HP. The Ecosirocco CO₂ HP is the only HT-HP model of Mayekawa. The heating capacity is around 120 kW and temperatures of 120 °C can be reached with an air supply of 80 °C. The exemplary use cases are food processing plants, meat processing plants, beverage plants, automobile plants, semiconductor plants and hospitals [17].

2.1.5 Sustainable Process heat GmbH (SPH)

Sustainable Process heat (SPH) is a very young company using the HP technology of Viking Heat Engines AS after their insolvency. SPH is a German company developing the Thermbooster HP, which has a power of 400 – 1000 kW. The working fluid is R-1233zd (trans-1-Chlor-3,3,3-trifluorpropen). The source temperature can vary between 8 – 120 °C and the sink temperature can be up to 165 °C. Figure 10 shows one possible use case from their website for producing hot water with 135 °C [18].

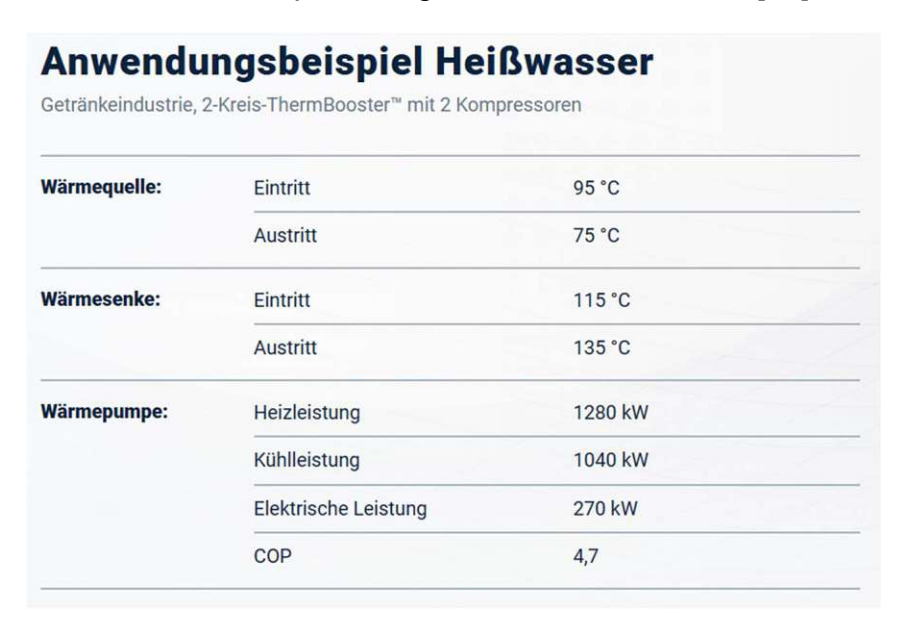


Figure 10 Possible use cases of SPH HP [18]

2.1.6 Ochsner

The HT-HP of Ochsner are labeled IWWDS, ISWDS and IWWDSS and have a power between 170 – 750 kW. The maximum temperature output is 130 °C, which can be achieved with special screw compressors. Ochsner uses a non-toxic and nonflammable working fluid called ÖKO1 (R245fa). There are no reference projects of this HP on the website [19]. Figure 11 (in this figure . (dot) is used in difference to , (comma)) gives an overview of Ochsner HT-HP [13].

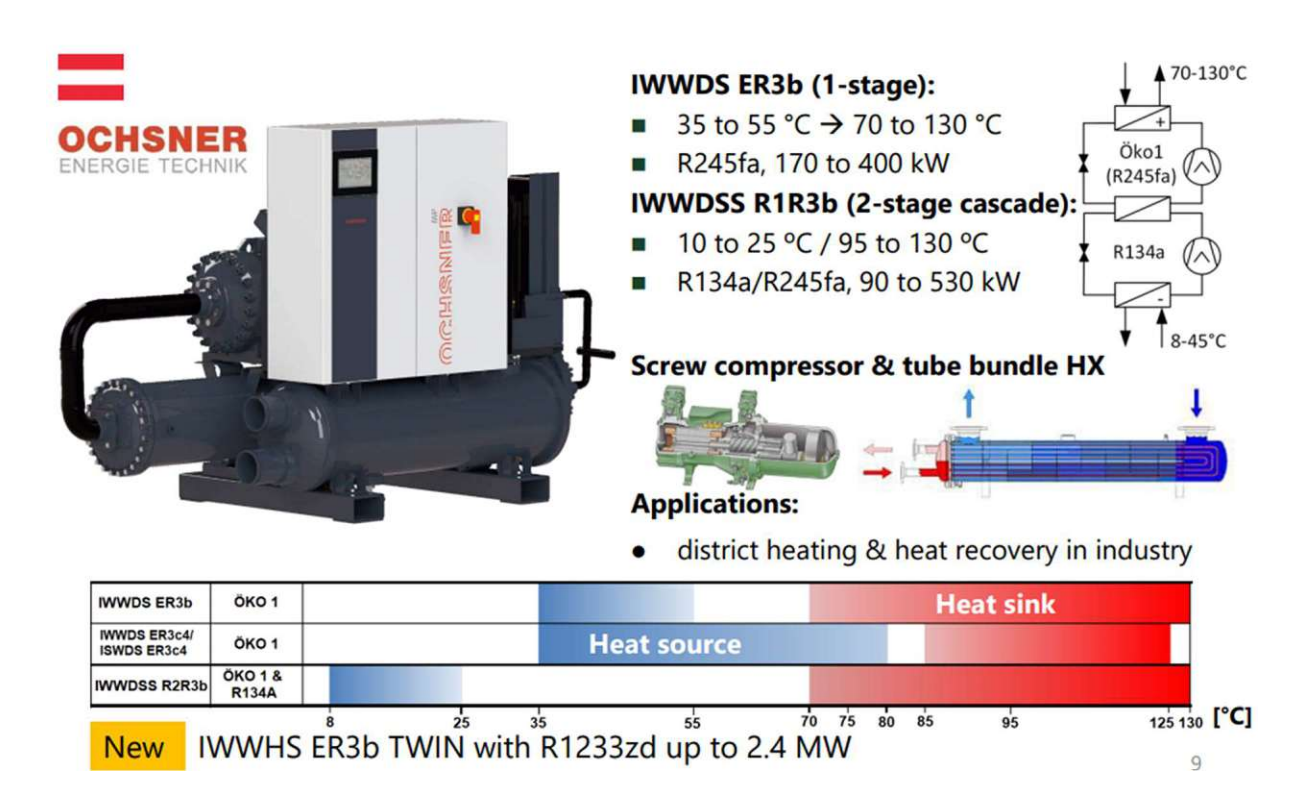


Figure 11 Overview of Ochsner HT-HP; ; in this figure . (dot) is used in difference to , (comma) [13]

Alternative Ochsner also offers another HP series with temperatures up to 95 °C with a power level of 60 – 850 kW. Such a HP (ISWHS 60 ER3) is operating at the Winery GVS Schaffhausen. The net power is 63 kW and a heating COP of 4,2 can be achieved. The HP uses the waste heat of a cooling machine with 37 °C as source producing a sink with 80 - 95 °C. The thermal energy is used in the facility for disinfection of the wine tanks, the bottling line and is additionally fed into a small DH system [19].

2.1.7 eNGie – thermeeco2

The flagship HP series (thermeeco2) of the company eNGie is available in the power range of 90 – 1000 kW. The maximum output temperature is 90 °C. The working fluid of this HP series is CO₂. Currently 90 thermeeco2 HP are in operation. In their brochure they show an exemplary customer (Osatina) using the thermal energy for different applications in greenhouses. The source is about 14 °C and the sink between 40 – 60 °C. Other exemplary use cases can be found on their website [20], [21].

2.1.8 Ecop Technology GmbH

Ecop Technology GmbH is an Austrian manufacturer of IHP. The working medium of the ecop rotation heat pump (RHP) are noble gases (helium, argon, krypton). The working medium is per- and polyfluorinated chemicals (PFAS) free, as well as nonflammable and has a global warming potential (GWP) < 1. This is made possible by the technology of the RHP, which is based on the Joule process. The ecop RHP cover

the temperature range between 5 °C (cooling) to 150 °C (heating). Technologically, the temperature range between - 50 °C and 250 °C is possible [22], [23].

2.2 Reference HP - ecop Rotation heat pump

This thesis uses the RHP of ecop as reference HT-HP. COP calculations of different setups and economic analysis are based on this HT-HP. Some specifications of the ecop RHP and technical details are given in 2.2.1 - 2.2.4.

2.2.1 General

In Table 2 technical data of the RHP is summarized. The nominal thermal energy output is between 400 - 700 kW. The maximum temperature of the sink is 150 °C. The working medium is either argon, helium, krypton, or mixtures of these three components. The temperature lift is currently limited to ~ 55 K by the maximum rotation of the heat exchanger [23].

Table 2 Technical specification of the ecop RHP [23]

Technische Daten				
Nominal heat output:	700 kW			
Working gas:	Noble gas mixture (He, Ar, Kr)			
Maximum outlet temperature of the sink:	150 °C¹			
Maximum inlet temperature of the source:	125 °C2			
Maximum temperature lift between sink outlet and source inlet:	55 K			
Minimum outlet temperature of the source:	5 °C			
Medium for heat transfer:	H ₂ O			
Dimensions ^{3 4} (W x H x L):	2200 x 2700 x 8100 mm			
Connection sink:	DN80 (3"), PN16			
Connection source:	DN80 (3"), PN16			
Mass:	16 t			
Nominal mass flows ⁵ / Kv-value ⁶ :	21m³/h / 15m³/h			
Maximum system pressure source/sink:	16 bar			
Electrical fuse protection:	500A gL/gG			
Supply voltage:	690/400 V - 3-N ~50 Hz			
Max. Nominal electrical power consumption (start-up): Average electrical power consumption in steady-state operation (depending on working parameters)	280 kW 150-200 kW			

2.2.2 Thermodynamic process of the RHP

In a conventional heat pump, the refrigerant is evaporated or condensed in a left-hand closed loop process, passing through the two-phase region (carnot process). In the RHP, the joule process is decisive, in which the working medium remains in the gaseous state the entire time. The two cycle processes are shown in Figure 12 [23].

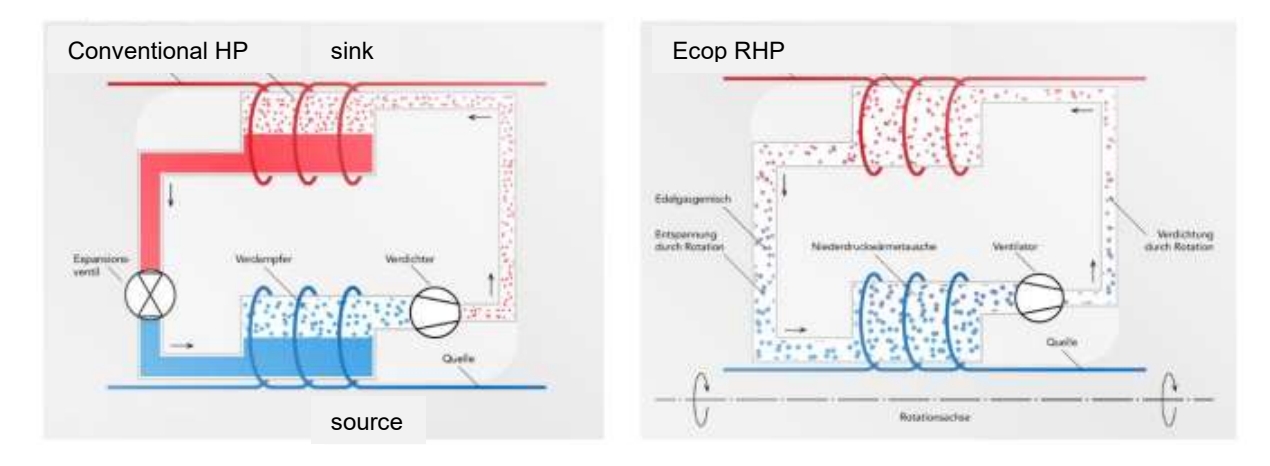


Figure 12 Cycle process of a conventional HP (left) and the Joule Process of the ecop RHP (right) [23]

Figure 13 shows the typical cycle of a conventional HP with Ammonia (NH₃) as working medium (left) and the Joule process of the ecop RHP (right) in T,s-diagrams [23].

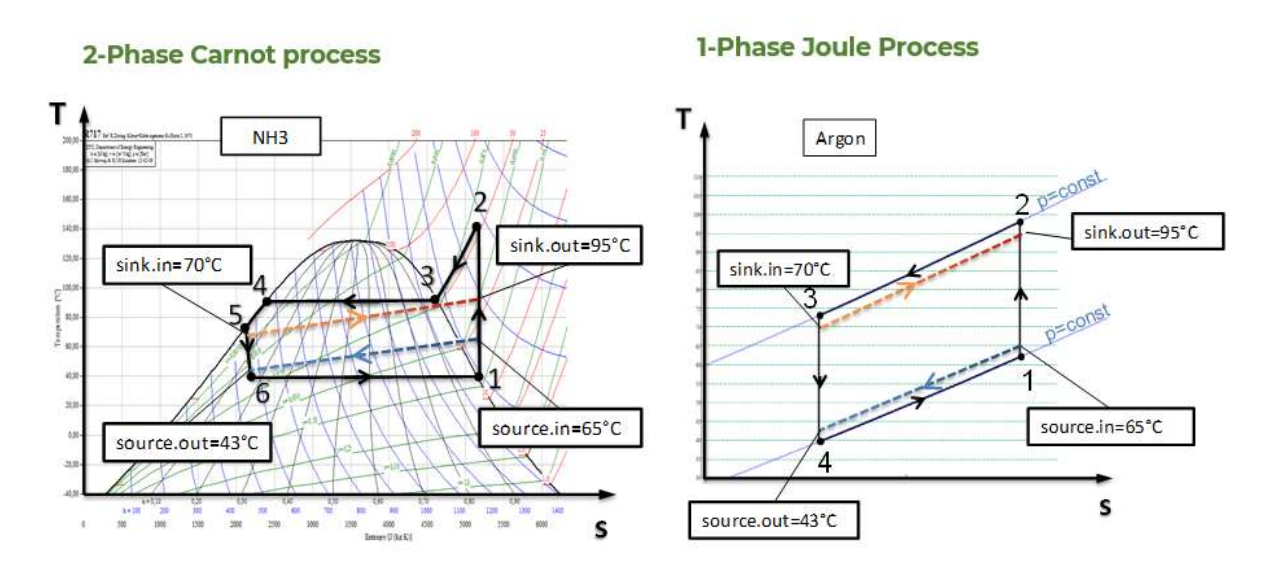


Figure 13 T,s diagrams which show the conventional HP typical Carnot process (left), Joule Process (right) [23]

In the RHP, the working medium is compressed via centrifugal forces by rotation of the rotor. The centrifugal force rise with increasing distance from the axis of rotation, which compresses and heats the working medium. In the expansion tube the working medium is being relaxed closer to the axis. A compression efficiency of up to 99% can be achieved. An additional fan is required to circulate the working medium in the tubes to overcome pressure losses, due to friction, deflections, and temperature changes. The main components of the system are the high-pressure (sink side) and low-pressure (source side) heat exchangers (HEX), compression lines, expansion lines, and the fan. At the high-pressure HEX, the thermal energy is transferred to the sink circuit, while



the low-pressure HEX absorbs energy from the source circuit. Figure 14 shows the rotor and the main shaft of the ecop RHP with the three fluid circuits (sink, source and working medium) [22], [23].

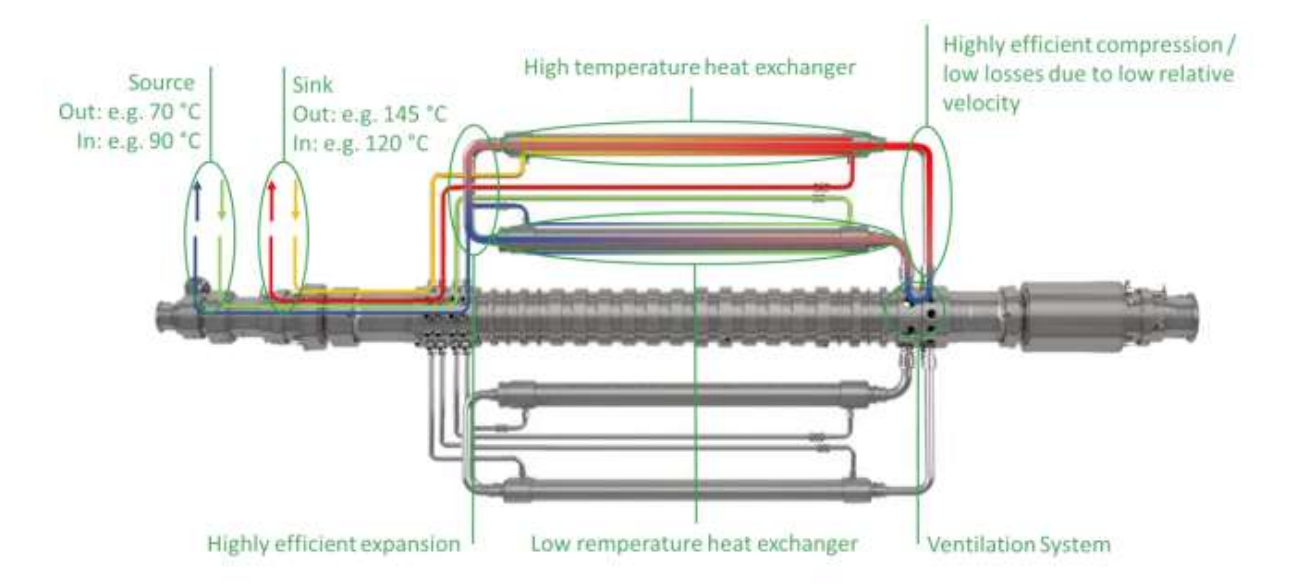


Figure 14 ecop RHP rotor with the three fluid circuits (sink, source and working fluid), the colors imply temperature levels (red hot > yellow > green > blue); e.g.: exempli gratia (exemplary) [22]

Figure 15 (in this figure . (dot) is used in difference to , (comma)) shows the joule process of the ecop RHP in a T,s-diagram. The temperatures and entropies listed are only given as examples. In the low-pressure HEX of the RHP thermal energy from a source (for example excess heat) is absorbed (4 - 5). For technical reasons, an extension tube is needed to connect the low-pressure heat exchanger to the fan (5 -5.1). In the next step, the fan compresses the working gas just as much to overcome the pressure losses during the cycle (5.1 - 5.2). In the compression tube, the working gas is compressed by the centrifugal forces and the temperature increases (1 - 2). In the high-pressure HEX, the thermal energy of the working gas is transferred to the sink (2 - 3) (for example DH feed). In the expansion tube, the pressure, and the temperature of the working fluid decreases (3 - 4) [23].

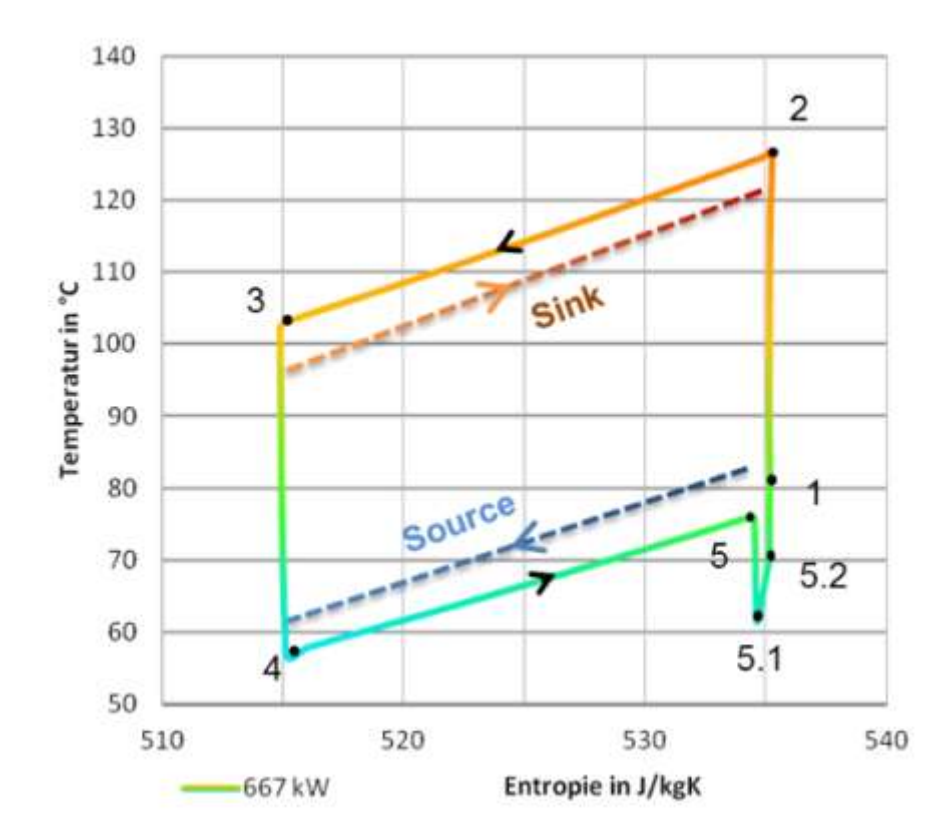


Figure 15 Cycle process (Joule process) of the ecop RHP divided in some steps in a T,sdiagram; in this figure . (dot) is used in difference to , (comma) [23]

Figure 16 (in this figure . (dot) is used in difference to , (comma)) shows the relevant sections of the joule Process (numbers comparable to Figure 15) in the schematic working fluid circuit. The colors are representative for the temperature level. The temperature is maximal in the sink HEX (red) and minimal in the source HEX and close to the lowest pressure before the fan (blue) [23].

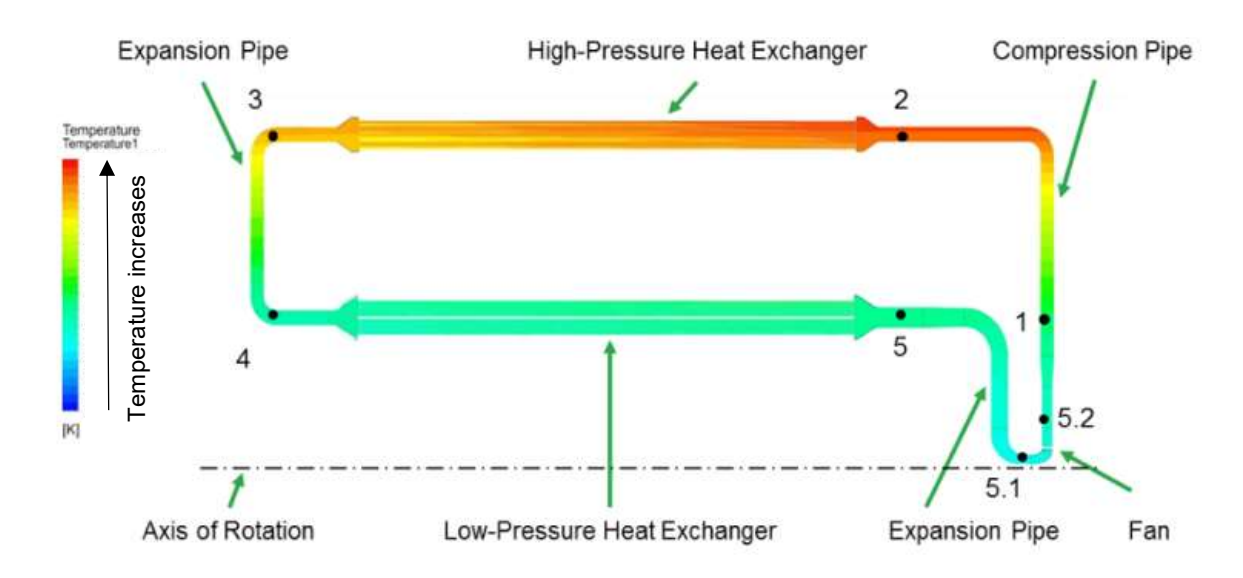


Figure 16 Relevant sections of the Joule process in the working fluid section; in this figure. (dot) is used in difference to, (comma) [23]

2.2.3 Demonstration plant

The first conventional rotation heat pump of ecop has been implemented in a biomass combined heat and power plant (CHP).

The CHP burns woody biomass to generate electricity in a steam cycle and thermal energy for DH. After the utilization of the steam in the turbine, the steam needs to be condensed completely. Before the integration of the RHP, the evaporation enthalpy of the utilized steam was released to the environment by a fan. The RHP is used to condense the steam using it as source to lift the temperature of the sink. The sink is the feedback of a district heating system being heated up from 55 °C to 95 °C. A schema of the combination between the CHP plant and the RHP is given in Figure 17 [22].

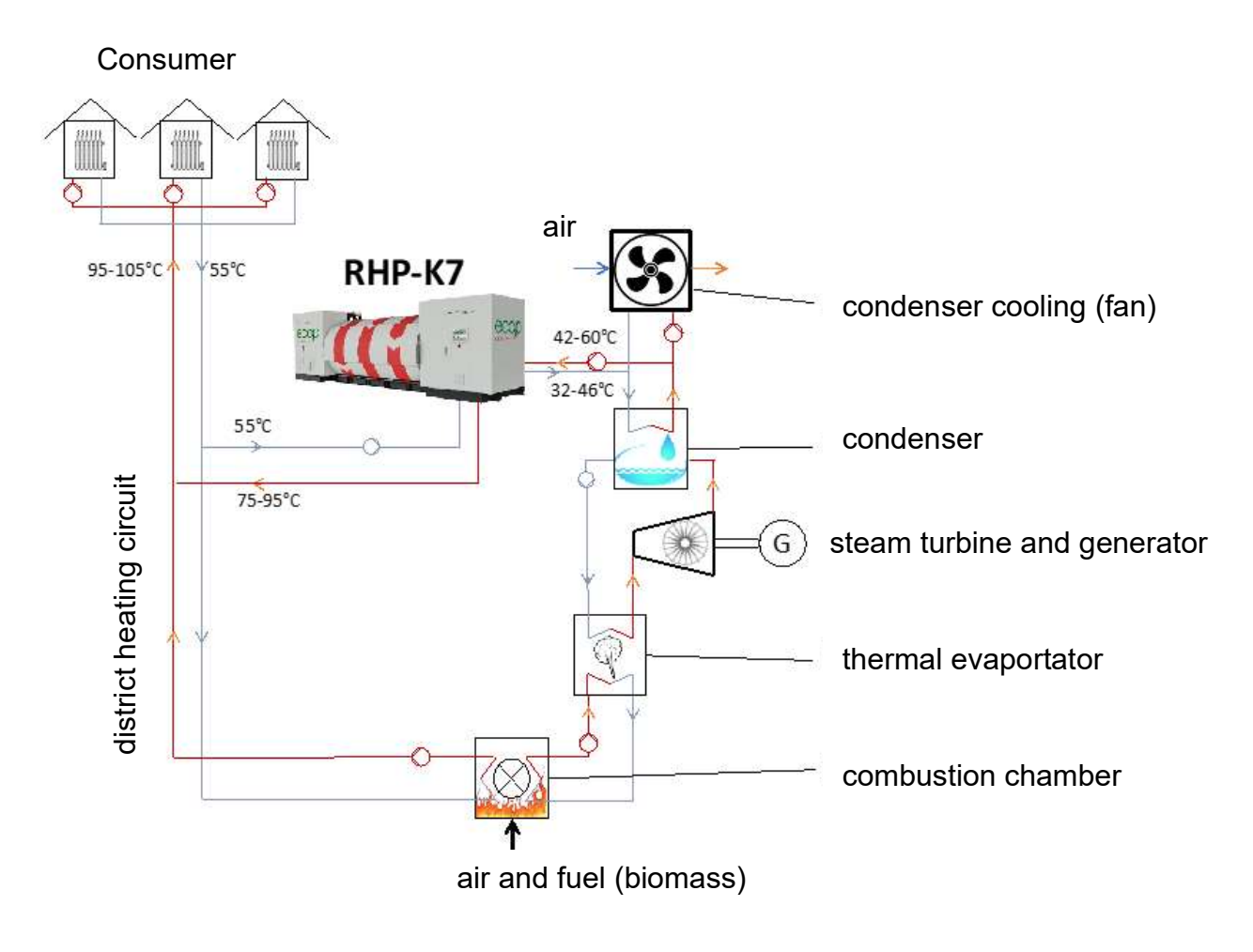


Figure 17 Schema of the rotation heat pump in a biomass CHP [22]

2.2.4 Advantages and Disadvantages of the RHP

The advantages of the RHP compared to conventional HP are as followed [23]:

Very high sink temperature, which opens use-cases that are not addressable by conventional HP. Especially the industry sector with use-cases up to 150 °C can be addressed.

- The operation in different temperature levels is very flexible, while being efficient. Therefore, the inlet and outlet temperatures of the source and sink can be variable. The flexibility results in the variable compressor pressure ratio of the working gas (variable rotation of the rotor). The mass flow and the resulting thermal energy transfer can be easily regulated by the fan.
- The working gas is not toxic, PFAS free, not flammable and has a GWP lower than 1.
- The temperature lift (source in to sink out) of the RHP (55 K) is higher than conventional HP (30 K).
- The RHP can reach higher COP than conventional HP, because of the use of the joule process (see Figure 18 – limitations by physics)

Figure 18 (in this figure . (dot) is used in difference to , (comma)) compares the maximum reachable COP of a conventional COP based on the Carnot process and the ecop RHP based on the joule process. The enthalpies (h) h1 – h5 refers for the carnot process to Figure 13 and for the joule process to Figure 15 [23].

2-Phase Carnot process

1-Phase Joule Process

$$COP = \frac{h2 - h5}{(h2 - h1)} = 6.05 \qquad COP = \frac{h2 - h3}{(h2 - h1) - (h3 - h4)} = 10.3$$

Figure 18 maximal reachable COP of the Carnot process (left) and the Joule process (right); in this figure. (dot) is used in difference to, (comma) [23]

3 Economic Analysis

The economic efficiency of a heat pump investment in general is determined by the payback period and the trade-off between the needed investment costs for the application including installation and the reduction of operational (energy) costs. For industrial investment decisions the payback period should be in a range of 1 to 3 years and maximum 5 years. To define a payback scenario the COP is needed as well as average energy costs. Furthermore, CO₂ prices become more and more important in total costs of ownership (TCO) calculations with a fossil reference scenario. In economic efficiency analysis different options are compared to choose the best fitting. In this thesis the reference scenario are natural gas (NG) boilers.

3.1 Investment decisions with Total Cost of Ownership

Investment appraisal using TCO is a calculation method for determining life cycle costs. The aim is to consider the income and the expenditures associated with an investment decision, which are incurred throughout the entire process from planning through construction to disposal [24], [25]. The goal of a TCO is to make statements about whether and in which form an investment pays off or which one causes the lowest costs [26]. Figure 19 shows the different investment decision procedures that can be applied in the context of a TCO. This thesis focuses on the single economic approach, which considers the cost / benefit issue of a specific project. The macroeconomic method is used for a company-wide view and considers issues such as sales, location, and financing considerations [24], [27].

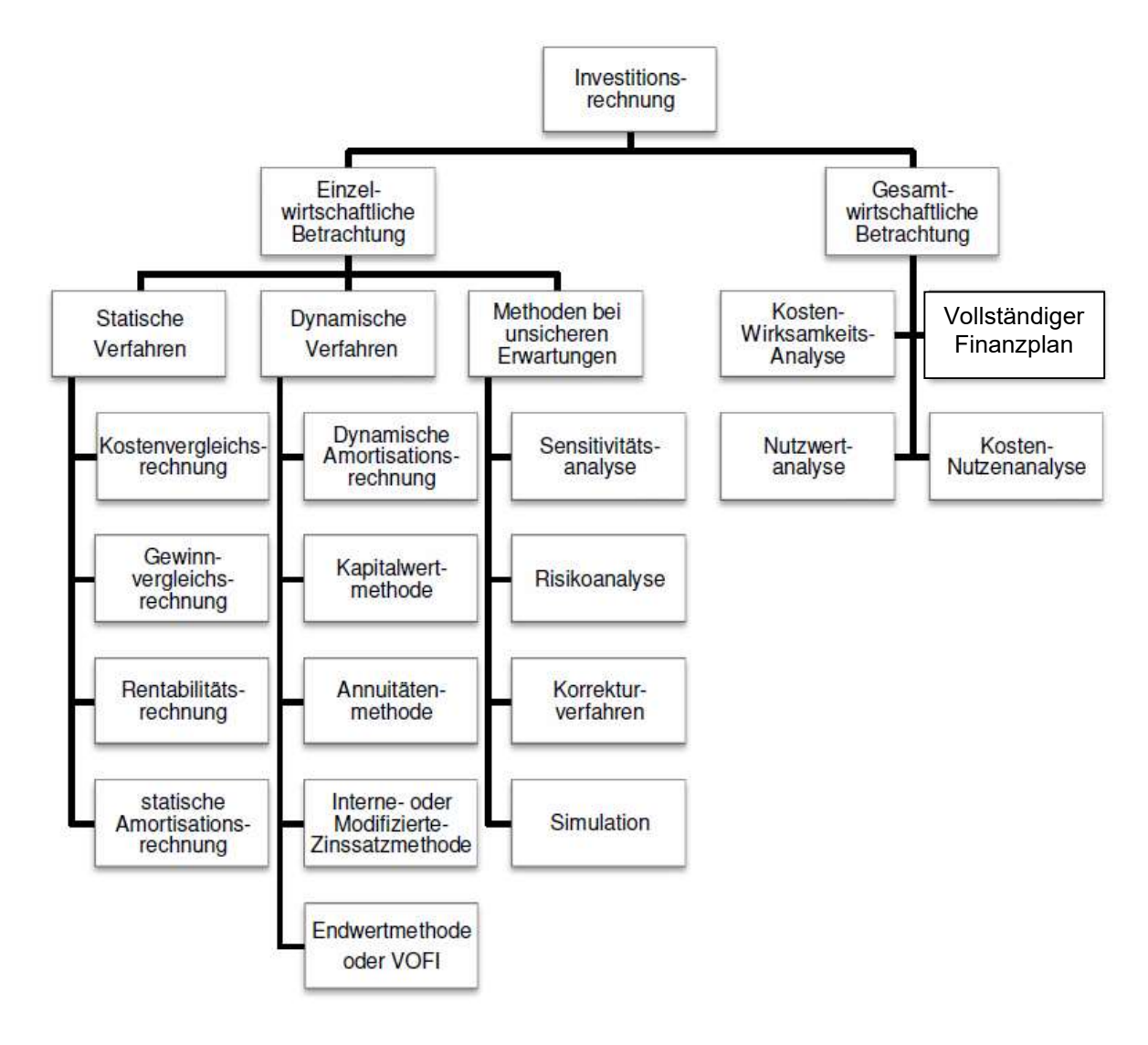


Figure 19 TCO investment decision-making processes [27]

3.1.1 The factor time in a TCO

The factor time considers in a TCO, if the calculation is done static or dynamic. Static methods not considering time as a factor are simple, but are not relevant for an investor in terms of a later profitability analysis. Static models do not respect real accounting, depreciation, and interest policy. In a static model cost are constant over a period, or the life of the investment. In the dynamic view, the timing of cash inflows and outflows is accounted for by interest. This interest can have decisive effects on investments and

must be calculated accordingly. In this thesis investment decision are calculated in a dynamic way [26], [28].

Income and expenses can be related to any point in time by "discounting" and "compounding". In Figure 20, this is illustrated by means of a time bar that can be divided into selectable time intervals. The compounding / discounting factor (q^{+/- n}) considers the interest rates between the reference and the observation period. The present value (K-n) is calculated according to Equation (1). Similarly, the future value (K_n) can be determined with the aid of the compound interest factor [26], [29].

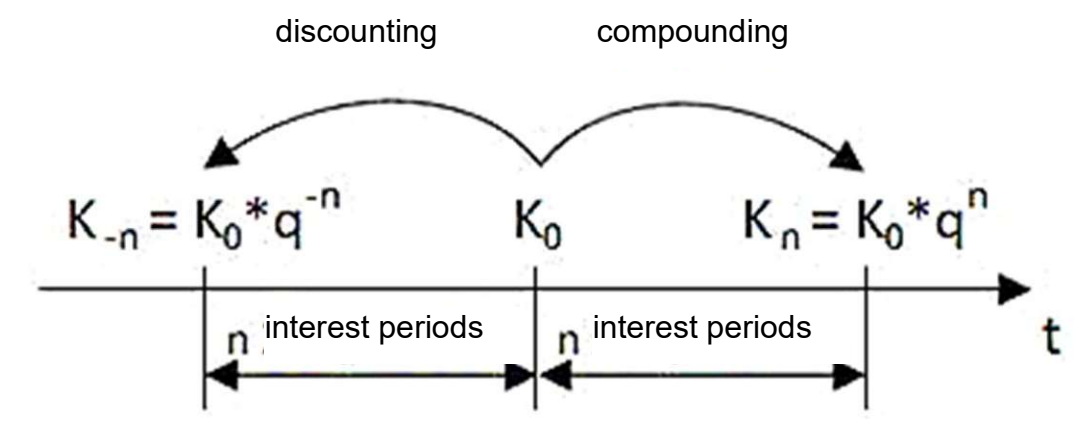


Figure 20 Visualization of discounting and compounding [30]

$$K_{-n} = K_0 (1 + i)^{-n} = K_0 q^{-n}$$
 (1)
 K_{-n} cash value in \in
 K_0 present value in \in
 q^{-n} discounting factor
 i discount rate in %
 n observation period in yr

3.1.2 Discounted payback period

This thesis is using the discounted payback period as dynamic investment makingdecision process, because the time until an investment is paid back is a major factor in industry investment decisions. The discounted payback period can be calculated according to (2). In this thesis the interest rate is assumed to be constant 3 % over an investment period of 20 – 30 years [10], [26], [31], [32].

$$DPP = \frac{-ln(1 - \frac{CAPEX}{OPEX_{savings}})}{\ln(1+i)} = \frac{-ln(1-PP)}{\ln(1+i)}$$
(2)

DPP discounted payback period in yr

PP static payback period in yr

CAPEX capital expenditures in €

*OPEX*_{savings} savings in the operational expenditures in €

The CAPEX in this section can me modeled in two different ways [10]:

- Investment costs of the HP including auxiliary system, what is specified in more detail in 3.3. In this case the HP substitute the existing heating system. The DPP show the payback period of the new HP system in difference to continuing to operate the old system.
- CAPEX difference between the HP system and the reference case. In this case DPP show the time needed that the HP system and the reference case have the same costs.

OPEX_{savings} clarify the difference in the OPEX in one year between a reference heating scenario (gas boiler) and a HP system. The OPEX of a gas boiler as reference scenario is calculated by Equation (3). The OPEX of the HP system is shown in Equation (4). Differences in maintenance costs are due to their small impact neglected [10], [32].

$$OPEX_{gas\ boiler} = \frac{Q_{demand}}{\zeta_{gas\ boiler}} \left(C_{NG} + \frac{f_{NG}}{10^6} C_{CO2} \right) \tag{3}$$

operational expenditures of a gas boiler in € $OPEX_{gas\ boiler}$

 Q_{demand} thermal energy demand in kWh

combustion efficiency of gas boiler $\zeta_{aas\ boiler}$

 C_{NG} NG price in €/kWh

Scope 1 CO₂ emission factor of NG in gCO_{2-ev}/kWh f_{NG}

 C_{CO2} EU-ETS price for Carbon emissions in €/t

$$OPEX_{HP} = \frac{Q_{demand}}{COP} C_{electricity}$$
 (4)

operational expenditures of a HP in € $OPEX_{HP}$

COPCOP of HP for given scenario

electricity price in €/kWh $C_{electricity}$

Figure 21 (in this figure . (dot) is used in difference to , (comma)) shows a sensitivity analysis of an exemplary HP case with 1 MW heating capacity. The sink / source temperature is 115 / 45 °C and the achievable COP is 2,53. PP result in 2,6 years and the DPP in 3,2 years. The sensitivity analysis shows the impact on the PP, if the different variables are adjusted between 50 and 150% of the current value. Very step curves show a very sensitive behavior. The most sensitive parameters are the FLH, electricity and fuel (gas, oil) price [10].



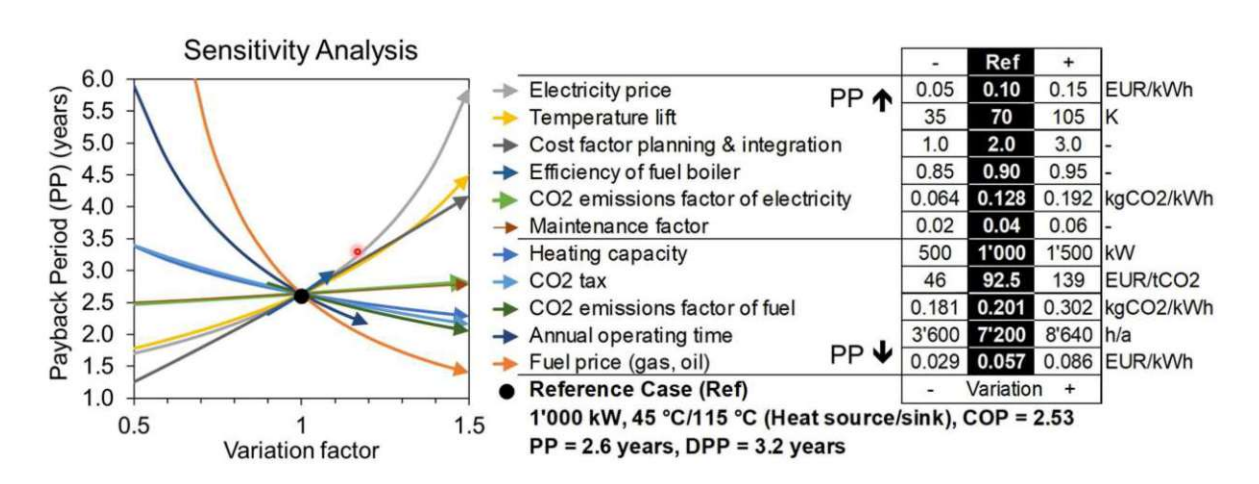
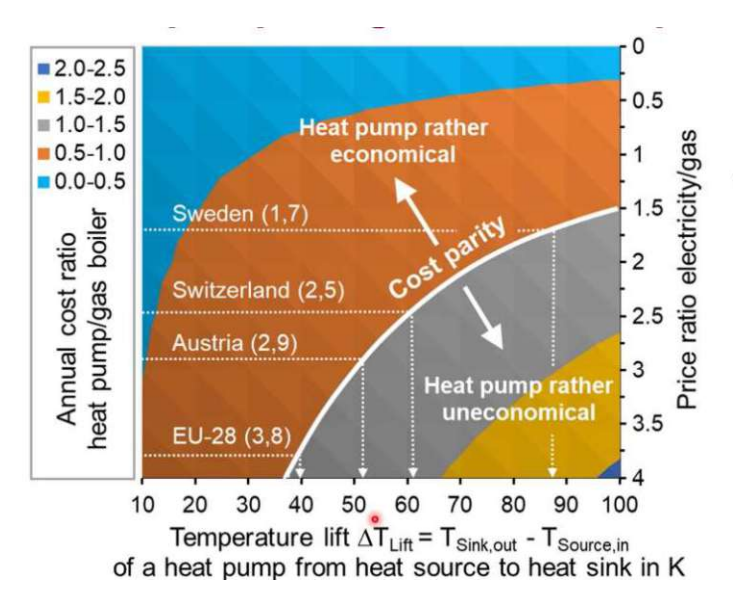


Figure 21 Sensitivity analysis of the PP according to their variation in the range of 50 – 150 % of the current calue; in this figure . (dot) is used in difference to , (comma) [10]

Figure 22 (in this figure . (dot) is used in difference to , (comma)) shows the cost parity between a HP and gas boiler depending on the power to gas price ratio and the temperature lift. Higher temperature lifts lead to decreasing COP. The relation between temperature lift and COP is shown in the figure. The assumptions for the graph are given on the right side of the figure. It is pictured that high electricity to gas price ratios and low temperature lifts lead to economical HP systems. Various power to gas price ratios in European countries lead to different national attractiveness of HP solutions. Exemplary is the electricity to gas price ratio in Sweden 1,7 and therefore the temperature lift boundary for an economical operation is 88 K [10].



The marked line shows the cost parity between the annual costs with a heat pump and a gas boiler

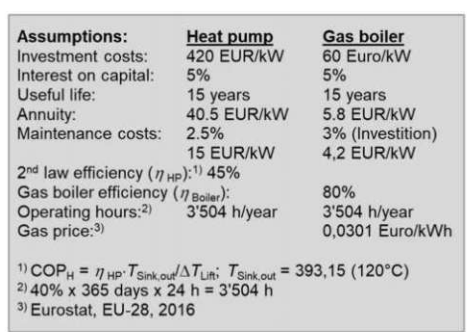


Figure 22 Cost parity of HP and gas boiler systems in accordance to the temperature lift and power to gas ratio; prices are based on 2016; in this figure . (dot) is used in difference to , (comma) [10]

Hence, an attractive market for HP are countries with a low ratio between electricity to gas prices such as Norway or Sweden. Figure 23 (in this figure . (dot) is used in difference to , (comma)) depicts the electricity to gas price ratio of some European



countries for a small-scale industrial end-user in 2020. Because of the importance of the electricity to gas price ratio the following chapter shows European trends [4].

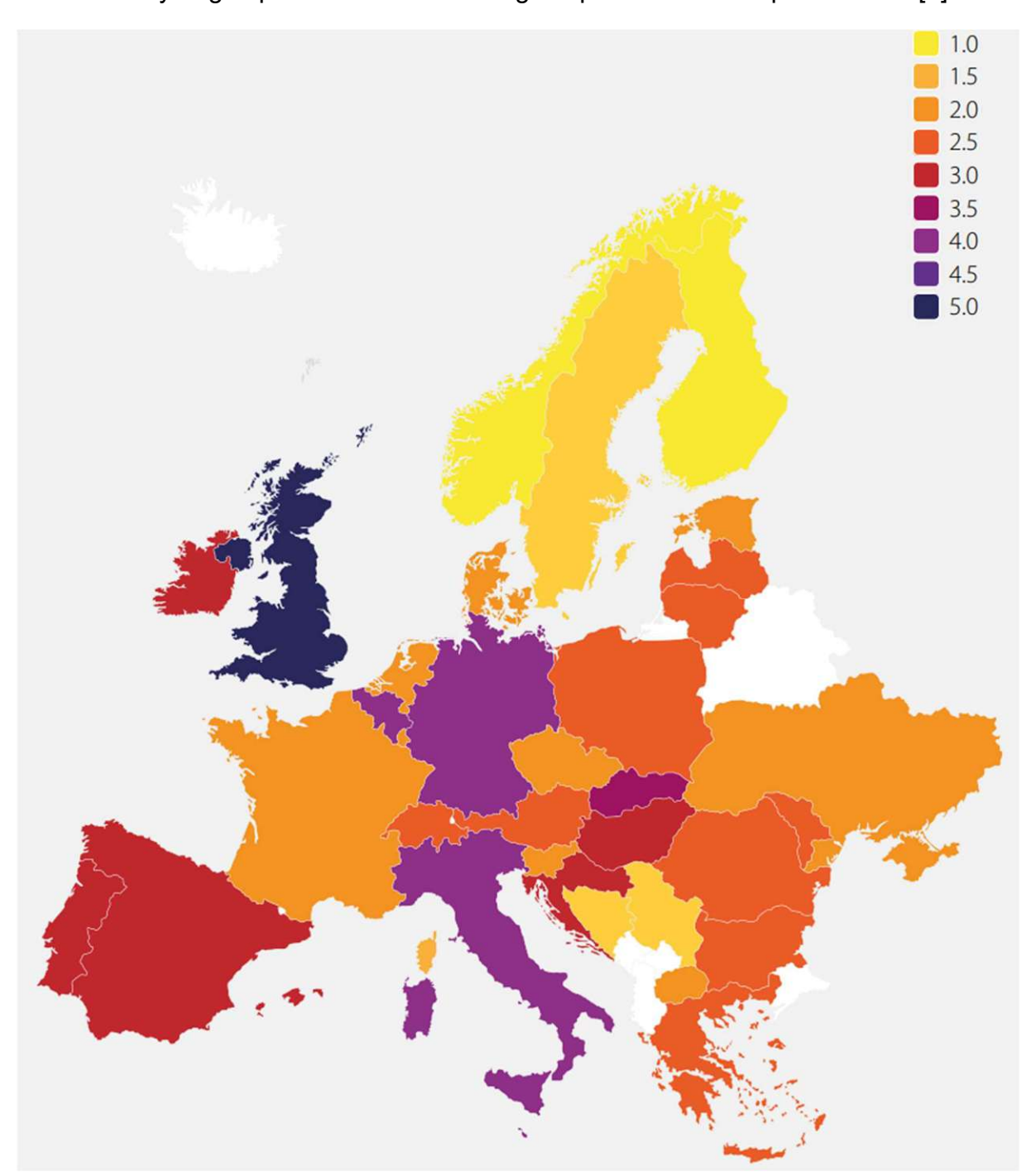


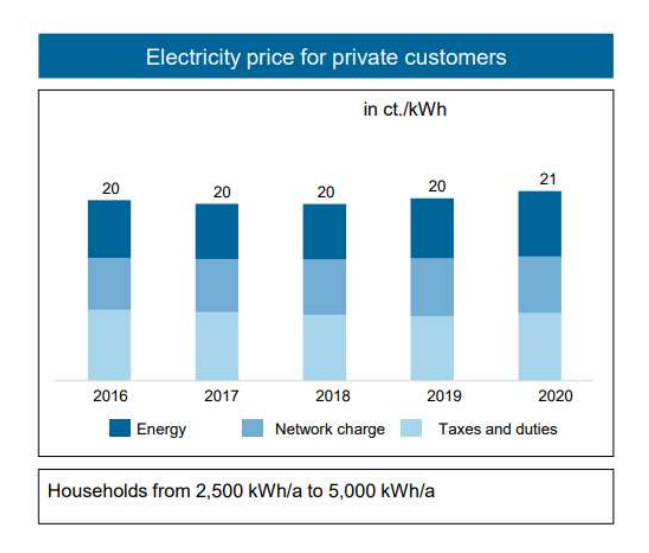
Figure 23 Electricity to gas price ratio of European countries for a small-scale industrial enduser (2 - 20 GWh/yr electricity; 3 to 28 GWh/yr gas); in this figure . (dot) is used in difference to, (comma) [4]

3.2 Electricity to gas price ratio

The electricity to gas price ratio is a very sensitive factor in HP economic analysis. While the CAPEX of HP solutions compared to gas boiler are usually higher, the OPEX are generally lower strongly depending on the electricity to gas price ratio. Because of usual COP between two and five of HP in industrial uses for the same amount of

thermal energy less electricity is needed than natural gas (NG). Therefore, if the electricity to gas price ratio is low the market is more attractive for HP solutions, because the plant operator can realize primary energy savings [33], [34].

Gas prices as well as electricity prices are different for households (private customers) and non-households (industrial customers). Among the industrial customers it must be distinguished between the quantity purchased. An example for the different electricity prices for private and industrial customers in Austria is shown in Figure 24 [33].



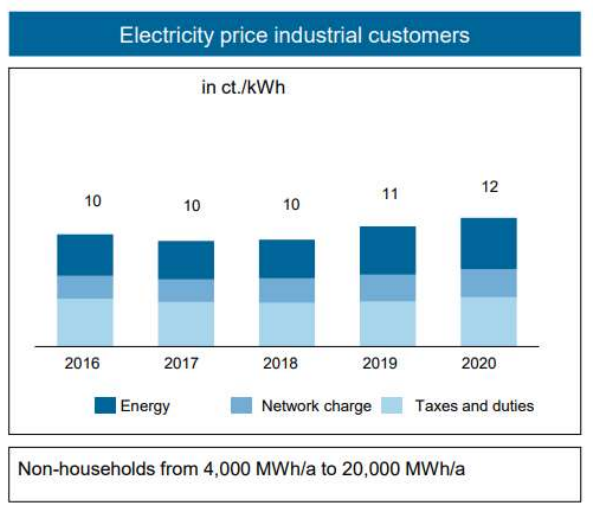


Figure 24 Electricity prices for private and industrial customers in Austria [33]

3.2.1 Electricity price

Electricity prices differ depending on the consumption volume. Therefore, electricity prices for private customers and industries are different. This thesis focuses on medium to large scale industries. Electricity for industries can be bought over the counter (OTC) that are bilateral contracts between the customer, supplier, and grid operator or on the exchange at very volatile prices. Figure 25 gives a short summary about OTC and the electricity exchange [33].

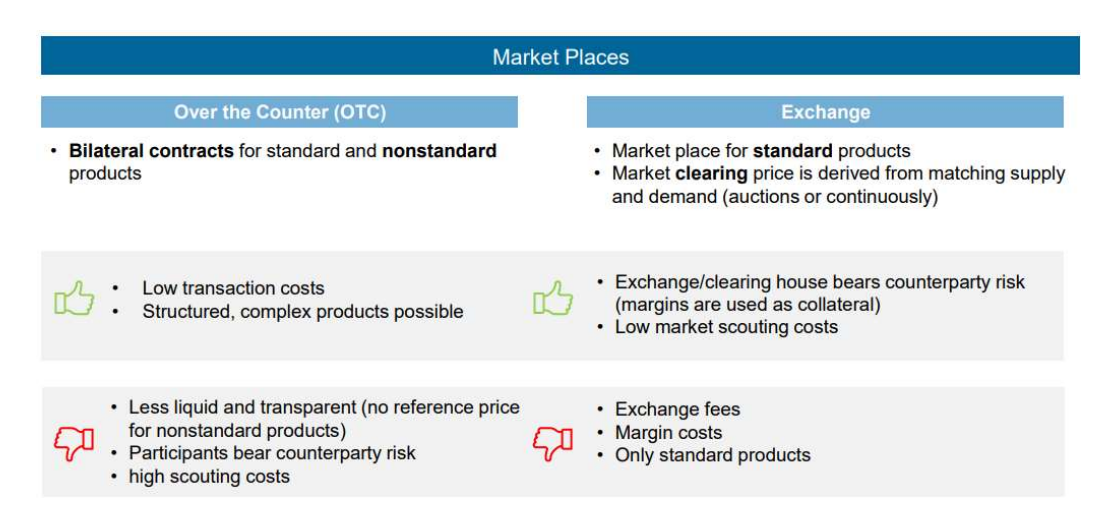
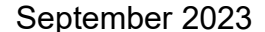


Figure 25 Electricity marketplaces in Europe [33]



Because of the different marketplaces and the unique contracts, it is very difficult to define the electricity price of an industrial customer. This section tries to define trends of the electricity prices for different countries in Europe.

In Europe, the electricity price on the day ahead auction at the European Power Exchange (EPEX) spot market is formed according to the merit order model. To explain this model, one needs to understand the concept of marginal cost of electricity generation. The marginal cost of a power plant determines the OPEX of the last kWh of energy produced. Different types of power plants have different marginal costs, which are shown in the example of Germany in Figure 26. Renewable and nuclear power plants have little marginal costs, while NG or oil plants have due to the need of a fuel input and carbon pricing higher marginal costs [33], [35].

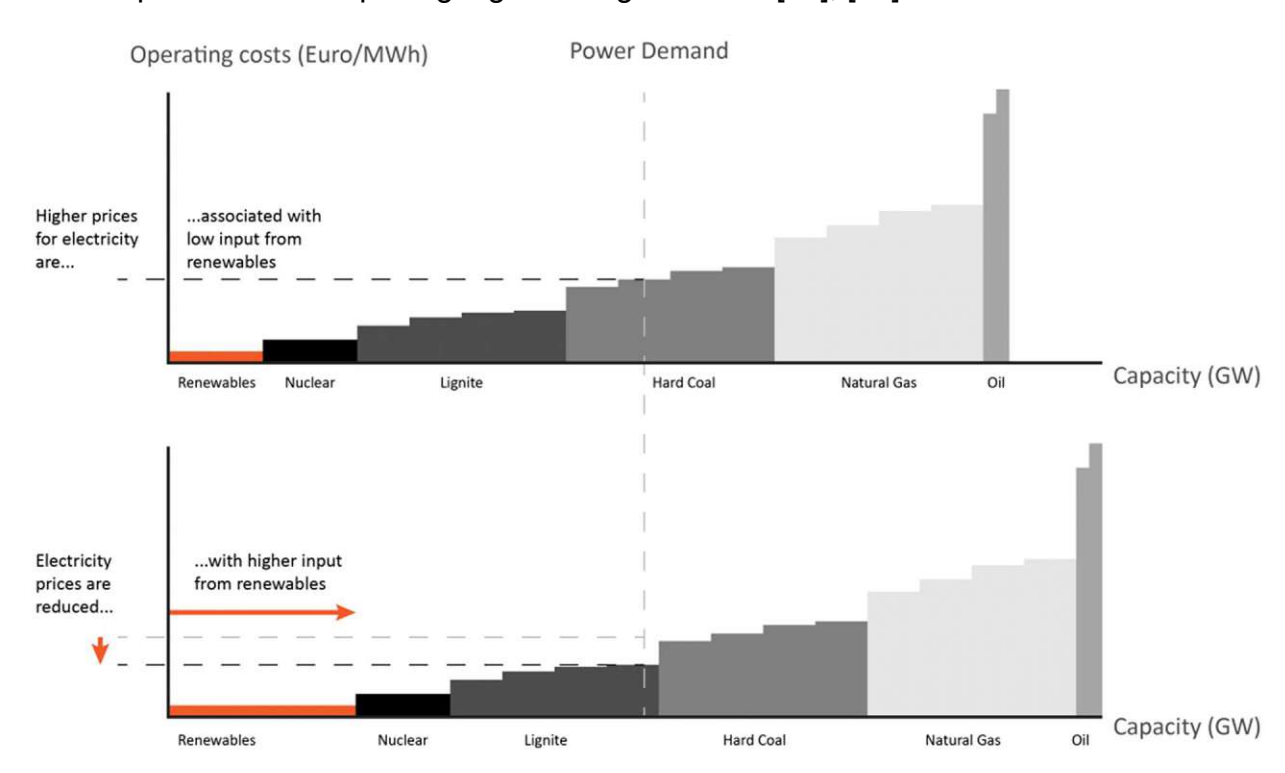


Figure 26 Electricity prices of the different plants based on the merit order model [36]

The electricity price is based on the price for the last kWh of electricity produced to meet the called demand. All power plants with lower marginal costs than the last kWh produced make a theoretical profit. Figure 27 visualizes the power price based on the merit order [35].

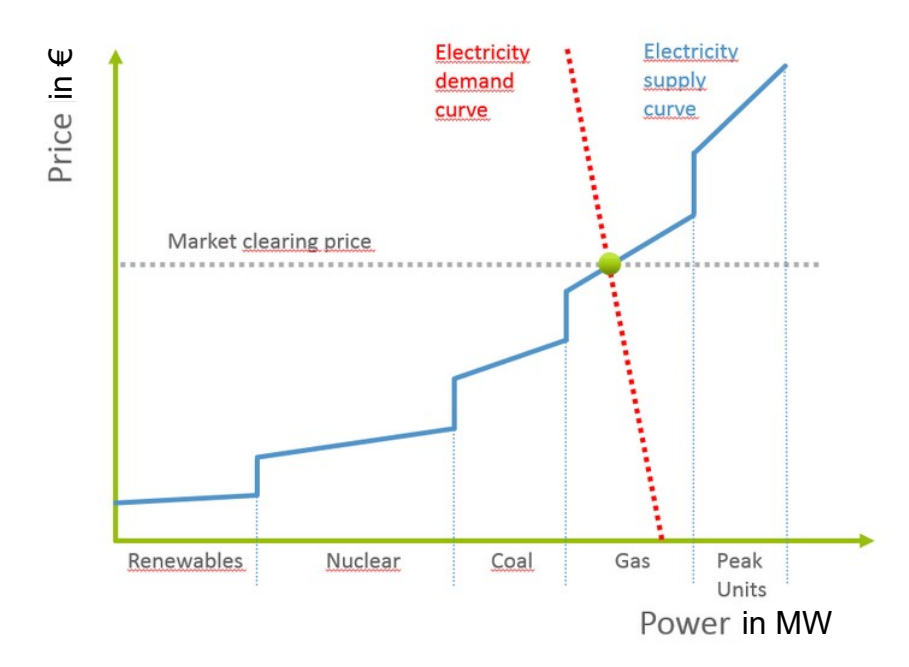


Figure 27 Simplified Diagram to visualize the electricity price based on the Merit Order principle [35]

A study by Energy Brainpool based on the world energy outlook 2022 predict the longterm development of average power prices for four scenarios shown in Figure 28. The investigated countries are the EU-27, United Kingdom, Norway, and Switzerland. The power price is declining until 2030 because of a recovery from the Ukraine war and is starting to increase from 2030 due to rising CO₂ prices. The scenario "central" is based on Europe stopping to import Russian gas. Therefore, the European NG price is determined by the global liquified natural gas (LNG) price. The energy system will strongly decentralize with a significant expansion of renewables. The "Tensions" scenario is based on increasing tensions between Europe and Russia and higher CO₂ prices. Therefore, the early NG prices are higher in this scenario. The "Relief" scenario is based on a better relationship between Europe and Russia. Europe decreases the amount of fossil fuels slightly. The renewable expansion target, which were set during the crisis, are kept in place. "GoHydrogen" focuses on a fully decarbonization until 2050 comparable to the IEA "Net Zero" scenario [34].

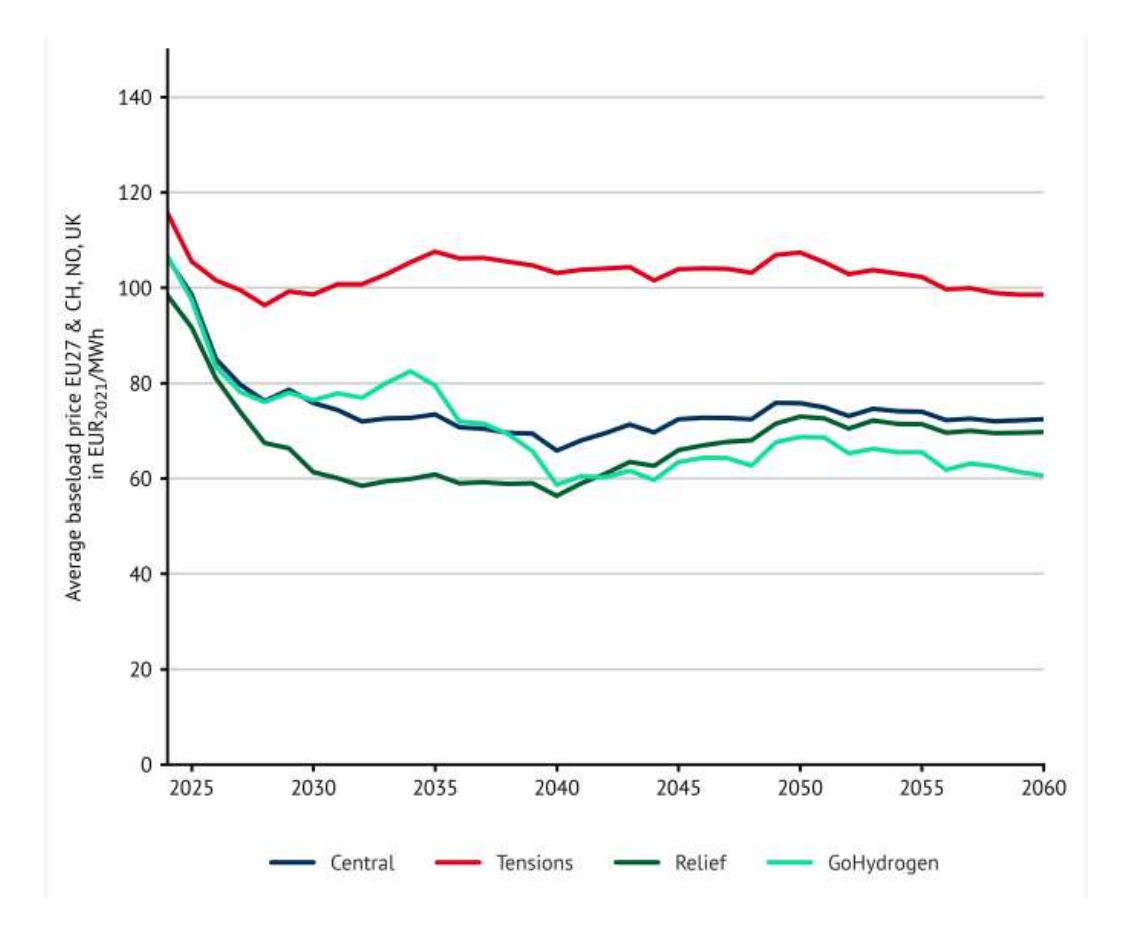


Figure 28 Long-term average power price in selected European countries for four scenarios [34]

Energy Brainpool predicts for future renewable power scenarios very volatile prices between summer and winter visualized for the central scenario in Figure 29. The prices will rise in winter due to the temperature sensitivity of the electricity demand and supply. The solar and hydroelectric power supply decrease in winter and the electricity demand increase due to greater energy losses and the need for heating [34].

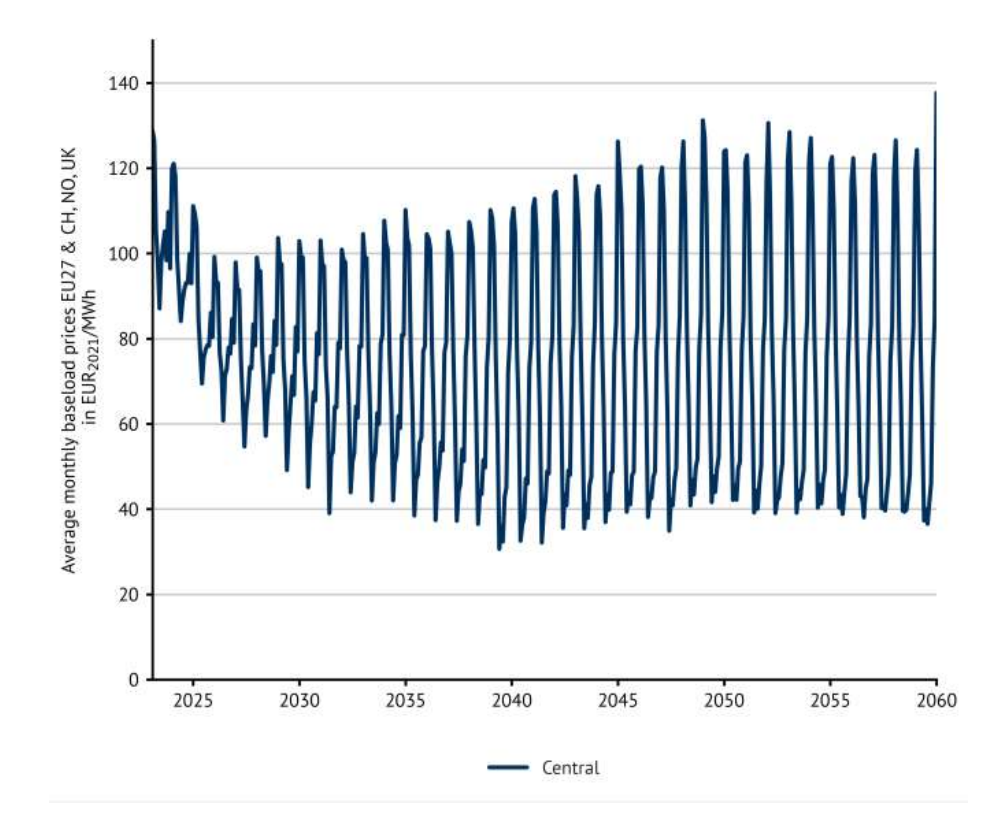


Figure 29 Increasing volatile power prices due to seasonal fluctuations in Europe [34]

There are also studies, which show long-term average power prices for countries with a lot of solar or wind power to decline to 30 – 40 €/MWh in the future [2].

Table 3 gives a summary of the different power price trends in Europe based on different scenarios [34].

Table 3 Summary of the European power prices between 2025 and 2050 by scenarios [34]

	r				1		
		Energy Brainpool					
source	Central [34]	GoHydrogen [34]	Relief [34]	Tensions [34]	Mean values		
EU power	€/MWh	€/MWh	€/MWh	€/MWh	€/MWh		
2025	95	95	90	105	96,25		
2030	75	76	61	99	77,75		
2040	66	59	57	103	71,25		
2050	77	68	72	108	81,25		
					81,63		

3.2.2 Gas price

A study by Energy Brainpool based on the world energy outlook 2022 predict the longterm development of commodity prices for an announced pledges scenario shown in Figure 30. It is assumed that all countries will fulfill their currently pledged goals.

According to Energy Brainpool the NG price will drop to around 26 €/MWh in 2026 and afterwards decline steady to 15 €/MWh until 2060 [34].

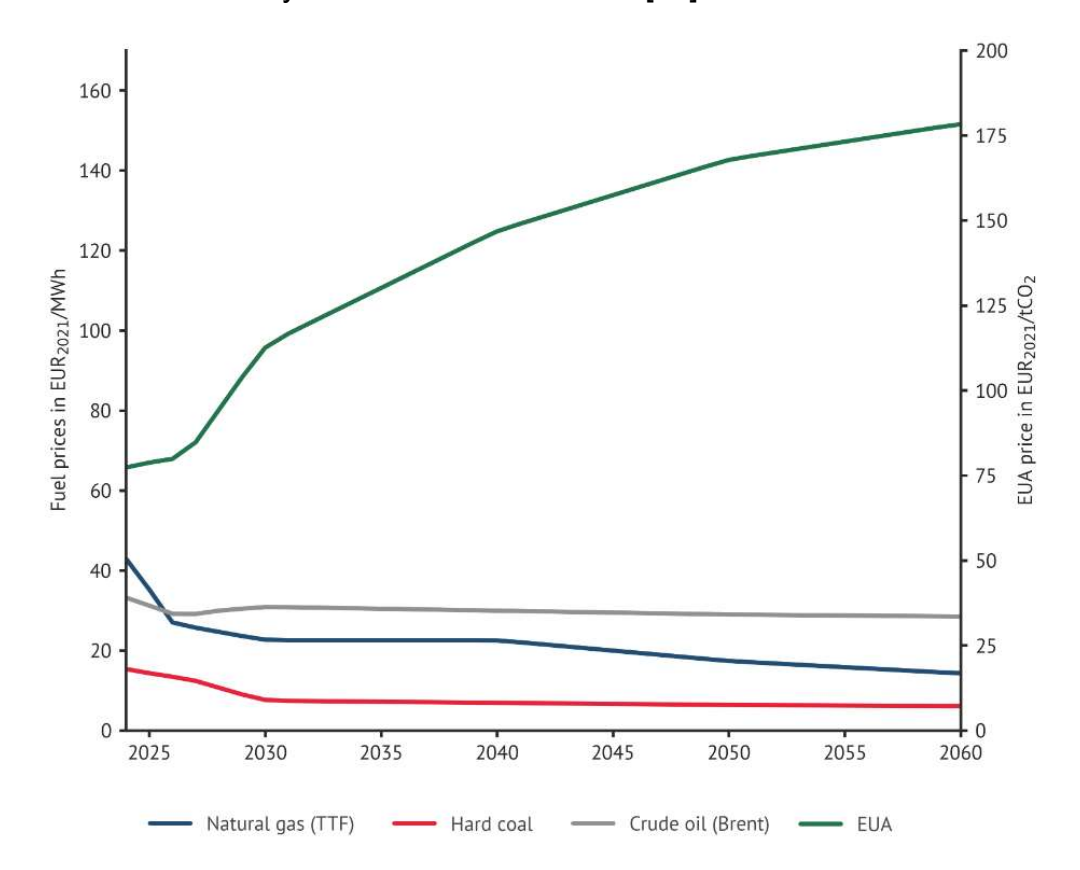


Figure 30 Long-term development of commodity prices, European Allowances (EUA): carbon pricing see 3.4 [34]

Table 4 (in this table . (dot) is used in difference to , (comma)) show the development of commodity prices based on research of the Aarlborg University. According to [32] the NG price is increasing until 2050 compared to prices before the Ukrainian war. The conversion factor between €/GJ to €/MWh is 3.6.

Table 4 Long-term price trends of commodities by Aarlborg University, conversion factor to €/MWh is 3,6 GJ/MWh; in this table . (dot) is used in difference to , (comma) [32]

(2009-€/GJ) Year	Oil (US\$/bbl	Natural Gas	Coal	Fuel Oil	Diesel	Petrol	Jet Fuel	Straw	Wood Chips	Wood Pellets	Energy Crops	Nuclear
2011	82.0	5.9	2.7	8.8	11.7	11.9	12.7	3.5	4.5	9.6	4.7	1.5
2020	107.4	9.1	3.1	11.9	15.0	15.2	16.1	3.9	5.1	10.2	4.7	1.5
2030	118.9	10.2	3.2	13.3	16.6	16.7	17.6	4.3	6.0	10.9	5.2	1.5
	87			Projecte	ed assumi	ng the sar	ne trend	s as in 202	0-2030			102
2040	130.5	11.2	3.3	14.7	18.1	18.2	19.1	4.7	6.8	11.5	5.7	1.5
2050	142.0	12.2	3.4	16.1	19.6	19.7	20.6	5.1	7.6	12.2	6.3	1.5

Table 5 (in this table . (dot) is used in difference to , (comma)) show the predicted longterm commodity prices by IEA based on the World Energy Outlook 2022 depending on different scenarios, which can be read in detail in [37]. The Conversion factor between USD/MBtu to €/MWh is 3 considering a currency conversion of 1,15 €/USD.

Table 5 Conversion factor from USD/MBtu to €/MWh is factor 3 considering 1,15 €/USD; in this table . (dot) is used in difference to , (comma) [37]

			Net Zero Emissions by 2050		Announced Pledges		Stated Policies	
Real terms (USD 2021)	2010	2021	2030	2050	2030	2050	2030	2050
IEA crude oil (USD/barrel)	96	69	35	24	64	60	82	95
Natural gas (USD/MBtu)								
United States	5.3	3.9	1.9	1.8	3.7	2.6	4.0	4.7
European Union	9.0	9.5	4.6	3.8	7.9	6.3	8.5	9.2
China	8.0	10.1	6.1	5.1	8.8	7.4	9.8	10.2
Japan	13.3	10.2	6.0	5.1	9.1	7.4	10.9	10.6
Steam coal (USD/tonne)			W	08 2	(O)	ė 15	8	
United States	63	44	22	17	42	24	46	44
European Union	113	120	52	42	62	53	60	64
Japan	132	153	59	46	74	59	91	72
Coastal China	142	164	58	48	73	62	89	74

Notes: MBtu = million British thermal units. The IEA crude oil price is a weighted average import price among IEA member countries. Natural gas prices are weighted averages expressed on a gross calorific-value basis. The US natural gas price reflects the wholesale price prevailing on the domestic market. The European Union and China natural gas prices reflect a balance of pipeline and LNG imports, while the Japan gas price solely reflects LNG imports. The LNG prices used are those at the customs border, prior to regasification. Steam coal prices are weighted averages adjusted to 6 000 kilocalories per kilogramme. The US steam coal price reflects mine mouth prices plus transport and handling costs. Coastal China steam coal price reflects a balance of imports and domestic sales, while the European Union and Japanese steam coal prices are solely for imports.

Table 6 gives a summary of the different NG price trends in Europe based on different sources and scenarios [32], [34], [37].

Table 6 Summary of the European NG prices between 2025 and 2050 by sources and scenarios [32], [34], [37]

		IEA	IEA	IEA		
source	Energy Brainpool ~ Announced Pledges Scenario [34]	Net Zero Emissions by 2050 [37]	Announced Pledges [37]	Stated Policies [37]	Aalborg University [32]	Mean values
EU natural gas	€/MWh	€/MWh	€/MWh	€/MWh	€/MWh	€/MWh
2025	40	21,15	26,1	27	34,74	29,80
2030	23	13,8	23,7	25,5	36,72	24,54
2040	23	12,6	21,3	26,55	40,32	24,75
2050	18	11,4	18,9	27,6	43,92	23,96
						25,76

3.2.3 Electricity to gas price ratio

According to [34] the electricity demand will rise by around 64 % until 2050 mainly due to national hydrogen strategies, enhanced electrification in households, and the expansion of electric cars. In the industrial sector, increased efficiency can prevent a significant increase in electricity consumption.

The historical power to gas price ratio of selected European countries between 2008 and 2022 is shown in Figure 31. The prices are based on an industrial customer with a consumption band of 500 – 2000 MWh for electricity and a gas consumption > 200 GJ per year. It is shown that Sweden has the lowest power to gas ratio. United Kingdom (UK) has the tendency to have a high ratio. The spikes between 2021 and 2022 are a result of the Ukrainian invasion. Turkey and Hungary had the most intensive reaction on the Ukraine war. The EU-27 average is shown in bold yellow and the linear trend of EU-27 in dotted yellow. Between 2008 and 2022 the EU-27 average was always between 2 and 2,5 slightly increasing. An extrapolation of the EU-27 power to gas ratio trend would lead to a ratio of 3 - 3.5 in 2050 [38].

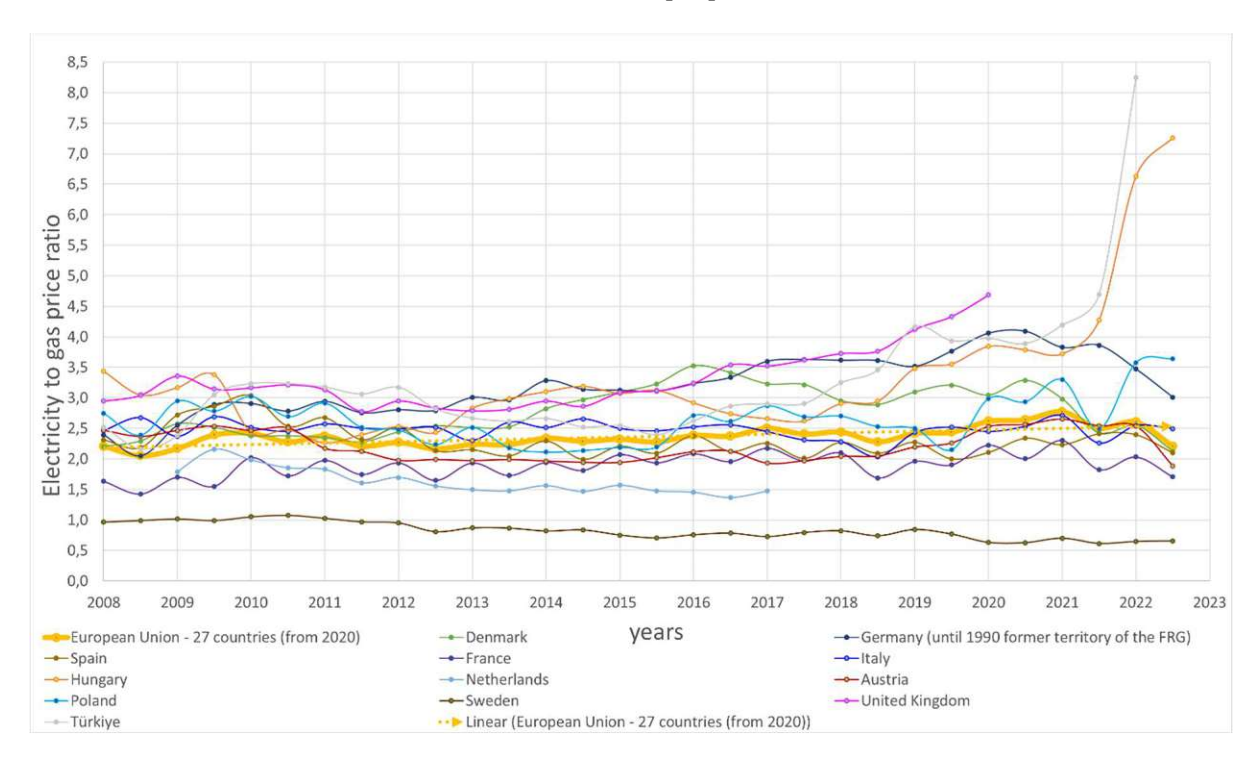


Figure 31 Historical electricity to gas price ratio of selected European countries between 2008 and 2022 [38]

Figure 32 shows the power to gas ratio in Europe between 2025 and 2050 based on different scenarios. The calculated values are shown in Table 7. This figure is based on the power and NG prices of the previos chapters. The ratio has been calculated for comparable scenarios of the different sources. The gray net zero scenario differs a lot from the others, because of significant lower NG prices. In 2040 all scenarios (except net zero) show similar ratios. From 2040, the scenarios show different trends between

2040 and 2050 leading to power to gas ratios between 2,0 and 4,2 in 2050 [32], [34], [37].

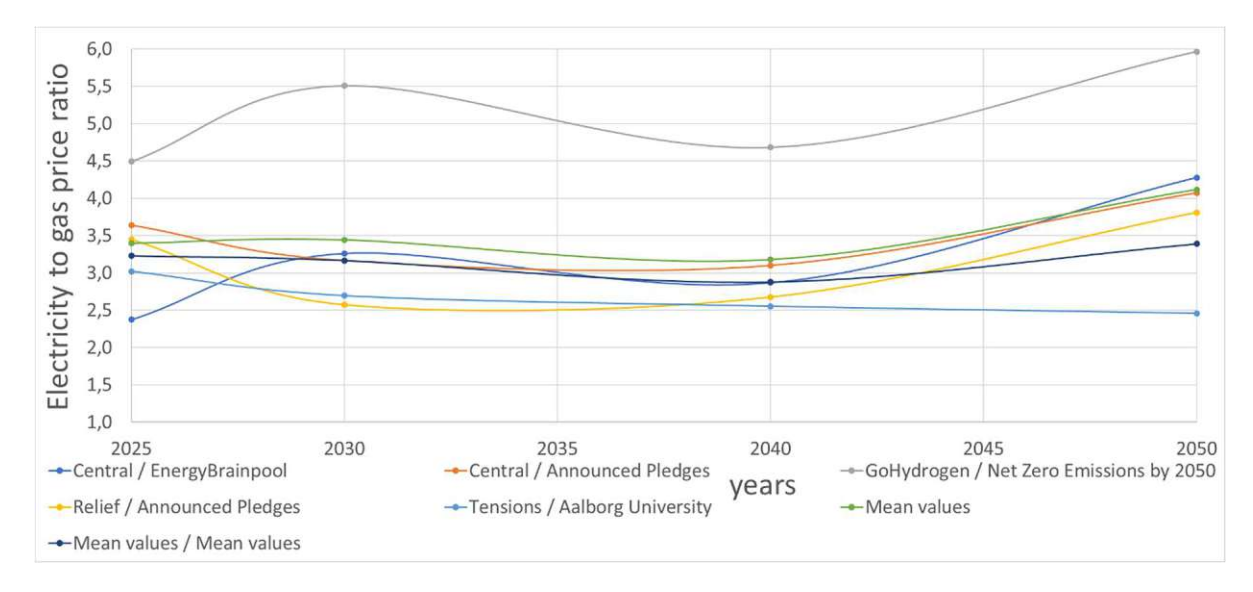


Figure 32 Power to gas ratio in EU-27 based on different sources and scenarios [32], [34], [37]

Table 7 Calculated power to gas ratio values for EU-27 based on different sources and scenarios [32], [34], [37]

power/gas ratio	Central / EnergyBrainpool	Central / Announced Pledges	GoHydrogen / Net Zero Emissions by 2050	Relief / Announced Pledges	Tensions / Aalborg University	Mean values	Mean values / Mean values
2025	2,38	3,64	4,49	3,45	3,02	3,40	3,23
2030	3,26	3,16	5,51	2,57	2,70	3,44	3,17
2040	2,87	3,10	4,68	2,68	2,55	3,18	2,88
2050	4,28	4,07	5,96	3,81	2,46	4,12	3,39
						3,53	3,17

In 2021 an average industrial user paid 40 - 45 €/MWh taxes for electricity and 6 - 6,5 €/MWh taxes for gas. Two-thirds of the revenues from power taxes are then used to subsidize renewable energies. The net effect is that the decarbonization of the electricity supply is subsidized, while disincentivizing the electrification of industry by favoring the use of gas. A review of the taxation framework by favoring the direct use of electricity would accelerate the switch away from fossil fuels. Figure 33 visualizes the influence of the power and NG taxation on the power to gas price ratio [1].

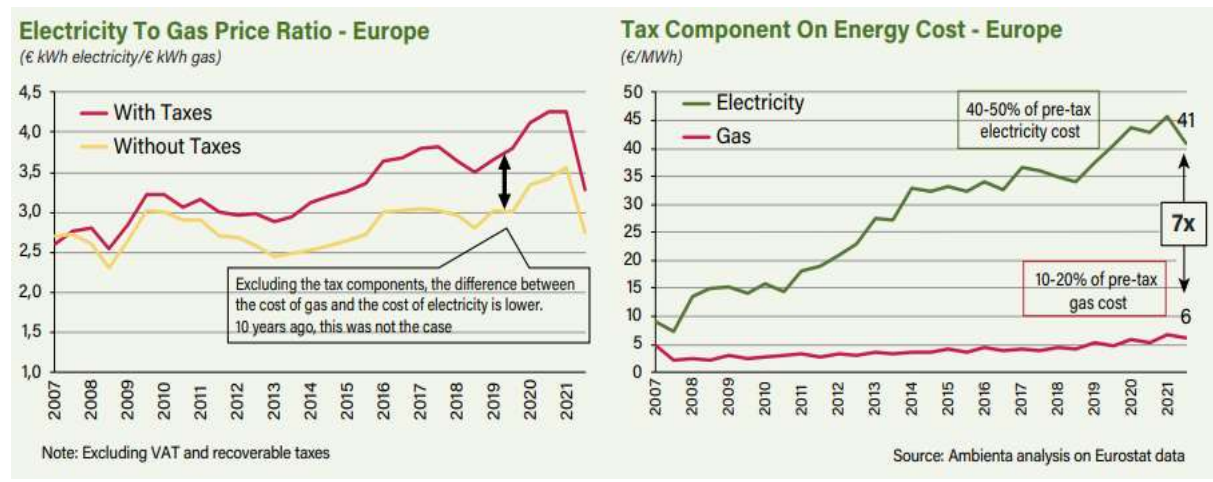


Figure 33 Influence of the power and NG taxation on the electricity to gas price ratio [1]

Figure 34 shows the electricity and gas prices in Europe and the United States of America (USA) in 2021 and 2022. The energy prices in Europe are generally higher than in the USA, while the power to gas price ratio in Europe is lower than in the USA. This is a result of low NG prices in the USA. Hence, from this perspective Europe is the more interesting market [1].

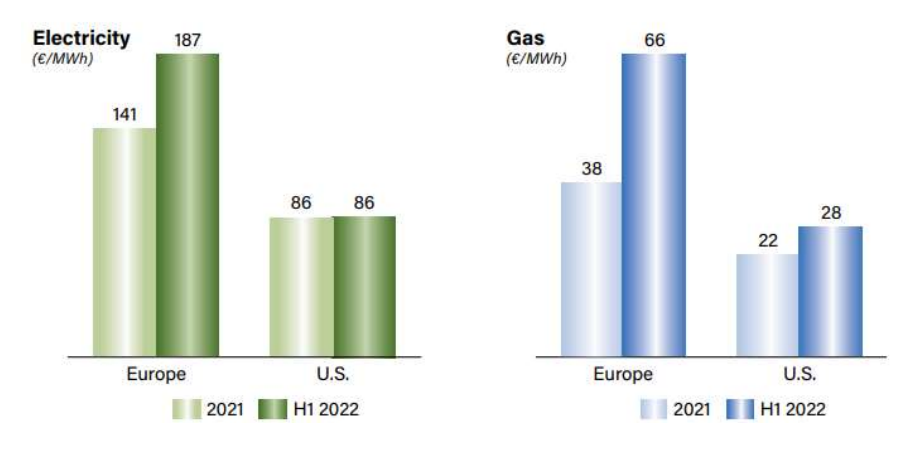


Figure 34 Electricity and gas prices in Europe and the USA in 2021 and 2022 [1], [39]

The key findings are that Europe is due to increasing carbon prices an attractive market for HP, but the power to gas ratio differs a lot within Europe. The most attractive market from this perspective is Scandinavia, as well as France, Portugal, and Bosnia. High ratios can be found in Romania, United Kingdom, Hungary, Croatia, and Slovakia. High national CO₂ prices combined with a high shares of renewable generated electricity result in low power to gas ratios. The considered long-term prices trends show similar results until 2040 and then vary a lot depending on the scenario. This thesis has decided to take an average power to gas ratio in Europe of three for an investment horizon of the next 20 – 30 years. Detailed economic analysis should consider country specific power to gas ratios [32], [34], [37], [40].



3.3 CAPEX and subsidies of a HP

The costs of a HP are usually given as HP specific investment costs in € / kWp. Prices for normal HP cannot be compared with IHP, because of the different requirements and temperature level. Whether additional equipment, labor associated with design and installation, and costs associated with design and installation are included in the price depends heavily on the manufacturer and the effort required for integration. Therefore, the specific HP investment costs found in the literature varies greatly between 300 and 1000 €/kWp [9].

There are also different kinds of CAPEX and OPEX subsidies in Europe. A summary of subsidies in selected Europe countries in 2022 is shown in Table 8 [41].

Table 8 Summary of CAPEX and OPEX subsidies in European countries for large heat pumps [41]

	Investment aid	Operating aid	Others	Comments
Czechia	V	Х	-	Investment aid for large-scale heat pumps in the heating industry is limited to one program within the Modernisation Fund, the HEAT program.
Denmark	y	х	CO2 taxation applying to the heat market and heat zoning	Investment aid is provided to operators to establish heat pumps or solar heating systems. District heating companies, where a minimum of 5% of the current heat production is based on coal, oil or natural gas, are eligible.
Estonia	V	X	-	Support will be continued under funding from EU structural funds to support fuel-switch, including large heat pumps.
Hungary	х	Х	-	No scheme dedicated to District Heating. The only incentives for heat pumps target small-size units in the form of a reduced price for electricity for end-users during the heating season.
Italy	Х	Х	-	There is an indirect mechanism linked to the white certificate schemes: the deployment of Efficient DHC systems can be rewarded with certificates proportionally to the amount of heat delivered to final customers, and heat pumps can be part of an efficient DHC system. But this aid is not sufficient to stimulate the market. According to calculations made by the Italian DH association, the aid would represent no more than 5% of total investment costs.
Finland	V	٧	CO2 taxation applying to the heat market	Investment support from July 2022, electricity to both heat pumps and electric boilers in district heating are included within tax class 2 (i.e. set to the EU minimum)
France	y	X	CO2 taxation applying to the heat market	The heat fund targets the development of renewable and waste heat projects, including Capex for DH deployment, and applies to large heat pumps projects.
Germany	V	V	a CO2 price signal on the heat market,	Both investment and operating aid (for thermal energy) are available under BEW, which aims to develop new DH schemes and upgrade existing ones, with a budget of Euro 3 billion until 2026. Operating aid is granted for the first 10 years of operation. Additionally, the iKWK (innovative CHP) provides operating aid for heat pumps in conjunction with CHP units.
Poland	V	X	-	Aid can be provided for heat pumps fuelled by renewable energy sources or in combination with CHP.
Norway	, v	Х	CO2 taxation applying to the heat market Fossil heating phase-out	
Sweden	V	X	CO2 tax applying to the heat market	Reduced energy tax for electricity used for heat pumps for district heat supplies to industry or cooling sold to large IT-infrastructure industries (i.e. data centres for the digital sector or other industries).

Figure 35 (in this figure . (dot) is used in difference to , (comma)) shows the specific investment costs of IHP according to different literatures. It is shown that the specific investment costs decrease with the heating capacity of the HP [10].

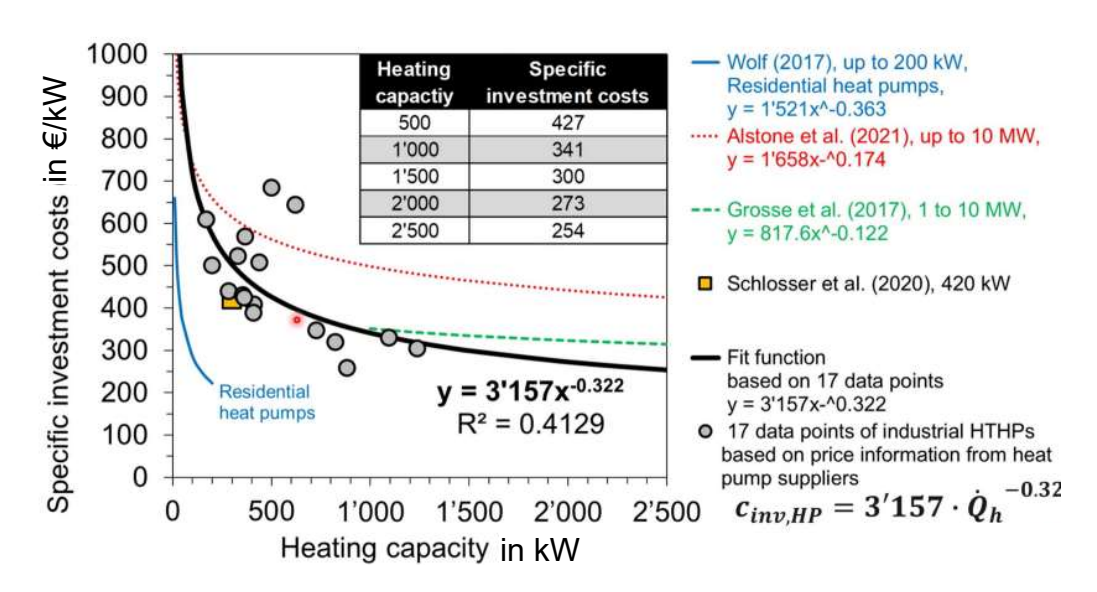


Figure 35 Specific investment costs of industrial HP according to different sources; in this figure . (dot) is used in difference to , (comma) [10]

This thesis uses a conservative specific investment cost of 700 €/kWp including subsidies, average costs for ancillary equipment, labour associated with the design and installation, and costs associated with the design and installation.

3.4 Carbon pricing in Europe

In Europe, greenhouse gas pricing distinguishes between industries with very high greenhouse gas emissions, which are priced directly via certificates, and all other emitters, which are priced indirectly via taxes for greenhouse gas emissions.

CO₂ of heavy industries

In 2005, a European Emissions Trading Scheme (EU-ETS) was introduced in the European Union (EU27), Norway, Iceland and Liechtenstein to implement the Kyoto international climate change agreement. The United Kingdom introduced its own national emissions trading scheme after its exclusion from the EU. The EU-ETS scheme includes > 10,000 plants in the energy sector and energy-intensive industries (oil refineries, steel mills and production facilities of iron, aluminum, metals, cement, unslaked lime, glass, ceramics, pulp, paper, cardboard, acids and basic organic chemicals, air and maritime transport), which are responsible for about 36% of greenhouse gas emissions in the specified countries. The target is to reduce emissions by > 55% until 2030 compared to 1990. Since 2012, intra-European aviation has also been included in the EU-ETS, which is not further referred in this thesis. The EU-ETS system is based on the "Cap & Trade" system in which emission allowances (CO2 certificates in CO_{2-ev}) are distributed or auctioned to the plants. Facilities can redeem them for released emissions or, if they are not needed, trade them on the market [42].

The allocation of CO₂ emissions depends on the current trading period. Between trading periods, prices are adjusted and regulations are adapted by means of amendments. The development of the trading periods is shown in Figure 36. As there was initially an oversupply of CO₂ - certificates on the market, which did not fulfill the purpose of climate protection, the market stability reserve was introduced. Its purpose is to regulate the supply and demand of certificates on the market and to ensure a future shortage. Details on the market stability reserve can be found at the following link (https://eur-lex.europa.eu/legal content/DE/TXT/PDF/?uri=CELEX:52014PC0020&from=EN).

The EU is currently in the fourth trading phase, in which significantly fewer allowances are available than in the previous trading periods, and in which the annual decrease is greater. According to "Fit for 55", the annual decrease in the cap is to be increased from 2,2 % to 4,2 % in order to achieve the climate targets. Detailed information on the fourth trading period are available at https://www.euromines.org/what-we-do/energyclimate-change/emissions-trading-system-phase-iv-2021-2030. Cap refers to the sum of all allowances that have always been higher than emissions (exception 2008) and are redistributed within the different installations through trading. In trading, a facility that does not need the allowances it has purchased or been awarded can sell them to other facilities. The link leads to the website of the European Energy Exchange (EEX) https://www.eex.com/de/maerkte/umweltprodukte/eu-ets-spot-futures-options [42].

Total cap and emissions in the ETS million tonnes of carbon dioxide equivalents

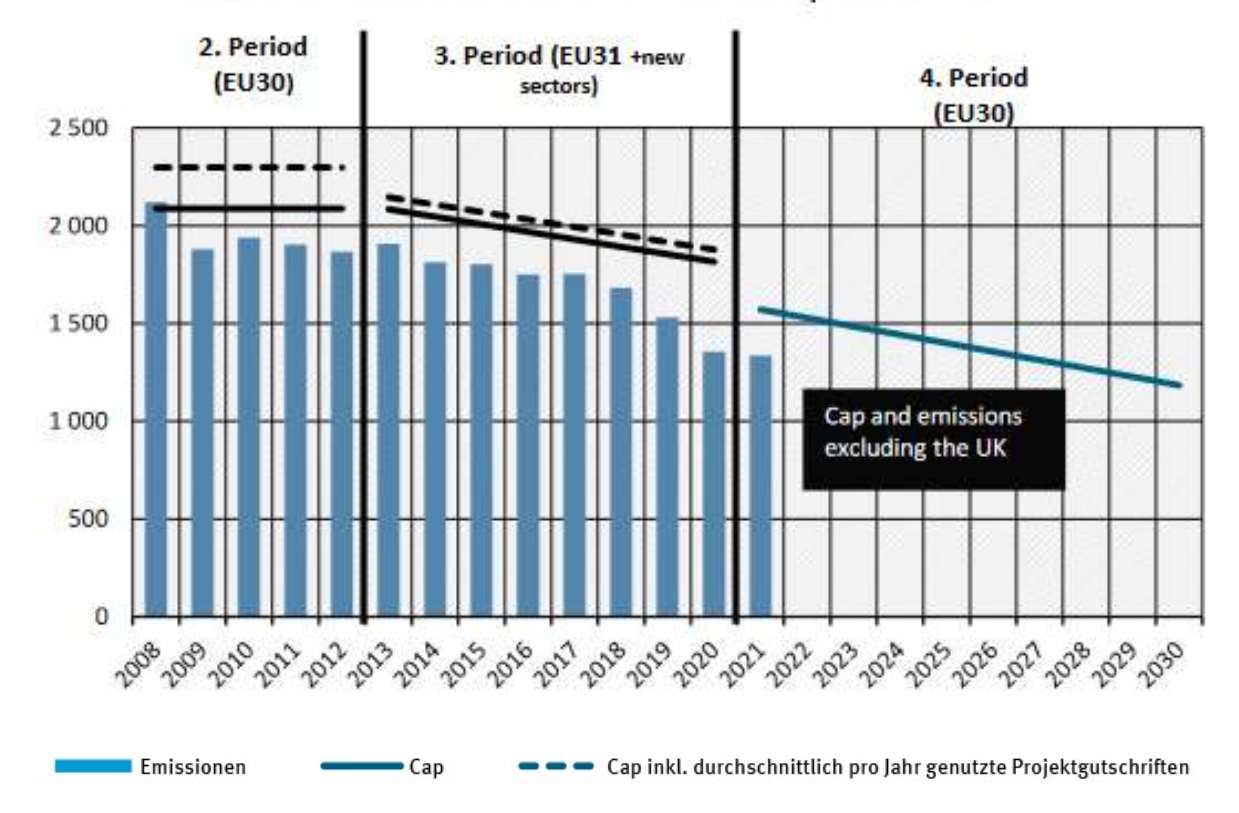


Figure 36 History of the total cap and the CO_{2-ev} emissions in Europe [42]



The fourth trading period provides allocation of free allowances only to industries that would otherwise no longer be competitive. The case where industries would relocate outside the EU due to the CO₂ price and thus only postpone their CO₂ emissions is referred to as carbon leakage (industries deemed to be at risk for carbon leakage can found be following the link https://eur-lex.europa.eu/legalcontent/EN/TXT/PDF/?uri=CELEX:32019D0708&from=EN). Industries with highest risk of relocating their production outside of the EU receive 100 % of their allocations for free, while less exposed sectors get a maximum of 30 %. All free allocations will be reduced beginning with 2026 giving the industries time to adjust. To ensure competitiveness of European industries energy intensive basic materials and products imported from outside the EU will be taxed equally to within the EU. This new method is called Carbon border adjustment mechanism (CBAM) and can be read in more detail following the link Carbon Border Adjustment Mechanism (CBAM) | Deloitte Germany. This regulation is currently still in draft status. A list of the European companies with allocations https://eur-lex.europa.eu/legalgranted can be found here content/DE/TXT/PDF/?uri=CELEX:32021D0728(01)&from=EN [42], [43], [44].

The falling cap lead to a shortage of CO₂ certificates in the medium term, which is why their price rise. Current model calculations assume prices between 90 - 130 €/t CO₂ in 2030. The price development of CO₂ certificates between 2008 and 2023 is shown in Figure 37 [43], [44].

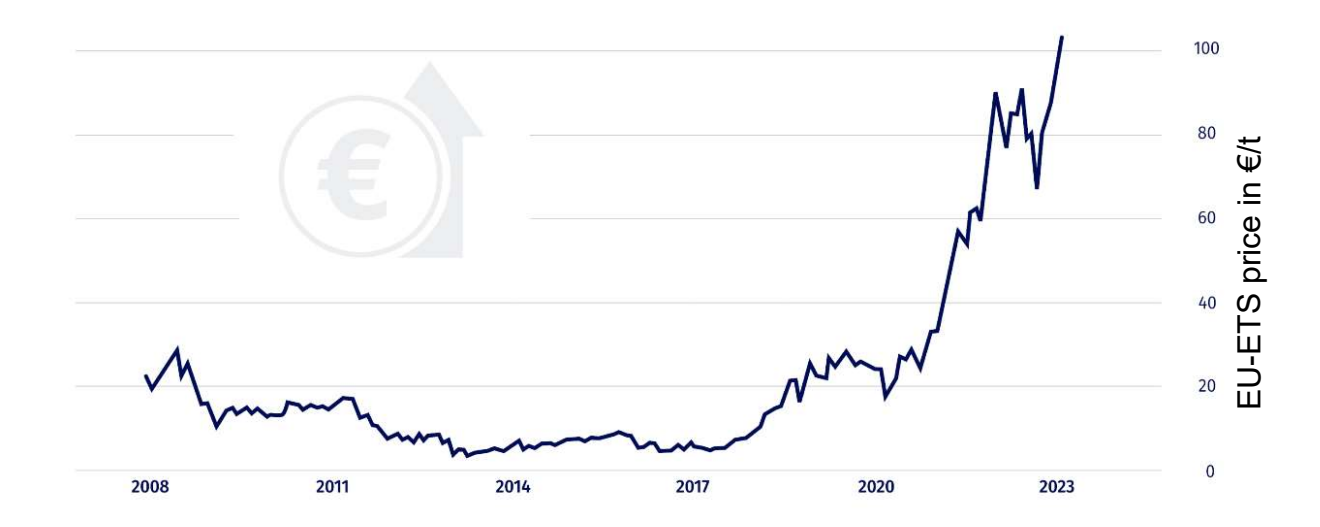


Figure 37 History of the CO₂-certificate prices between 2008 and 2023 in € / ton CO_{2-ev} [45]

In terms of corporate emissions, a distinction is made between Scope 1, 2 and 3 emissions, which are shown in Figure 38. Scope 1 emissions are generated in the plant itself, for example through the conversion of fossil fuels for the generation of thermal energy. Scope 2 emissions result from the purchase of electricity, thermal energy, or steam from other plants. Scope 3 emissions arise from the upstream extraction of raw materials, the supply chain, and any waste disposal [46].

Understanding Scope 1, 2 and 3 Emissions Graphic by Stacy Smedley, 2021

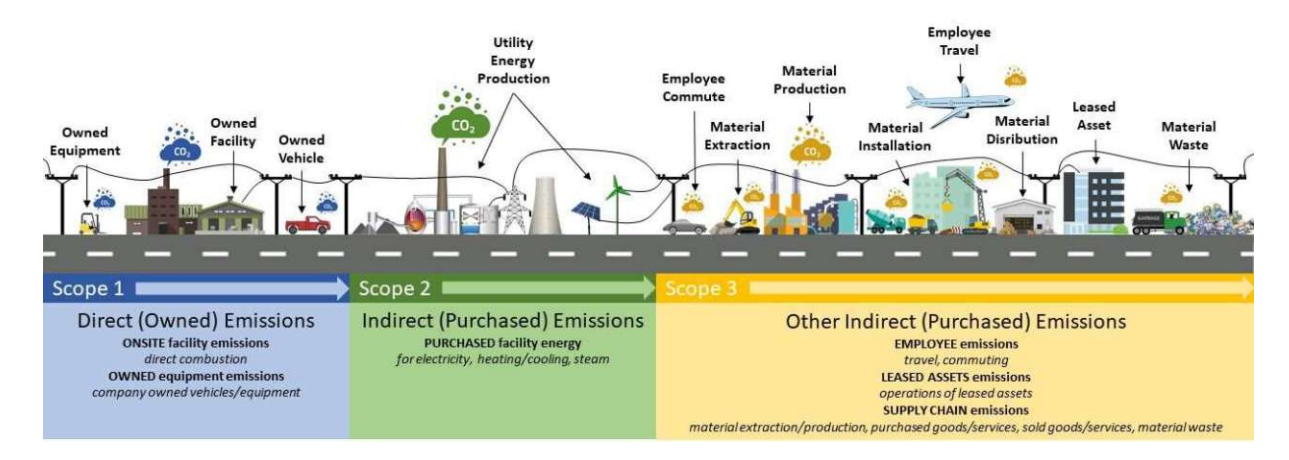


Figure 38 Visualization of Scope 1,2 and 3 Emissions [47]

Companies must cover their Scope 1 emissions with certificates. Scope 2 emissions are only paid indirectly. For example, if electricity is purchased externally for which CO₂ certificates have been paid, these certificate prices are added to the electricity price [48]. CO_{2-ev} emissions consider CO₂ emissions as well as other greenhouse gases with GWP > 0. CO_{2-ev} emissions of different fuels for the generation of thermal energy using modern technologies are shown in Table 9. The combustion technology used is relevant due to the efficiency of different plants. For example, for the generation of 1 kWh of thermal energy using NG 202 gCO_{2-ev} (fgas) need to be considered. The CO_{2-ev} of other fuels, as well as a calculation tool (Excel) for CO_{2-ev} emissions for thermal energy and electricity production can be found in [49]. Further CO_{2-ev} emissions can be found in [9].

Table 9 CO_{2-ev} emissions of different fuels according to the generation of 1 kWh of thermal energy [49], [50]

Fuel	Scope 1 Emissions g CO ₂ . _{ev} /kWh	Scope 2 & 3 Emissions g CO _{2-ev} /kWh	total Emissions g CO ₂ . _{ev} /kWh
Pellets	0	25	25
Wood chips	1	26	27
Wood ¹⁾			368
Lignite	369	58	427
Peat			367

Hard coal	349	52	401
light heating oil	267	51	318
Liquefied natural gas			260
Natural gas	202	45	247

1) with not-sustainable use without reforestation

CO₂ Emissions of other sources

In addition to the EU-ETS system, further mechanism (EU-ETS 2) is introduced to take account of sectors outside the ETS, such as transport, housing, waste, and agriculture. Taking Austria as an example, 48 % of the national CO_{2-ev} is emitted in these sectors. This further mechanism will be determined via the national climate protection law and the burden sharing ordinance. Currently, the emissions of these sectors are indirectly priced via taxes. Decisive for the tax burden are the nationally determined CO2 prices of the different countries. These are shown for European countries (2021) in Figure 39. The chart also shows the years in which the CO₂ tax was introduced. It can be seen large national differences within the EU [45], [51].

Nationale CO2-Preise in der EU

in Euro pro Tonne CO2

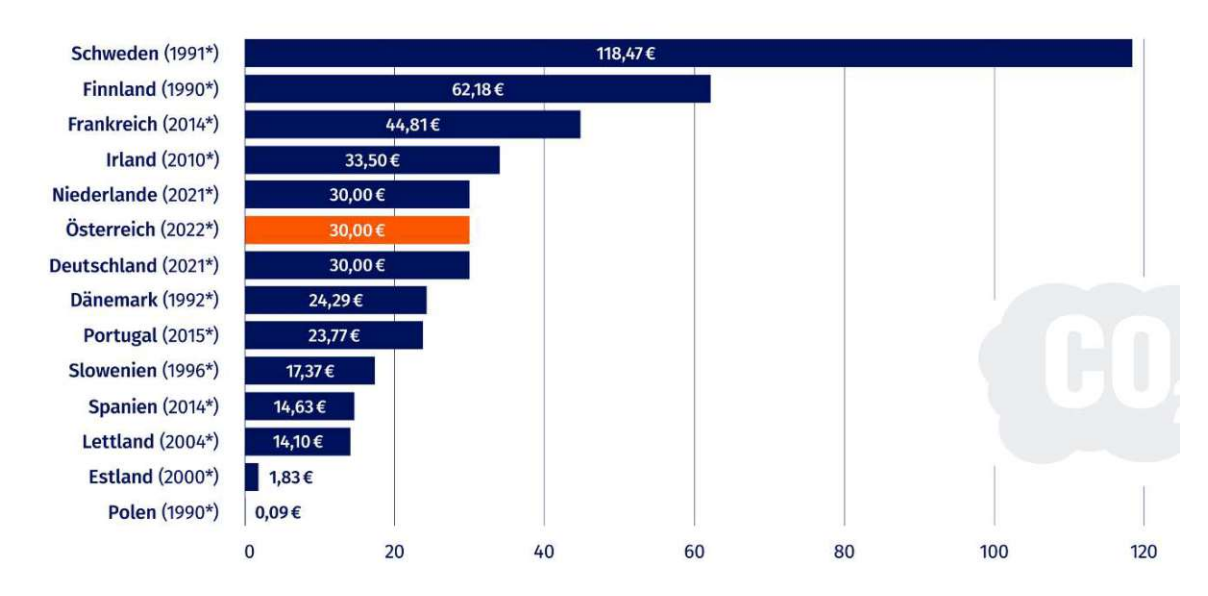


Figure 39 CO₂ prices of EU countries in 2021 and the beginning year of CO₂ taxation [45]

The CO₂ price is to be increased annually to give the different sectors time to adjust, but to create an incentive for savings. Table 10 shows the adjustment of the CO₂ price using Austria as an example [51].

Table 10 CO₂ tax trend of Austria, Anm. 1.: for 2023 taxes of 32,5 € where applied [51]

Kalenderjahr	Betrag
2022	30 Euro
2023	35 Euro(Anm. 1)
2024	45 Euro
2025	55 Euro

This indirect pricing is to be gradually converted into an emissions certificate trading system in Europe by 2027, based on the EU-ETS system [51].

Table 11 shows a comparison between the national CO₂ pricing (example for Germany) and the EU ETS system [45], [51].

Table 11 Comparison between national CO₂ prices (example Germany) and the EU ETS System [45], [51]

	BEHG	EU ETS	
Zielgruppe	– Alle Anlagen die Treibhausgase ausstoßen	 Feuerungsanlagen mit >20 MW Leistung und Produktionsanlagen energie-intensiver Branchen 	
Anzahl der <mark>Zertifikate</mark>	- Unbegrenzt	– Begrenzt (1,8 Milliarden für 2021)	
Ausnahmen	- Bereits von EU ETS betroffene Anlagen - In Wettbewerbsfähigkeit eingeschränkte Unternehmen	Zertifikatspreissensible Branch (Carbon Leakage)	
Zeitpunkt der Fälligkeit	- Bei Brennstoffbezug	- Bei Brennstoffeinsatz / Ausstoß Treibhausgas	

3.4.2 Carbon price trend and influence on the power to gas ratio

Figure 40 shows on the top the electricity prices and on the bottom the gas prices of selected European countries in €/kWh. The prices have three components. Prices excluding all taxes and fees (blue) is the price of the energy, supply component and the network component. Value added tax (VAT) and other recoverable taxes and levies (yellow) includes all recoverable taxes, fees and charges (including VAT). Rest of taxes includes all taxes, fees, levies and charges (brown) that are declared as nonrecoverable like carbon taxes. The resulting price for non-household consumers are the sum of all three bars. Countries with higher carbon taxes do have bigger brown bars at the gas prices. Comparing different countries show, why the power to gas ratio

is even high or low. For example, Sweden has very low electricity prices, but very high NG prices [38]. In [38] is an interactive tool for power and gas prices for European countries and different years, customers, and consumption levels.

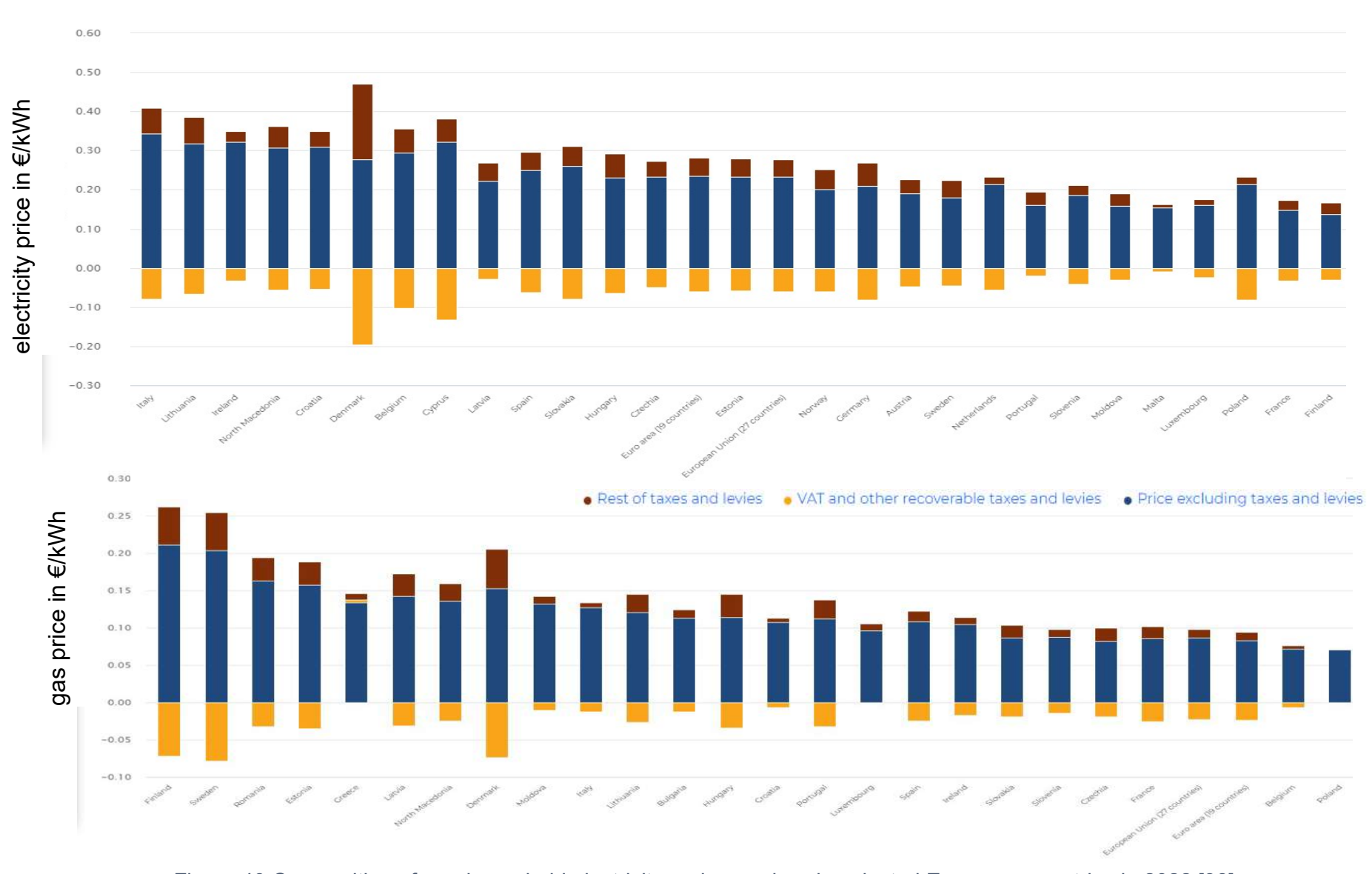


Figure 40 Composition of non-household electricity and gas prices in selected European countries in 2022 [38]

Figure 41 show the EU-ETS trend between 2023 and 2060 predicted by Energy Brainpool. According to Brainpool the EU-ETS price will skyrocket between 2028 and 2032 to 125 €/t and then increase decelerating to 177 €/t in 2060 [34].

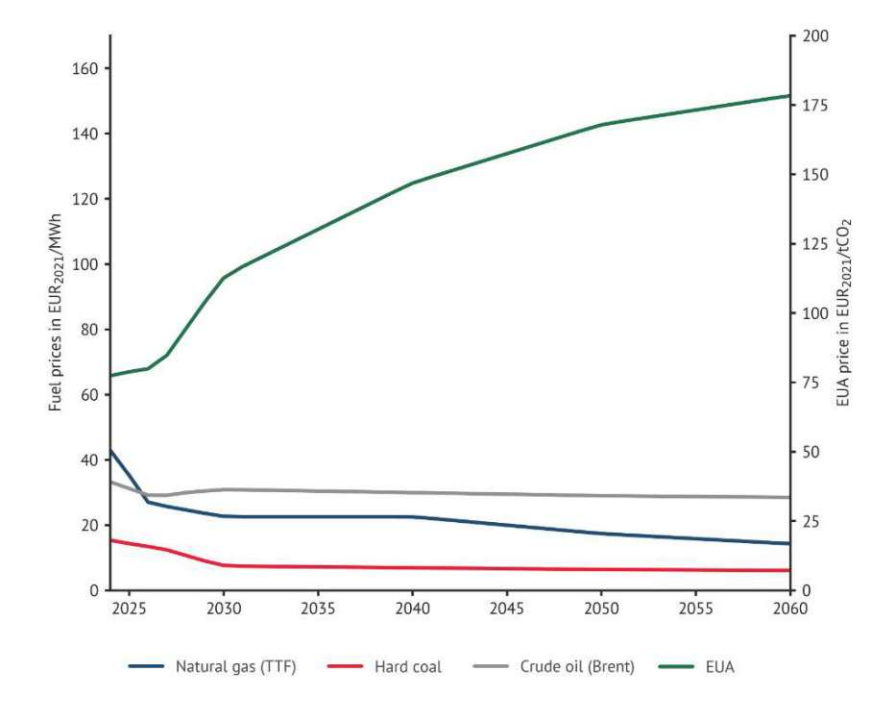


Figure 41 Future trend of the EU-ETS price in the Energy Brainpool scenario [34]

Table 12 show predicted trends of ETS prices in different regions based on different scenarios [37].

Table 12 Carbon price for certificates in selected areas based on different scenarios [37]

USD (2021) per tonne of CO ₁	2030	2040	2050
Stated Policies Scenario			
Canada	54	62	77
Chile, Colombia	13	21	29
China	28	43	53
European Union	90	98	113
Korea	42	67	89
Announced Pledges Scenario			
Advanced economies with net zero emissions pledges ¹	135	175	200
Emerging market and developing economies with net zero emissions pledges ²	40	110	160
Other emerging market and developing economies	0 0 0	17	47
Net Zero Emissions by 2050 Scenario			
Advanced economies with net zero emissions pledges	140	205	250
Emerging market and developing economies with net zero emissions pledges	90	160	200
Other emerging market and developing economies	25	85	180

Note: Values are rounded.

¹ Includes all OECD countries except Mexico.

² Includes China, India, Indonesia, Brazil and South Africa.

Figure 42 also shows the scenario with a constant EU-ETS price of 113 USD/t considering that carbon capture and storage is economical feasible at that price [2], [34], [37].

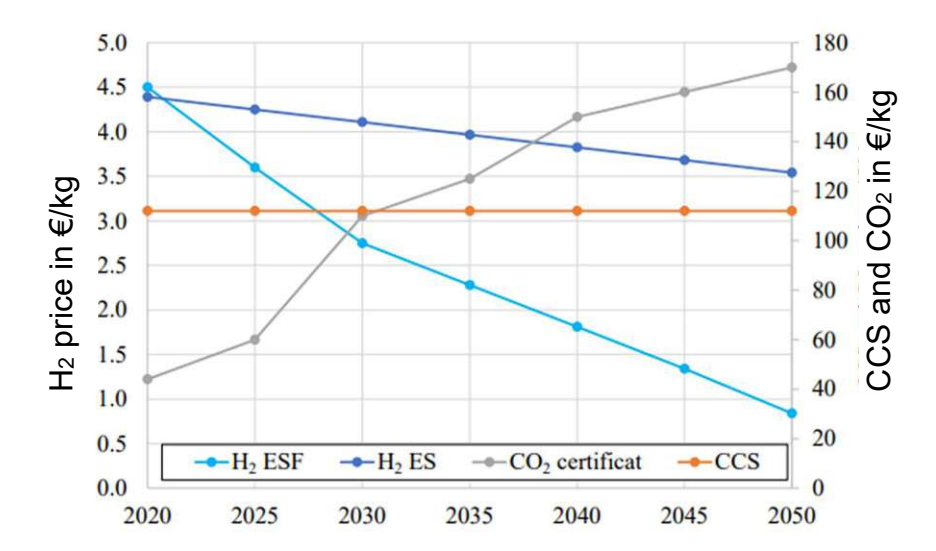


Figure 42 EU-ETS price trend in a hydrogen scenario [2]

This thesis will use an EU-ETS price of 113 €/t (C_{CO2}) assuming that carbon capture and storage will become technological and economical feasible. Furthermore, with this assumption the early future with more solid price forecasts is weighted more than more distant time periods.

3.5 Summary economic parameters

Table 13 shows a summary of the most important parameters of the reference scenario (gas boiler) and the HP scenario for later economic efficiency calculations [2], [32], [34], [37], [40].

Table 13 Summary of gas boiler and HP parameters for later economic calculations [2], [32], [34], [37], [40]

	Variable	Value	Unit
reference scenario	η _{gas boiler}	0,9	-
	C _{natural gas}	0,025	€/kWh
	f _{natural gas}	202	g/kWh
	C _{CO2}	113	€/t
	CAPEX _{gas boiler}	150	€/kW
HP scenario	C _{electricity}	0,075	€/kWh
	COP	case depending	-
	CAPEX _{HP}	700	€/kW
interest rate	i	3	%
full load hour	FLH	case depending	h/yr



3.6 Contracting model

As mentioned before is the industry looking for short payback periods. Because of the more CAPEX intensive renewable solutions, the industries tendency to switch to OPEX based energy contracts can be seen [10], [26], [31], [32].

An example for such a OPEX based energy contract is shown in Figure 43. Figure 43 is based on a COP of 4 and depicts the costs for thermal energy as a function of the FLH and the electricity price. For the further calculations 4000 - 6000 FLH and an average price for electricity is assumed to be 0 €/MWh (self-production with photovoltaic cells) to 200 €/MWh. Therefore, the specific heating costs of the HP result in 24 - 86 €/MWh. Such contracts usually include more details like heat purchase commitments, maturities, and others [22].

OPEX SALES MODEL, indicative prices	cost of heat excl. electricity	cost of heat incl. electricity	cost of heat incl. electricity	cost of heat incl. electricity
electricity price	•	100 EUR/MWh	200 EUR/MWh	300 EUR/MWh
2.500 FLH	58	83	108	133
4.000 FLH	36	61	86	111
6.000 FLH	24	49	74	99
8.000 FLH	18	43	68	93

Indicative costs of HEAT in EUR pro MWh Costs of implementation are paid by the customer

Figure 43 Exemplary OPEX sales model for thermal energy [22]

3.7 Definition of market potential

In this section it is briefly the difference between different kinds of potentials defined. In general, it is differentiated between the resource potential, technical potential, economic potential, and the market potential pictured in Figure 44 [40].

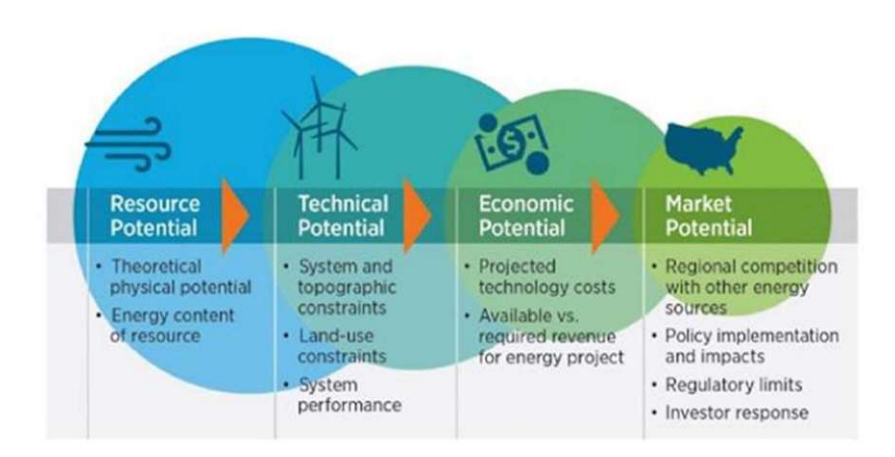


Figure 44 Different kinds of potential and what they include [40]

The resource potential considers the theoretical potential of a technology with its physical and technical boundaries. For instance, is it possible that HP can provide temperatures greater than 200 °C in the future [40].

The technical potential includes all technical feasible solutions in the market no matter if they are economical feasible or not. That would mean in the HP sector, that any waste heat source would be utilized by a HP [40].

The economic potential is the share of the of the technical potential that is economical feasible [40].

The market potential includes future decision and developments of the market, which can speed up or stop the trend. The market potential is the economic potential including future changes [40].

In this thesis the economic / market potential is analyzed. The methodology to do so is to determine the economic potential as fraction of the technical potential. By incorporating future changes in key economic parameters, the economic potential is translated into the market potential. These key economic parameters are HP CAPEX, subsidies, CO2 prices, electricity prices and gas prices, which were analyzed in the previous chapters [40].

Market segments and potential

Thermal energy has become one of humanities basic needs since humans learned to use fire about 40 000 years ago. Around 40 % of the global final energy demand (~ 10 billion tonnes of oil equivalent (Btoe) = 4,652 * 10⁴ TWh/yr) accounts for the industry (see Figure 45). 55% of the industries energy demand is thermal energy being provided by around 75 % with fossil fuels. A significant amount of the needed thermal energy is below 200 °C. This temperature level is often provided by burning NG reaching 2 000 °C leading to high exergy losses. To minimize these exergy losses this

thesis focuses if, where and how HP can provide temperatures up to 200 °C in the industry [1].

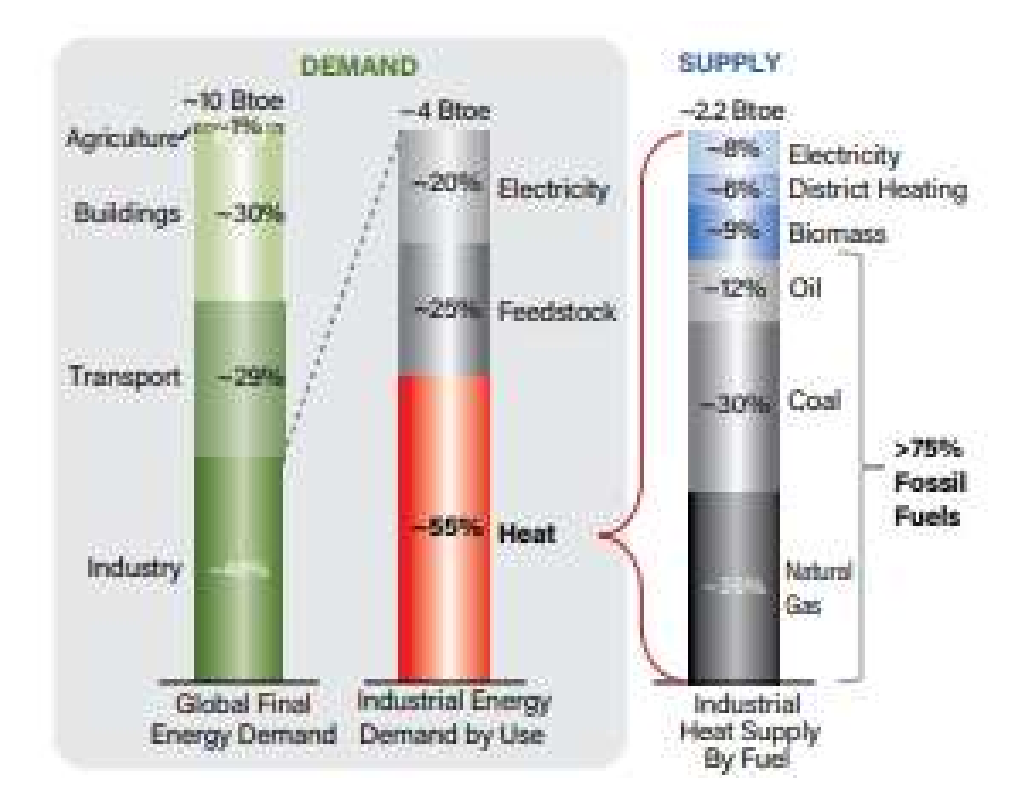


Figure 45 The share of the industrial thermal energy demand in the global energy demand and the primary energy sources, 1 Btoe = 1,163 * 10⁴ TWh [1]

Industry

In this section the potential of IHP in Europe will be outlined. Figure 46 is based on data of Eurostat, which compares the thermal energy end-use of 33 countries within Europe. The total amount of thermal energy consumption in Europe are roughly 3000 TWh/yr (7200 PJ/yr). According to Figure 46, 66 % (~2000 TWh/yr) of this thermal energy is used as process heat. 77 % of the process heat is provided by burning fossil fuels. In the next step it is differed between temperature levels, industries and how this energy is currently provided [4].

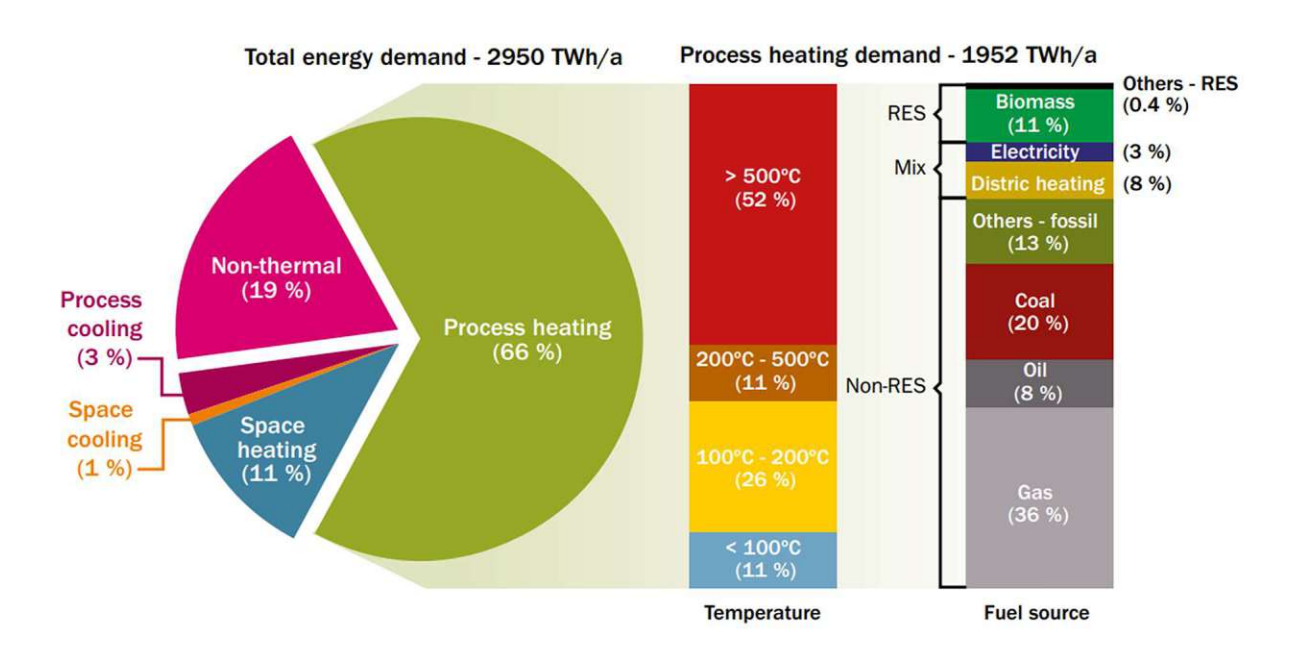


Figure 46 Breakdown of the total thermal energy demand in Europe (RES = renewable energy sources), "a" means anno and stands for year [4]

Table 14 (in this table . (dot) is used in difference to , (comma)) shows the industries thermal energy demand at different temperature levels in the EU28+3. In the range of 100 – 200 °C the thermal energy demand is 531,2 TWh/yr. The greatest potential in this temperature range is in Germany, Italy, UK, France, Finland, Spain, and Sweden [8], [9], [52].

Table 14 Process and space heat / cooling demand in the EU28+3 countries in TWh/yr; (in this table . (dot) is used in difference to , (comma)) [8], [9], [52]

TWh	PH <100°C	PH 100- 200°C	PH 200- 500°C	PH >500°C	SH	Total heating	Cooling		PH <100°C	PH 100- 200°C	PH 200- 500°C	PH >500°C	SH	Total heating	Cooling
Austria	3.3	22.0	5.3	35.5	13.4	79.4	1.9	Latvia	0.5	3.0	1.0	2.2	1.4	8.2	0.1
Belgium	7.1	14.8	6.7	42.4	13.9	84.8	4.5	Lithuania	2.7	1.7	0.6	2.2	1.7	8.8	0.3
Bulgaria	5.1	3.5	1.5	6.9	5.4	22.5	1.0	Luxembourg	0.1	0.5	0.7	3.9	0.6	5.7	0.1
Croatia	1.4	2.9	1.1	3.6	1.3	10.3	0.4	Malta	0.0	0.0	0.0	0.0	0.0	0.1	0.0
Cyprus	0.1	0.2	0.2	0.9	0.1	1.5	0.1	Netherlands	17.4	21.1	7.6	66.5	14.9	127.6	5.8
Czech Rep.	7.7	13.1	5.5	30.3	9.4	66.0	2.3	Norway	0.5	5.0	1.1	14.8	5.6	27.0	1.5
Denmark	3.1	5.6	1.8	4.3	3.5	18.4	1.2	Poland	15.4	29.5	10.7	62.0	10.0	127.6	4.9
Estonia	0.4	1.3	0.4	0.9	1.6	4.5	0.2	Portugal	4.0	15.0	2.5	13.1	6.7	41.4	1.7
Finland	16.1	45.7	5.3	15.6	6.2	89.0	2.2	Romania	4.0	8.5	4.0	33.1	10.4	60.0	1.4
France	8.6	38.5	15.8	97.7	46.8	207.3	11.3	Slovakia	1.7	4.0	0.9	26.7	6.1	39.4	0.9
Germany	64.3	92.1	34.6	251.1	58.3	500.3	18.5	Slovenia	0.6	2.2	0.5	3.6	1.7	8.6	0.2
Greece	2.7	5.6	2.0	9.7	4.2	24.2	1.4	Spain	4.4	45.3	14.5	82.3	31.4	177.8	9.9
Hungary	3.8	2.3	1.1	9.3	4.7	21.2	0.8	Sweden	4.9	49.6	7.0	15.4	7.6	84.4	1.5
Iceland	0.1	0.1	0.0	1.5	0.4	2.2	0.3	Switzerland	2.8	6.1	2.2	9.6	2.0	22.7	1.0
Ireland	1.4	4.5	1.7	5.3	3.9	16.8	1.0	United Kingdom	16.4	61.0	22.1	66.3	25.6	191.3	6.6
Italy	27.9	26.5	16.6	117.7	47.7	236.4	14.9	EU28+3	228.1	531.2	175.3	1034.6	346.3	2315.6	98.0

Table 15 shows the EU28 usage of thermal energy in different industries at variable temperatures. The total thermal energy consumption in the EU28 industry is 1 821 TWh/yr. The currently by IHP addressable temperatures of 80 – 150 °C result in 281 TWh/yr (16 %). 80 TWh/yr of thermal energy are in the range between 150 – 200 °C.

In specific the industrial sectors iron and steel, chemical, non-metallic minerals, food and tobacco, and paper, pulp and print have a particularly high demand for the accounted temperature level of IHP [7], [11], [53]

There is also a broad range of low temperature applications (< 80 °C). The most common are space heating, general heating uses or district heating [7], [11], [53]

Table 15 Thermal energy consumption at temperature levels in EU28 industry [11]

	Heat Consumption (TWh/a)	EU-28	
	Space heating	297	16%
	Hot water	25	1%
	PH <60 °C	55	3%
_	PH 60 to 80 °C	53	3%
lea	PH 80 to 100 °C	89	5%
S	PH 100 to 150 °C	192	11%
Process heat	PH 150 to 200 °C	80	4%
2	PH 200 to 500 °C	151	8%
_	PH 500 to 1'000 °C	376	21%
	PH >1'000 °C	504	28%
	Total Heat Consumption (TWh/year)	1'821	100%
	Total Process Heat <60 °C to >1'000 °C (TWh/year)	1'499	
	Total Process Heat 90 °C to 160 °C (TWh/year)	237	16%

Process Heat Consumption (TWh/a)						
Industrial sector	PH 100 to 150 °C P	H 150 to 200 °C				
Iron and steel	19.8	7.3				
Chemical	19.3	15.4				
Non-ferrous metal	2.7	1.0				
Non-metallic minerals	36.5	0.0				
Food and tobacco	68.0	8.8				
Paper, pulp and print	10.0	39.4				
Machinery	6.9	2.9				
Wood and wood products	0.2	0.7				
Transport equipment	1.2	0.2				
Textile and leather	6.9	0.0				
Other	19.1	4.2				
Total	191	80				

The industries as well as the temperature levels coverable by IHP are visualized in Figure 47. According to [11] 174 TWh/yr of the EU28 process heat demand are coverable by IHP. 41 % (71,3 TWh/yr) of this thermal energy is in the temperature range between 80 - 150 °C. Figure 47 shows food and tobacco, chemical and paper as the most interesting industrial sectors for IHP [11], [40].

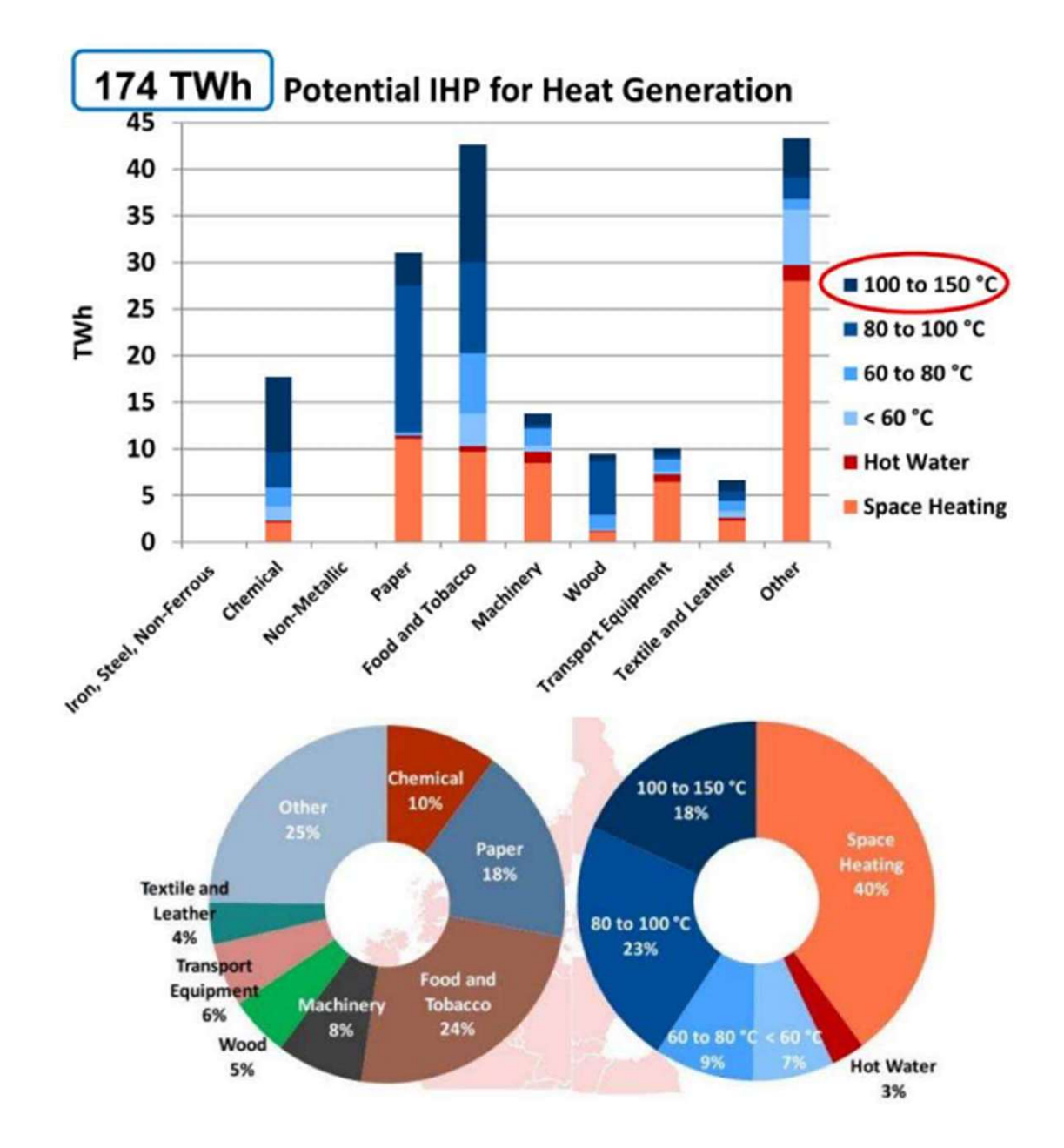


Figure 47 Market potential of IHP in EU28 based on industries and temperature levels [11]

The studies [9] and [52] also investigated the pulp and paper, chemical, food and beverages and refinery sector as the most promising ones for the use of IHP. They estimated the IHP suited thermal energy potential among these industries for < 150 °C to ~750 PJ (208 TWh/yr) and < 200 °C to ~1100 PJ (306 TWh/yr). Table 16 shows the IHP coverable thermal energy demand among these industries. The term coverable means that in the given industries suitable processes were identifying under the perspective of the simultaneous availability of suited waste heat [8], [9], [52].

A switch from fossil fuels to HP (< 200 °C applications) in the four mentioned industries would lead to CO_{2-ev} savings of 146 Mt/yr [4].

Table 16 Cumulative IHP suited process and waste heat in EU28 in the defined temperature intervals [9]

Sector	<15	0°C	<200°C		
	Process Heat Q _P (PJ/a)	Waste Heat Qw (PJ/a)	Process Heat Q _P (PJ/a)	Waste Heat Qw (PJ/a)	
Paper	228	231	356	231	
Chemical	295	320	355	337	
Food	130	96	193	97	
Refinery	92	393	219	465	
Total (Σ)	745	1039	1123	1130	

Figure 48 shows the cumulative waste and process heat suited for HP < 200 °C depending on the temperature level of the four named industrial sectors. The heat pump has the duty to utilize the low temperature waste heat (mainly moist air and condensate streams) to provide the process heat at higher temperatures [9].

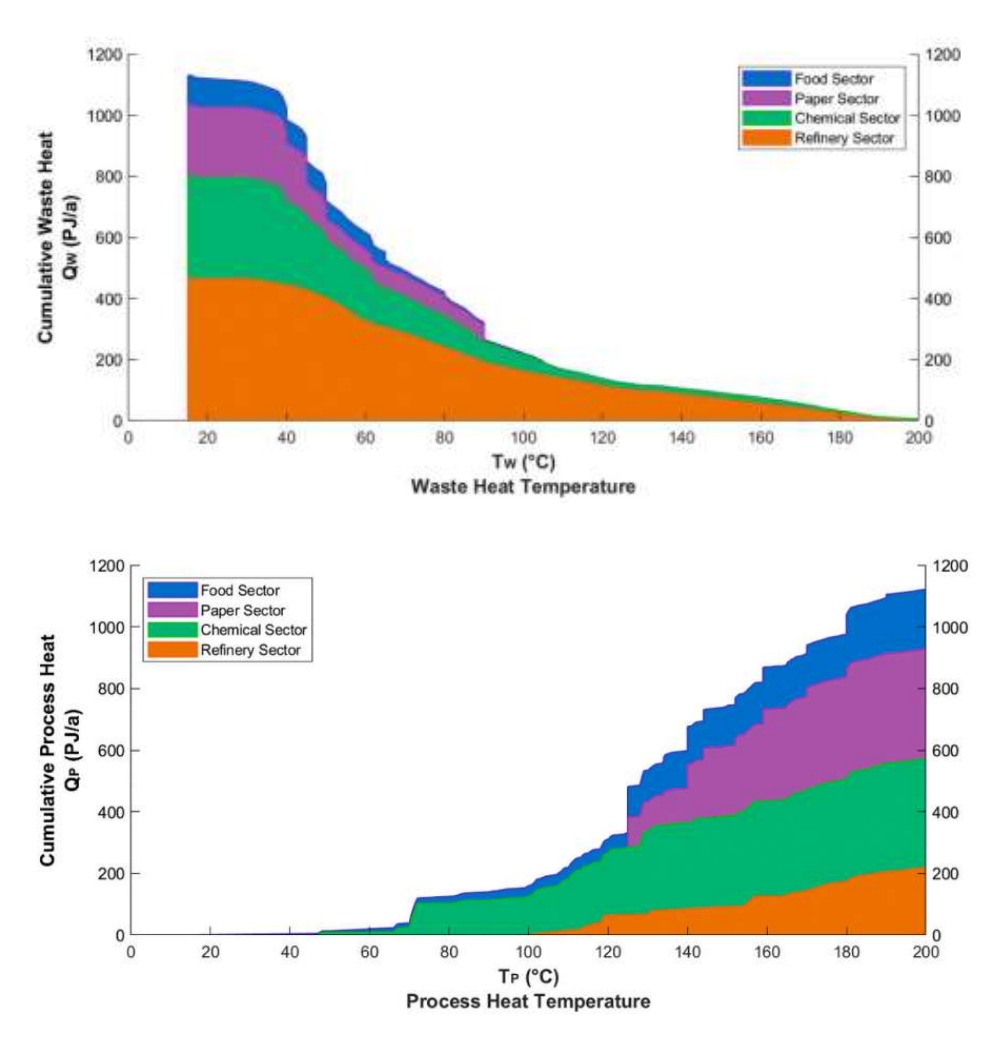


Figure 48 Cumulative waste (top) and process (bottom) heat below 200 °C in the four investigated sectors in the EU28 [9]

Because of some technical reasons such as a limitation of the temperature lift of heat pumps to 100 K or missing waste heat sources just 73 % of the process heat < 150 °C and 57 % < 200 °C can be supplied by industrial heat pumps. The study calculated that 20 GW are needed to provide the process heat < 150 °C and additional 3 GW to cover process heat up to 200 °C. According to the study 4 174 heat pump units ranging from < 0,5 MW to > 30 MW are necessary to provide the suited process heat (641 PJ/a). Detailed information about the relative achievable process heat coverage by industrial heat pumps can be found in Table 17 (in this table . (dot) is used as decimal point instead of a, (comma) [9].

Table 17 Heat pump units per sector and relative process heat coverage; in this table . (dot) is used as decimal point instead of a , (comma) [9] Summary of the EU28 industrial heat pump market potential.

Seite | 54

Heat pump m	arket to 150°C				
Sector	Cumulative Heating Capacity, Q _{P.HPmarket} (GW)	EU28 Heat Pump Units, NitPatarket (#)	Heat Pump Process Heat Coverage, Qr. HPmarket (PJ/a)	Electricity Requirement, E _{r,HPmurket} (PJ/a)	Heat Pump Relative Process Heat Coverage, Q _{P,HPmarket} /Q _P (%)
Paper	6.6	938	203	78	89%
Chemical	8.1	1164	252	59	85%
Food	5.0	1107	83	25	64%
Refinery	0.3	20	9	4	10%
Total (Σ)	20.0	3229	547	166	73%
Heat pump <mark>m</mark>	arket to 200 C				
Sector	Cumulative Heating Capacity, Qr. HPmarket (GW)	EU28 Heat Pump Units, NHPmarket (#)	Heat Pump Process Heat Coverage, Qp.HPmarket (PJ/a)	Electricity Requirement, E _{e HPmarket} (PJ/a)	Heat Pump Relative Process Heat Coverage, QP.HPmurket/QP (%)
San San San	22000	1000	202	74/40	10000
Paper	7.9	1351	245	94	69%
Chemical	9.1	1291	283	65	80%
Food	5.5	1463	98	31	51%
Refinery	0.5	69	14	6	6%
Total (Σ)	23.0	4174	641	195	57%

Figure 49 (in this figure . (dot) is used as decimal point instead of a , (comma)) shows detailed information about the 4 174 calculated heat pump units. On the left side the operating temperatures and the unit size is visualized. The right side shows the distribution of the expected coefficient of performance. In general, high heating capacities do not lead directly to high temperature levels and vicar versa [9].

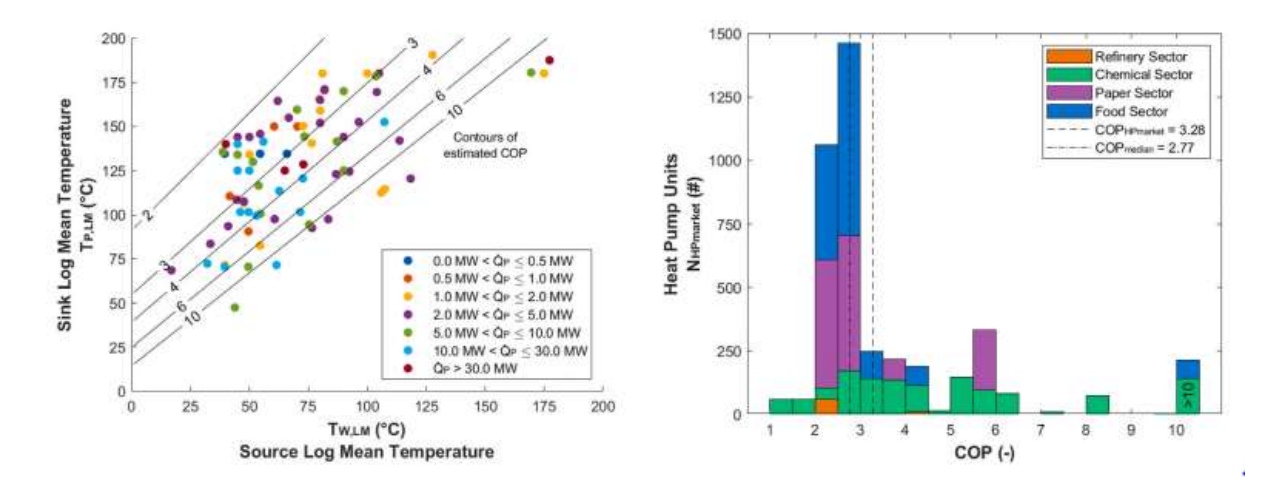


Figure 49 Specification of the 4 174 heat pump units in the EU28: (left) by power and sink/source temperature, (right) by calculated COP; in this figure . (dot) is used as decimal point instead of a, (comma) [9]

Figure 50 (in this figure . (dot) is used as decimal point instead of a , (comma)) shows a more detailed visualization of the 4 174 heat pump units. The upper part shows the number of calculated heat pump units depending on the heating capacity. Around 88 % of the heat pump units are below 10 MW. The bottom show that around half of the heating capacity can be provided by units smaller than 10 MW and the rest are units greater than 10 MW [9].

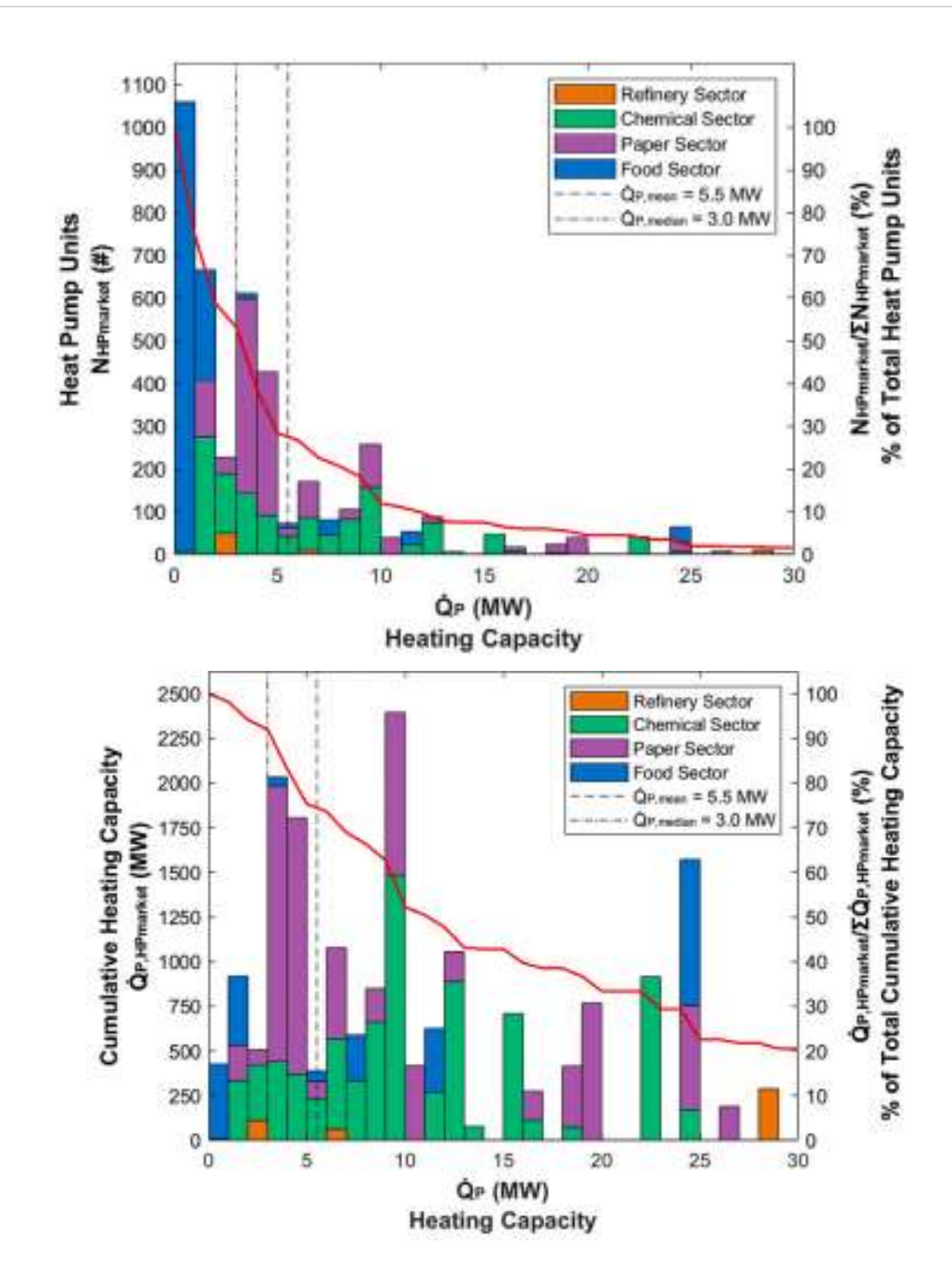


Figure 50 HP units and relative HP units (top) related to the cumulative heating capacity and relative heating capacity (% of total cumulative heating capacity) (bottom) depending on the heating capacity per unit; in this figure . (dot) is used as decimal point instead of a , (comma) [9]

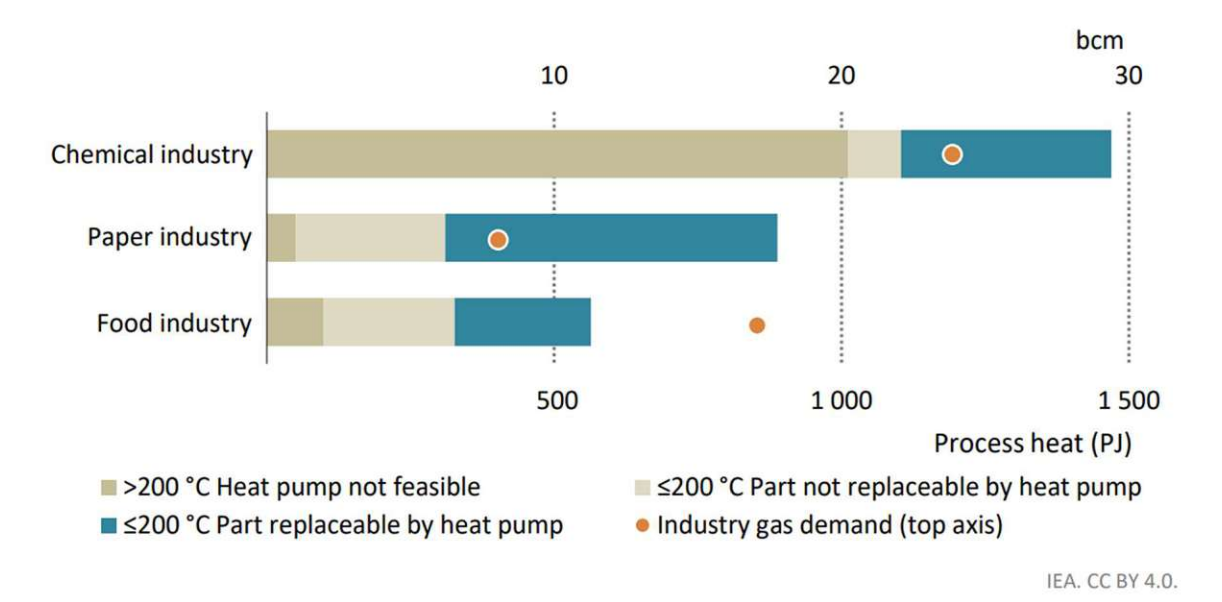
The needed investment to realize the discussed industrial heat pump market with unit costs ranging from 200 – 500 €/kW result in 4,5 – 11,5 billion €. The study names these values as conservative calculations. The investment costs per sector are shown in Table 18 (in this table . (dot) is used as decimal point instead of a , (comma)) [9].

Table 18 Needed investment to realize the European IHP market with unit costs between 200 – 500 €/kW; in this table . (dot) is used as decimal point instead of a , (comma) [9]

Sector	Cumulative Heating Capacity, Q _{P.HPmarket} (GW)	Lower Bound Investment (G€)	Upper Bound Investment (G€)
Paper	7.9	1.58	3.95
Chemical	9.1	1.82	4.55
Food	5.5	1.10	2.75
Refinery	0.5	0.10	0.25
Total (Σ)	23.0	4.60	11.50

The key message of [9] is that there are many relatively small units (88 % of total HP units) providing around 50 % of the heat capacity. To provide solutions for the whole industries manufacturer should provide small standardize machines in high numbers and very big, customized machines depending on the needed use case [9].

Also [7] investigated the paper, food and chemical industries as the most promising ones for HP. Figure 51 shows the 2019, process heat (in PJ) and gas (in bcm = billion cubic meters) demand of paper, food and chemical industry in Europe. The figure divides the process heat demand in the three categories HP not feasible, not replaceable by HP and partly replaceable by HP. The greatest HP potential is in the paper industry. The highest NG consumer is the chemical industry [53].



The food and paper industries are prime candidates for deploying industrial heat pumps on a large scale, helping to reduce energy use, gas demand and emissions

Notes: PJ = petajoules. Europe = European Union and the United Kingdom.

Sources: IEA analysis based on European Commission (2016) and Marina et al. (2021). Feasibility based on TRLs from Table 1.2.

Figure 51 Industrial gas and process heat demand by temperature level and HP replacement potential in Europe 2019, 1 bcm = 10 TWh [7]

Comparing the different studies, one can see that they do not agree on what is coverable by HP. Variable assumptions and border conditions lead to different results. The usefulness of integrating an IHP into an industrial process must be examined in detail in each individual case.

Figure 52 shows exemplary industrial processes different HP technologies can provide depending on the temperature level. Exemplary applications in the food industry are steam production for sterilization, concentration, boiling, baking, vaporization, and pasteurization processes. Furthermore, hot water is used during the bottling process (washing and sterilization), and the brewing process (mashing, lautering, wort boiling). But also, in the polyethylenterephthalat (PET) bottle industry process heat between 100 – 150 °C is needed for injection molding of plastic preforms or pellets drying. There are several drying processes, which need < 150 °C such as starch drying, wood drying, paper drying, laundry drying, brick drying (air preheating), drying of animal fodder and others. In the chemical industry steam and hot water is needed for distillation, concentration, boiling and thermoforming processes. The wood sector needs temperatures greater than 100 °C for gluing, pressing and drying processes. The textile industry works in the processes of coloring, washing, and bleaching above 100 °C [7], [53].

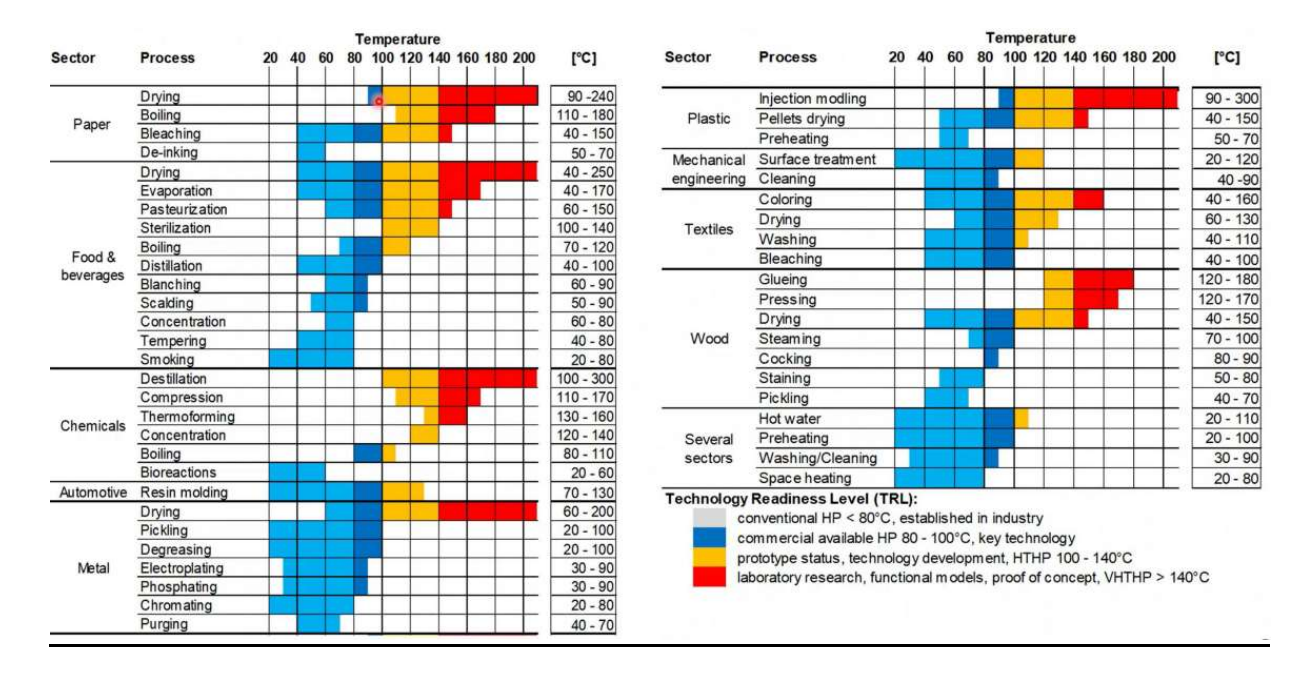


Figure 52 Typical processes in given industries and their temperature level [53]

HP applications without thermal buffer storages are limited by the simultaneous need for heat demand and waste heat availability. Table 19 shows typical excess heat streams and their temperature level [54].

Table 19 Industrial excess heat and their typical temperature levels by [54]

Excess heat source	temperatur level in °C
Flue gas	50 - 400
Cooling fluids	20 - 45
Compressor cooling	30 - 70
Washing fluids	30 - 60
Cooking processes	< 100
Power unit cooling	< 100
injection molding	20 - 80

Summarizing the European market potential, it can be said that roughly 3000 TWh/yr of thermal energy are used in the industry and around 600 TWh/yr are < 200 °C. 200 - 300 TWh/yr are estimated to be suited for IHP due to the availability of suited waste heat sources. To cover the lower bound of 200 TWh/yr around 23 GW of thermal power are necessary. Around 50 % of the plants are < 10 MW leading to an economical potential of 16 428 ecop RHP having each a thermal power of 0,7 MW [4], [8], [9], [11], [40], [52].

District heating

DH is growing massively all over the world. Most of the thermal energy in DH is provided by fossil fuels. There are different generations of DH networks, which mainly vary in their temperature and pressure level as well as the transportation medium. Figure 53 gives an overview of the different DH generations and their different thermal energy sources. The integration of HP in DH systems of the third and fourth generation is useful because of the lower temperature level. Combinations between renewable energy sources and HP are used in newer DH systems. Some of these combinations will be outlined in the following chapters [55].

Europe is market leader in the transition to the integration of excess heat and renewable sources in the DH system. Possible heat sources for a HP integration are data centers, metro tunnels, waste heat, hydrogen generating electrolyser, sewage water treatment facilities, nuclear power plants and renewable sources. Examples for renewable sources are geothermal energy, solar thermal energy, or the burning of waste [56].

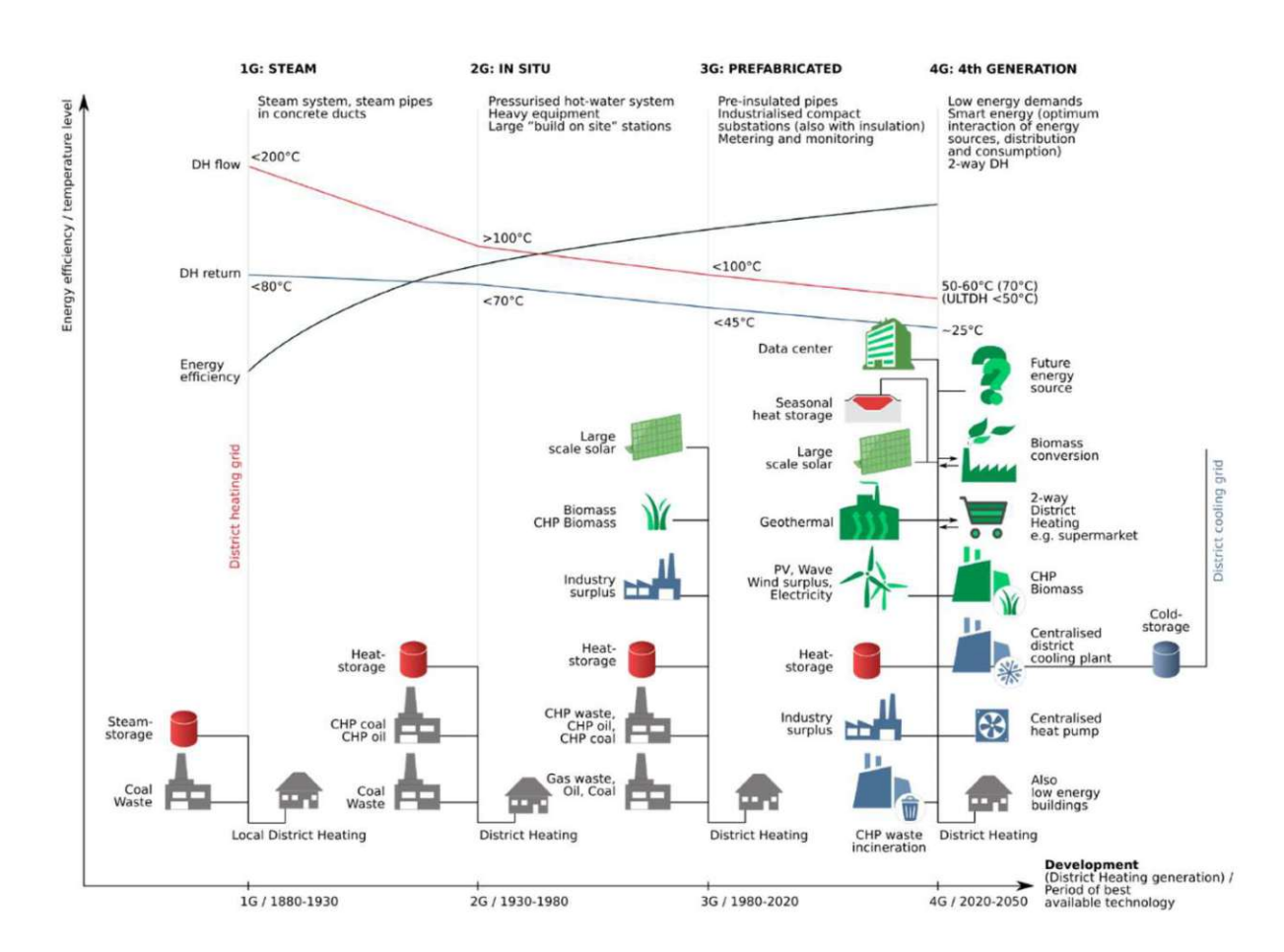


Figure 53 DH generations with their temperature level and typical thermal energy sources [55]

The two different ways of integrating a HP into a DH system are shown in Figure 54. The parallel integration (a) heats the DH return side or parts of it lifting it to the feed temperature level. The serial integration (b) lifts the temperature of the DH feed (after another heating plant). In the serial setup exergetic losses occur, if just a part of the feed is heated due to mixing the streams with different temperatures. The feasibility of any configuration must be considered on the specific project, mostly depending on achievable COP and FLH [57].

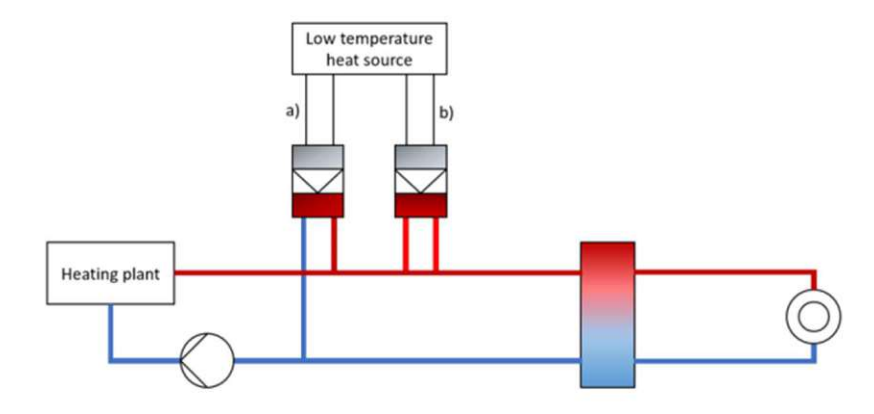


Figure 54 Two ways to integrate HP into DH networks a) parallel b) serial [57]

The target of district heating and cooling (DHC) is to connect 350 million buildings globally by 2030, providing 20 % of the space heating needs. The total installed DH EU28+3 capacity in 2021 where around 300 GW. Roughly 43 % of the DH thermal energy is supplied by renewable and waste heat sources pictured in Figure 55. The DH sales in 2021 where around 500 TWh/yr [58].

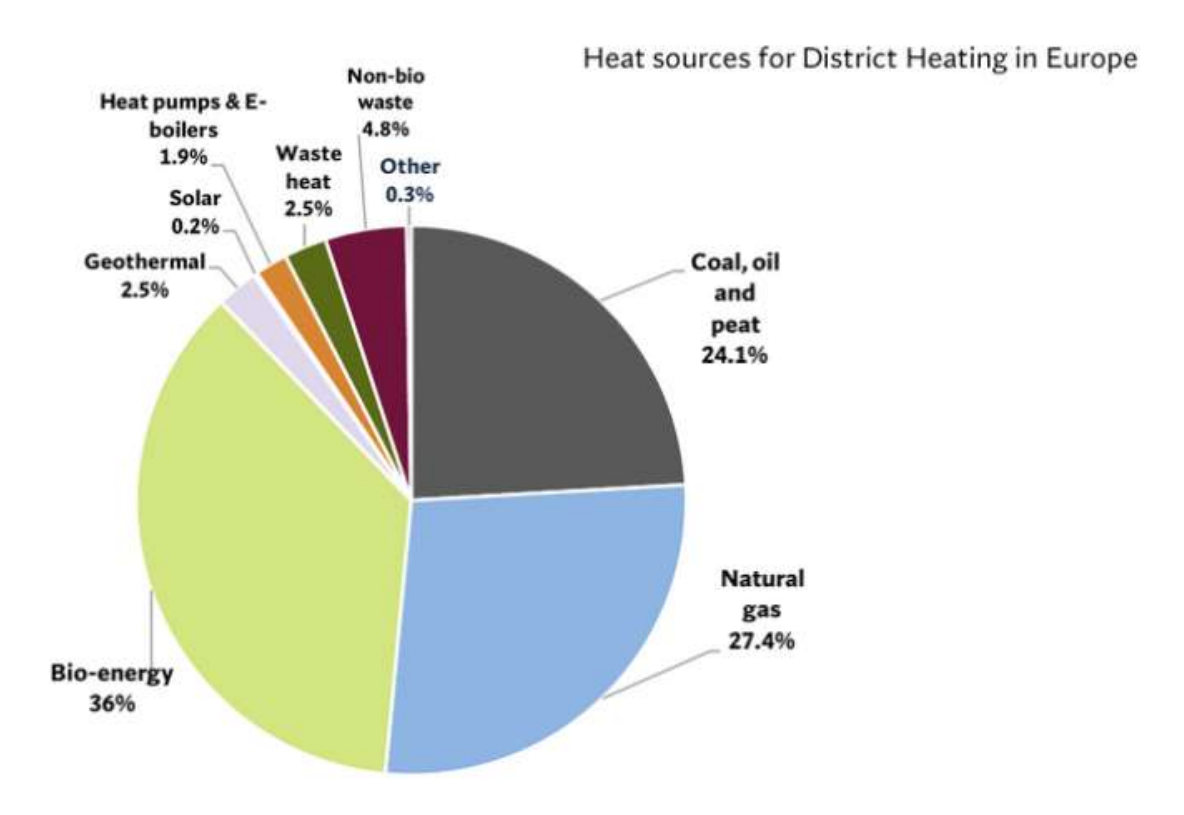


Figure 55 Heat sources for DH in Europe in 2021 [58]

Figure 56 (in this figure . (dot) is used in difference to , (comma)) shows the production and capacity of large scale HP in European DHC systems. The current capacity is around 2,43 GW. The key players are Sweden, Finland, and Denmark. According to predictions the amount of HP power in European DHC will increase at least by 80 % until 2030 which corresponds to 2 GW or 2 857 ecop RHP [58].

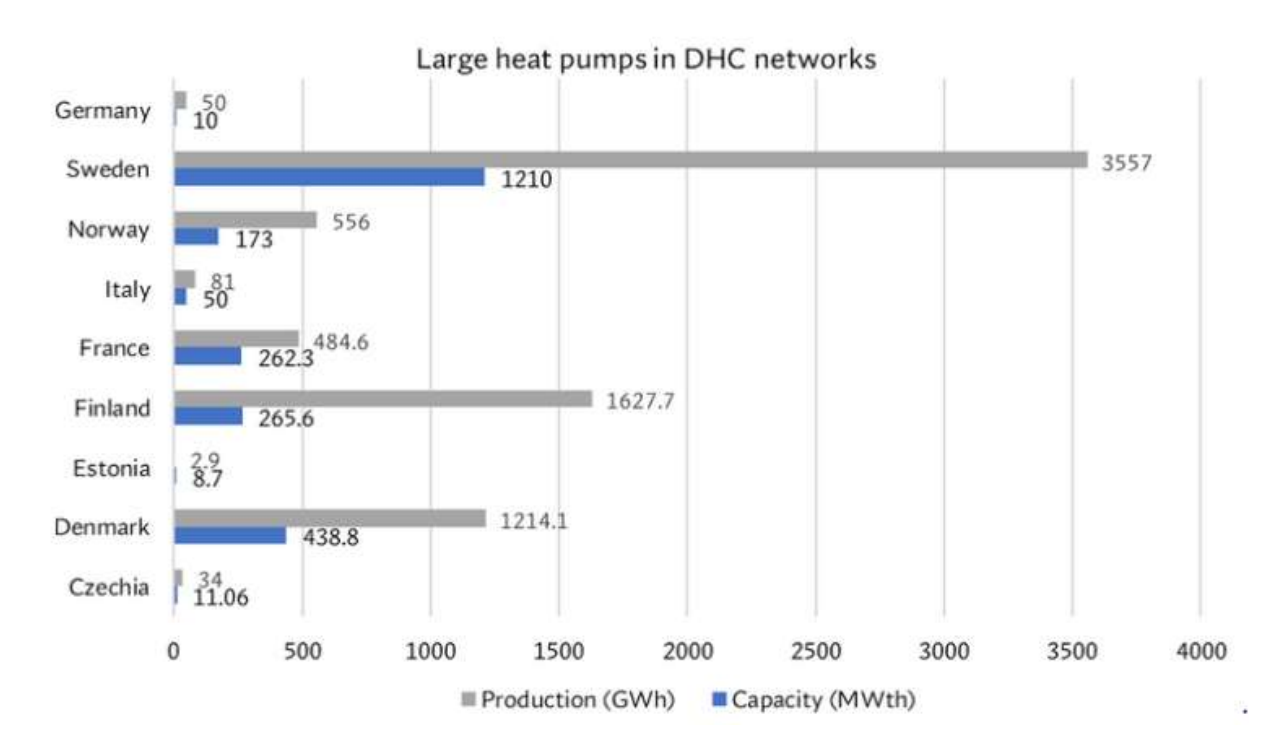


Figure 56 Large heat pump stock for DHC in selected European countries and their thermal energy supply in 2021; in this figure . (dot) is used in difference to , (comma) [58]

Overview investigated areas

In this section the necessity and the justification of the following chapters is clarified.

- Geothermal energy (4.1): Geothermal energy is a renewable energy sources that opens the possibility to supply thermal energy with a HP if no waste heat sources are available. The HP can increase the thermal power output of a geothermal energy well or increase its temperature level.
- Hydrogen Electrolysis (4.2): Green hydrogen will become an important energy carrier in the European Union towards its path to "net zero emissions". The major technology to provide green hydrogen is electrolysis generating a lot of waste heat. This waste heat can be utilized by an HP and lifted to valuable temperature levels.
- Solar thermal heat (4.3): Solar thermal energy can provide thermal energy for industries and DH, but is subject of large seasonal fluctuations. Systems that can store solar oversupply and make it available at later times typically require a HP.
- Flue gas utilization (4.4): Flue gas is still one of the major excess heat sources leaving the plant usually at temperatures greater than 100 °C.
- Steam production (4.5): Much of the European process heat is needed as process steam. All conventional steam supplies are based on fossil fuels and need to be replaced by a renewable technology in the future.

4.1 Geothermal energy

4.1.1 Geothermal energy general

Regardless of the temperature of the ambient air, the temperature inside the earth is constant. The deeper one enters the earth's surface, the warmer it gets [59]. The thermal power of the earth's crust comes from the radioactive decay of long-lived nuclides like ²³⁵U, ²³⁸U, ²³²Th and ⁴⁰K. This geothermal energy can be used by different technologies. Regarding the thermal energy deposits, a distinction is made between hydrothermal geothermal systems (hot and usually very salty water in great depths) and petrothermal systems (warm rock in fracture structures) [59].

About extraction, a distinction is made between open and closed loop systems. Open hydrothermal systems work through a geothermal doublet. In this system thermal energy in the form of hot water is pumped to the surface through a producer well. The thermal energy is extracted from the hot water through a heat exchanger and returned to the subsurface through an injection well [59], [60]. Closed systems, which are also often referred to as borehole heat exchangers, are usually designed in the form of coaxial pipes. A thermal energy transfer fluid is pumped to depth in the outer annulus, using the surrounding rock as a heat exchanger. The heated-up fluid rises to the surface in the middle through an insulated riser [60].

In terms of depth, it can be distinguished between:

- Near-surface geothermal energy (depth 20 200 m), rock temperature < 25°C
- Medium geothermal energy (depth 800 3000 m), rock temperature 40 -100°C
- Deep geothermal energy (depth >3000 m), rock temperature > 80 °C

The indicated depths and temperatures are to be understood as approximate values.

Figure 57 gives an overview of different geothermal energy systems and their extraction methods. This thesis focuses on the direct use of hydrothermal sources [60].

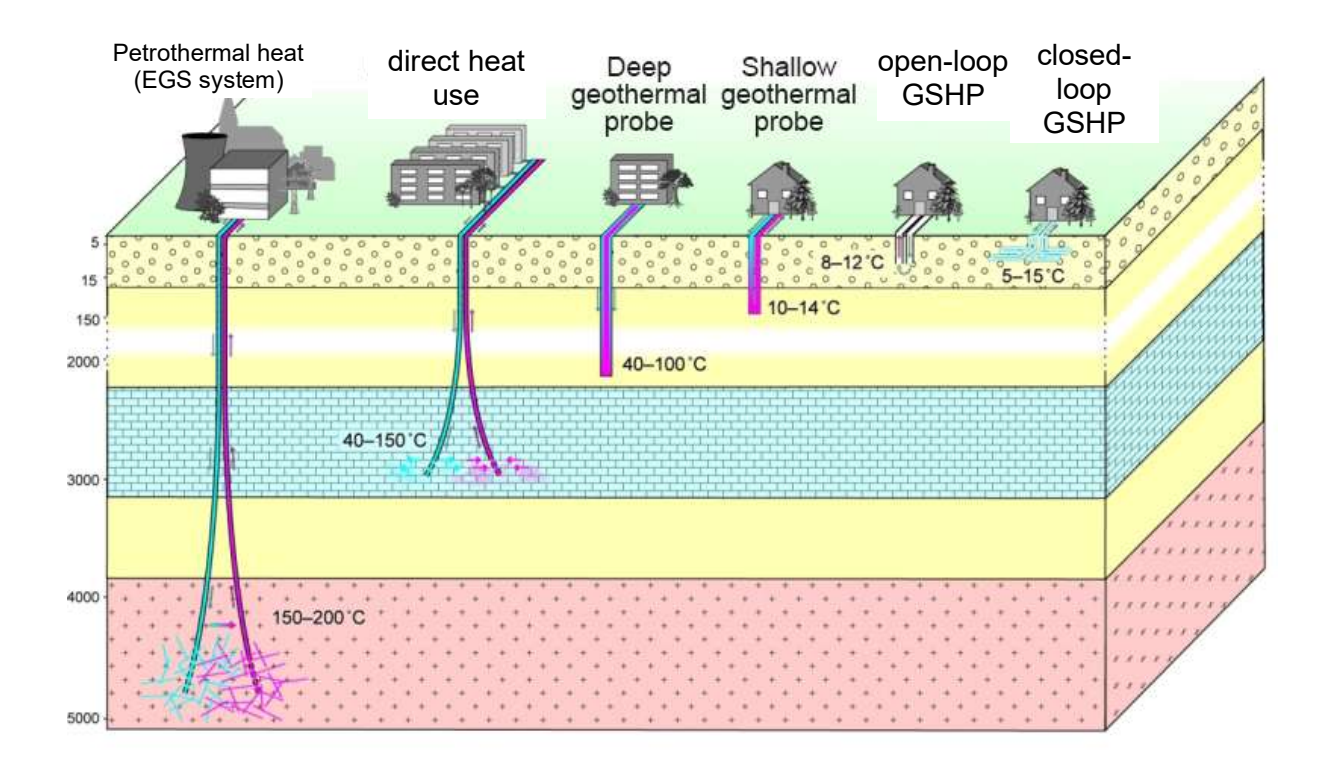


Figure 57 Overview hydrothermal, petrothermal systems; open and closed systems; EGS: enhanced geothermal system, GSHP: ground source heat pump [61]

4.1.2 Geothermal energy in Europe

The geothermal potential in Europe comprises several gigawatts, whereby the geographic and topographic distribution varies considerably. Figure 58 visualizes the geothermal resources in Europe. Europe's largest deposits are in Iceland, France, Turkey, Germany, Hungary, Italy, and Serbia [62]. Further visualizations of the geothermal resources in Europe can be found at (https://heatroadmap.eu/peta4/).

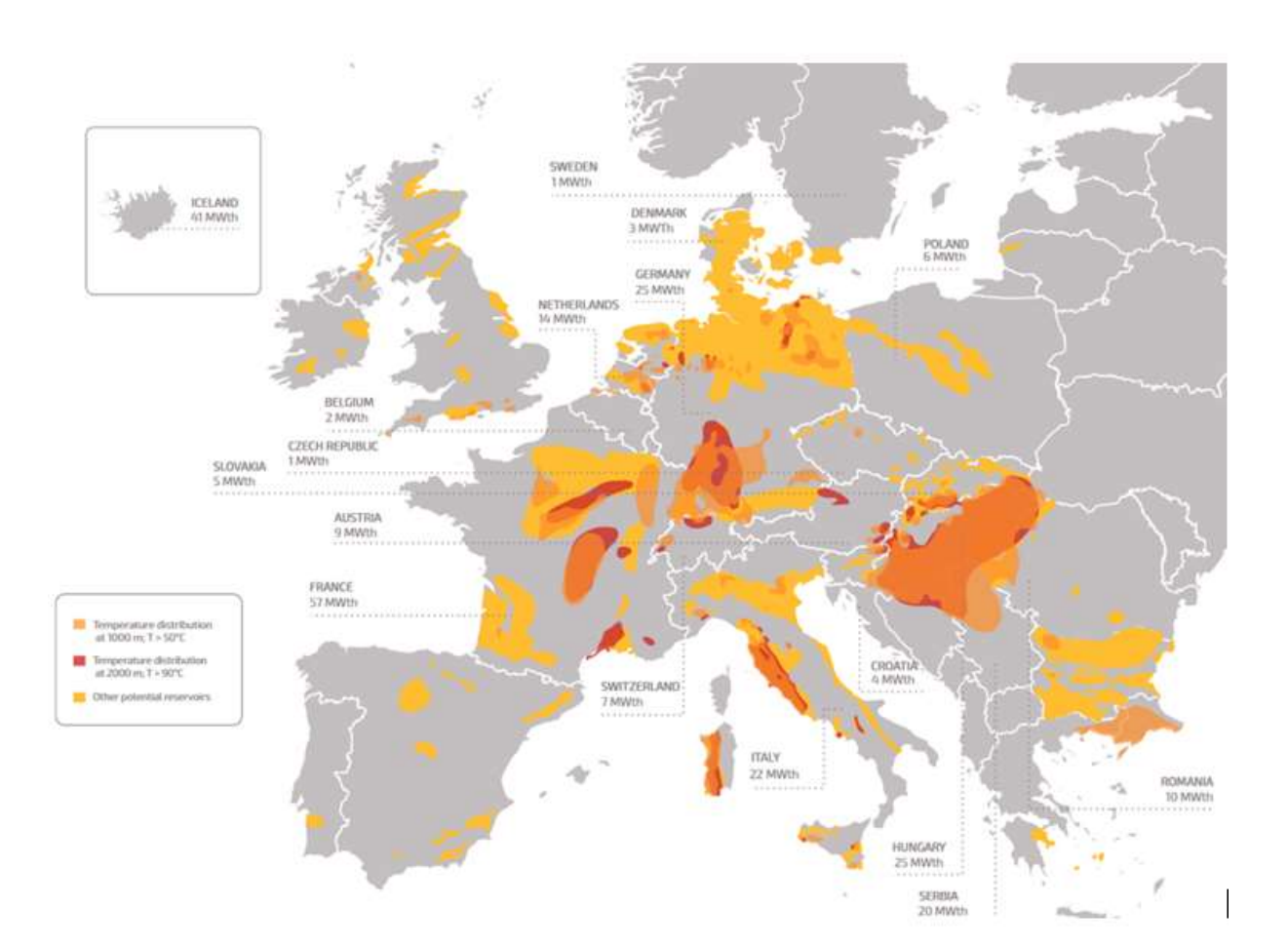


Figure 58 Overview of the geothermal sources in Europe, the color indicates the temperature at different depths [63]

An investigation of the commercially used geothermal wells in Germany has shown a distribution of the most used temperature ranges in combination with the plant size. A summary of the findings can be found in Figure 59. The largest plants and the most utilized geothermal potential are in the temperature range of 120 - 140 °C. Very low temperature levels 20 - 40 °C are hardly used industrially, while very high temperature levels > 160 °C are very rare [64].

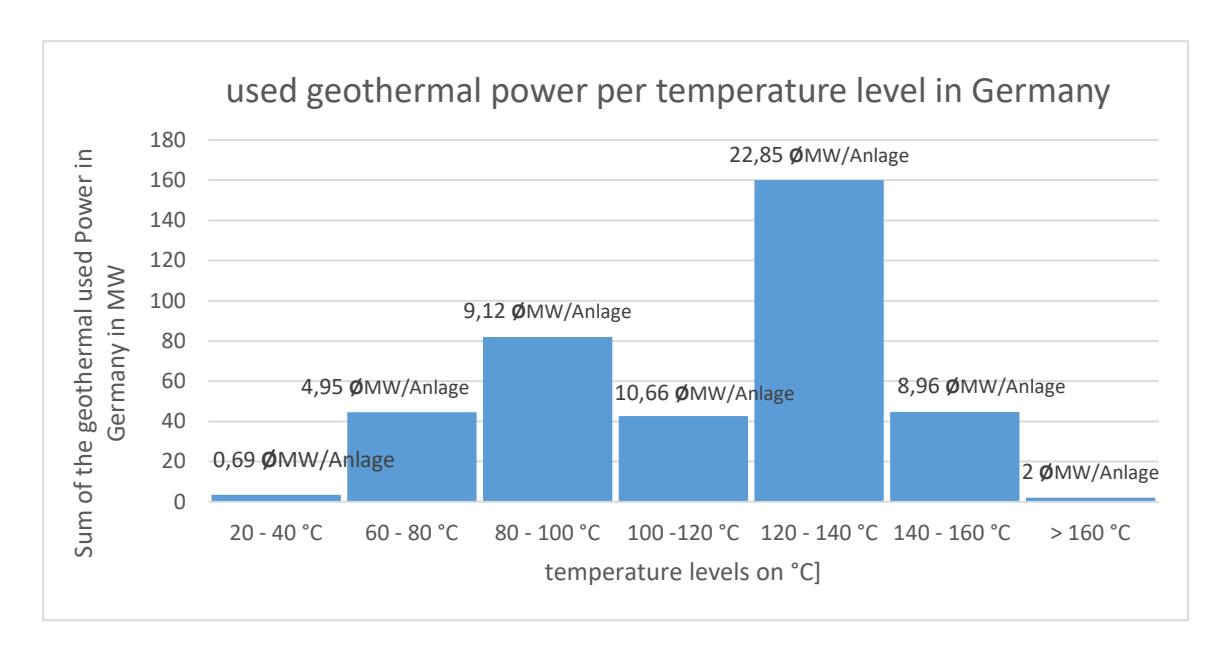


Figure 59 Stock of the geothermal plants as a function of the temperature level data based on [64]

4.1.3 Geothermal applications for heat pumps

The found low temperature level in near-surface geothermal storages is usually used for space heating. This thesis focuses on temperatures between 40 – 150 °C in depts greater than 800 m. The major European applications in these temperature levels are process heat and DH systems [65].

The temperature levels of the commercial used geothermal heat storages in Europe differ a lot. Figure 60 shows geothermal storages in Europe and their expected temperature level. Highest temperatures can be found in Italy, Turkey, and Germany [65].

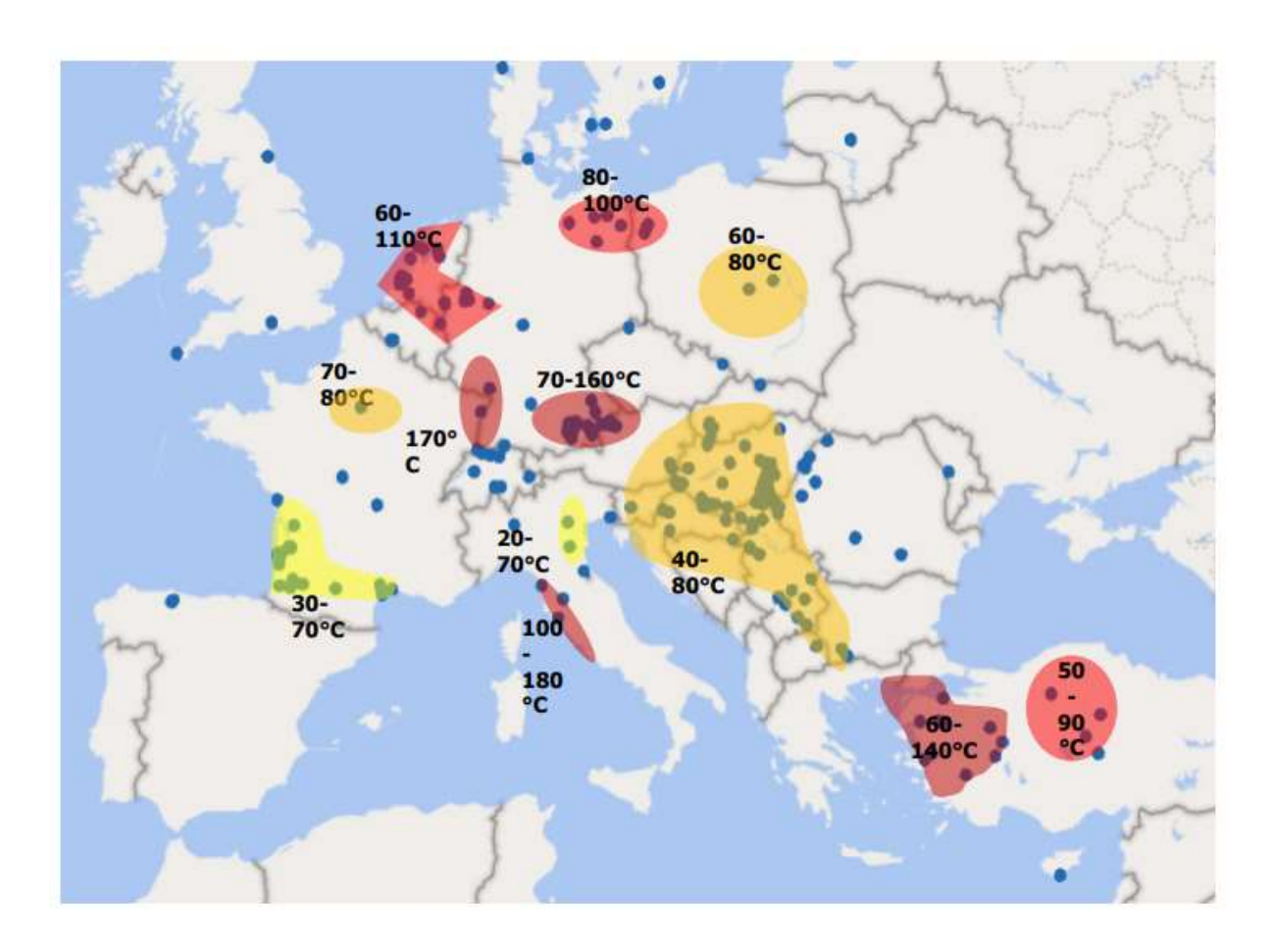


Figure 60 temperature levels of the commercialized geothermal areas in Europe [65]

The thermal energy from geothermal deposits can either be used directly or serial in combination with a heat pump. Figure 61 shows the direct-use (left) and serial concept (right). For the direct-use the geothermal energy reaches higher temperatures than the return flow of the DH. In this setup the geothermal energy is transferred via a HEX to the DH system. Additionally, a parallel installed heat pump can be used to lower the temperature level of the DH-return flow using it as source to increase the DH-feed temperature. This setup is used to increase the efficiency of the HEX (increased temperature difference) and if the geothermal source cannot lift the DH-feed to the needed temperature level. The serial concept (right side) directly uses the geothermal energy as source in a HP. The hot sink of the HP is used to heat the DH-feed. Geothermal energy is used in the same way for process heat in industrial applications [66].

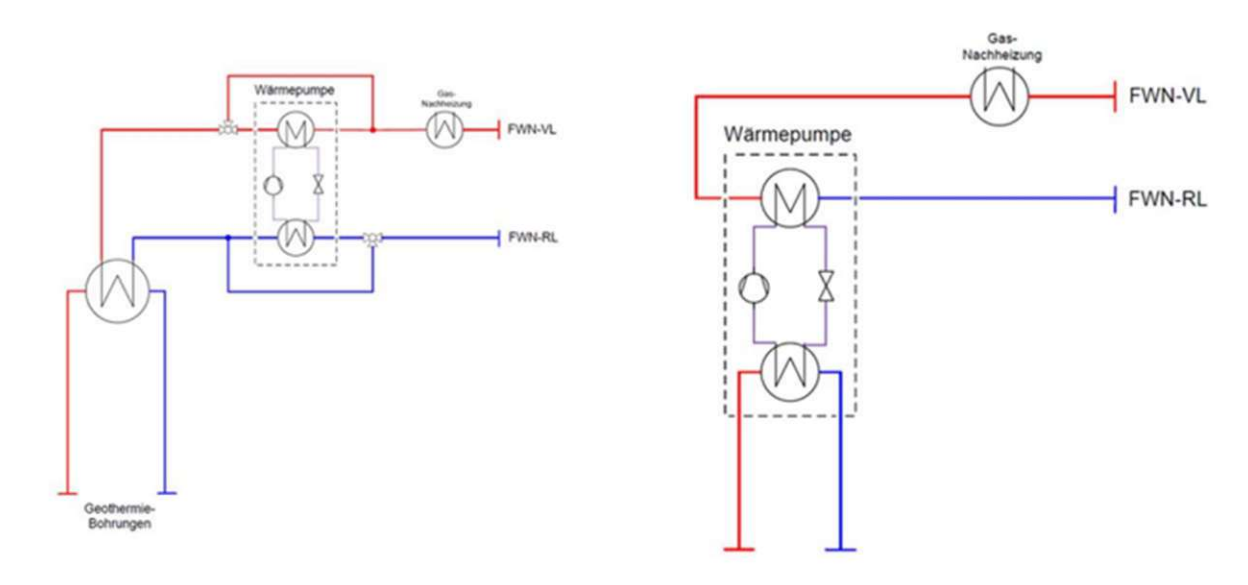


Figure 61 District heating concepts for geothermal systems direct (left) serial (right) [66]

On the following pages three use cases how the ecop RHP can be integrated in geothermal applications are shown.

Increase the geothermal heating capacity (Use case Geo-1)

The use case Geo-1 (Increase the geothermal heating capacity) is exemplary shown in Figure 62. This setup can be installed as retrofit to existing plants or in new plants to increase the geothermal capacity or to lift the temperature level of the geothermal energy. The geothermal energy at a temperature level of 80 °C is used directly to heat the district heating return flow (55 °C). In this process step, the geothermal water is cooled down to 60 °C. Next the 60 °C geothermal water is used as a source in an ecop RHP, cooling it down to 33 °C. At the sink side of the RHP, water with 70 – 115 °C can be extracted. The hot water can either be used as process heat or to lift the DH feed. Alternative also the preheated DH feed with 75 °C can be used as HP sink inlet being lifted to 130 °C for high temperature applications. The given temperatures are only examples for a integration in a typical DH network [63], [64], [65], [66], [67].

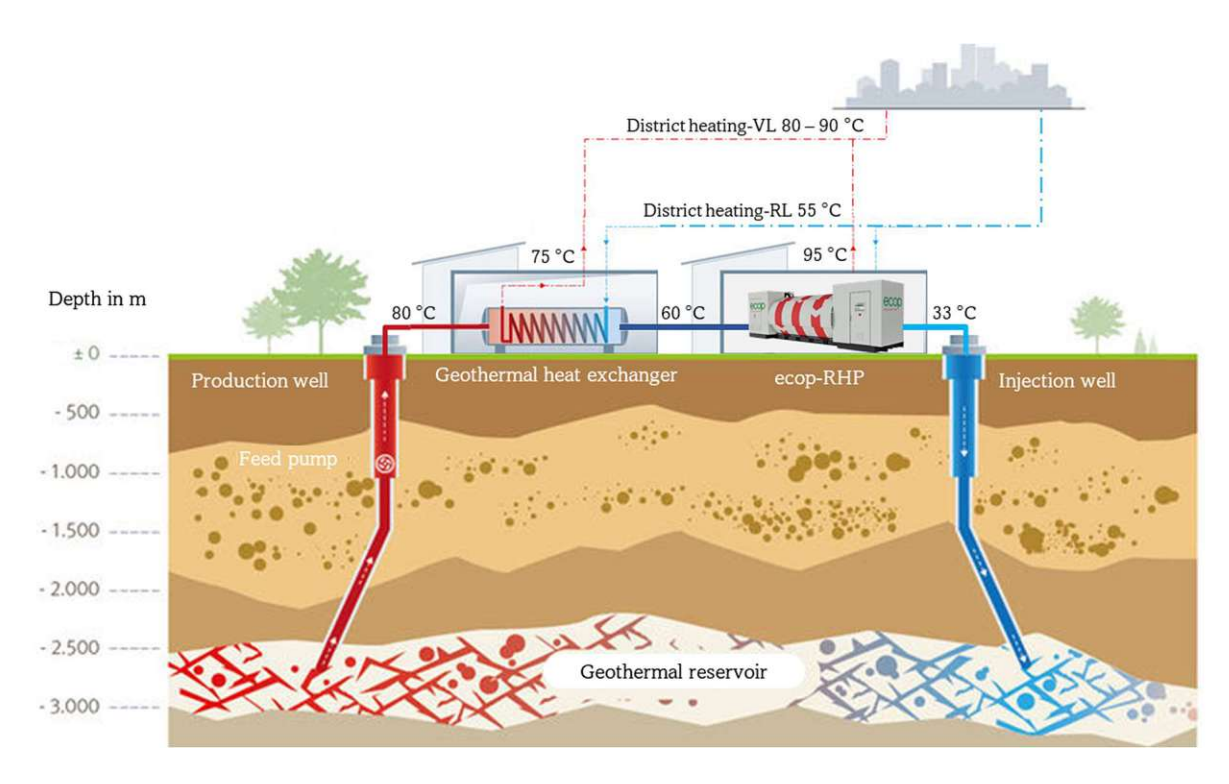


Figure 62 Doubled use of the geothermal energy based on [67]

The advantage of this application is that more thermal energy can be extracted from the geothermal reservoir with the same amount of water pumped from the depth. Thus, the specific pumping costs are reduced. A simulation of the operating data of the ecop RHP is shown in Figure 63. The direct cooling of the geothermal feed via a heat exchanger from 80 °C to 60 °C results in a thermal power of 467 kW. The ecop RHP can further cool the water from 60 °C to 33 °C extracting 617 kW as source energy. The output of the ecop RHP result in 700 kW thermal power lifting a sink from 55 to 95 °C with a COP of 4,41. In this setup the thermal power of the geothermal well is increased by 150 % from 467 kW to 1,167 MW [68].

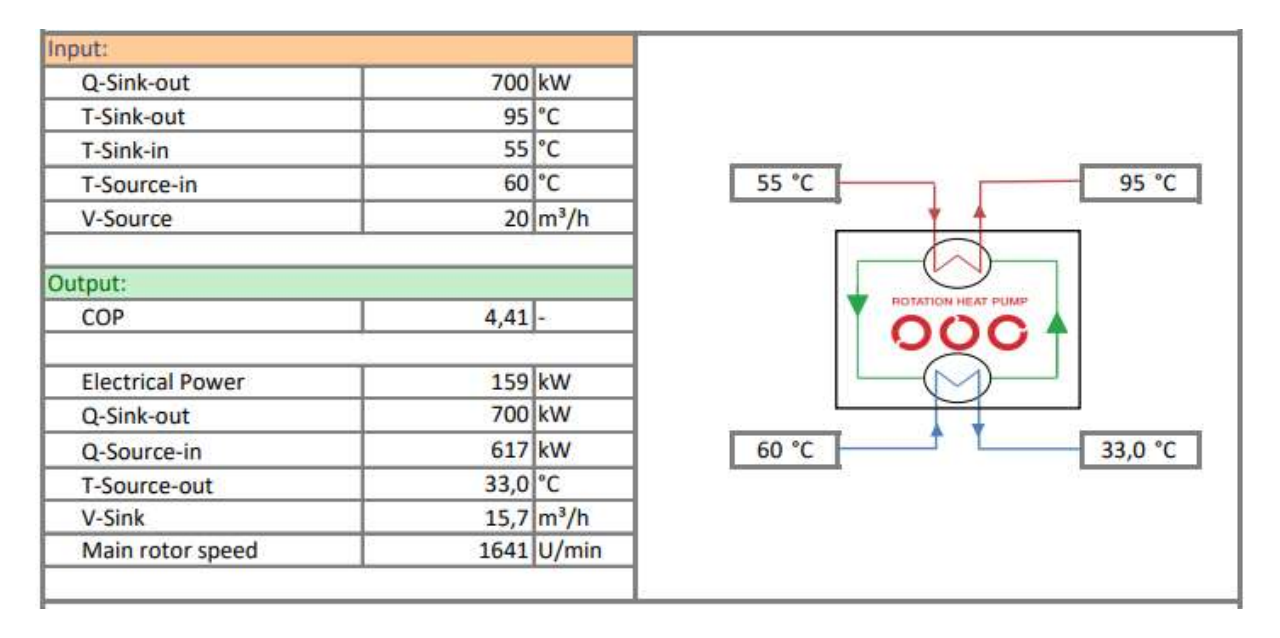


Figure 63 Simulation of the ecop RHP in use case Geo-1 [68]

Temperature rise of existing / new geothermal sources (Use case Geo-2)

Another application is the supply of high temperatures for industry or old DH system with heat pumps. If heat pumps should provide high temperatures, reasonable waste heat sources are necessary. Often no excess heat sources with temperatures around 90 °C are available. In this case geothermal energy is a renewable option for a constant heat pump source. Figure 64 shows use case Geo-2 where the heat pump is used in a serial design to lift the temperature of the geothermal well [63], [64], [65], [66], [67].

000

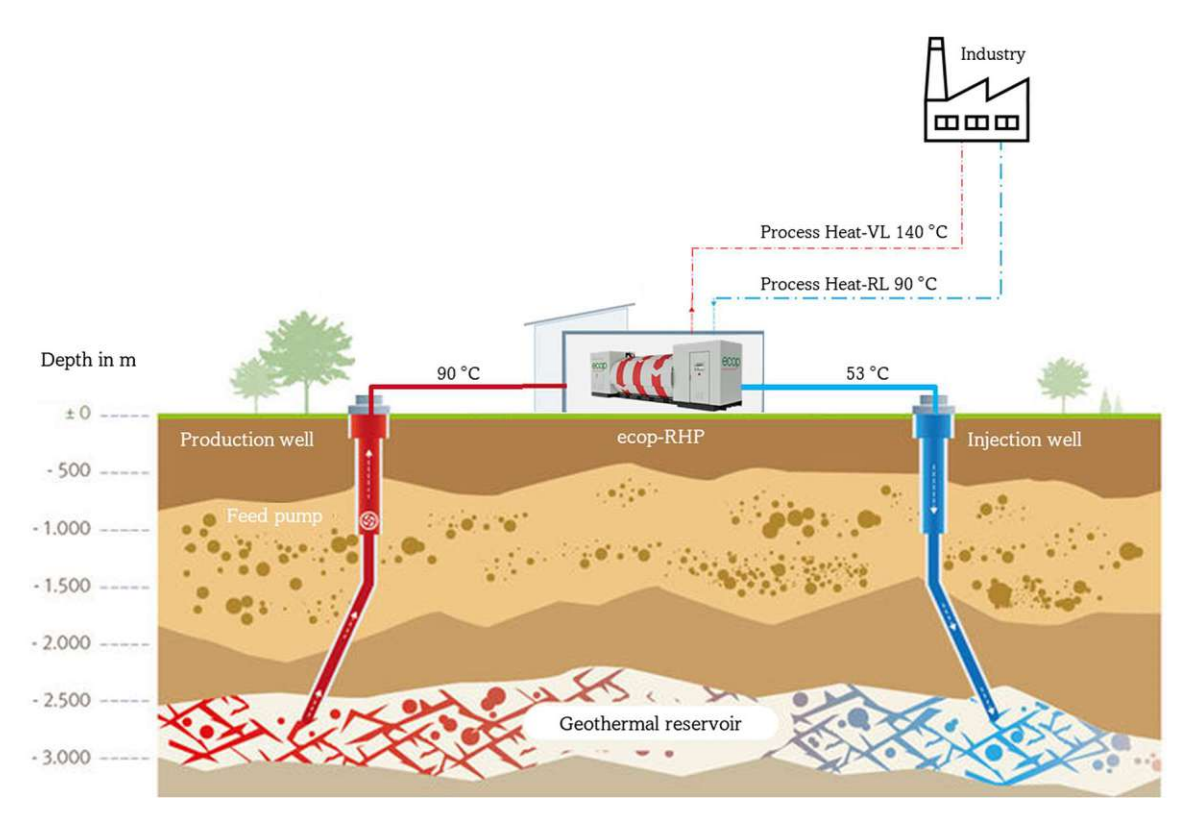


Figure 64 Visualization of use case Geo-2 with a serial use of the geothermal energy based on [67]

A simulation of the ecop RHP in this setup is pictured in Figure 65. The advantage of the ecop RHP in this configuration is that it creates a high temperature lift (55 K) and can reach temperatures up to 150 °C. In an exemplary simulation (see Figure 65), the geothermal water was cooled down from 90 to 53 °C and thus process heat could be heated from 90 to 140 °C. In some applications, it might me reasonable to switch another ecop RHP in series (compare Geo-1) using the cooled down geothermal water with 53 °C as source extracting additional thermal energy for low temperature applications [68].

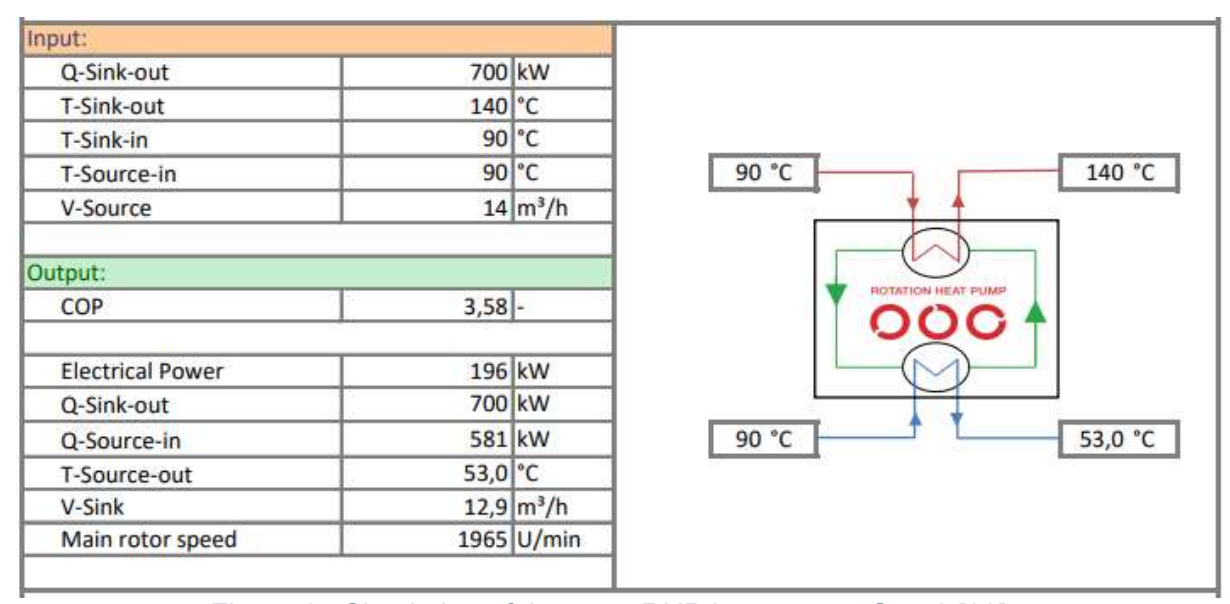


Figure 65 Simulation of the ecop RHP in use case Geo-2 [68]

High temperature swing of low temperature geothermal sources (Use case Geo-3)

This use case is based on low temperature geothermal sources of 30 – 50 °C. Without a HP these geothermal sources cannot be used for DH or in industry, beside for space heating tasks. Such low temperatures can usually be found in depths between 800 -2000 m having significant lower drilling expenses. Furthermore, old oil wells can be used in this application reducing the drilling costs to zero. Also, some geothermal drillings fail or the expected temperature level is not found in reasonable depths. A describing visualization is shown in Figure 66 [63], [64], [65], [66], [67].

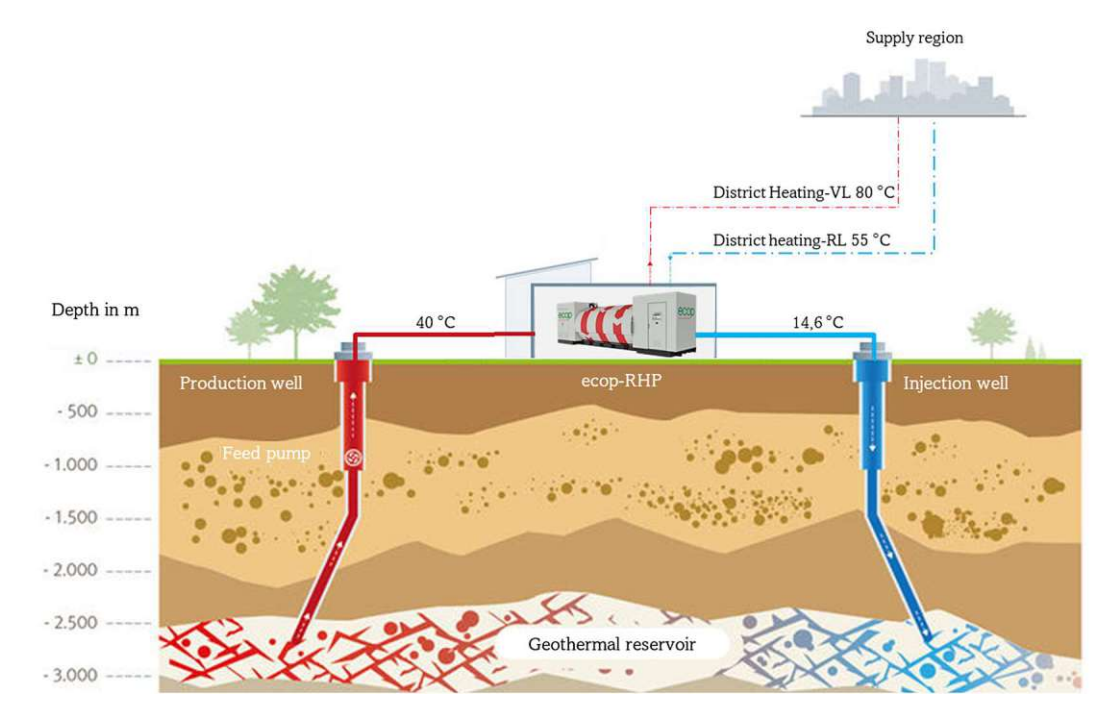


Figure 66 Use case Geo-3 with a direct use of low temperature geothermal energy based on [67]

In Figure 67 the ecop RHP has been simulated for an exemplary use case 3 Geo-3 [68].

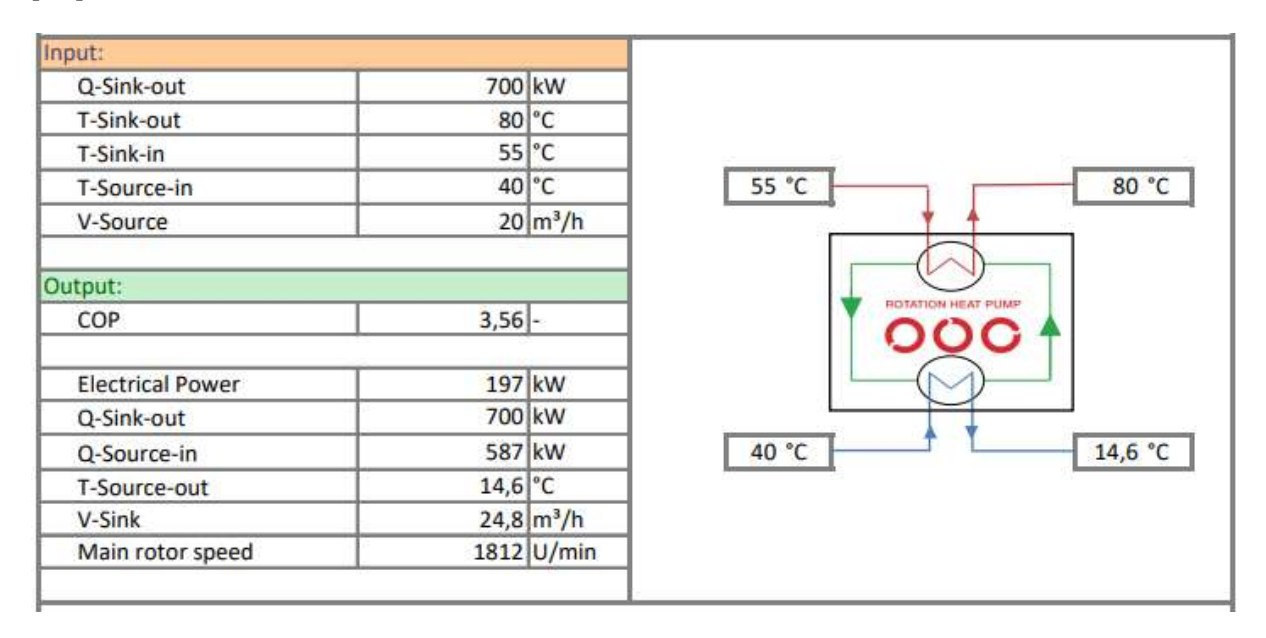


Figure 67 Example of the ecop RHP in use case Geo-3 [68]

4.1.4 Economic efficiency for the geothermal use cases

According to [69] the average levelized costs of heat (LCOH) for geothermal district heating (GeoDH) projects are ~ 80 €/MWh. Using exemplary the ecop contracting model shown in Figure 43 and the LCOH of 80 €/MWh for GeoDH systems and the LCOH of use case Geo-1 result in 46,4 - 83,6 €/MWh depending on the FLH and the electricity price. Therefore, the HP add on can lower the price significantly compared to the GeoDH without HP. The corresponding calculation is shown in Equation (5), where 467 kW is the geothermal power without the ecop RHP and 700 kW is the power added by the RHP. The calculation has been visualized in Figure 68 [63], [64], [65], [66], [67], [70].

$$LCOH_{Geo-1} = 80 \frac{\text{ }}{\text{MWh}} \frac{0,467 \text{ MW}}{0,467 \text{ MW} + 0,7 \text{ MW}} + \left(24 \frac{\text{ }}{\text{MWh}} \middle| 86 \frac{\text{ }}{\text{MWh}} \right) \frac{0,7 \text{ MW}}{0,467 \text{ MW} + 0,7 \text{ MW}}$$

$$= \left(46,4 \frac{\text{ }}{\text{MWh}} \middle| 83,6 \frac{\text{ }}{\text{MWh}} \right)$$
(5)

LCOH_{Geo-1} levelized cost of heat for use case Geo-1 in €/MWh

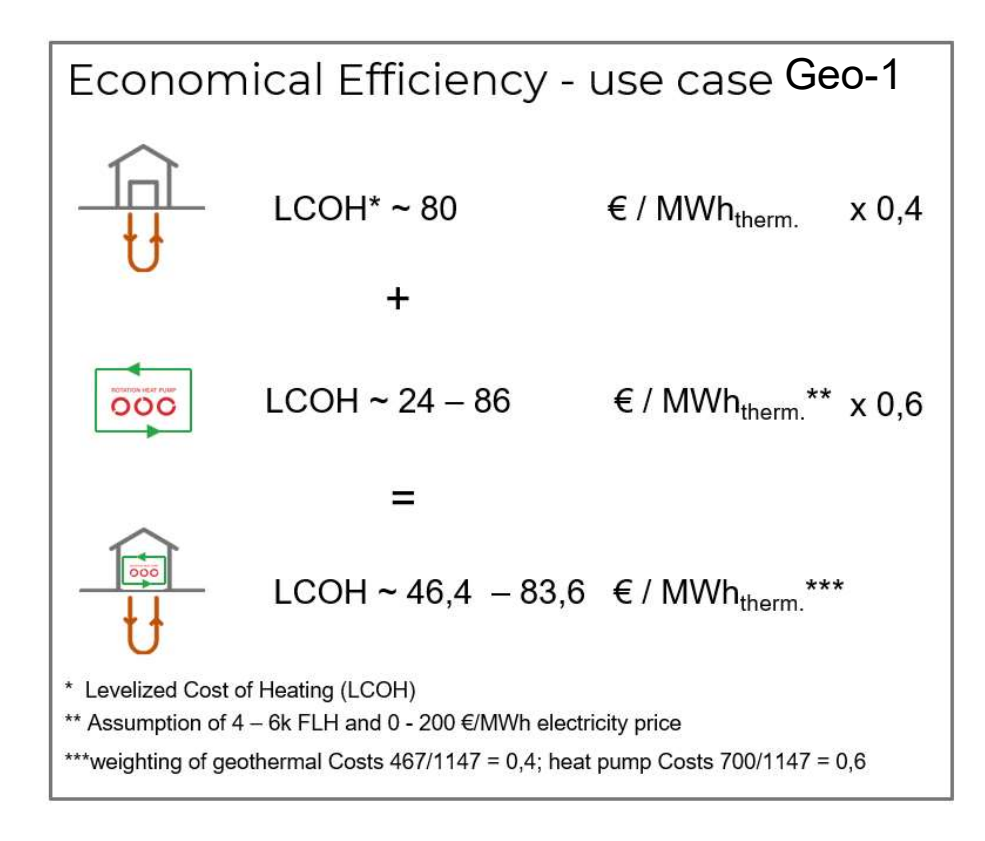


Figure 68 Visualization of the levelized costs of heating for use case Geo-1 [70]

Based on the calculation given in Equation (5) the use cases Geo-2 and Geo-3 were calculated in a very similar way visualized in Figure 69 and Figure 70. Use case Geo-2 result in significant higher costs, because higher temperatures (up to 150 °C) are generated. Compared to most other options of delivering temperatures of 150 °C this setup has very low CO_{2-ev} emissions [63], [64], [65], [66], [67], [70].

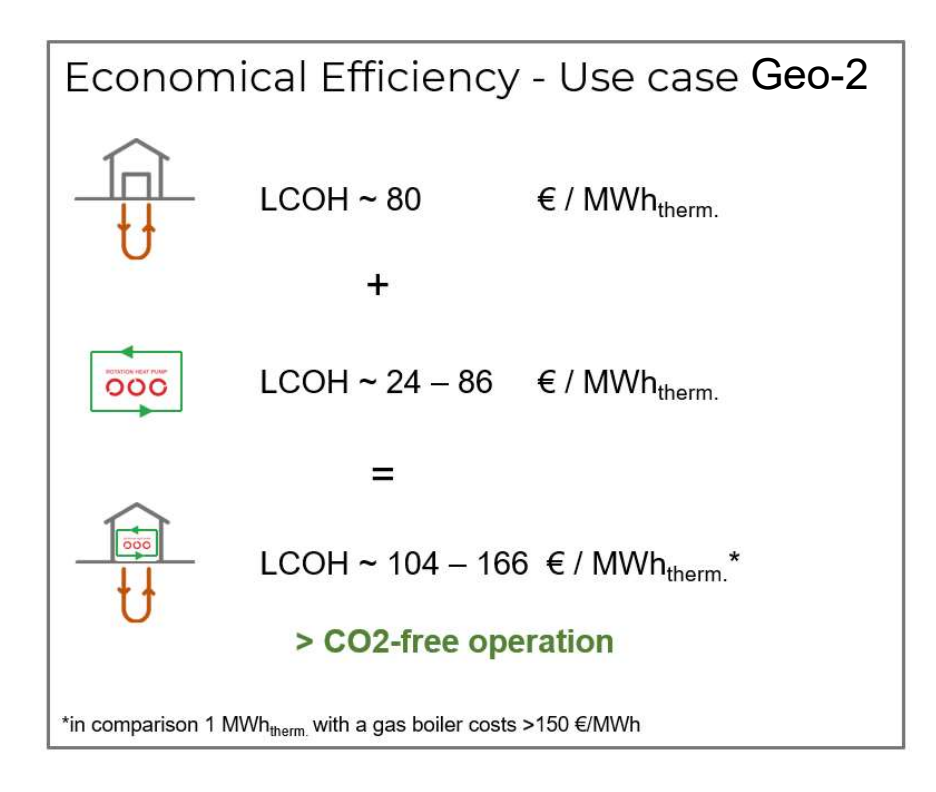


Figure 69 Visualization of the levelized costs of heating for use case Geo-2 [70]

Use case Geo-3 aims on existing boreholes with geothermal energy of around 40 °C (unused oil wells) or stopped drilling approaches. Drilling approaches might stop early if the expected temperature gradients are not found. Around 30 % of all drilling approaches do not find the expected temperature level. Use case Geo-3 for stopped drilling approaches can be a better solution than an expensive deconstruction of the failed borehole. The economic viability is depending on the given case (further investment costs for Geo-3, reached temperature level, possibility to extract thermal energy, ...) [71], [72], [73], [74]. The economic calculation of use case Geo-3 in Figure 70 assumes that an extraction of low temperature geothermal energy in a failed borehole is reasonable and better than a deconstruction. Therefore, the construction costs of the geothermal well are set to zero.

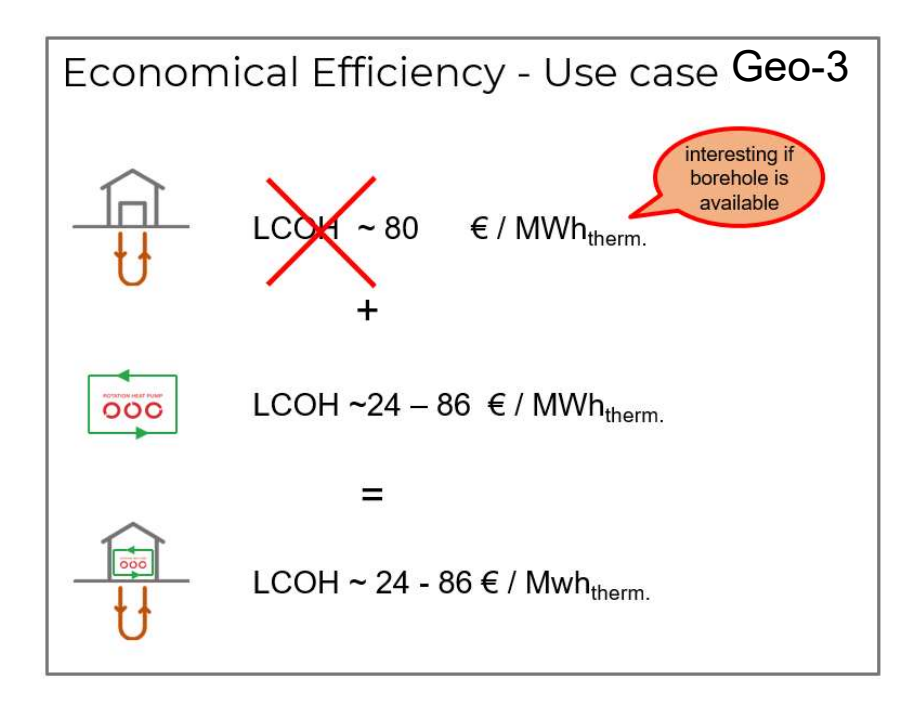


Figure 70 Visualization of the levelized costs of heating for use case Geo-3 [70]

4.1.5 Market potential geothermal systems

The European potential for geothermal energy is huge and growing fast. Figure 71 shows the number of existing and planned geothermal plants in selected European countries. In France, Germany, and Poland are the most geothermal plants in development. Currently mostly hydrothermal storages where tapped, but new technologies such as hot dry rock open the possibility of a better use of petrothermal storages. Hot dry rock is basically a technology for cracking the rock of petrothermal storages in depths of 3000 – 5000 m by pumping water with a very high pressure. The technology is related to fracking technologies [65], [75].

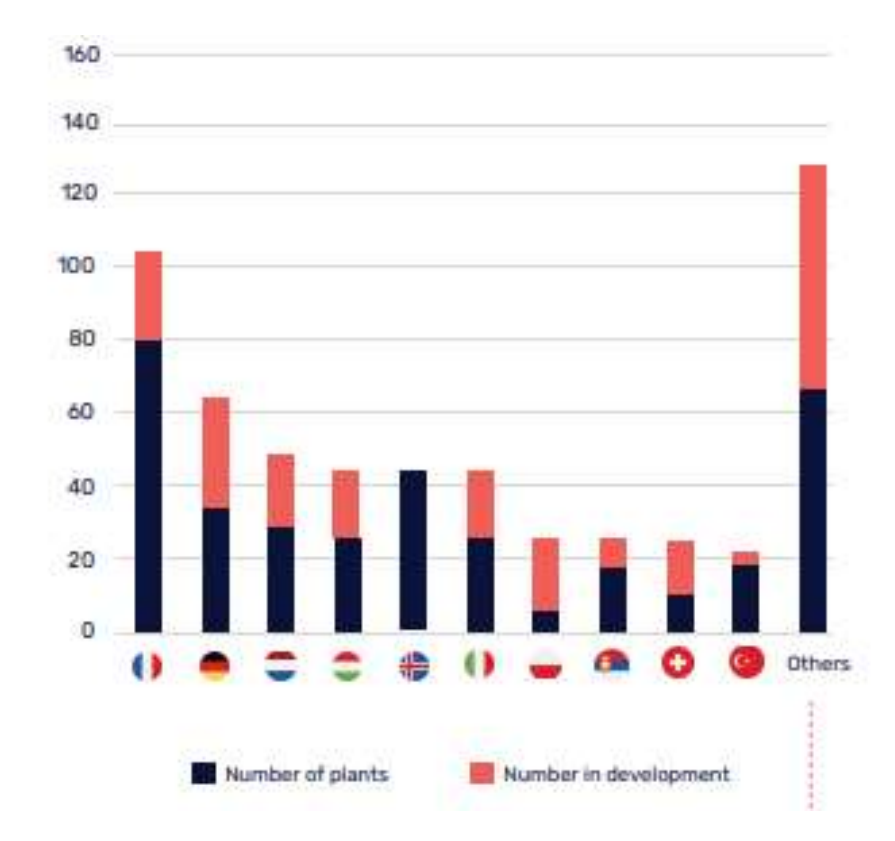


Figure 71 Number of GeoDH plants in Europe in operation and under development [65]

Figure 72 shows an existing GeoDH project in Neustadt Glewe using the geothermal feed flow directly to heat the DH return. This project could be extended by the defined use cases Geo-1-3. Currently the geothermal water is fed back with 50 °C in the injection well. The thermal power of the GeoDH system can be increased by use case Geo-1 by further cooling down the geothermal return. Alternative the ecop RHP can be used for reserve / peak load heating (see point 4 in Figure 72 - use case Geo-2) [71], [72], [73], [74].

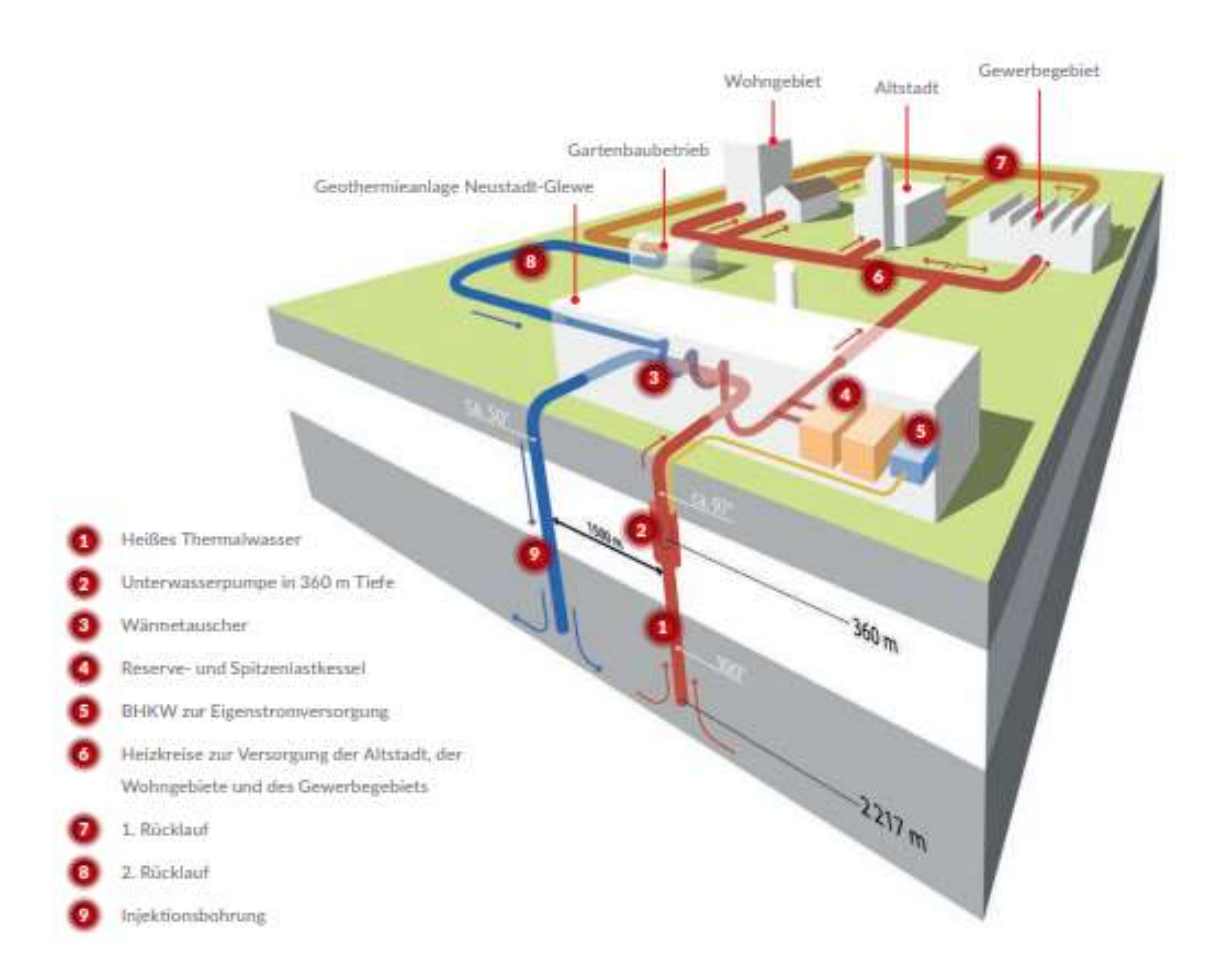


Figure 72 Existing GeoDH project in Neustadt Glewe (Germany) based on [71], [72], [73], [74]

This thesis assumes that use case Geo-1 can be implemented to most of the 4,8 GW installed GeoDH stock in Europe. With the assumption, that it is possible to use the geothermal return flow with 60 °C of all the European GeoDH stock and cool it down to 33 °C (use case Geo-1) the economic potential would result in 2,35 GW. Further assuming that such CO_{2-ev} free heating solutions are subsidized and the FLH are typical very high all solutions are economical feasible. Therefore, the market potential is equal to the economic potential. This would result in 3 357 pieces of ecop RHP having each a power of 700 kW [71], [72], [73], [74]...

According to [74] the total unused potential of geothermal heat with close by DH plants are 350 TWh with temperatures of > 60 °C in < 2 km depth and 1 428 TWh with temperatures of > 80 °C in < 2 km depth. The author of [74] estimated that this European GeoDH potential could result in 30 000 pieces of 18 MW plants (= 540 GW). Figure 73 gives an idea of how the potential for heat pumps can be derived from the geothermal potential. Considering the defined use cases Geo-1 to 3 the technical HP integration potential in geothermal systems result in 378 GW. If just 1 - 2 % of the technical HP potential is economical feasible the market potential result in 5 400 – 10

800 pieces of 700 kW ecop RHP. In this calculation the potential of ~40 °C in 1 km depth or use case Geo-3 is not considered in more detail [71], [72], [73], [74].

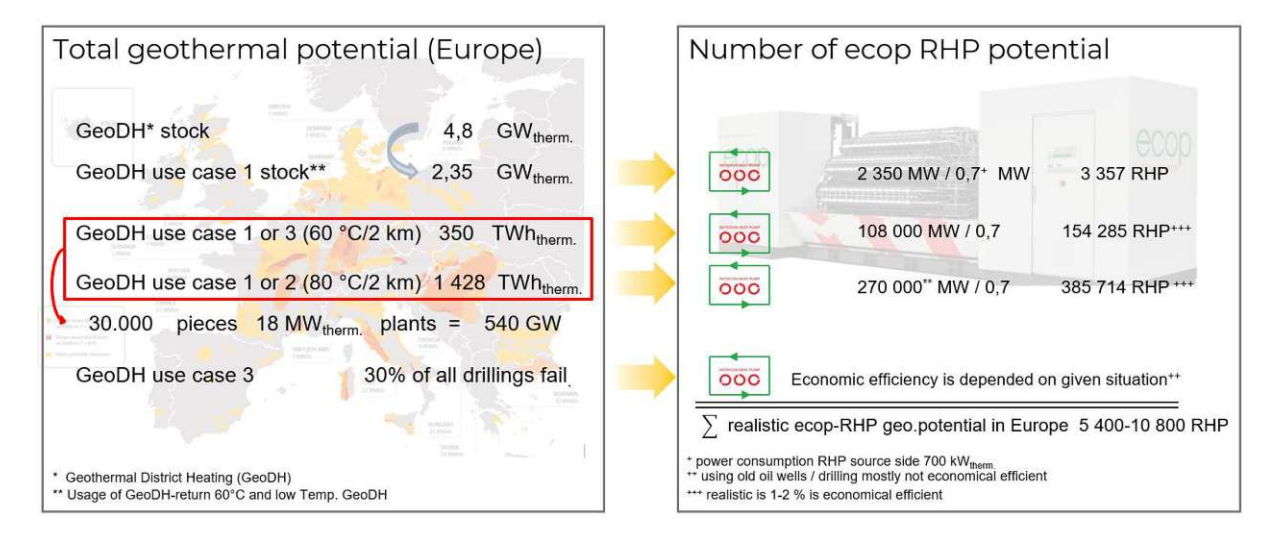


Figure 73 Total geothermal technical, economic, and market potential for the integration of a HP into geothermal systems by using use case Geo-1-3 [71], [72], [73], [74]

4.2 Hydrogen Electrolysis

Green hydrogen will become an important clean energy carrier helping to decarbonize sectors with high CO₂ emissions. Hydrogen is suited as energy carrier, because it has a high energy density (heating value ~ 120 MW/kg) and existing transport infrastructure can partly be used. Nowadays approximately 80 % of the hydrogen production is classified as brown or grey. This means it is produced by fossil fuels. Another possibility to produce hydrogen is by electrolysis. If the used electricity is from renewable sources, electrolysis can be declared as green hydrogen source. To make green hydrogen production economical more feasible, the potential of waste heat recovery of electrolysis facilities is determined in this section [57], [76].

Figure 74 gives a short overview of the current major electrolyser technologies [76]. This thesis focuses on current state of the art Alkine electrolysis (AEL) and Polymer exchange membrane (PEM) electrolyser [57]. High temperature electrolysis is a promising technology with high efficiencies, which is currently under development, but not included in this thesis.

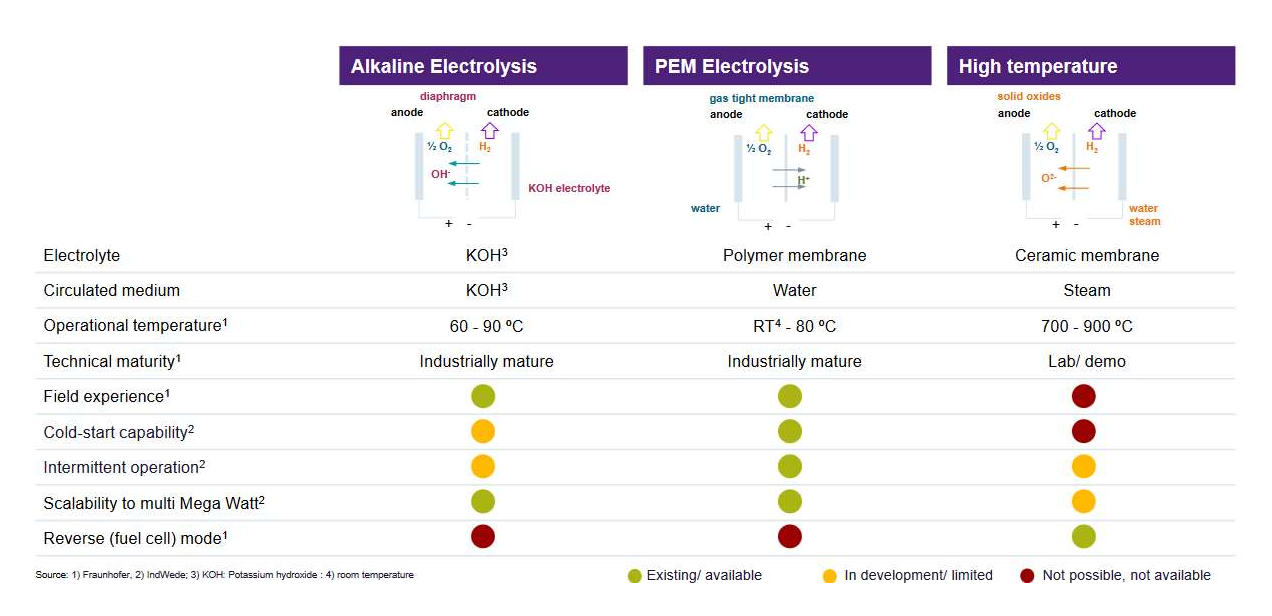


Figure 74 Overview of the current state of the art electrolyser technologies [76]

4.2.1 Production of green hydrogen

Electrolysis is an energy intensive process, which happens in an electrolyser powered by electricity. Electrolysis is the process when liquid water is split into hydrogen (H₂) and oxygen (O₂). The chemical formula is given in Equation (6) [57].

$$H_2 O_{lig} = H_2 + O_2 \tag{6}$$

(liquid) water H_20_{lia}

 H_2 (gaseous) hydrogen

 0_2 (gaseous) oxygen

Polymer exchange membran electrolyser

A PEM cross section as well as the related chemical reaction equations are shown in Figure 75. In a PEM electrolyser the anode is located at the water inlet. At the anode the liquid water is decomposed into ions and oxygen. The oxygen and the not decomposed water leaves the cell. The ions migrate driven by an electric field through the membrane to the cathode side, where these ions are reduced to hydrogen. On both sides of the membrane are porous catalyst layers supporting the chemical reactions [57].

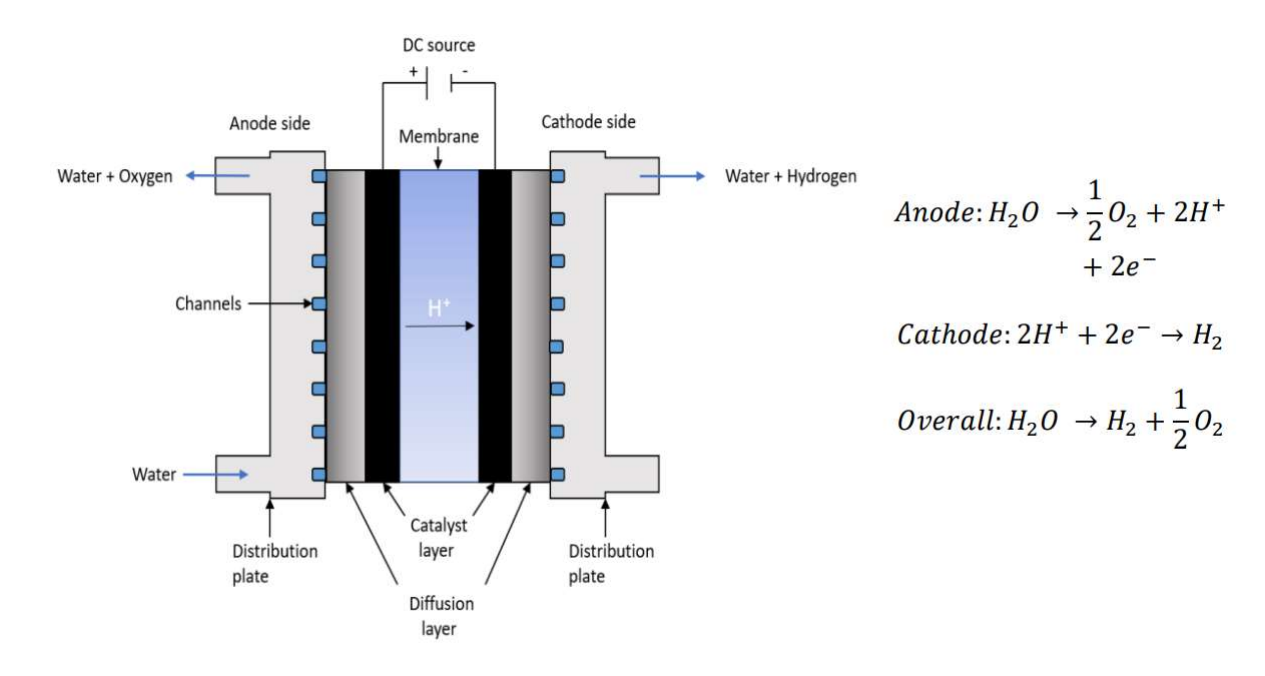
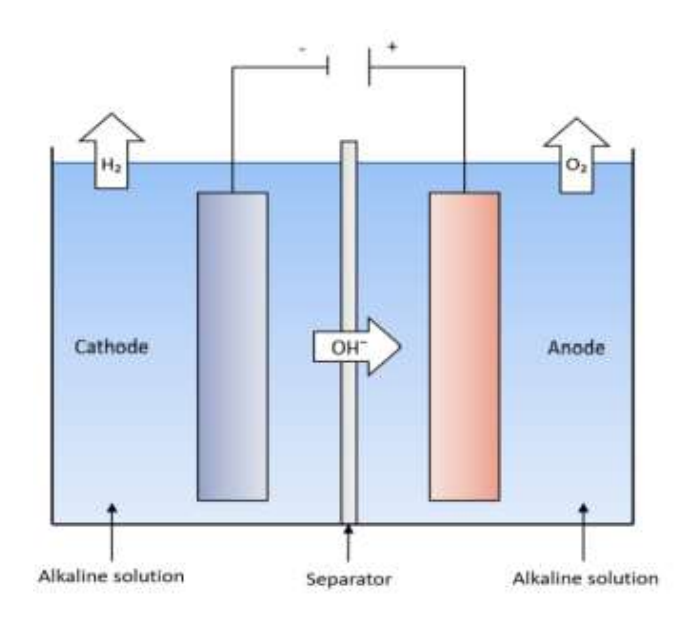


Figure 75 Cross section and chemical reaction equations of the PEM electrolyser [57]

PEM electrolyser allow high current densities (> 2 A cm²), cell voltages of 1,6 – 2,0 V and work at cell temperatures up to 80 °C, while having high efficiencies of 70 – 80 %. The generated hydrogen is very pure (99,99 %). Another advantage of PEM electrolyser is their short response time and a very wide dynamic operation range, which makes them perfectly suited for the use of fluctuating renewable power. Due to the use of noble metals the challenge is to increase their capacity, while keeping the production costs of the stacks low [57].

Alkine water electrolysis

The AEL differs from the PEM electrolyser in the liquid alkaline electrolyte instead of the membrane. The electrolyte transports the negative charged hydroxide ions from the cathode through the separating diaphragm to the anode. At the anode the hydroxide ions release electrons forming water and oxygen. The negative charged electrons return to the cathode, where they are consumed by the hydrogen ions to form hydrogen. Figure 76 depicts an AEL cell including the chemical equations [57].



Anode:
$$20H^- \rightarrow H_2O + \frac{1}{2}O_2 + 2e^-$$

Cathode:
$$2H_2O + 2e^- \rightarrow H_2 + 2OH^-$$

Overall:
$$H_2O \rightarrow H_2 + \frac{1}{2}O_2$$

Figure 76 Scheme of a AEL cell and the related chemical reaction equations [57]

The structure of the AEL is easier and the materials are cheaper and more durable, why AEL facilities are in general cheaper. The cell temperature can be up to 90 °C reaching efficiencies between 60 – 80 %. The operating pressure in the AEL stack is lower than in PEM cells, which is why a higher compression for transportation is needed. AEL cells with higher pressures are under development [57], [77].

Table 20 shows typical specifications of PEM and AEL electrolyser. These typical specifications are the base for further calculations. The specifications of electrolysers can vary in a broad band depending on their individual use [57].

Table 20 Typical specifications of a PEM and AEL electrolyser modified by [57], [78]

	PEM	AEL	
current density	1,5	/	A/cm²
efficiency	80	80	%
cell temperature	80	/	°C
anode pressure	5	7	bar
cathode pressure	30	7	bar
cell area	/	2082	cm²
operating current	/	200	А
max. DT in stack	5	5	K

4.2.2 Stack-cooling (Use case H₂-1)

During the electrolysis more thermal energy is produced by the electrodes than consumed by the endothermal splitting of water. The generated thermal energy follows the formula given in Equation (7). The temperature difference within the electrolysis stack should be kept very small (0 K (isothermal) - 10 K). The small temperature difference helps to drive the electrolyser in a stationary way. Furthermore, higher

temperature differences lead to an increase of aging and fouling processes. Hence, the stack must be continuously cooled. The cooling of the stack is done by small water flown channels inside the electrolyser. The thermal energy losses of the stack are small compared to the thermal energy extracted by the cooling circuit [57], [78], [79], [80].

$$\dot{Q}_{gen} = n_C \left(V_{cell} - V_{tn} \right) i A_{cell} \tag{7}$$

 \dot{Q}_{gen} generated thermal power in electrolyser in W

number of cells n_{C} V_{cell} cell voltage in V

 V_{tn} thermoneutral voltage in V i current density in A/cm²

cell surface in cm² A_{cell}

A simplified scheme of the use case H₂-1 is shown in Figure 77. The cooling fluids exits the electrolysis stack with around 79 °C. Usually, the thermal energy is dissipated via a fan to the environment. In this setup in a HEX the thermal energy is transferred to the closed-loop source circuit of the HP. In the HEX the stack cooling circuit is cooled down to 74 °C before it reenters the electrolysis stack. The additional HP source circuit allow greater temperature spreads than 0 – 10 K, which improves the efficiency of a HP. The HP utilizes the absorbed thermal energy of the source circuit and uses it to lift the sink to higher temperatures. The sink of the HP with 90 – 130 °C can be used for DH or as process heat [57], [79], [81].

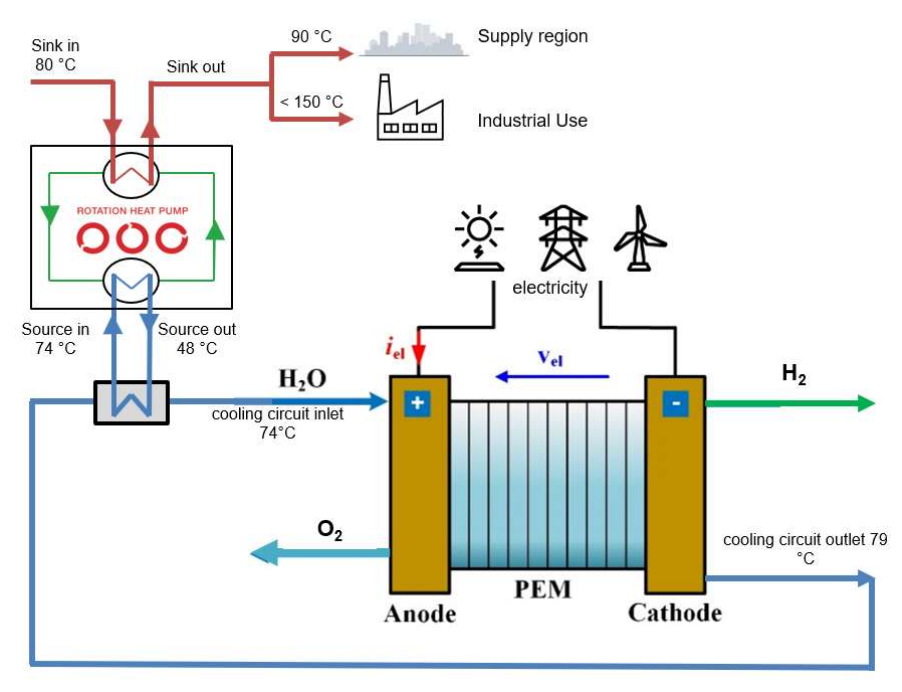


Figure 77 Simplified scheme of an electrolysis stack and the cooling circuit including the ecop RHP modified by [22], [81]



In an ecop internal simulation tool the ecop RHP as shown in Figure 77 has been simulated. The result of the ecop RHP simulation is shown in Figure 78. With the given temperatures an COP of 3,84 can be achieved. A further cooling down of the source flow is not reasonable, because of the temperature difference within the HEX [68].

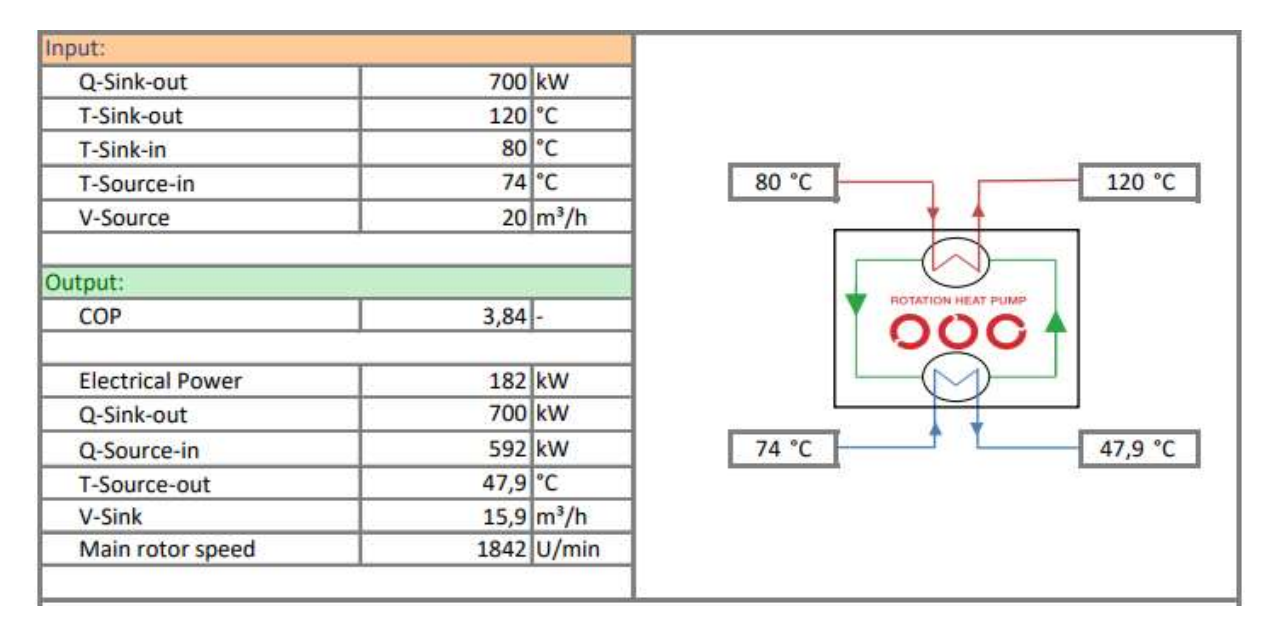
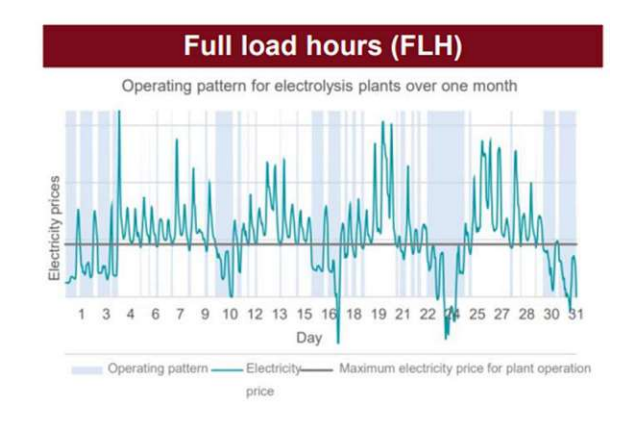


Figure 78 RHP simulation for electrolyser stack cooling use case H₂-1 [68]

Figure 79 (in this figure, (comma) are used as thousand-digit-draw) shows the predicted market share of AEL, PEM and solid oxide electrolyser cell (SOEL) electrolysers in 2030 and 2040. PEM and SOEL will gain increasingly market shares by 2040 compared to AEL. The FLH very much depend on the gird integration concept, but are assumed to be around 3 500 h/yr [82].

Technology data				
	Waste	Waste heat temperature	Technology share	
	share		2030	2040
AEL	20%	70°C	80%	52%
PEM-EL	25%	70°C	18%	40%
SOEL	-	-	2%	8%



Alkaline electrolysis (AEL)

- Most mature technology
- Polymer electrolyte membrane (PEM-EL)
- Increasing market shares

Solid oxide electrolysis (SOEL)

No useable waste heat

- FLH depending on integration concept
- Grid connected electrolyser
- Dedicated RES (no grid connection)

Assumed FLH value: 3,500 h

Figure 79 Market share of electrolyser technologies and predicted full load hours; in this figure, (comma) are used as thousand-digit-draw [82]

In Lulea (Sweden) a similar project as described above has been planned and is currently under construction. The concept of Lulea is shown in Figure 80. There, a combination between renewable energy sources (wind power), H₂ electrolysers, DH, H₂ transportation and Methanol synthesis is planned. The methanol synthesis works as a Power-to-fuel plant as storage unit [57].

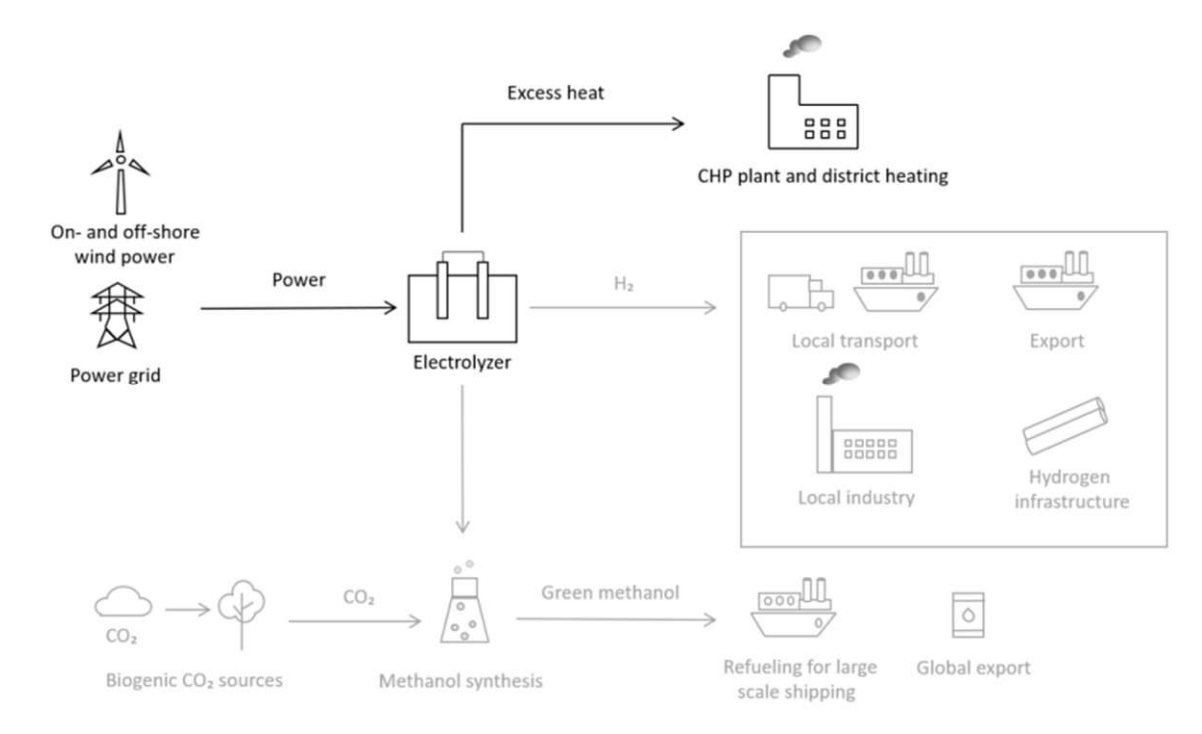


Figure 80 Waste heat utilization of an electrolyser reference facility in Sweden [57]

In Lulea an electrolyser capacity of 100 MW is planned. The amount of extractable thermal energy by stack cooling for either a PEM or AEL is shown in Table 21 (in this table . (dot) is used in difference to , (comma)). In Table 21 it can be seen, that due to the lower efficiency of the AEL the waste heat potential is greater than for PEM electrolyser. Nevertheless, further calculations are focused on the PEM, because the bigger part of new electrolysis plants will follow this technology [57], [83].

Table 21 Specifications and waste heat potential of a 100 MW electrolyser (left) PEM or (right) AEL; in this table . (dot) is used in difference to , (comma) [57]

	PEM	AEL
Parameters	Value	Value
Required number of cells	34 530	218 030
Cell voltage [V]	1.93	2.29
Current density [A/cm ²]	1.5	200
Cell temperature [°C]	80	80
Waste heat temperature [°C]	79	80
Cooling fluid temperature [°C]	74	75
Hydrogen production [kg/hour]	1929	1624
Electrical efficiency [%]	76.7	64.5
Mass flow of cooling fluid [kg/s]	1108	1694
Heat/Electric power ratio	0.23	0.35
Waste heat output from stack [MWth]	23.2	35-5
Extracted waste heat from stack [%]	23.2	35.5
Extracted heat from the stack [MWth/yr]	203 060	310 630

Figure 81 shows the integration of the HP for stack cooling in Lulea. In the given scenario the DH feed / return is depending on the summer or winter period 40 °C / 80 °C or 60 °C / 100 - 115 °C. During the summer months (around 50 % of the time) the heat pump is not used. In this time thermal energy of the electrolyser is transferred via a HEX to the DH system. In winter the HP operates in a parallel setup to heat the DH return to the needed temperature [57].

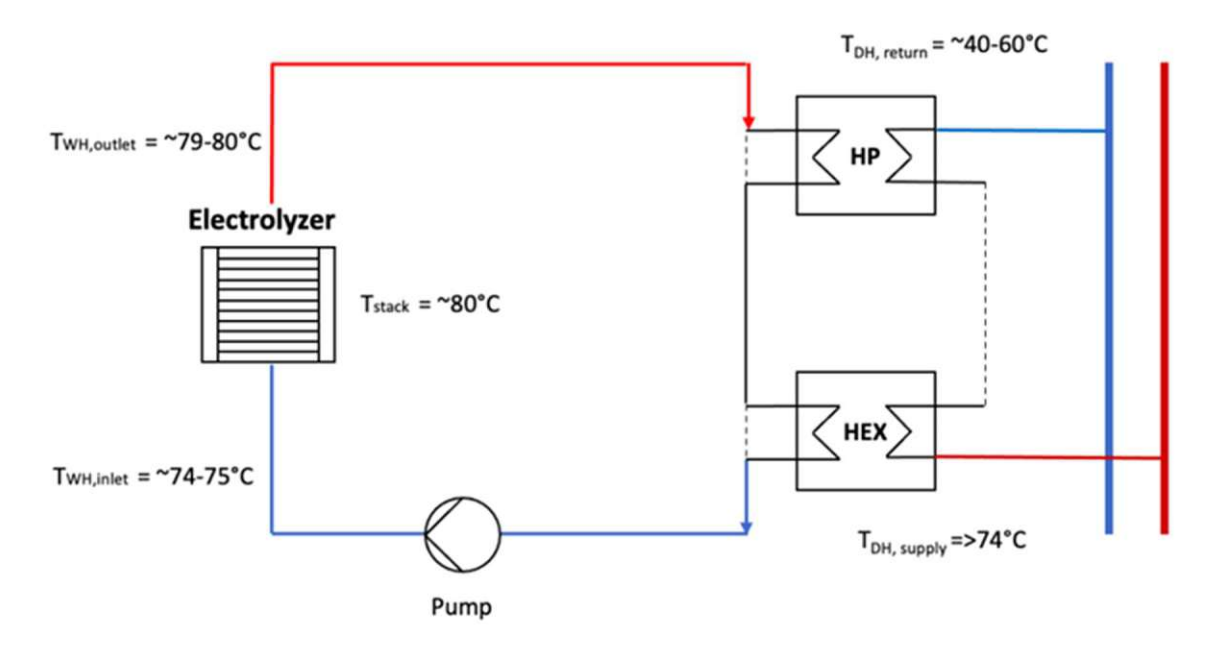


Figure 81 Cooling circuit and DH connection of the stack cooling in Lulea [57]

The planned heat pump in Lulea is not specified in detail. It is mentioned that the HP works with a two staged compressor (for the high temperature lift) and the refrigerant is R1234ze(Z). Some HP parameters are summarized in Table 22 (related to the ambient temperature) (in this table . (dot) is used in difference to , (comma)). The COP given in Table 22, is referred to the ambient temperature and therefore not comparable with the COP given in the ecop simulations [57].

Table 22 HP specifications of the Lulea project, COP is reffered to the ambient temperature by; in this table . (dot) is used in difference to , (comma) [57]

	PEM	AEL
HP parameter	Value	Value
Thermal waste heat input to HP [MWhth/year]	105 690	151 090
Compressor electricity requirement [MWh _e /yr]	11 760	16 510
Heat pump output to DH [MWhth/year]	116 630	166 470
Peak thermal power [MW _{th}]	29.35	44.7
Maximum COP	16.5	16.7
Average COP	9.9	10.1
Annual operation ratio [%]	52	48.5

Regarding the literature this application is economical feasible. This means that the LCOH of the cooling system including HP, HEX and auxiliary system are comparable to other thermal energy sources. The sensitivity analysis of the LCOH for the PEM electrolyser is shown in Figure 82 (AEL is very similar). The CAPEX is the most sensitive part followed by the discount rate and electricity price [57].

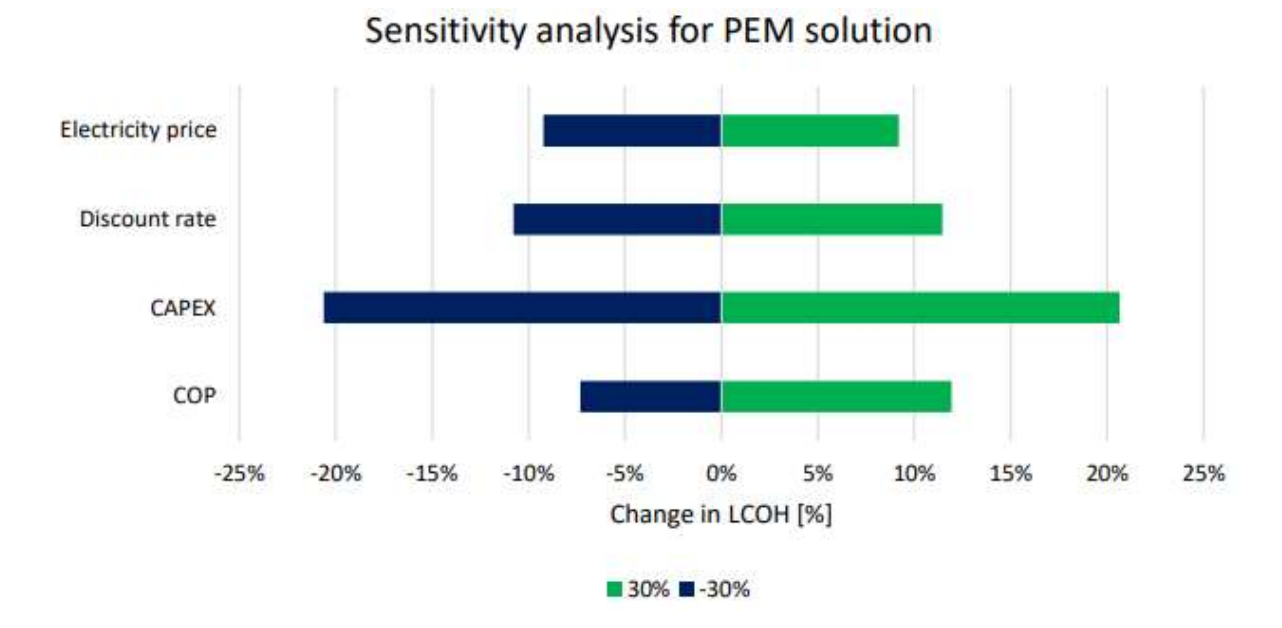


Figure 82 Sensitivity analysis of the reference scenario cooling system [57]

The ecop RHP in the more important winter period would have specifications given in Figure 83. The COP of the ecop RHP in this specific exemplary scenario would result in 5,97 [68].

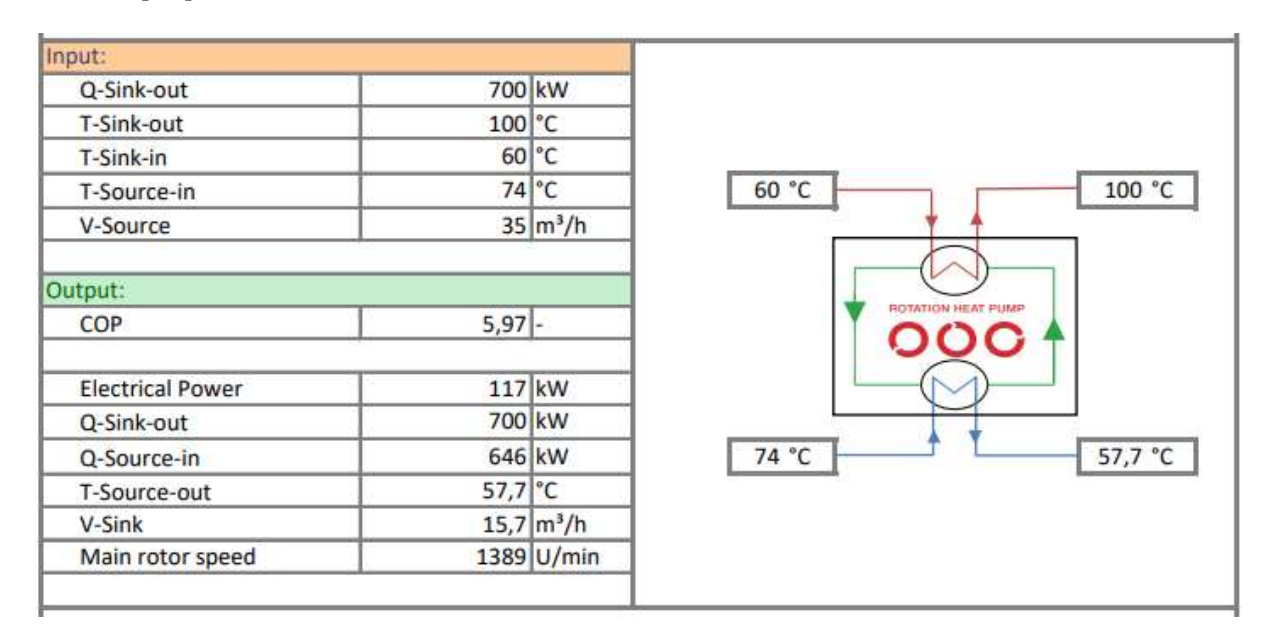


Figure 83 Specification of the ecop RHP for the Lulea DH application [68]

The thermal power for stack-cooling of a 100 MW PEM-electrolysis plant result in 23,2 MW (Table 22). To utilize the whole thermal energy around 39 ecop RHP would be needed in this facility. The total output of the ecop RHP would result in 613,3 m³/h water with 100 °C (27,37 MW) (based on Figure 83) [70].

4.2.3 Gas drying of hydrogen (Use case H₂-2)

After the production of green hydrogen by electrolysis the hydrogen is fully saturated with water vapor. To increase the purity of hydrogen and the efficiency of the compression a two-staged gas drying process, to reduce the amount of gaseous water in the hydrogen is added. Figure 84 shows the relative humidity of hydrogen in accordance to the hydrogen pressure and temperature. The values are calculated by the saturation vapor pressure of water in hydrogen [80]. Depending on the further use of hydrogen residual moistures between 62 ppm in Pipeline applications and < 5 ppm in fuel cell applications are needed [80].

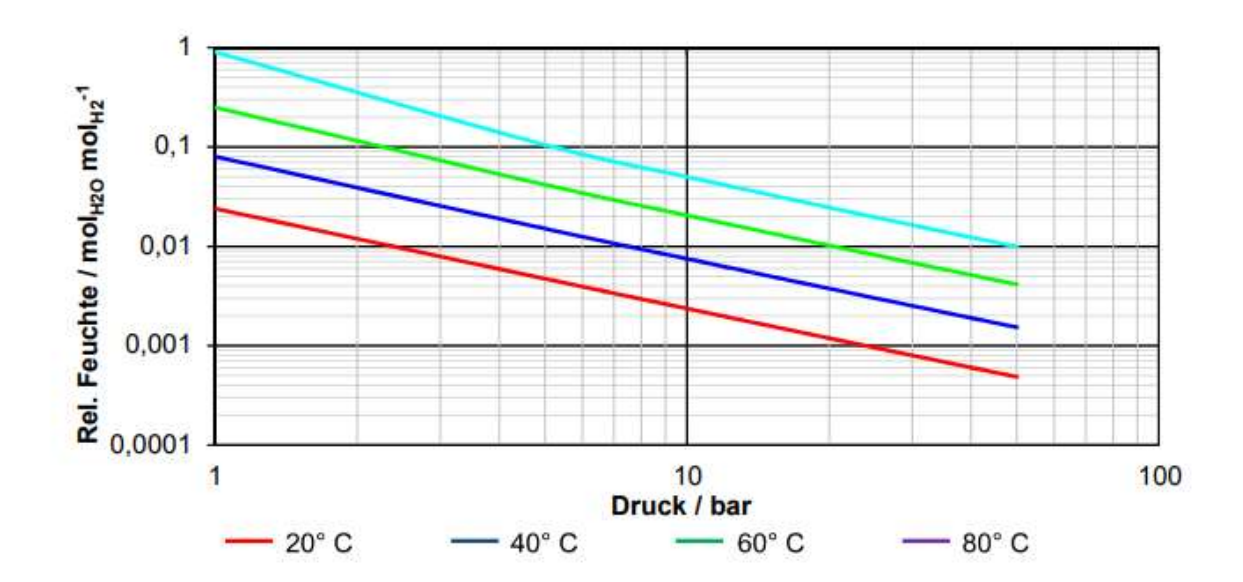
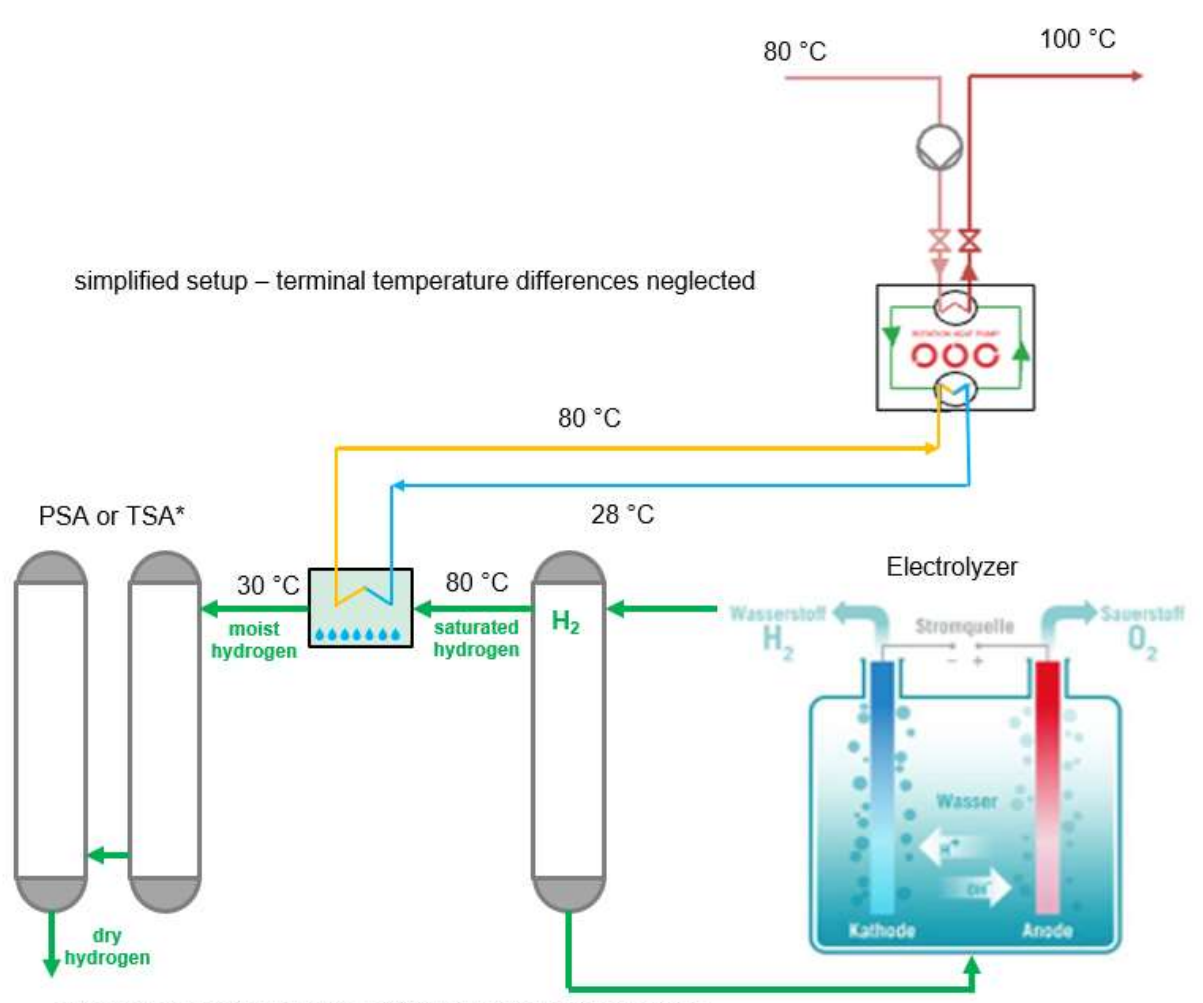


Figure 84 Relative humidity of hydrogen depending on the pressure and temperature [80]

In the first drying step hydrogen is cooled down from its production temperature of around 80 °C to 20 – 40 °C. In this step around 90 % of the water condensates and can be removed [57].

The second step is based on the absorption of water on molecular sieves or silica gel. The hydrogen flows through the drying bed and the water is being adsorbed. After the saturation of the drying bed, the bed must be regenerated. For a continuous operation this process is executed as a swing adsorption dryer with two absorption beds. In form of the regeneration process it can be differed between temperature swing adsorption dryer (TSA) and pressure swing adsorption (PSA). To avoid contamination of the hydrogen the desorption is done with a part of the dry hydrogen stream [57].

The ecop RHP can be used to utilize the low temperature thermal energy of the first step of the gas drying process. Figure 85 shows an exemplarily example how this process could look. The generated saturated hydrogen is cooled down from around 80 °C to 30 °C loosing around 90 % of the absorbed water. The ecop RHP uses the thermal energy of the drying circuit as source to lift a sink to valuable temperatures. In the next drying step, the hydrogen is further dehumidified in a PSA or TSA [57].



PSA: Pressure swing absorption, TSA: temperature swing absorption

Figure 85 Simplified scheme of waste heat recovery of the hydrogen drying process [57], [70]

In this model the hydrogen is cooled down from 80 °C to ~ 30 °C. In the case of a 100 MW electrolysis with a hydrogen mass flow of 1 929 kg/h 400 kW of thermal energy (calculated by Equation (8)) is released during the first step of the drying process. The specific heat capacity is simplified as the arithmetic mean between the start and end state of hydrogen leaving the water vapor unheeded [57].

$$P_{cool, gas \, drying} = \bar{c}_{H_2} \, \Delta T_{H_2, cooling} \, \dot{m}_{H_2, production}$$
 (8)

 $P_{cool, gas \, drying}$ cooling power for gas drying in kW

 \bar{c}_{H_2} mean specific heat capacity of hydrogen in kJ/(kg K)

 $\Delta T_{H_2, cooling}$ cooling circuit temperature difference in K

 $\dot{m}_{H_2, production}$ mass flow of hydrogen in kg/s

Figure 86 shows the simulation of the ecop RHP for a gas drying use case. The RHP uses the extracted energy to heat the sink from 80 - 100 °C with a COP of 3,56. In Figure 86 is a Q_{source,in} of 584 kW given, which is greater than the extractable 400 kW

of a 100 MW electrolysis facility. This leads to the fact, that waste heat utilization of hydrogen drying is only feasible in electrolysis facilities > 100 MW [68].

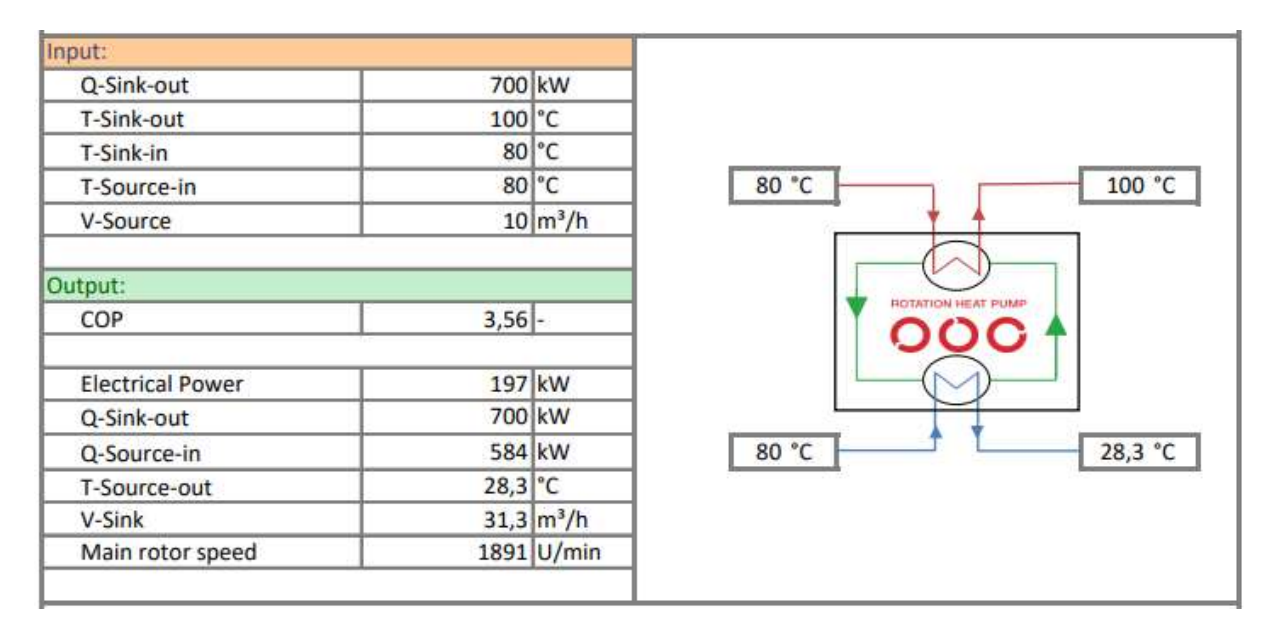


Figure 86 RHP simulation for gas drying use case H₂-2 [68]

4.2.4 Hydrogen compression (Use case H₂-3)

Hydrogen is a very light gas (density = 0,08375 kg/m³ at 20 °C and 1 atm), which is why it occupies a very large volume. To make hydrogen storable it is either compressed or liquified. Liquification is due to the cooling down to < -150 °C very energy intensive and former even more expensive than compression. Hence, hydrogen is usually compressed to different pressure levels depending on the further usage [84], [85], [86], [87]. Hydrogen pipelines operate between 50 - 100 bar, while cavern storages can have a pressure up to 200 bar. Hydrogen refueling stations usually have hydrogen storages with 750 bars for cars and 350 bar for trucks and buses.

The compression of hydrogen is an energy intense process and there have been different types of compressors developed (mechanical, non-mechanical: cryogenic compression, metal hydride compression, electrochemical compressors, adsorption compressors) [88]. Mechanical driven compressors are currently the state of the art and most widely used. Figure 87 shows the needed specific energy consumption to compress one kg of hydrogen starting from a specific cathode pressure to 100, 200 or 750 bar [80], [89], [90].

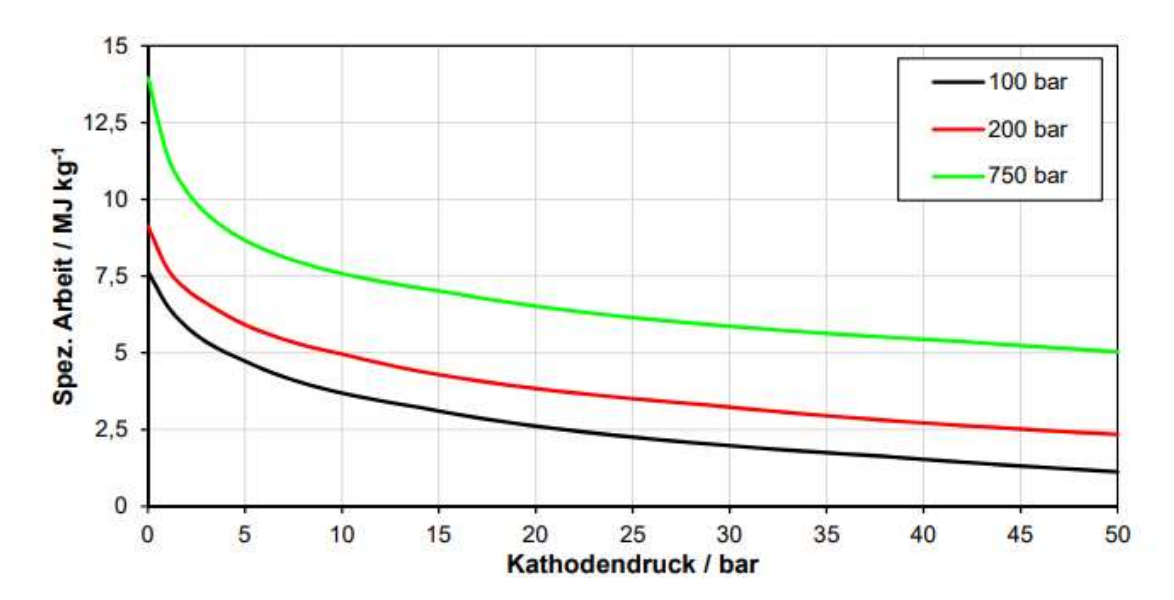


Figure 87 Specific energy consumption for the compression of hydrogen [80]

In terms of compression, it needs to be distinguished between an isothermal compression (temperature changes are steadily balanced) and isentropic compression (no thermal energy transfer while compression). The isothermal process is less energy consuming, but technical not feasible. The used compromise to decrease the energy consumption, while being compact and technically feasible are compressors with interstage cooling.

Figure 88 shows the compressor work as a function of the compression ratio for an isothermal, isentropic and intercooled compression process. The isothermal process needs the least energy. The intercooled process is cooled twice at 5 and 25 bar [80], [85].

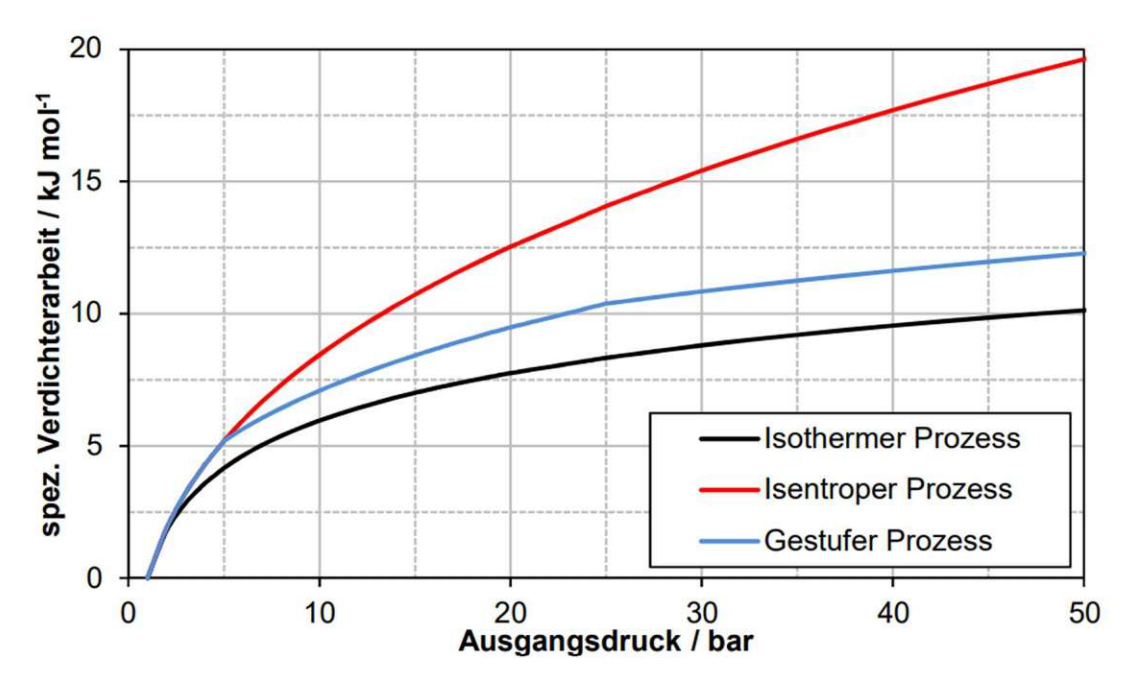


Figure 88 Specific compressor work for an isothermal, isentropic and intercooled compression [80]

To reach very high pressures several compressors are installed in series having intercooling stages in between. The intercooling stages are heat exchanger, exemplary cooled by water or other cooling fluids. Such an intercooled compressor arrangement is shown in Figure 89 [89].

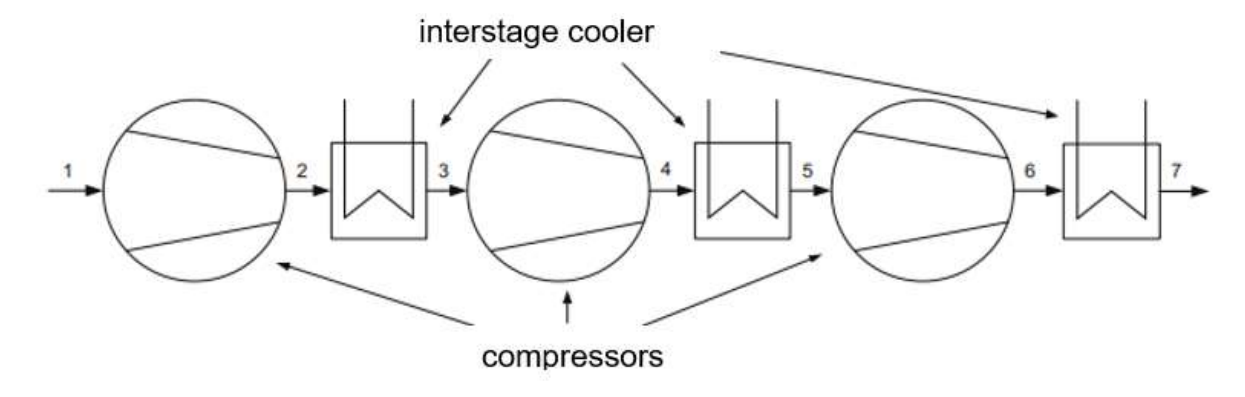


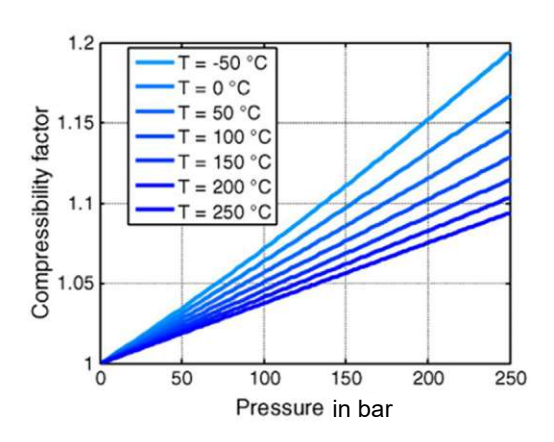
Figure 89 Exemplary intercooled compressors in series [85]

The temperature change of a real gas during an isentropic compression as a function of the compression ratio can be calculated by Equation (9). The gas is characterized by the compressibility factor and the real isentropic exponent [85].

$$T_{2} = T_{1} \frac{Z_{1}}{Z_{2}} \left(\frac{p_{2}}{p_{1}}\right)^{\frac{\kappa_{p,\nu}-1}{\kappa_{p,\nu}}}$$
(9)

 T_1 initial temperature in K T_2 final temperature in K Z_i compressibility factor p_2 compression ratio p_1 real isentropic exponent $\kappa_{p,v}$

The compressibility factor and real isentropic exponent as a function of the pressure and temperature for hydrogen are visualized in Figure 90 [85].



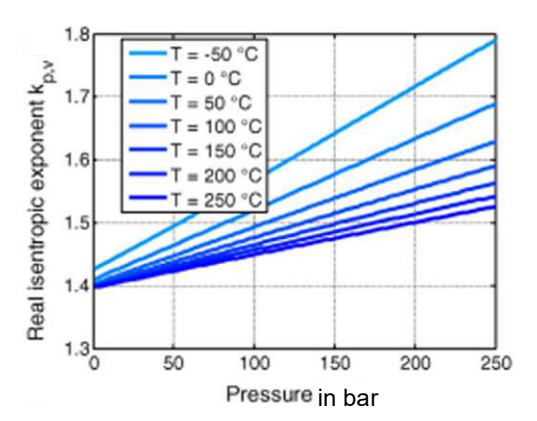


Figure 90 Compressibility factor (left) and real isentropic exponent (right) of hydrogen as a function of pressure and temperature [85]

The resulting final temperature of an isentropic compression of hydrogen starting from 10 °C and 50 bar depending on the compression ratio is pictured in Figure 91 [85].

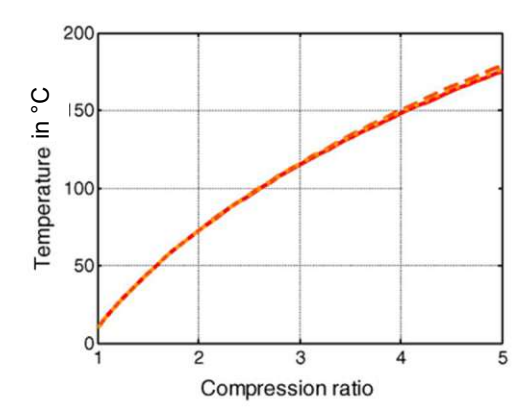


Figure 91 Resulting temperature of an isentropic compression of hydrogen starting at 10 °C and 50 bar [85]

The thermal energy of the intercooling stages is usually dissipated by a fan to the environment. Alternative a HP can be used for cooling down the cooling circuit of the compressor interstage cooler. The HP uses the cooling circuit as source extracting thermal energy to lift the sink circuit. Depending on the temperature level the sink can be used in different matters. The extractable energy of the cooling circuit varies depending on the end compression pressure and the compressor type [70].

Figure 92 shows a simplified visualization of a single stage compression. The calculated values are based on a compression from a cathode pressure of 30 bar to 80 bar for pipeline transportation and the hydrogen mass flow of a 100 MW electrolyser. "Q° waste heat" is the thermal energy produced by the compressor during the compression in dependence of the compressor efficiency. During the compression the temperature of hydrogen increases according to Equation (9). "T2" is the end temperature after the compression to 80 bar. "Q°cool" is the energy that can be extracted by cooling down the hydrogen from the compression end temperature ("T₂") to the needed storage temperature ("T₃") [70].

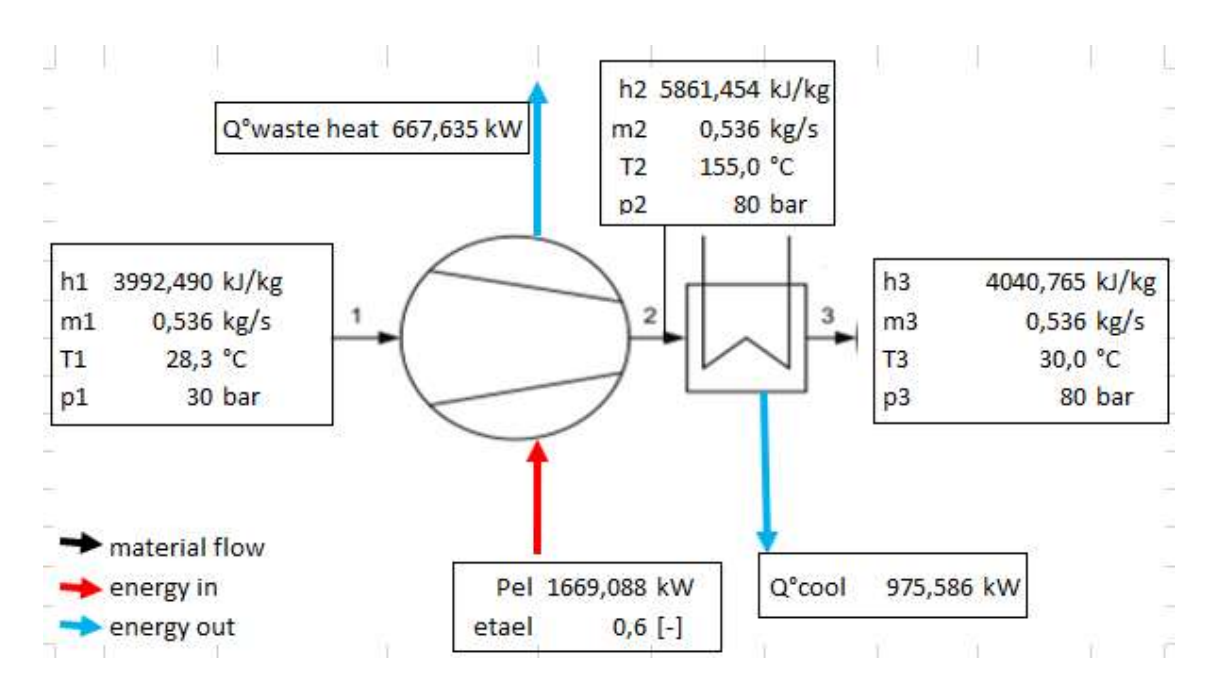


Figure 92 Simplified visualization of energy flows during compression and possible thermal energy extraction [70]

Table 23 shows a summary for the extractable thermal energy depending on the cathode pressure, initial temperature (hydrogen temperature after gas drying) and the storage type (final pressure). If higher end pressures than 80 bar are necessary, more compressor stages with intercoolers are used. The stages are set to have approximately equal compression ratios. Between each stage the partly compressed hydrogen is cooled down to 30 °C. The mean temperature after compression is the mean temperature of all isentropic compression stages ("T2"). The possible thermal energy extraction is approximated by the sum of "Q°waste heat" and "Q°cool" (see Figure 92) [80], [89], [90].

Table 23 Parameters of the different storage facilities and thermal energy generation during compression *calculated according to Equation (9), parameter estimated by Figure 90 [80], [89], [90]

	Pipeline	cavern storage	hydrogen car refueling station	
initial pressure: cathode pressure	30	30	30	bar
end pressure	80	200	750	bar
initial temperature	28,3	28,3	28,3	°C
compression stages	1	2	3	pcs.
mean temperature after compression	126*	125*	142*	°C
gas temperature after interstage cooling	30	30	30	°C
thermal energy extraction potential	1 264,5	2 518	4 601	kW

The extracted thermal energy can be used in the ecop RHP as source to lift the sink to the desired temperature level. The end temperature of a compressor stage is usually around 100 - 150 °C and is cooled down to around 30 °C. There are different possibilities how the thermal energy of the interstage coolers can be used depending on the temperature level [70].

An example to fully utilize the extracted thermal energy by HP is shown in Figure 93. HP are set in series to cool down the cooling circuit low enough to reach hydrogen temperatures of 30 °C. In this case the highest temperature level can be utilized by the RHP for steam production or other high temperature applications. The lower temperature level can either be used for process heat or for DH [70].

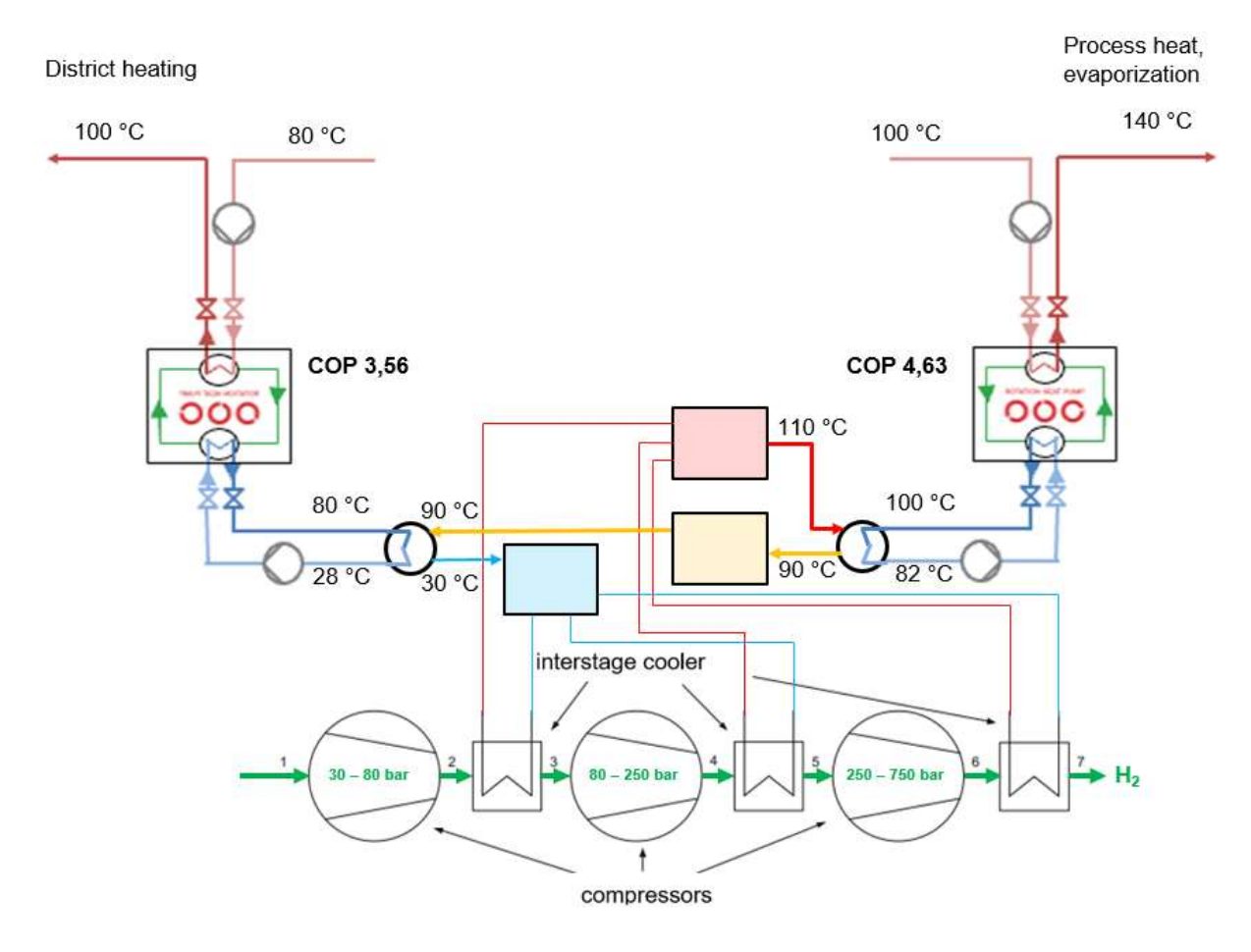


Figure 93 Integration of the RHP in the interstage cooling of the hydrogen compression [70]

Another possibility is to use the highest temperature level directly and only lift the lower temperature levels with the RHP. This waste heat utilization could look like [68]:

- temperature level of 110 140 °C directly used for process heat or steam generation
- temperature level of 90 110 °C lifted with RHP to 140 °C and used for process heat or steam production (RHP according to Figure 94, COP 4,63)

another RHP in series utilizing the lower temperature level (RHP according to Figure 86). Cooling down the source to 28 °C and lifting the sink from 80 to 100 °C for DH.

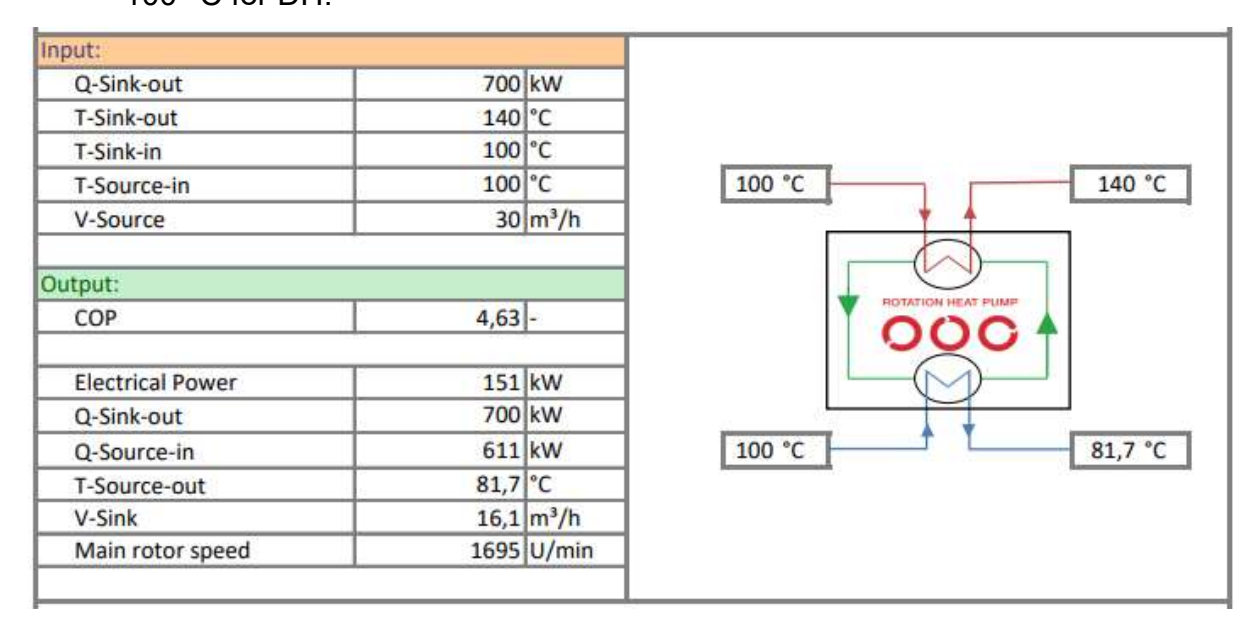


Figure 94 RHP for utilization of hydrogen compression waste heat H₂-3 [68]

4.2.5 Economic efficiency for the H₂ use cases

In all hydrogen use cases the thermal energy is generated anyway and must be extracted or dissipated. Nowadays and especially in small facilities the extracted thermal energy is dissipated by a fan to the surrounding. In contrast to that the thermal energy can be used as source circuit for an HP. The electrolyser and the following facilities must not be adapted to utilize the waste heat with a HP. Therefore, the LCOH for the thermal energy exemplary provided by the ecop RHP can be set to be the costs for the RHP itself. Using the contracting model pictured in Figure 43 the LCOH result in 24 - 86 €/MWh depending on the FLH and the electricity price [70].

4.2.6 Market potential green hydrogen

The 2020 electrolysis capacities in Europe was 130 MW divided 60 and 40 % between AEL and PEM. The highest capacities are in Germany (57 MW), followed by Spain (25 MW), Switzerland (14 MW), Austria (10 MW) and Great Britain (9 MW). Until 2030 the green hydrogen capacity in Europe is going to increase to 40 - 113 GW. From today's perspective is seems like PEM is going to be the major technology for new installations till 2030. The electrolysis capacities by countries in 2030 is shown in Figure 95 (in this figure . (dot) are used as thousand-digit-draw). According to Figure 95 Spain, Netherlands and Germany have the highest electrolysis capacities in development [83], [91].

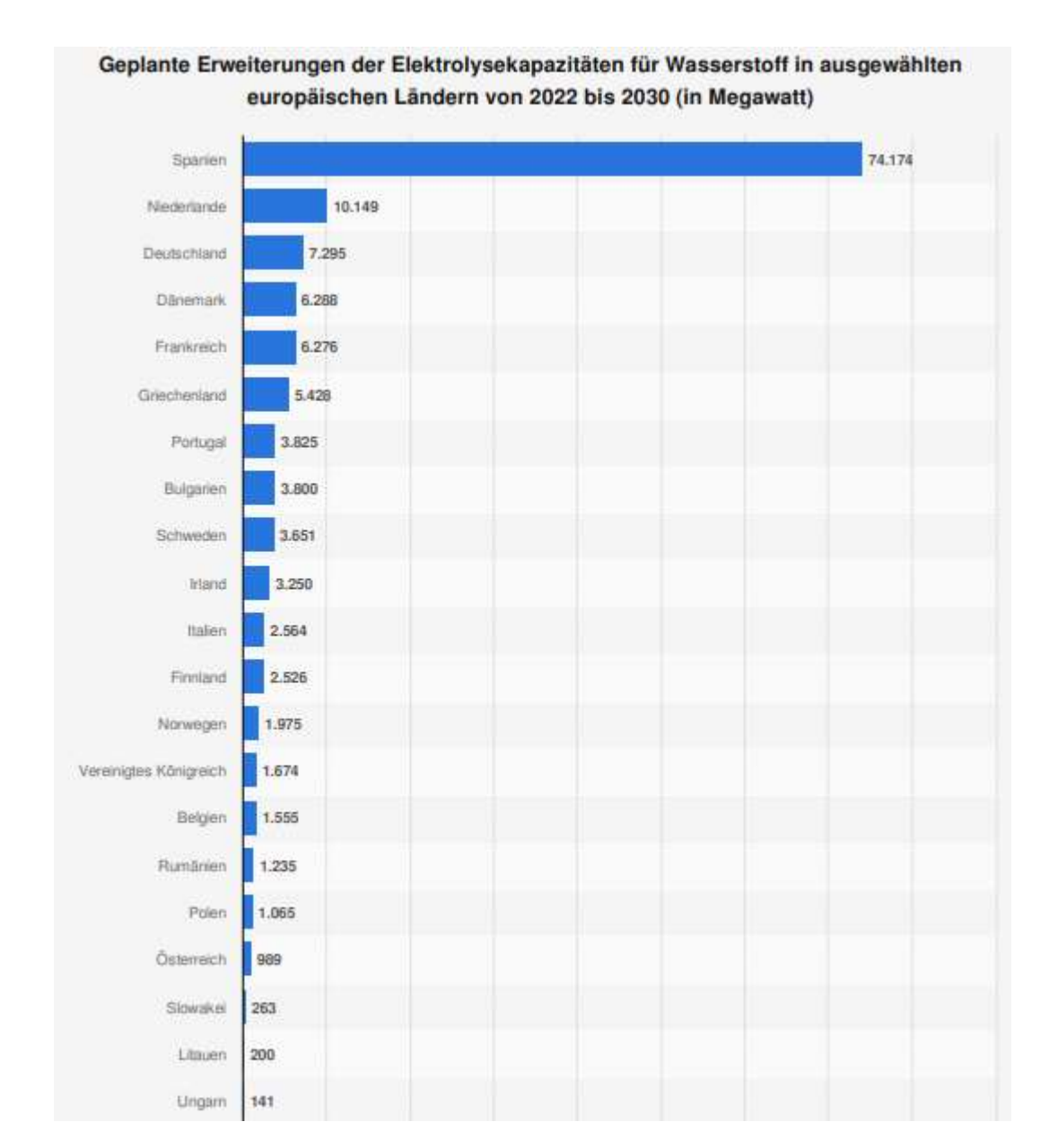


Figure 95 Electrolysis capacity extension from 2022 till 2030 in selected countries; in this figure . (dot) are used as thousand-digit-draw [83]

Figure 96 (in this figure . (dot) is used as thousand-digit-draw) shows the expected AEL and PEM elctrolysers waste heat potential in EU27+UK and in the rest of the world in 2030 and 2040. In 2030 and 2040 the EU27+UK waste heat from electrolysers are expected to be 35 TWh/yr and 250 TWh/yr [91].

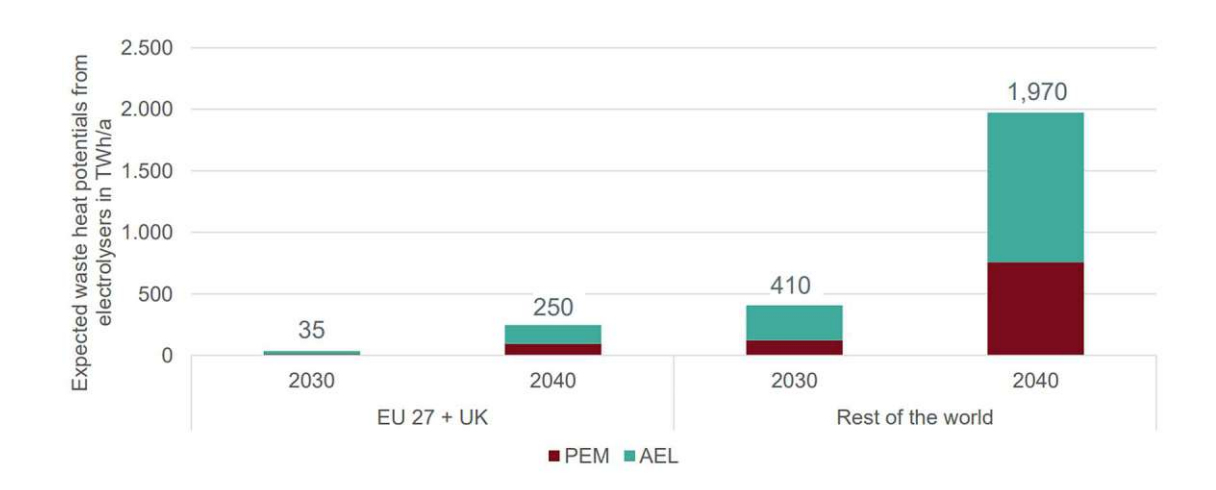
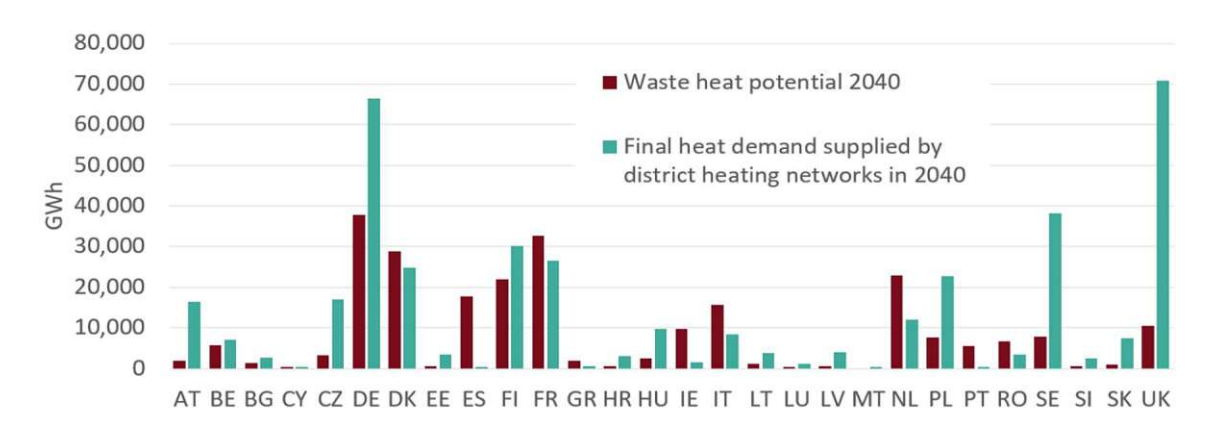


Figure 96 Expected waste heat potential from PEM and AEL electrolysers in the EU27+UK and the rest of the world in 2030 and 2040; in this figure . (dot) is used as thousand-digitdraw [91]

Figure 97 (in this figure, (comma) is used as thousand-digit-draw) shows a comparison between the 2040 electrolyser waste heat potential and DH thermal energy demand in selected European countries. Across all countries, 64% of DH demand can be met by waste heat from electrolysers in 2040. According to Figure 97 Germany, Denmark, Spain, Finland, France, and Netherlands will have the greatest electrolyser capacities. The explanation of the country shortcuts can be found following the Link https://www.gesis.org/fileadmin/upload/dienstleistung/daten/soz indikatoren/eusi/Abb reviations.pdf#:~:text=CY%20Cyprus%20CZ%20Czech%20Republic%20EE%20Esto nia%20H,Switzerland%20N%20Norway%20U.S.%20United%20States%20JAP%20J apan [91].



Waste heat potential: 64% of projected district heating supply in 2040

Figure 97 Comparison between electrolyser waste heat potential and DH heating demand in 2040 in selected European countries; for a explanation of the country shortcuts follow the Link Microsoft Word - Country Abbreviations.doc (gesis.org), in this figure . (dot) is used as thousand-digit-draw [91]

To utilize the waste heat of 40 - 113 GW electrolysis capacity till 2030 by applying the use cases H₂-1 to H₂-3 the technical potential of ecop RHP result in 14 864 to 41 991 plants having each a power of 700 kW. The calculations are based on the 100 MW PEM-electrolyser shown in Figure 98. The biggest potential is in the stack cooling with 13 257 – 37 451 pieces, the potential of gas drying is relatively small with 228 - 645 pieces and the potential of waste heat utilization of hydrogen compression is 1 379 -3 895 based on a given storage / transport mix shown in Figure 98. The calculations are based on the extractable thermal energy per use case and the needed ecop RHP to utilize the thermal energy. Assuming that a HP implementation is technical and economical feasible in most cases the market potential equals the technical potential and is between 14 864 and 41 991 ecop RHP pieces [70].

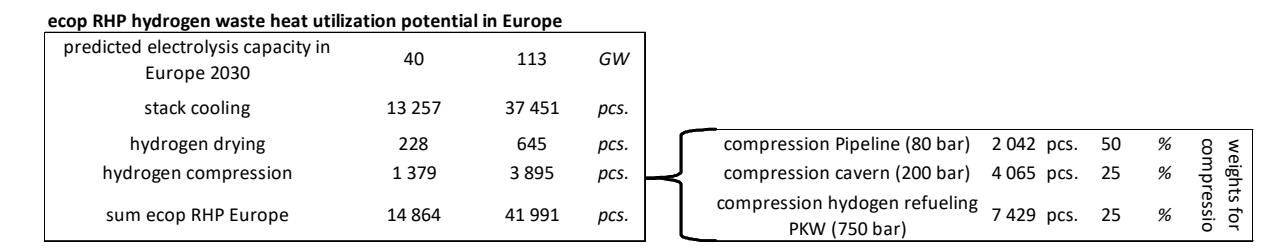


Figure 98 Potential of ecop RHP for the waste heat utilization of green hydrogen production [70]

4.3 Solar thermal energy

With solar energy, a distinction must be made between energy as electricity and as thermal energy. Photovoltaic (PV) cells are used to generate electricity with solar radiation. A combination between HP and PV is reasonable in most cases, because the generated electricity can directly be used to power the HP. To analyze the feasibility of the combination between HP and solar thermal energy (STE) is the aim of this section [92].

The first question is if HP, and STE are competitors or teammates. According to research for this thesis a combination of both systems is reasonable, because it increases the efficiency of the overall system, while it gives the operator more flexibility and redundancy for the energy supply [93].

This section focuses on solar thermal district heating applications (SDH) and the combination of STE, HP, and thermal energy storages (TES) for industries. In this thesis it will not be looked deeper in the different kinds of STE applications, nor in different kinds of storage technologies. In general, it can be said that in Europe flat plate collectors (FPC) are mostly used. Evacuated tube collectors (ETC) are more efficient in the upper temperature level (~ 80 °C). Parabolic through collectors (PTC) reach higher temperatures but are more expensive. Standard FPC reach temperatures of 40 - 60 °C, modified FPC and ETC 80 - 100 °C and PTC 70 - 150 °C. Also,

combinations between different collector types can be used to provide different temperature levels [3]. Usually, a factor of 0,7 kW/m² is used for FPC (thermal power/collector aperture area) to convert collector area to nominal power [94]

In this section the HP will be modeled as an ecop RHP, because of the advantages below. The opportunity of the RHP to flexible adjust the source temperature, while having high COP offers a great advantage in the combination with STE and TES. The adaptability in the sink and source flow offers the prospect to cool down the source sharply to increase the efficiency of the STE system. In the winter arise small STE fractions and low TES temperatures. Nevertheless, provides the RHP due to the temperature lift of up to 55 K also in this case reasonable supply temperatures [22], [95].

There are two major ways how STE, HP and TES can be combined (parallel and serial). The parallel setup is with 61 % the more common one, while 6% are serial applications and 33 % are combinations of both types [96].

A parallel setup is shown in Figure 99. In parallel applications both, STE and the HP feed the TES with thermal energy. Depending on their temperature level they might feed the TES at different heights (temperature stratification) [97]. The integration of a HP offers the possibility to use cheap electricity during the night or during renewable overproduction and save it as thermal energy in the TES (Power-to-heat) [3]. The TES is used to cover the thermal energy demand [97].

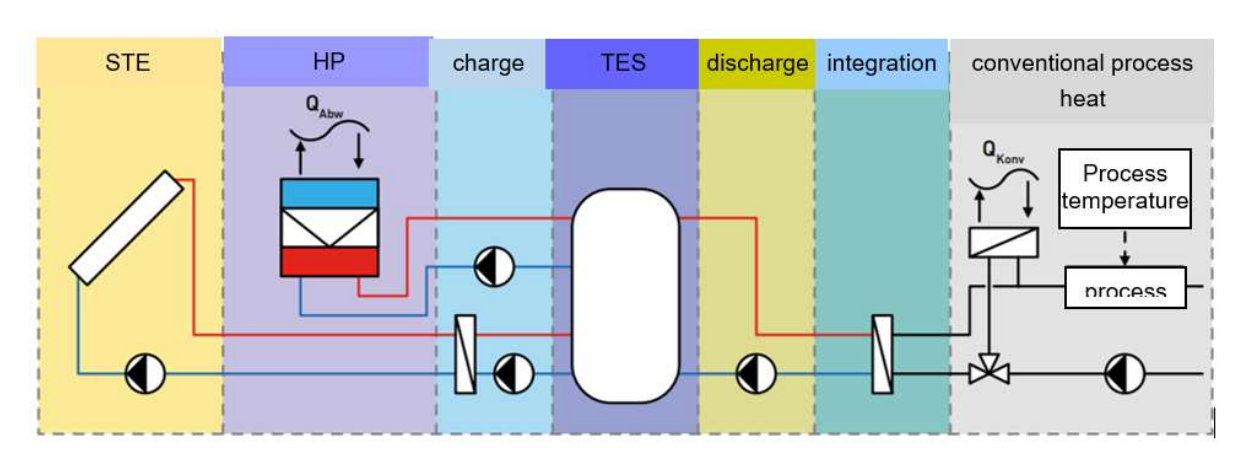


Figure 99 Parallel combination of STE, HP, and TES [97]

In the literature the parallel concept is exemplary used in the chemical industry. STE and HP charge a TES, which cover a washing water demand with 60 – 75 °C. The HP uses low-pressure steam of the evaporation plant with around 35 °C as source. The HP extract thermal energy from the low-pressure steam to lift the TES to the needed temperature level for the washing application [97].

A setup of a serial combination is shown in Figure 100. In the serial combination either the STE (b) or the HP (a and c) is used to reheat the feed for the end consumer.

Respectively the other one is used to charge the TES. If the HP is used for end heating the source can either be any kind of waste heat (a), environmental thermal energy (exemplary ground or air source - a) or the TES feedback (c) [97]. The translation of the descriptions in Figure 100 to English are shown in Figure 99.

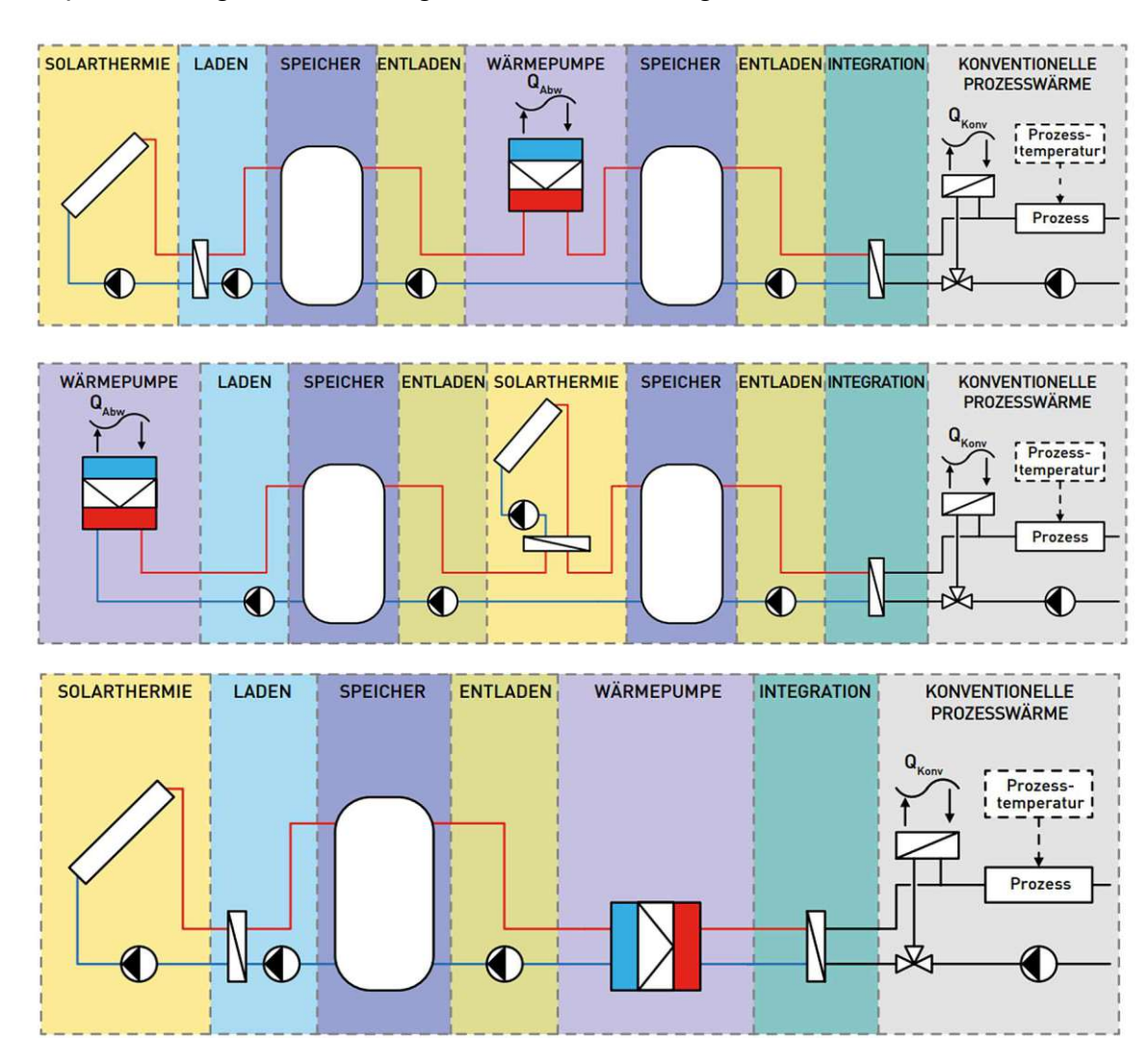


Figure 100 Serial combination of STE, HP and TES; a) top: preheating STE and HP reheat (source for HP waste heat or environment); b) middle: preheating HP and STE reheat (source for HP waste heat or environment); c) bottom: preheating STE and HP reheat (source for HP is the TES return flow) [97]

A possible use case in the literature for the serial application (a) is the supply of hot dry air with 80 – 160 °C for drying applications in an industrial laundry. The STE with up to 40 °C is used to charge the TES. The HP using the moist exhaust air from the drying process as source, to reheat the fluid from the TES. The reheated fluid is used to heat the dry air for drying applications. If necessary, an additional (re-)heater can be ordered [97].

Another serial application for (a), (b) or (c) is the heating and cooling of electroplating baths in the metalworking industry. Electroplating baths needed to be heated up to around 90 °C. In the case of (a) the STE would charge the TES and the HP would lift the TES temperature to the needed level. In the case of (b) and (c) the cooling down electroplating bath can be used as source for the HP to feed thermal energy in the TES or provide thermal energy for other processes [97].

TES are needed because the thermal energy supply of renewable sources is often shifted to its demand. For example, in Europe is the thermal energy demand in winter on average 10 times larger than in summer. For STE the greatest thermal energy supply is during the summer months. Therefore, arises the need of long-term seasonal storages. Short-term buffer storages are necessary for daily fluctuations of the thermal energy demand and supply. Figure 101 shows the solar contribution for heating in accordance with the storage availability. The integration of a TES increases the solar fraction (SF) for heating. The SF is 5 - 20 % with shrot term TES and 30 - 60 % with seasonal TES [98].

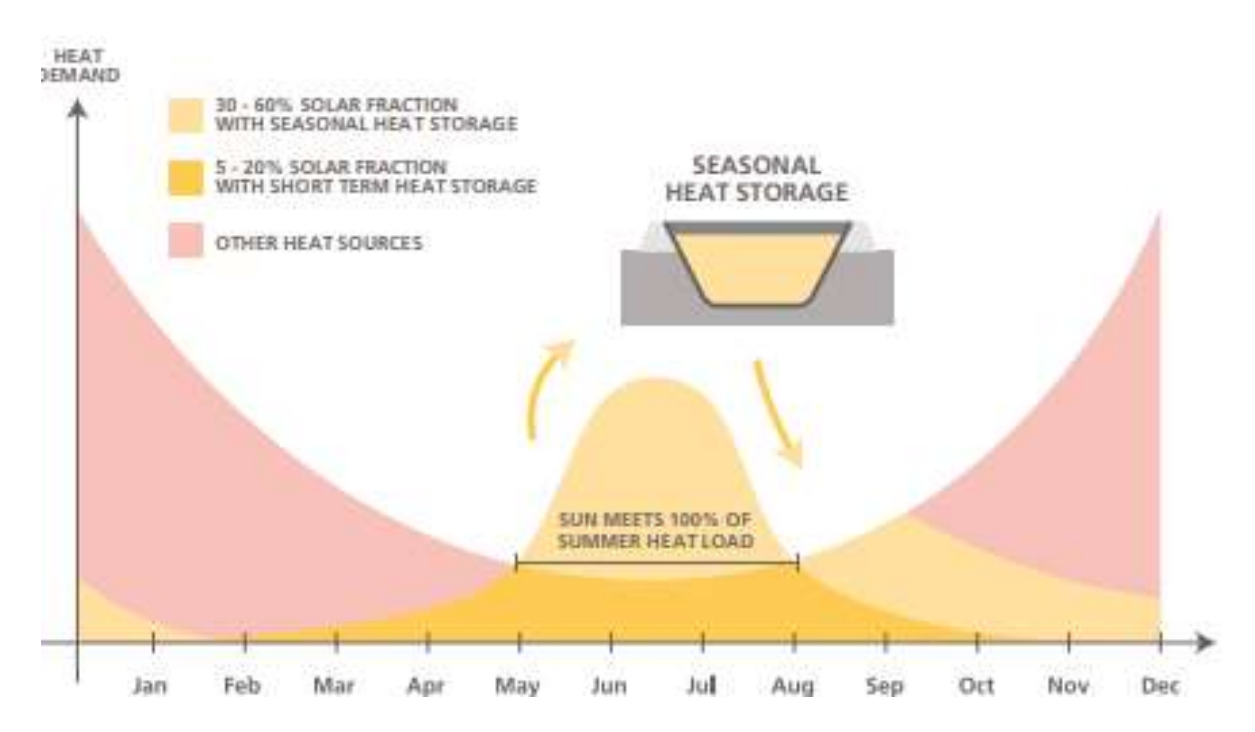


Figure 101 Solar contribution for heating in accordance with the storage availability [98]

Figure 102 shows the four most common long-term sensible TES. Pit thermal energy storages (PTES) are the simplest, cheapest, and have almost no limitation in the size, but consume a large area to build. PTES are the most widely used seasonal TES. Aguifer thermal energy storages need natural aquifers to be realized [99].

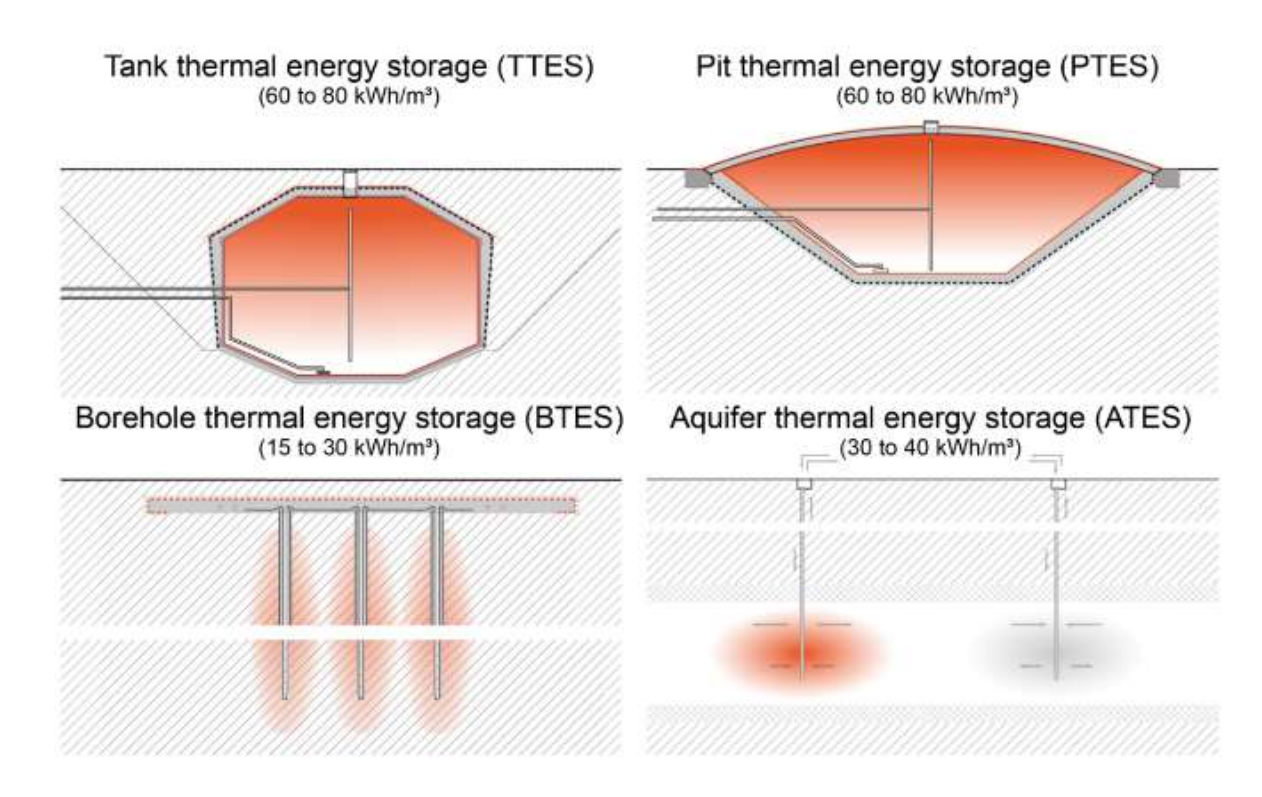


Figure 102 Types of sensible thermal energy long-term storages [99]

4.3.1 Solar district heating (Use case Solar-1)

A concept for cities, towns, and villages to increase the share of solar thermal energy for space heating, domestic hot water (DHW) and industries is solar district heating (SDH). SDH uses solar thermal collectors to capture STE, which is stored in a TES and lifted by a HP to cover the heating demand and to provide the needed temperature level. Furthermore, the additional integration of HP in a SDH systems enable [100]:

- The possibility to reduce the storage temperature, leading to lower thermal losses and higher STE efficiencies.
- The storage capacity increases by the possibility to reach higher temperatures with the HP.
- The possibility to integrate volatile energy sources (sector-coupling: Power-toheat options).

SDH accounts for around 88% of the total installed and operating capacity of largescale STE. Solar process heat (described in 4.3.2) in the industry makes up around 12 % and is currently most used in the mining, textile, and food industry. A STE plant is defined as large-scale if the collector aperture area surpasses 500 m² or 350 kW nominal thermal output [3].

Figure 103 shows an exemplary integration of a HP in a SDH system. In this case the HP heats a buffer storage, to avoid back-mixing and disturbance of the stratification in the large-scale TES. The HP uses the large TES as source and supply a small daily buffer storage to cover the daily heating demand. The additional buffer storage is optional and lead to higher investment costs and higher thermal losses, but a more efficient operation [100].

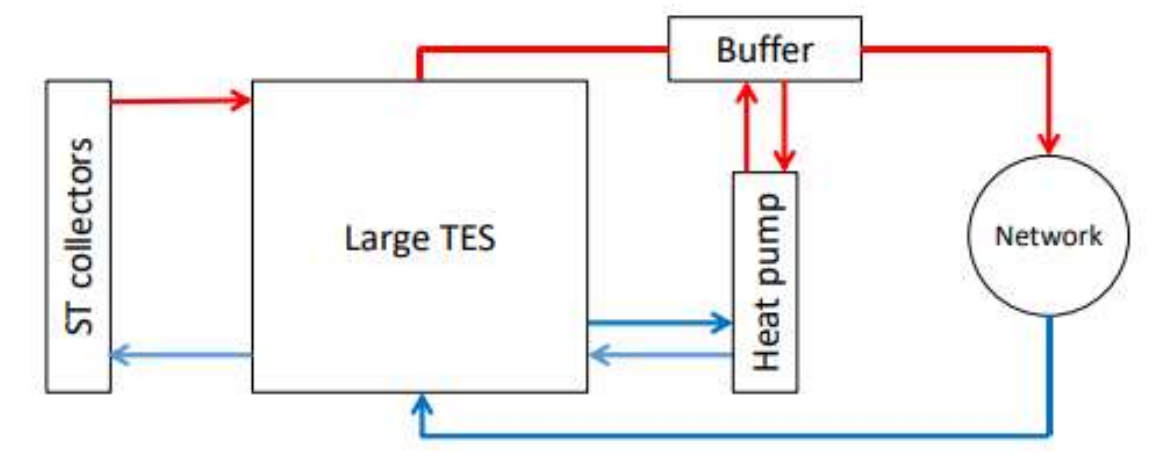


Figure 103 Typical integration of a HP in a SDH system [100]

Figure 104 shows a combination between a DH network and several renewable thermal energy sources. There are two different kinds of STE collectors providing different temperature levels for either a direct use or charging the seasonal thermal storage. HP are used to lift the temperature of the seasonal storage to the needed temperature level of the consumer or to charge the storage using excess heat. A biomass boiler is available to cover peak loads or very high temperature levels. The ecop RHP could substitute the biomass boiler in facts of providing high temperatures of up to 150 °C, while also handling the other HP tasks [101].

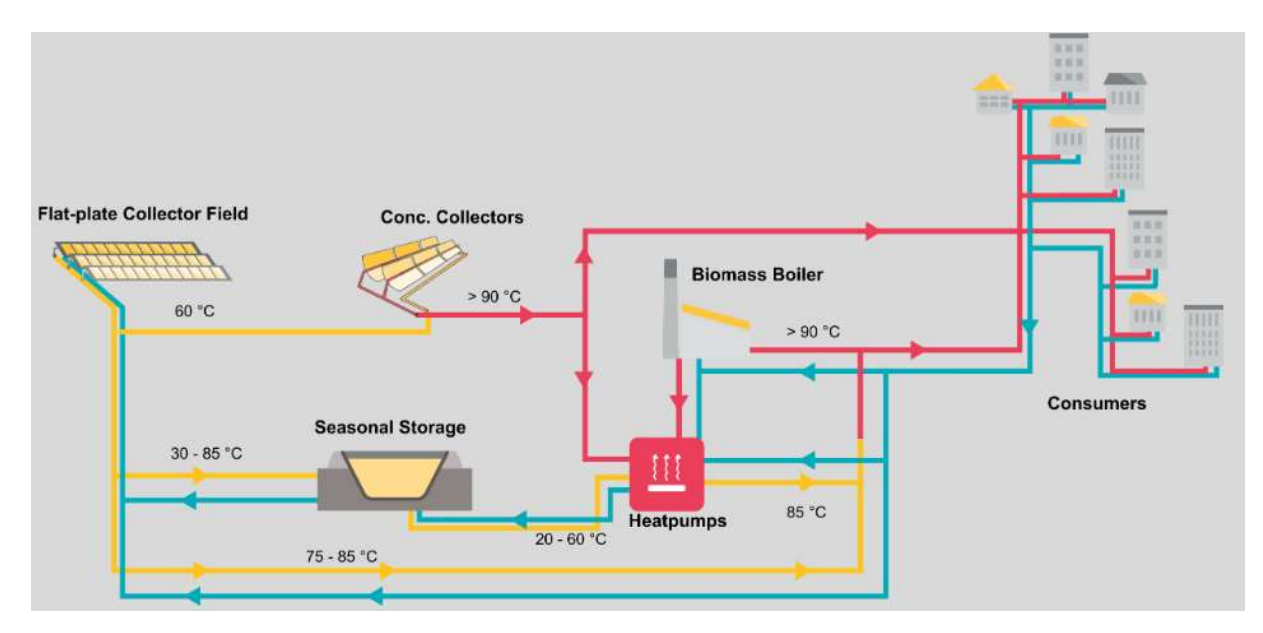


Figure 104 Possible set up of a SDH system with several renewable energy sources [101]

The goal of a SDH system is to minimize the LCOH, while maximizing the renewable energy fraction. To do so, the solar yield must be maximized, while keeping the investment, operation, and maintenance costs low. To achieve this the major hurdles of SDH systems are [3], [94], [101]:

- High capital expenditures (CAPEX)
- High complexity of the system
- Missing system certifications
- Heating supply and demand are staggered
- High space requirement for the collectors close to the demand
- Most existing DH systems require high network temperatures

The effect of the SDH feed and return flow temperature on the solar yield is shown in Figure 105. A reduction of both the feed and the return flow temperature result in higher solar yields. For example, a reduction of 2 K (57 °C – 55 °C) of the return flow offers an 2,8 % increase of the solar yield. Respectively a reduction of 10 K (57 – 47 $^{\circ}$ C = 4th Generation DH network) provide an 10 % increase of the solar yield [102].

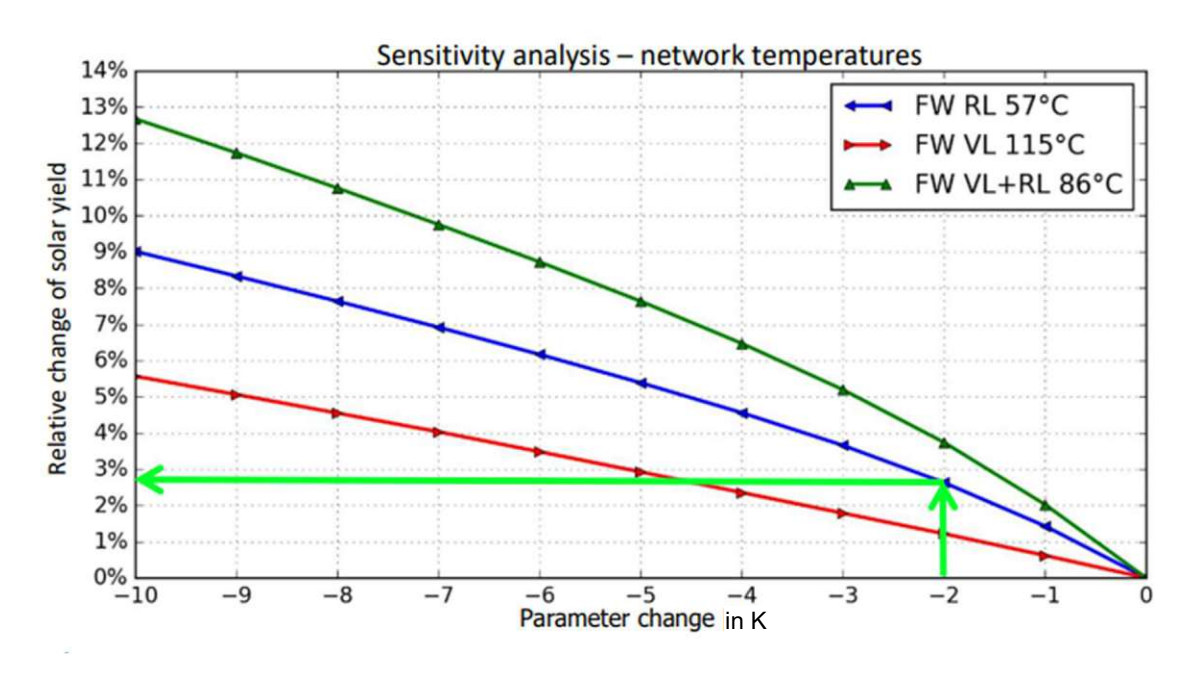


Figure 105 Sensitivity analysis of the SDH feed and return flow temperature on the solar yield [102]

SDH use-case Dronninglund

A best practice example for a SDH system is the Danish city Dronninglund. The SDH system in Dronninglund consists of a combination between FPC, PTES, peak load boilers and a HP. Specifications of this SDH network can be found in Table 24 (in this table . (dot) is used in difference to , (comma)). In Dronninglund 1 350 consumers are supplied by the SDH network. The solar fraction of the 35 726 MWh/yr (SDH heating demand in 2018) was 52 %. The STE was provided by FPC with an aperture area of 37 573 m². The feed and return temperature are 75 and 40 °C. Two storages are used to maximize the SF [3].



Table 24 Specifications of the SDH system in Dronninglund; in this table . (dot) is used in difference to , (comma) [3]

Plant		Dronninglund SDH (DK)		
Latitude	[deg]	57.2 N		
Longitude	[deg]	10.3 E		
Global irradiance (TRY)	$[kWh/m^2/y]$	1030		
Operation start	[y]	2014		
Life time	[y]	30		
Application				
Туре		SH, DHW		
Supply/return temperature	of connected	(1900 € \$ • 100 ±		
(district) heating network	[°C]	75/40		
Collector array				
Collector type		FPC (glass and foil)		
Aperture area	$[m^2]$	37,573		
Slope (inclination)	[deg]	35		
Orientation	[deg]	180 (south)		
Land area	[m ²]	130,000		
Storage				
Diurnal heat storage (size,	type)	865 m ³ steel		
Seasonal heat storage (size, type)		62,000 m ³ pit		
Additional heat sources				
Type, capacity		CHP natural gas (6.4 MWth)		
		2 bio-oil boilers (15 MW)		
		natural gas boiler (8 MW)		
		absorption heat pump (4.7 MWth)		
Performance				
Measurement period		2018		
Irradiance collector plane	$[kWh/m^2/y]$	1,244		
Heat demand	[MWh/y]	35,726		
Solar yield	$[kWh/m^2/y]$	493		
Solar fraction	[%]	52%		
Utilization ratio	[%]	40%		

A simplified visualization of the SDH network in Dronninglund is shownn in Figure 106. The output temperature of the FPC is between 40 °C (winter) and 90 °C (summer). During the summer, if the solar output exceeds the thermal energy demand the surplus STE is used to charge the 62 000 m³ PTES to a maximum temperature of 90 °C (see Figure 107). In autumn hot water from the PTES is used to cover the heating demand of the SDH network. The cooled down return flow with around 40 °C reenters the PTES at the bottom. If the PTES temperature is below the required DH feed temperature the absorption HP with superheated hot water (160 °C) from the bio-oil boiler is used to lift the temperature level. In this combination the PTES can be cooled down to 10 °C. If the PTES is fully discharged the thermal energy is supplied by another bio-oil boiler, a natural gas boiler and natural gas CHP boiler [3].

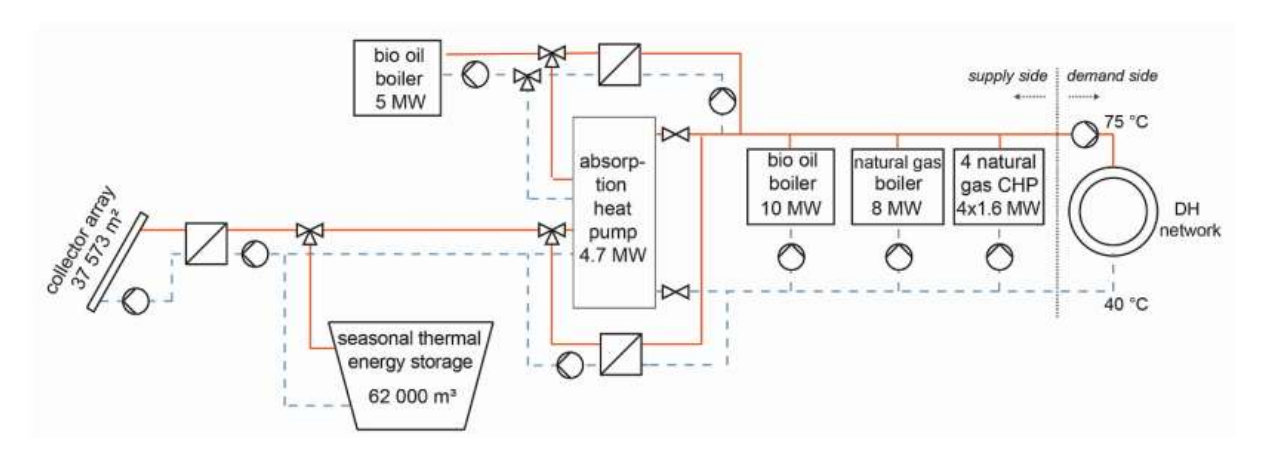


Figure 106 Simplified layout of the SDH network in Dronninglund, pumps indicate the flow direction [3]

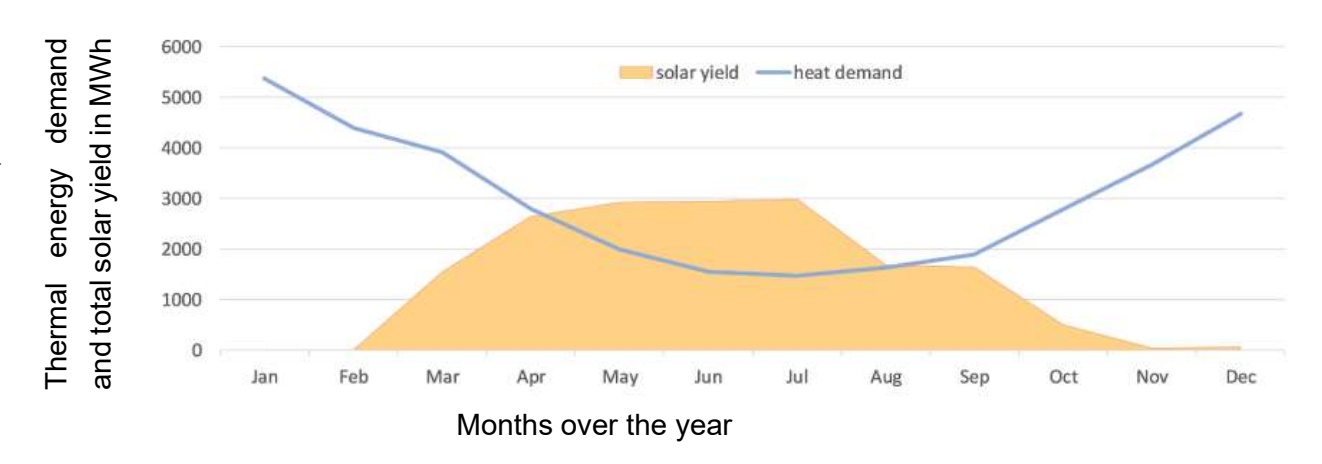


Figure 107 Thermal energy demand and solar yield over the year in the Dronninglund-SDH

The absorption HP can be substituted by the ecop RHP. In this case the bio-oil boiler with 5 MW is not necessary, reducing the CAPEX. The RHP allows a further cooling down (< 5 °C) of the PTES offering a larger storage capacity and a higher efficiency of the FPC. An exemplary operating point of the ecop RHP is shown in Figure 108 [68], [70].

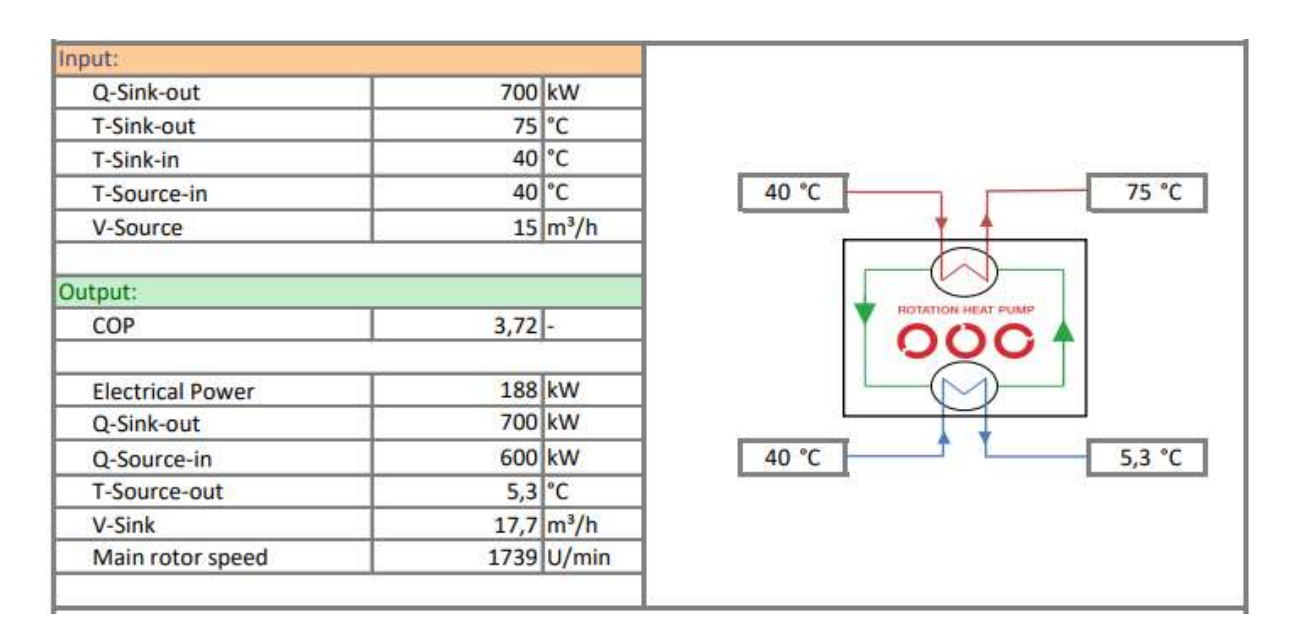


Figure 108 ecop RHP for Dronninglund [68]

Figure 109 shows the large-scale FPC system and the TES in Dronninglund. The specific costs of the collectors are 389 €/m² (per aperture collector area). The LCOH of the system before subsidies are 50 €/MWh [3].





Figure 109 FPC arrays (left) and PTES (right) in Dronninglund [3]

Most European DH systems have supply temperatures greater than Dronninglund. Conventional HP usually cannot generate temperatures greater than 90 °C, what implicates the need for fossil, biomass, or electric based reheating. The ecop RHP offers the possibility to also provide high DH feed temperatures, while cooling down the source significantly. An exemplary simulation of the ecop RHP for this operating point is shown in Figure 110 [3], [68].

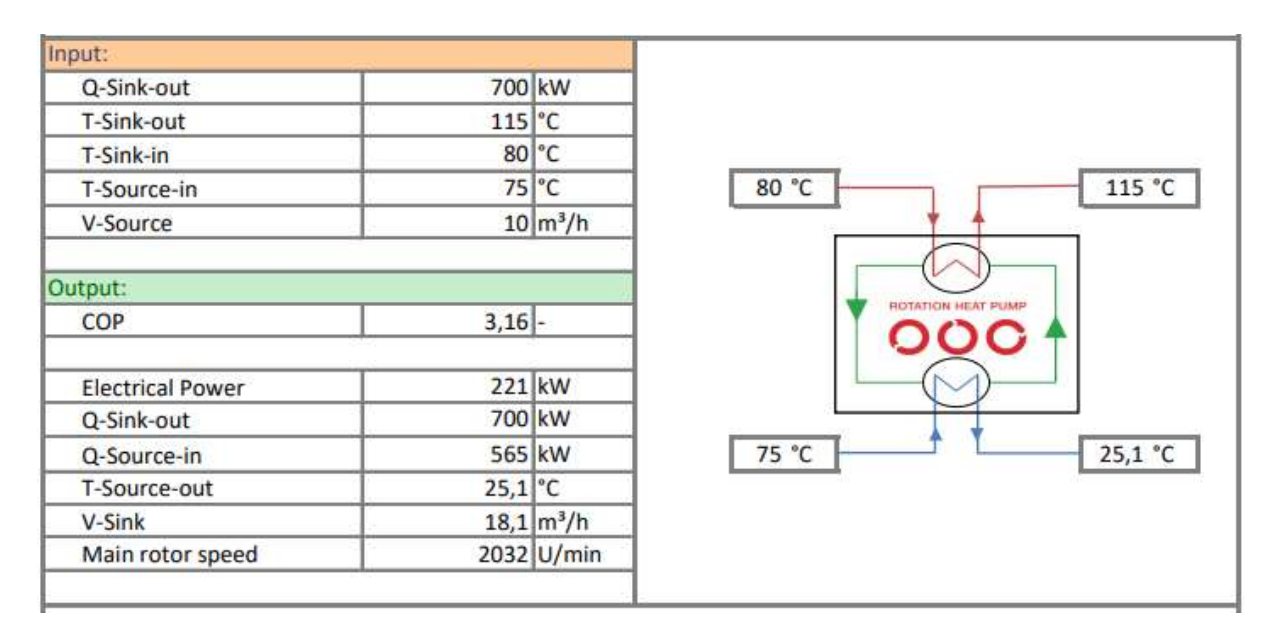


Figure 110 ecop RHP for providing high temperatures for conventional DH networks [68]

To achieve higher COP a serial configuration of RHP can also be realized showed in Figure 111 and Figure 112. In this case the source is cooled down in two steps. Both RHP can provide the same sink temperature. By adding another RHP the source can be cooled down further [70].

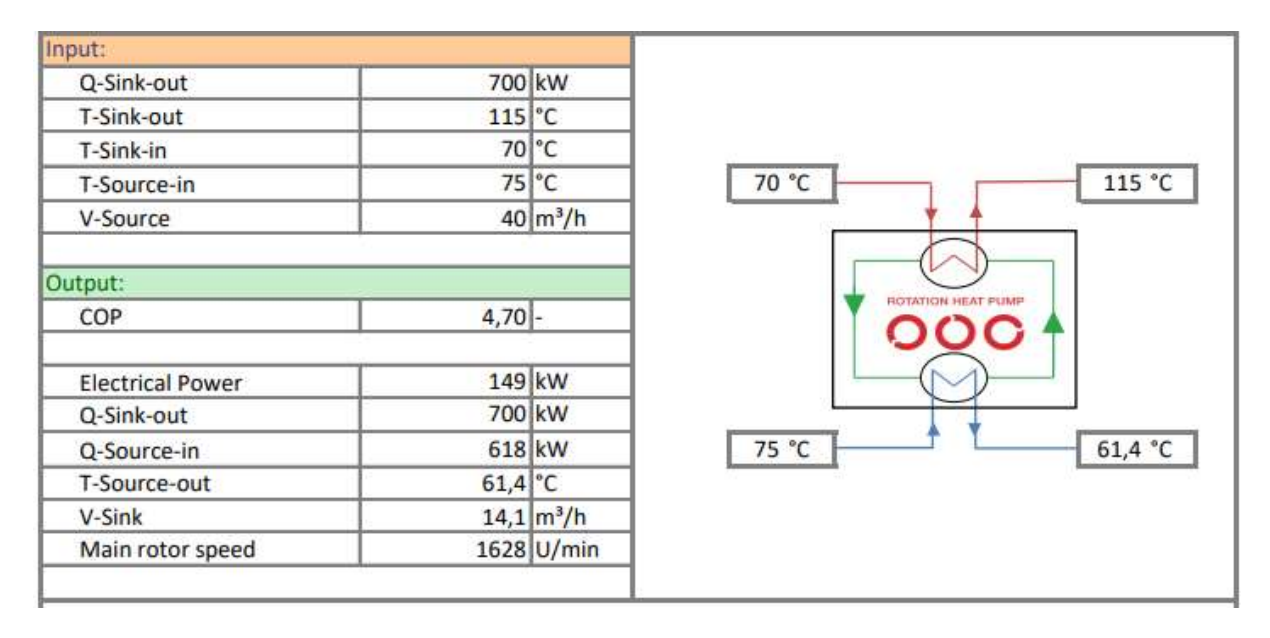


Figure 111 1/2 ecop RHP switch in series for providing high temperatures for conventional DH networks with high COP [68]

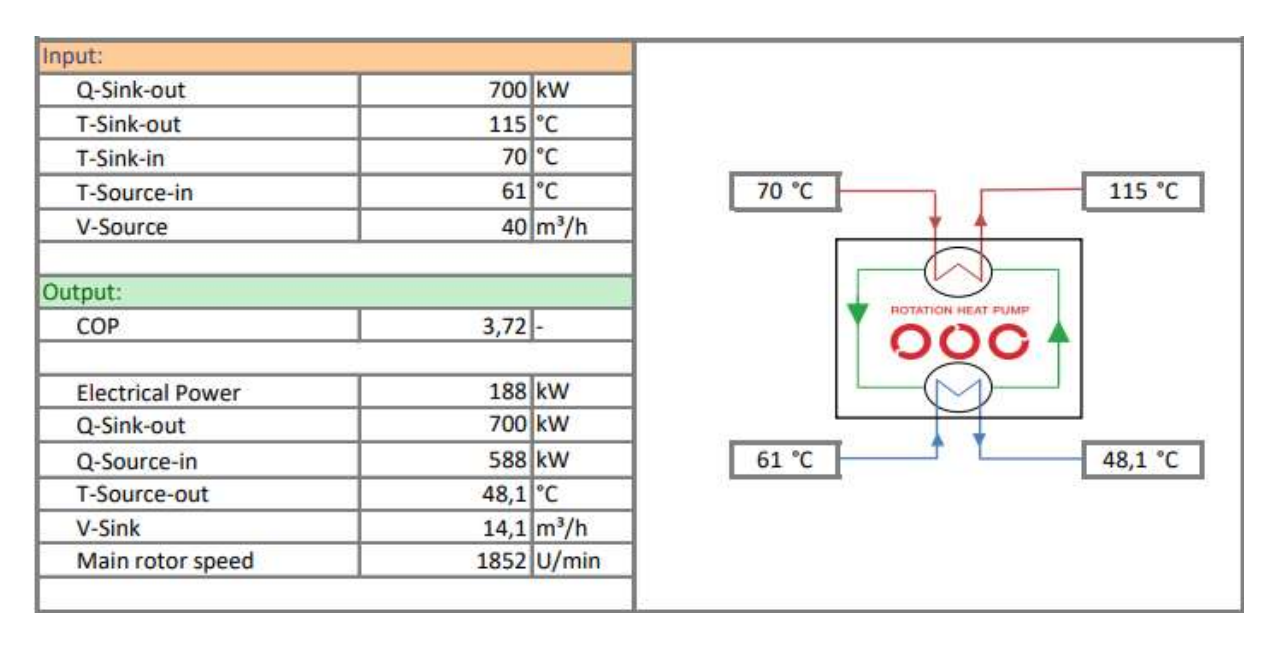


Figure 112 2/2 ecop RHP switch in series for providing high temperatures for conventional DH networks with high COP [68]

Local solar heating network

A feasibility study of a small SDH system is outlined in this section. The data is based on a "BAFA-Machbarkeitsstudie" on the topic "Wärmenetzsysteme 4.0" (DH-networks 4.0). In this study Stadtwerke Aachen AG in cooperation with EEB Enerko Energiewirtschaftliche Beratung GmbH investigate, if a SDH system is technical and economical feasible based on the given situation on site. The exemplary project has in the first stage of development a thermal energy demand of 4,3 GWh/yr and a peak load of 3,3 MW. It is assumed that until 2034 the thermal energy demand will rise to 5,94 GWh/yr and a peak load of 5 MW. The DH network has a feed temperature of 70 °C and a return of 40 °C. The system is a combination between solar thermal collectors, a RHP, heat exchanger, a PTES, and a daily buffer storage [103].

The planned operation is described by some simplified process visualization. In the visualization the red lines show the DH feed and blue lines the DH return flow. Gray lines are in the current operating status unused. Figure 113 and Figure 114 show typical summer operations where STE is directly used to cover the heating demands of the SDH network and the overproduction is used to charge the buffer storage and the PTES [104].

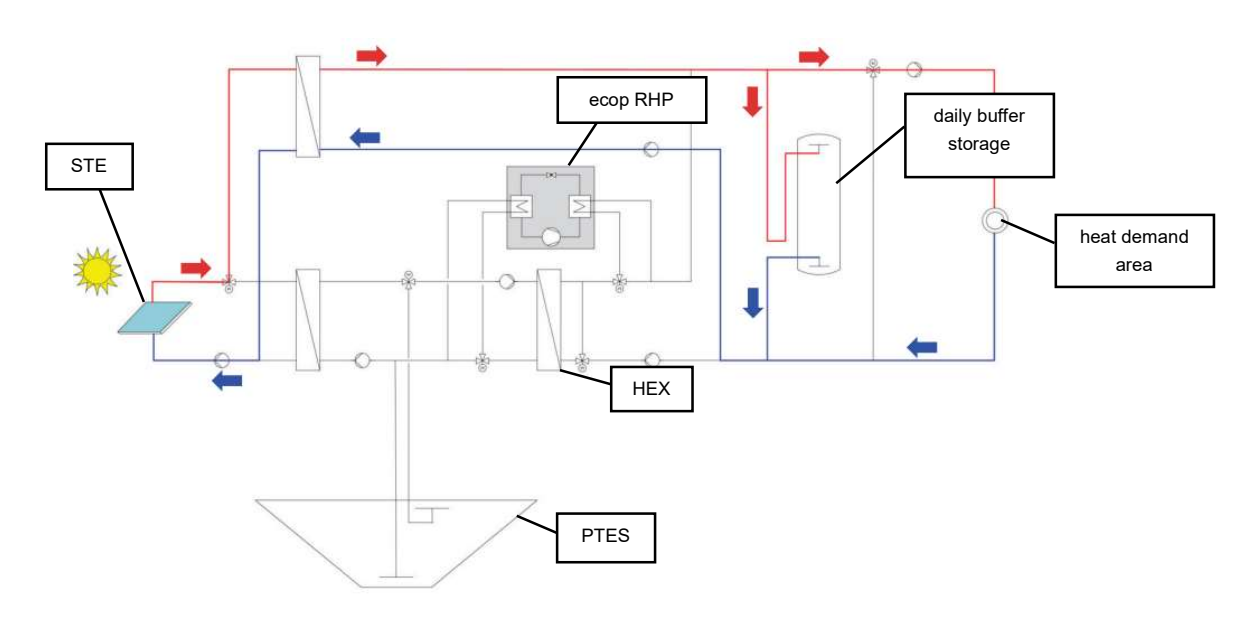


Figure 113 Simplified visualization of the thermal energy supply in a typical summer operation: direct solar usage and charging of daily buffer storage [104]

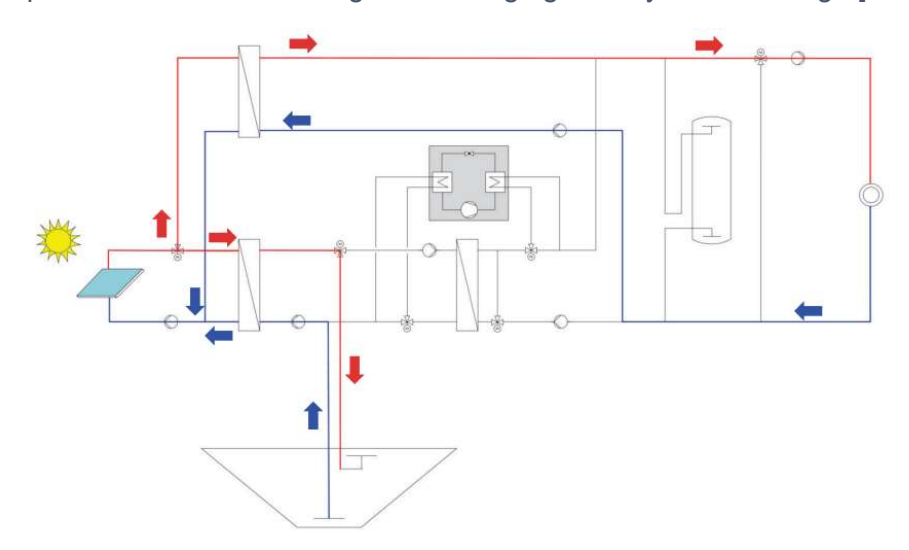


Figure 114 Simplified visualization of the thermal energy supply in a typical summer operation: direct solar usage and charging of PTES [104]

Figure 115 shows a typical operation in autumn, when the PTES is fully charged and the PTES temperature exceeds the DH feed. In this case the thermal energy can be transferred directly via a HEX from the PTES to the DH system [104].

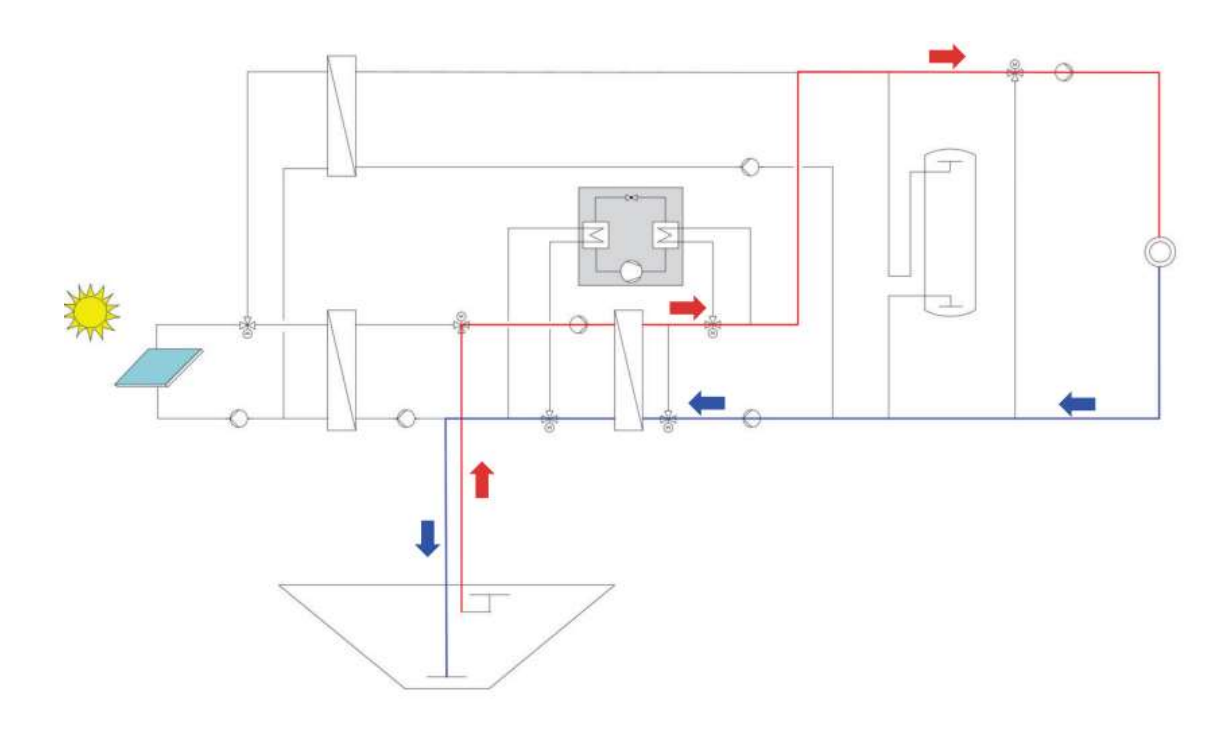


Figure 115 Simplified visualization of the thermal energy supply in a typical autumn operation: discharging PTES directly via HEX into DH network [104]

If the PTES temperatures drops below the DH feed, the RHP is used to lift the temperature level. First the PTES is used to preheat the DH return flow and afterwards the remaining thermal energy of the PTES flow is used as source for the RHP. The RHP lifts the preheated DH return flow to the needed DH feed temperature. This situation is shown in Figure 116 [104].

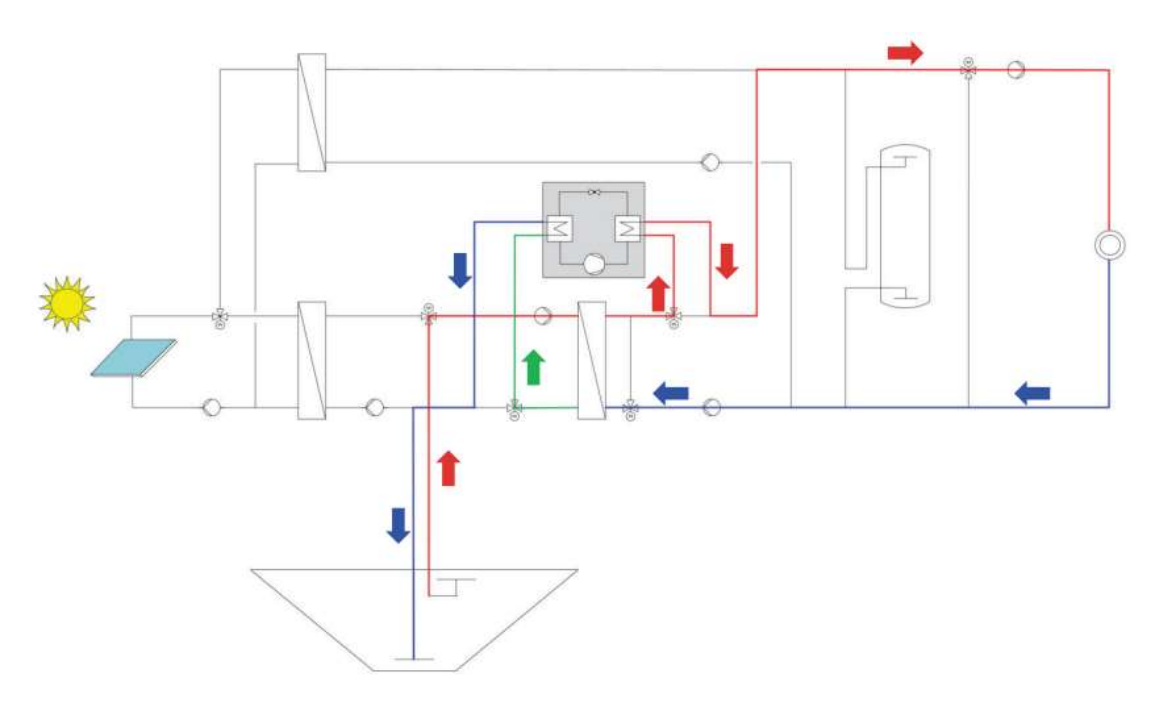


Figure 116 Simplified visualization of the thermal energy supply in a typical autumn operation: using PTES via HEX for DH return preheating and afterwards as source for RHP, RHP does the end heating of the DH feed [104]

Another operation mode is, if the PTES is already partly discharged and the temperature level is below the DH return flow. In this case the PTES is used as source for the RHP to lift the DH return flow to the needed feed temperature level. A schema for this case is shown in Figure 117 [104].

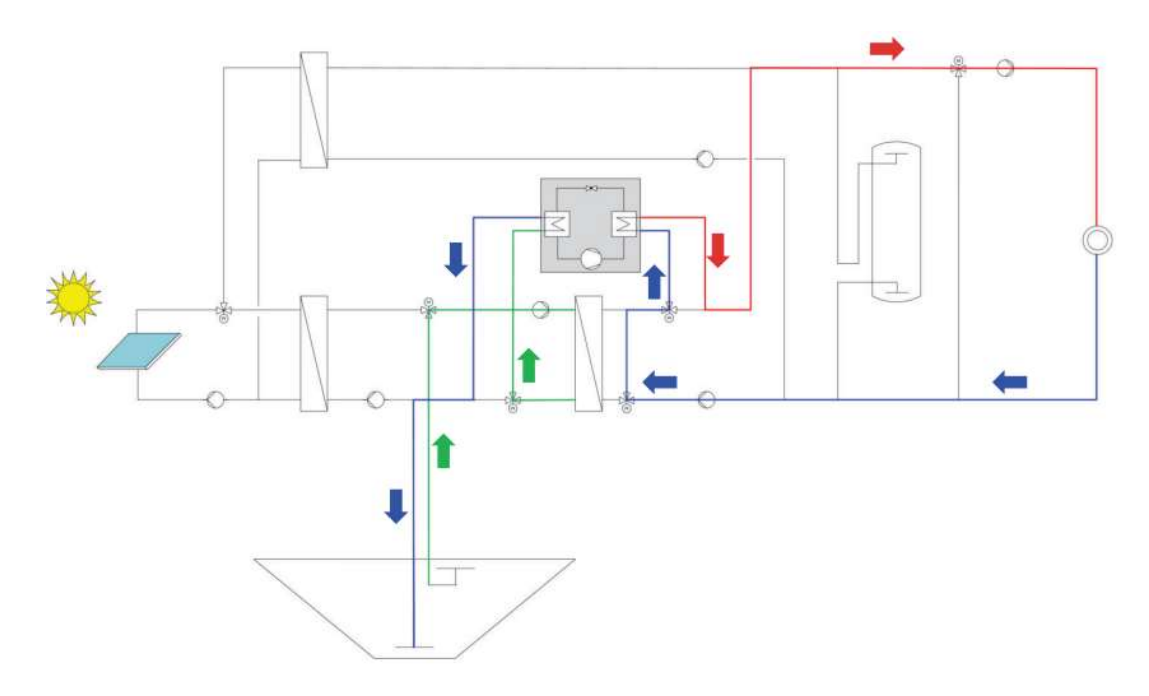


Figure 117 Simplified visualization of the thermal energy supply in a typical winter operation: using PTES as source for RHP, RHP is used for lifting the DH return flow [104]

If the PTES is fully discharged the RHP can use the STE of sunny winter days directly as source pictured in Figure 118. The RHP is used to lift the DH return flow to the needed DH feed temperature [104].

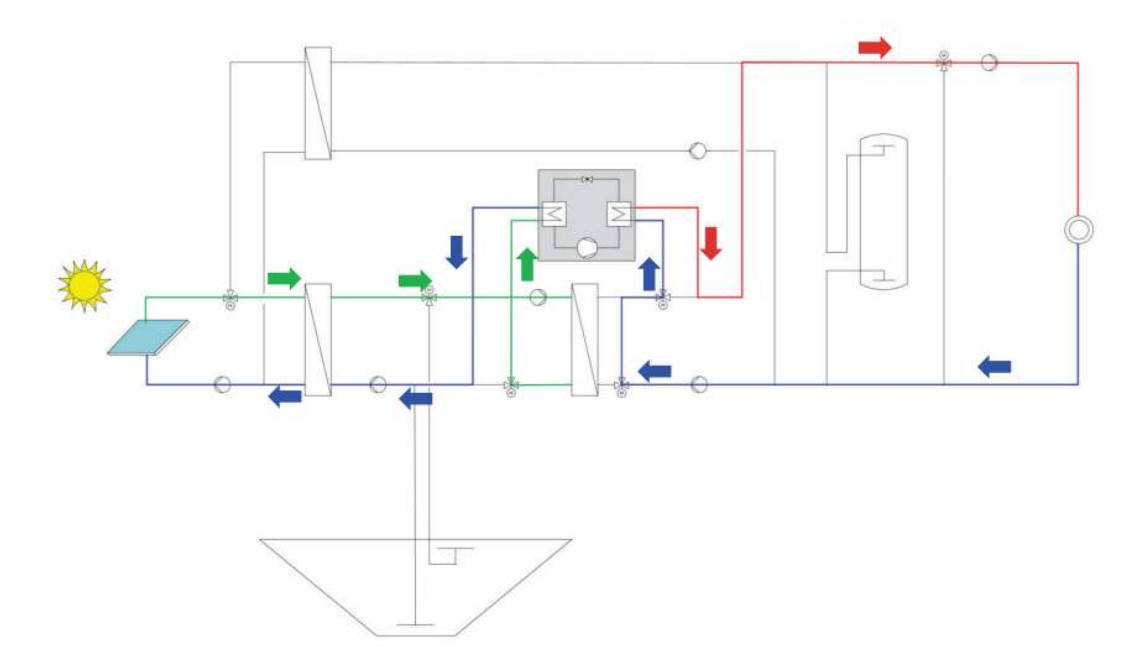
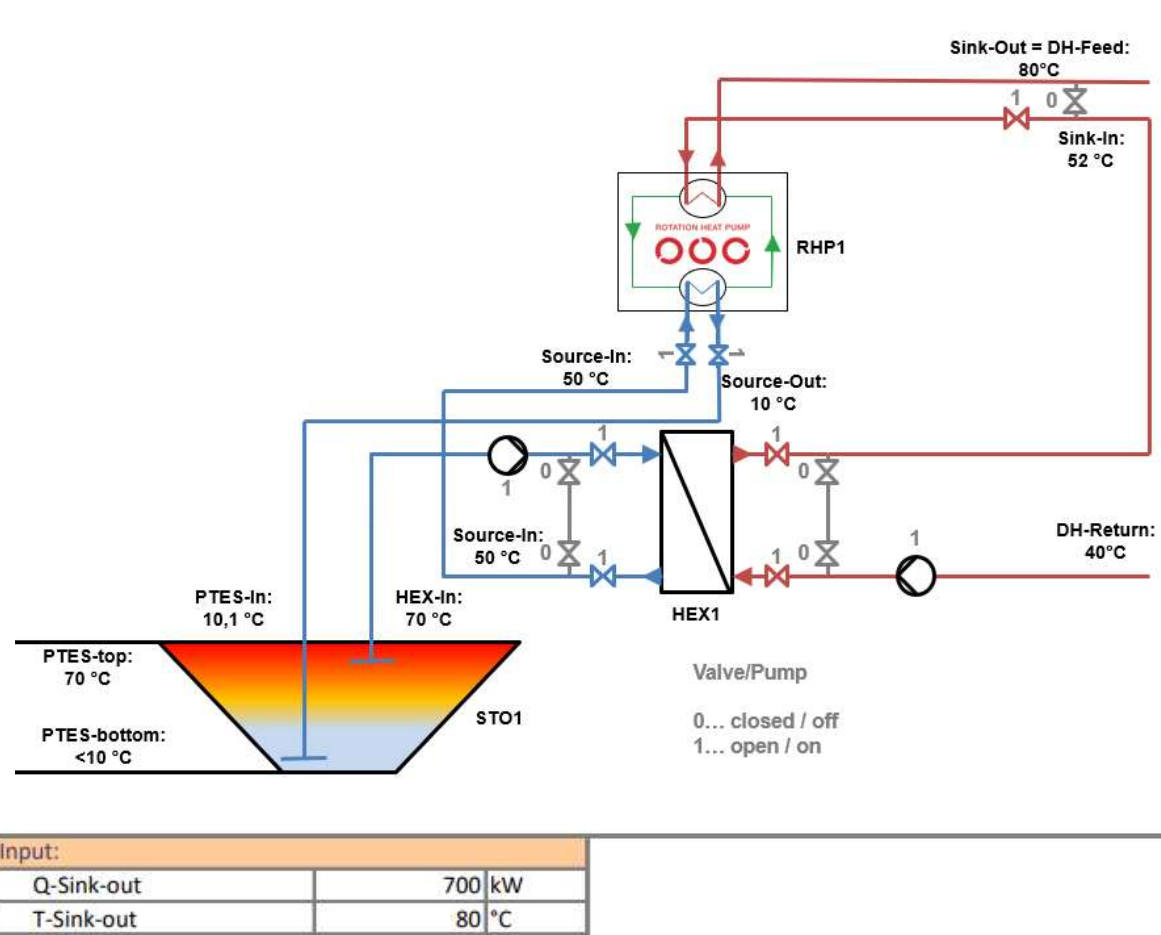


Figure 118 Simplified visualization of the thermal energy supply in a typical winter operation: using STE as source for RHP, RHP is used for heating the DH return flow [104]

Figure 119 shows an COP simulation of the operation pictured in Figure 116. The maximal temperature of the PTES is limited to 70 °C due to material durability. The PTES feed with 70 °C is used in the HEX to preheat the DH return from 40 to 52 °C. In the HEX the PTES feed is cooled down to 50 °. Afterwards the RHP uses the 50 °C PTES stream as source cooling it down to 10 °C. The ecop RHP is used for end heating from 52 °C to the DH feed temperature of 80 °C. The ecop RHP in this use case reaches a COP of 3,67 [68], [70].



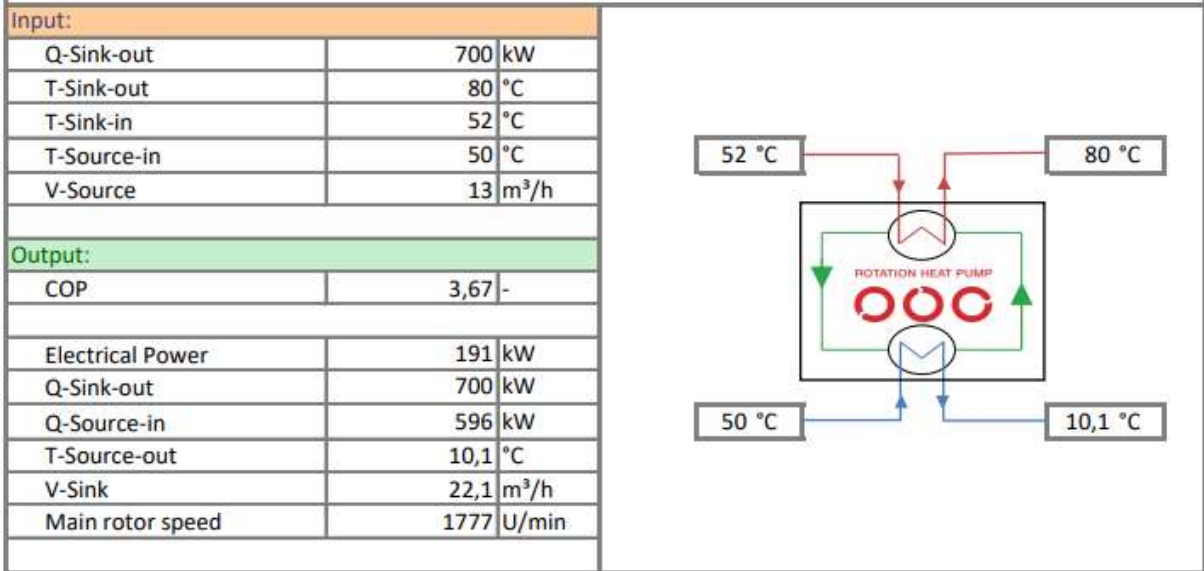
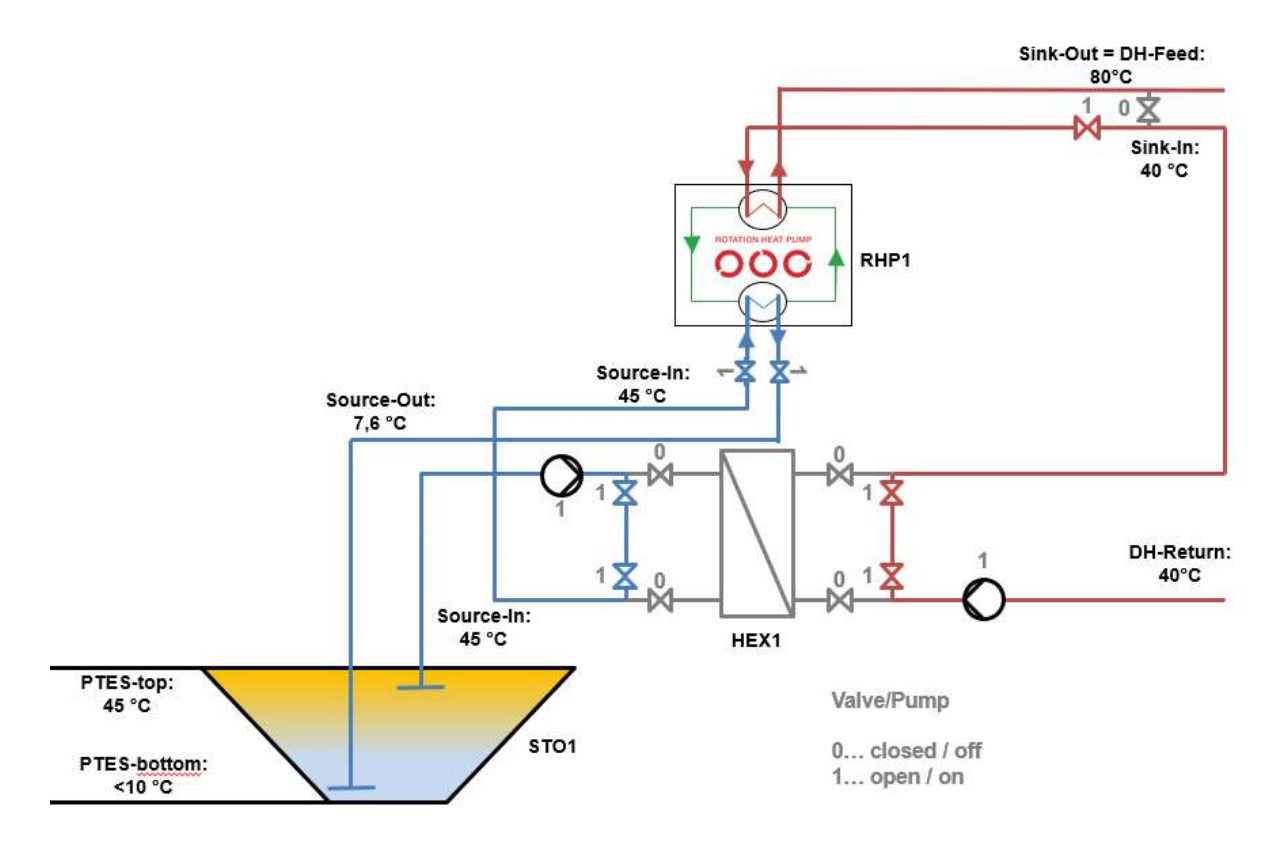


Figure 119 Simplified visualization of the thermal energy supply using PTES via HEX for DH return preheating and afterwards as source for RHP for DH end heating (top); Specifications of the ecop RHP in this operation point (bottom) [68], [70]

Figure 120 shows an COP simulation of the operation pictured in Figure 117. The PTES in this case is already partly discharged and has a temperature of 45 °C. The HEX cannot be used for preheating, because of the low PTES temperature. Therefore, the PTES flow is directly used as RHP source being cooled down to 7,6 °C before reentering the storages at the bottom. The ecop RHP is used for lifting the DH return from 40 to 80 °C. The ecop RHP in this use case reaches a COP of 3,77 [68], [70].



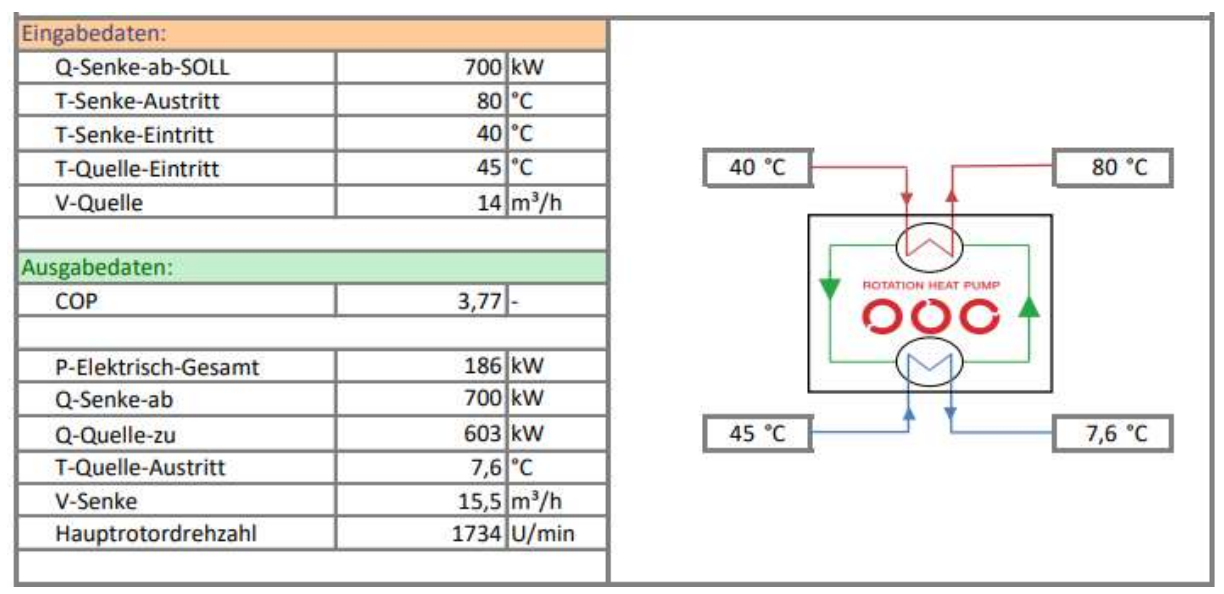


Figure 120 Simplified visualization of the thermal energy supply using PTES as source for RHP to lift the temperature of the DH feed; Specifications of the ecop RHP in this operation point (bottom) [68], [70]

The great advantages of the RHP in this case are [70]:

- The DH return flow can be lifted to the needed feed temperature with a single HP stage
- The cooling down of the storage temperature from 45 to below 10 °C is achievable in one stage
- Easy hydraulics and control of the RHP due to parallel setup
- Very broad control area (partial load) of the RHP, while having good COP

4.3.2 Solar heat for industrial processes (Use case Solar-2)

In this section a combination between STE, HP and TES for an industrial use is presented. These systems are called SHIP (solar heat for industrial processes) in the literature. This use-case is based on an existing insulation manufacturer. SHIP systems are similar to SDH systems, but the seasonal PTES is often substituted by small-scale tank storages (daily or weekly buffer storages) and the temperature level is higher [70].

In the industry the generation of saturated steam is often required. Figure 121 shows a possible renewable set up for the generation of saturated steam with 120 °C from a 10 °C freshwater feed. The set up consists of a HEX, a steam generator, two tank storages, STE and an RHP. The plant release waste heat with around 40 °C, which is used together with the low temperature storage for preheating the fresh water from 10 to 30 °C. In the next step the freshwater is heated via a HEX with hot water from the high temperature storage to 85 °C. In the following step the water is reheated by the RHP sink to > 100 °C. Afterwards the hot water enters a steam generator where it is converted into saturated steam. In this setup two RHP are set in series, while one provides high temperatures for the steam generator. The second serial RHP ensures a constant source temperature of the steam generating RHP by compensating the fluctuating / decreasing storage temperatures. The source providing RHP uses the buffer storages as source. The STE is used to charge the storages. The STE charges prioritized the LT storage due to higher efficiencies. During the night the RHP can be used to charge the HT-storage using excess heat from cooling down the process or the LT-storage as source [70].

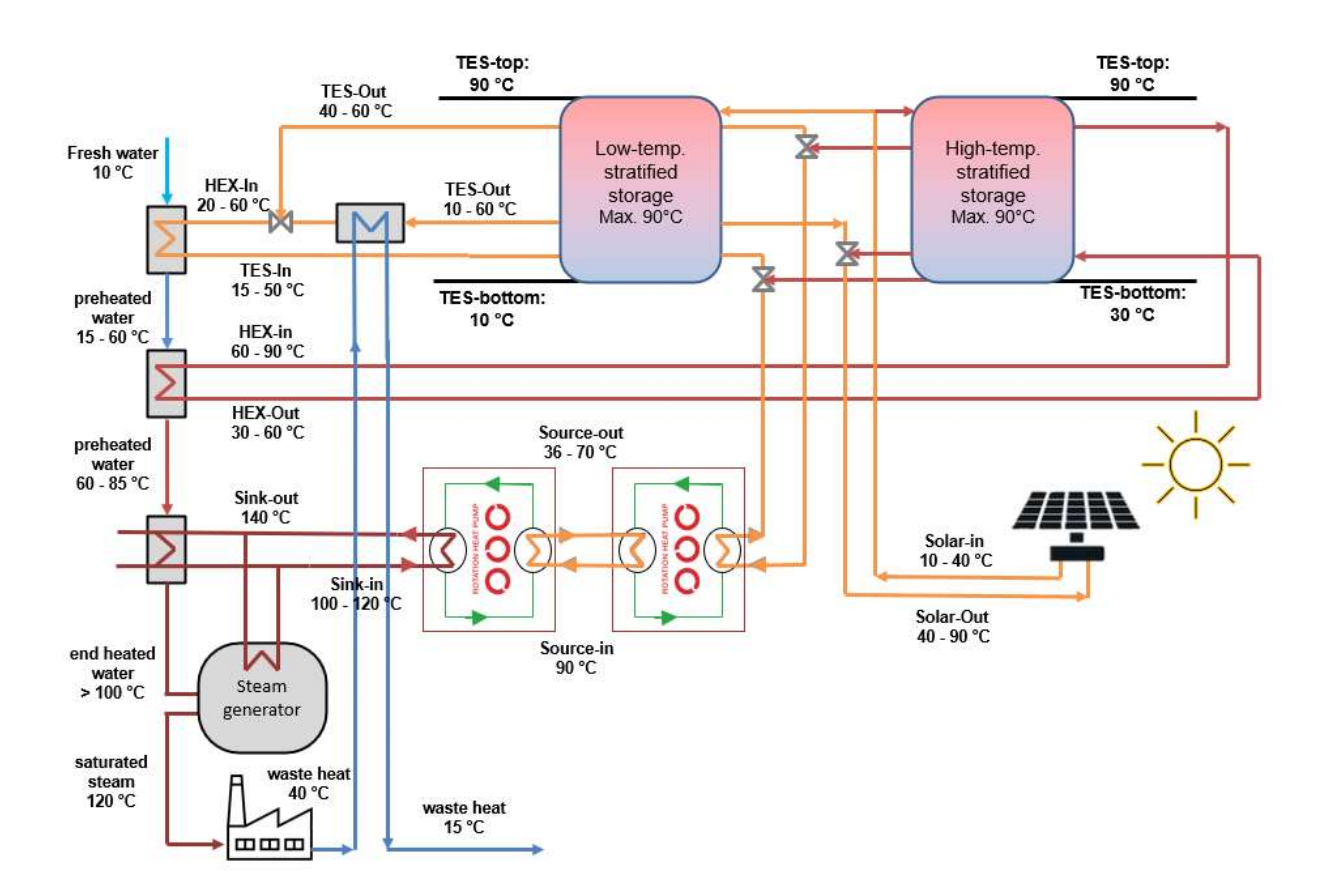


Figure 121 Set up for the generation of saturated steam with a RHP and STE combination, max. stands for maximum [70]

To transform 1 t/h fresh water with 10 °C to saturated steam with 120 °C 741 kW thermal power is needed. The setup was dimensioned to provide this thermal energy for 16 h from 6 AM to 10 PM. It is assumed that the buffer storages are at the beginning of the day fully charged. The solar collectors are dimensioned that during a weekend with average solar irradiance enough thermal energy can be provided to fully charge the storages. The dimensions of the system components for the renewable set up are shown in Table 25 [70].

Table 25 Set up for renewable thermal energy supply [70]

thermal power demand for 1 t/h 10 °C fresh water to 120 °C		
saturated steam	741	kW
LT-temperature storage capacity	55	m³
HT-temperature storage capacity	45	m³
installed Solar peak power	750	kW
installed ecop RHP (700 kW)	2	piece

Figure 122 shows a simulation of the ecop RHP providing the HT-level for reheating and steam generation. The RHP reaches a COP of ~ 4 in this setup [70].



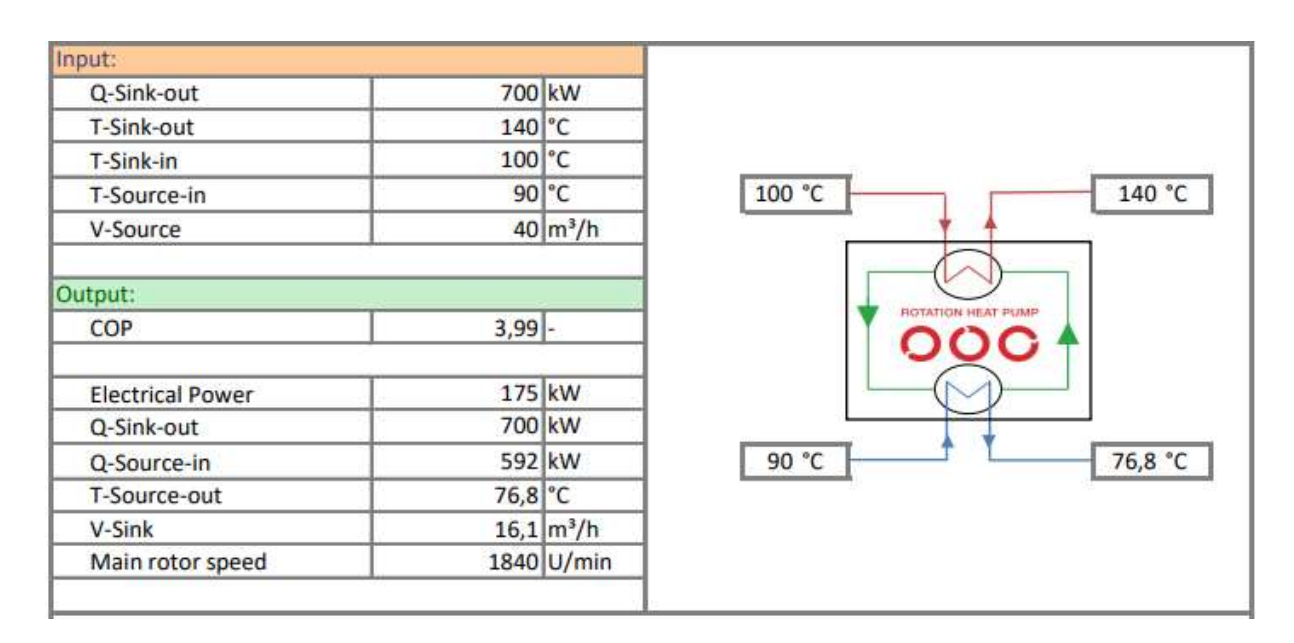


Figure 122 Simulation results of the ecop RHP for reheating and vaporization – use case Solar-2 [68]

Figure 123 shows the thermal energy demand (differentiated between HT / LT) and the thermal energy suppliers. The energy supply exceeds the demand. The difference are conversion losses. The LT-demand is the preheating of the freshwater and the source for the RHP (all demands covered by the LT-storage) and the HT-demand includes the needed thermal energy between 30 °C and 120 °C saturated steam (covered by the HT-storage and the RHP sink) [70].

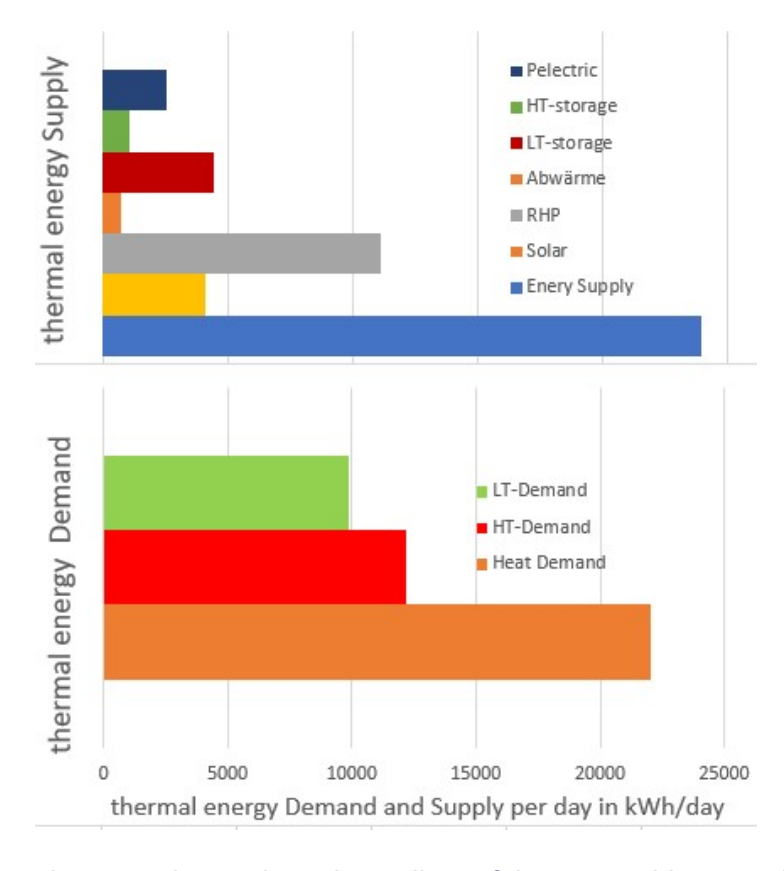


Figure 123 Thermal energy demands and suppliers of the renewable setup for one day [70]

Figure 124 shows the mean-temperature history of the HT- and LT-storages for a day. The temperature of the HT-storage decreases linear. The temperature of the LTstorage decreases stronger when the solar yield is low or not available (6 AM - 7 AM& 6 PM – 10 PM). During the rest of the day the high solar yield reduce the discharging rate of the LT-storage [70].



Figure 124 Daily mean-temperature history of the LT and HT storages and the considered solar yield history; Temp. stands for temperature [70]

This example show that a renewable operation of HT applications is feasible. If the buffer storages and the STE are dimensioned bigger several days can be covered fully renewable [70].

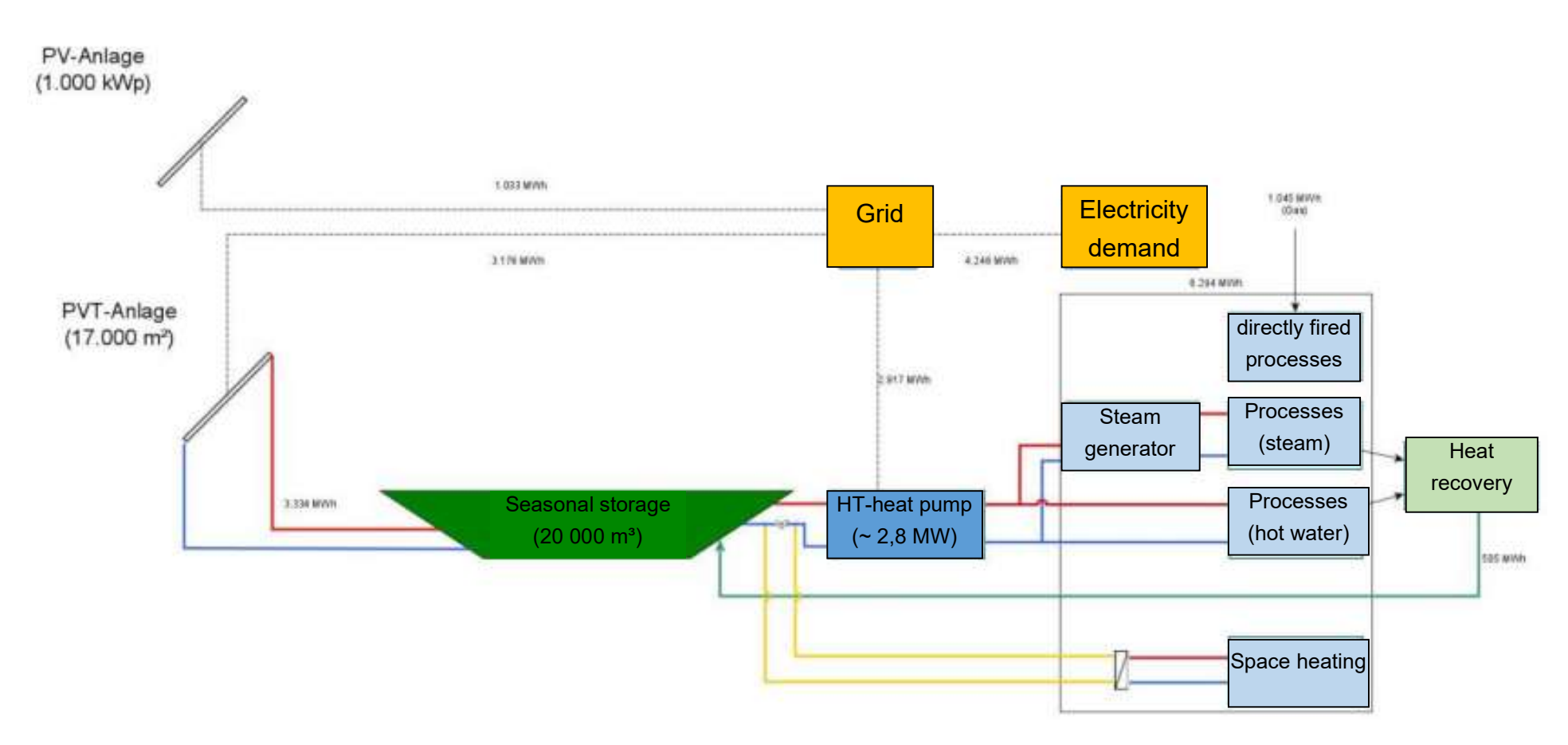
Textile industry

An example for the combination of PV, STE, TES and HP is the project of an Austrian textile manufacturer. In the plant textile products like exemplarily towels are produced. Currently the thermal energy requirements are provided by two gas boilers with a total power of 11,7 MW. This thermal energy is used to power the processes shown in Table 26. Some of these processes require steam, marked with the letters "DD". The waste heat of these processes is used for space heating and DHW requirements [105].

Table 26 Processes in the textile industry and their temperature level [105]

Prozess	Temperatur		
Schlichte, Schlichtemittelvorbereitung (DD)	90 °C		
Färben/Farbmittelaufbereitung (DD)	60-70 °C		
Waschen, Bleichen (DD)	100 °C		
Trocknen	110 °C		
Tumbler 1, Tumbler 2	75°C, 140 °C		
Spannen	150 °C		
Garnfärberei	?		
Warmwasser	60 C° (?)		
Heißwassernetz	80 °C (?)		
* DD - Bedarf Direkt-Dampf	72		

The operator of the plant plans to substitute the gas boilers by a renewable alternative. The renewable alternative is a combination of photovoltaic/thermal collectors (PVT), a PTES, a RHP and PV collectors. The envisioned concept is shown in Figure 125 (in this figure . (dot) are used as thousand-digit-draw). The PVT generate electricity and thermal energy simultaneously, the PV only electricity. The thermal energy is fed into the PTES and the electricity is used for the RHP or other electricity demands. The RHP is used to lift the PTES temperature to the needed level. For the processes which require steam the RHP sink is fed into a steam generator. A gas peak boiler is used if temperatures > 150 °C are needed [105].



Seite | 121

Figure 125 Visualization of the future envisioned SHIP heating of a textile manufacturer; combination of a PV, PVT, TES and RHP; in this figure . (dot) are used as thousand-digit-draw [105]

The dimensions of the plant components are pictured in Table 27 [105].

Table 27 Renewable energy concept components [105]

PVT-Anlage [m²]	17 000,0
Erdbeckenspeicher [m³]	20 000,0
Hochtemperatur-Wärmepumpen [MW]	2,8
Nahwärme-Anschluss [MW]	-
PV-Anlage [kWp]	1 000,0
PV-Anlage [m²]	7 800,0

Figure 126 shows the energy supply (simulated) and demand (reference year 2019) of the different sources. Between March and August, the supply exceeds the demand. During this time thermal energy is fed into the PTES. During the other months thermal energy of the PTES is consumed [105].

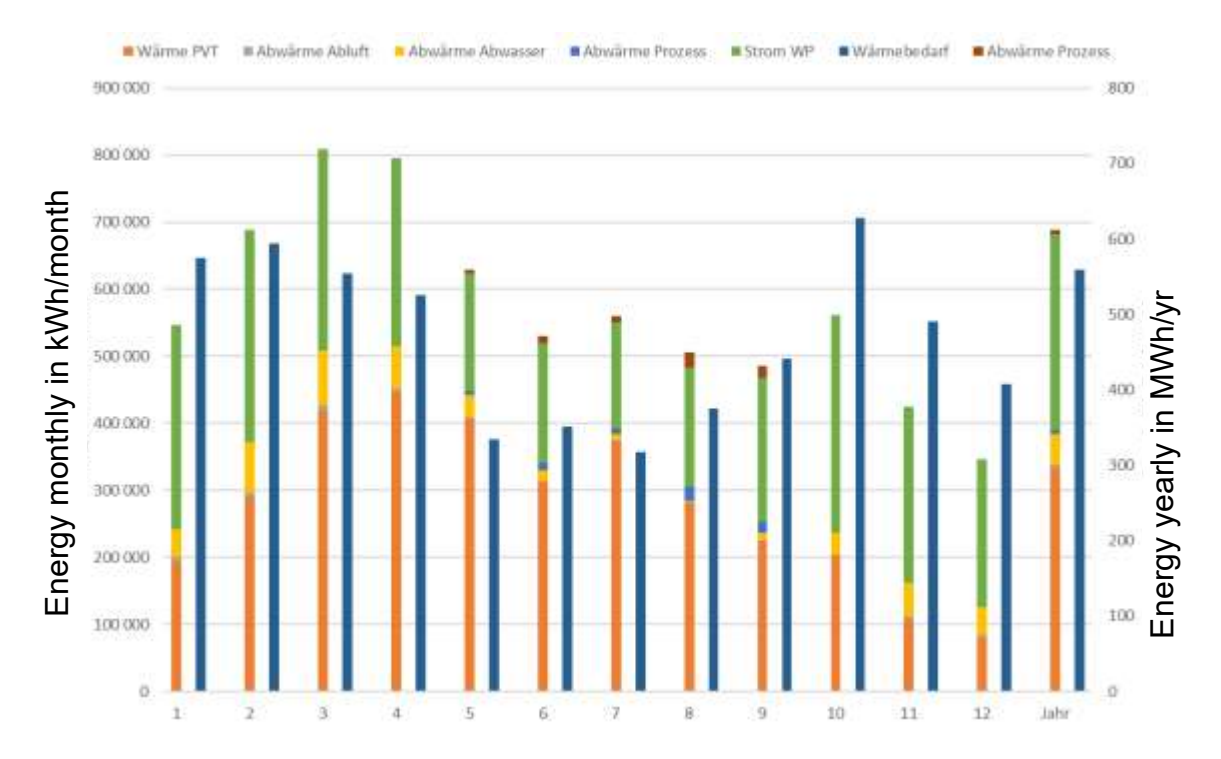


Figure 126 Simulated energy balance of the SHIP system; the energy demand is on the basis of 2019 [105]

Figure 127 depicts the mean temperature profiles of the PTES at different heights over the year. Between March and August, the PTES temperature is rising, reaching a maximum in August. In the following months thermal energy from the PTES is consumed which is why the temperature is declining [105].



Figure 127 Mean temperature profiles at different heights in the PTES over the year [105]

Figure 128 shows the electricity supply of the PVT and PV system and the electricity demand of the consumers like the RHP over a year. The electricity demand of the RHP can be covered almost over the whole year by the PVT and PV system. The additional electricity supply is consumed by other consumers in the plant [105].

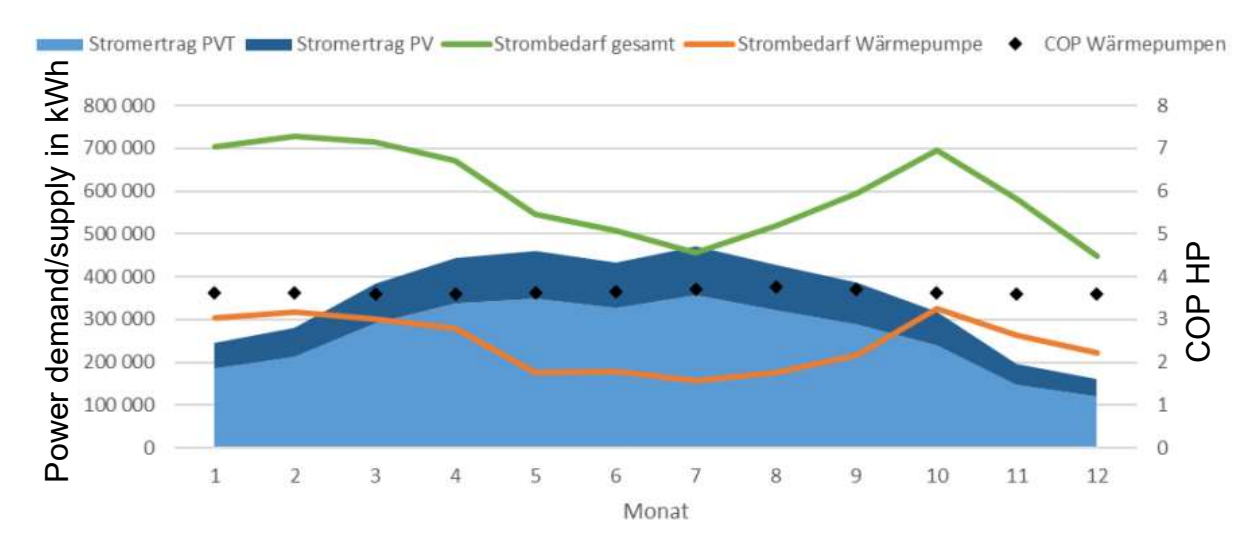


Figure 128 Electricity supply of the PVT and PV system and the electricity demand of the RHP and other consumers, COP of the RHP is assumed to be constant [105]

For the renewable thermal energy supply as described above an economic efficiency calculation based on the data given in Table 28 were done [105].

Table 28 Parameters for the economic efficiency analysis based on ÖNORM M7140 [105]

Betrachtungsperiode	50 Jahre
Kalkulationszinssatz	3,5%
CO2-Preissteigerung	2%
Spez. CO2-Kosten (Projektion)	100 €/Tonne
Preissteigerung Energie, Wartung und Investition	4%
Lebensdauer PVT und PV	30 Jahre
Lebensdauer Erdbeckenspeicher	50 Jahre
Lebensdauer Wärmepumpen	20 Jahre
Lebensdauer FW-Übergabestation	50 Jahre
Spez. Kosten PVT-Anlage	600 €/m²
Spez. Kosten PV-Anlage	200 €/kWp
Spez. Kosten Erdbeckenspeicher	200 €/m³
Spez. Kosten Wärmepumpen	1,035 Mio. €/MW
Anschluss Fernwärme	50.000 €
Energiekosten	
Strom	0,21 €/kWh
Gas	0,2 €/kWh
Fernwärme	0,19096 €/kWh
Wartungskosten	*
PVT, PV, Erdbeckenspeicher	0,05% der Investitionskosten
Wärmepumpe und FW-	1% der
Übergabestation	Investitionskosten
Förderungen	45
30% der Investitionskosten von PVT-	
Anlage, Erdbeckenspeicher und	
Wärmepumpen	8
Evtl. PV-Förderung nicht berücksichtigt	25

Figure 129 shows the outcome of the economic efficiency calculation. The life cycle costs for the reference scenario (only OPEX) are significantly higher than the planned scenario with and without subsidies (including OPEX, CAPEX and fixed system costs) [105].

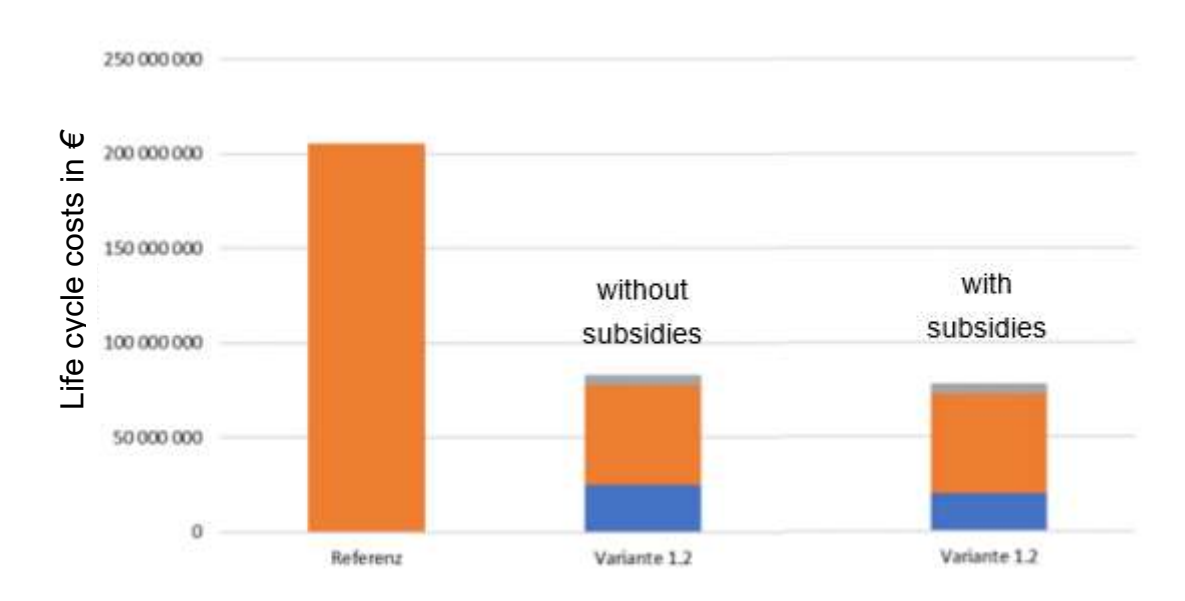


Figure 129 Life cycle costs of the reference case and the planned case without/with subsidies, orange: OPEX, blue: CAPEX, gray: fixed system costs [105]

The resulting LCOH and the dynamic amortization time are visualized in Table 29. The LCOH of the planned scenario including subsidies are 51 €/MWh and the DPP are 7,2 years. This price is competitive with the current fossil energy supply, while having approximately on fourth of the GWP [105].

Table 29 LCOH (in €/kWh) and dynamic amortization period of the project based on [105]

	reference scenario	Option		
	(fossil energy supply)	without subsidies	with subsidies	
capital LCOH	/	0,16	0,13	
consumption based LCOH	0,84	0,34	0,34	
operational LCOH	/	0,04	0,04	
sum	0,84	0,54	0,51	
discounted amortization period		9,3 yr	7,2 yr	

4.3.3 Economic efficiency of SDH and SHIP systems

In Europe several SDH systems are under construction, investigation or in operation. The competitiveness of SDH systems compared to other technologies rely on several facts [3], [106], [107]:

Availability of land as well as the price of land

- DH temperature level
- Existing infrastructure for heating (gas boilers, biomass CHP, ...)
- Difference between maximum and minimal thermal energy demand (winter / summer)
- Necessity of seasonal storage (high CAPEX)
- Prices of other technologies (reference scenario is usually fossil fuels), taxes on fossil fuels are in nordic countries for example Denmark significantly higher
- The size of the DH system, because smaller SDH systems are already well explored, while bigger SDH systems with several thermal energy sources are more complex and only little experienced

Generally, it can be said that SDH systems have very low operation and maintenance (O&M) costs. Regarding to [3] the O&M costs of the STE collectors can be set to be 0,5 % of its investment costs. In Denmark the O&M of STE systems are calculated with approximately 0,27 €/MWh. SDH systems have higher O&M costs, because of electricity costs for the pumps and the HP. Small Danish SDH systems reach LCOH of 36 €/MWh, while bigger systems with the need of a seasonal storage are around 50 €/MWh. More cost parameters are pictured in Table 28 [3].

Figure 130 shows an average CAPEX structure for SDH systems depending on the SF. The costs for land are based on average prices for arable land and are expected to be nearby the thermal energy demand. Therefore, short transmission lines are taken into account. In the analyzed SDH system no HP where intended, which is why they are missing in the CAPEX structure. Nevertheless are the CAPEX of the HP small compared to the storage and the collector field costs. Larger SF lead to larger storages and therefore they also take a larger cost position [108].

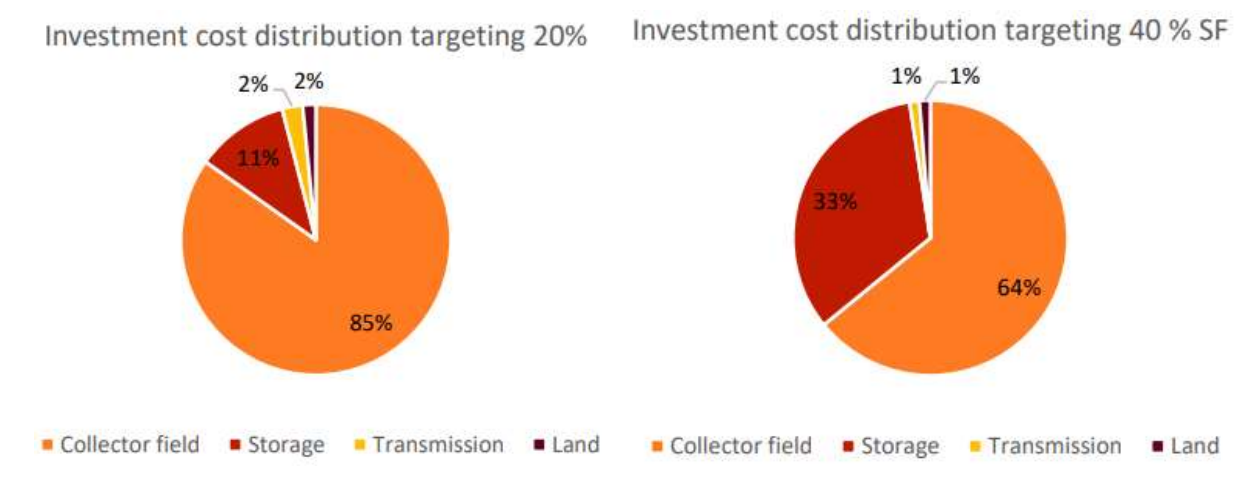


Figure 130 Average CAPEX structure of a SDH system without a HP and short transmission lines for SF of 20 % (left) and SF of 40 % (right) [108]

The cost structure for a small and large-scale SDH system is pictured in Table 30 (in this table . (dot) is used as decimal point and , (comma) as thousand-digit-draw). The large-scale SDH system result in higher costs. This is mainly a result of the needed PTES instead of a more compact TTES [32].

Table 30 Cost structure for a small and large scale SDH system; in this table . (dot) is used as decimal point and , (comma) as thousand-digit-draw [32]

Solar thermal system category	SDH: Solar district heating Solar assisted district heating (ground mounted collector field)			
All systems of this category are ground- mounted and may be equipped with either - short-term (diurnal) storages (A) or - long-term (seasonal) storages (B)				
Energy/technical data	A) with diurnal storage	B) with seasonal storage		
Kind of solar thermal collector used optional	FPC -	FPC -		
Kind of solar energy storage used optional	Non-pressurized TTES pressurized TTES	PTES BTES, (ATES)		
Typical size per unit [m² _{gross}] -range (from - to)	10,000 5,000 – 20,000 (up to 150,000)	50,000 20,000 – 70,000		
Typical thermal peak capacity per unit [kW] - range (from - to)	7,000 3,500 – 14,000	35,000 14,000 - 140,000		
Typical storage volume per unit [m³.H200]	1,200	125,000		
Typical annual production per unit [MWh/a]	4,100	17,500		
Specific storage volume per unit [ltr./m² grass] -range (fram - to)	120 90 – 150	2,500 1,500 - 3,500		
Typical solar energy yield SE [kWh/m ² groot/a] - range (from - to)	410 380 - 460	365 340 – 390		
Typical solar fraction sf [-] - range (fram - ta)	12% 5-20%	50% 40 - 60%		
Technical life time [years]	25	25		
Financial data	A) with diurnal storage	B) with seasonal storage		
Specific cost <u>ready installed</u> [1,000€/m ² gross] (excl. VAT, excl. subsidies)	0.24 (*/- 12%) (0.21 - 0.27)	0.29 (+/- 15%) (0.25 – 0,33)		
Specific cost (material only) [1,000€/m ² gross] (excl. VAT, excl. subsidies)	0.22 (+/- 12%) (0.19 – 0.25)	0.27 (+/- 15%) (0.23 – 0.31)		
Specific cost (labor only) [1,000€/m² _{gross}] (excl. VAT, excl. subsidies)	0.02 (0.02 - 0.02)	0.02 (0.01 - 0.02)		
Investment per unit ready installed [1,000€/unit] (excl. VAT, excl. subsidies)	2,400 (+/-12%) (2,100 – 2,700)	14,500 (+/-15%) (12,325 – 16,675)		
Fixed O&M per unit [€/m³ _{g/oss} /a]*	1.7	2.0		
Variable O&M per unit [€/m² _{gross} /a]*	1.5	1.3		
Levelized cost of heat LCOH [€-ct/kWh] - range (from - to)	4.1 (+/- 11%) 3.7 – 4.6	5.5 (+/- 14%) 4.7 - 6.3		

^{* 0.75%} of net investment cost (excl. labor)

Figure 131 shows the average LCOH of SDH systems based on their thermal energy demand. It is shown that in DH networks with low heating demands (< 0,05 TWh/yr)

^{**} Electricity for solar pump and control (around 1.5 kWh electrical / 100 kWh heat produced). Electricity: 24€-ct/MWh

SDH concepts are not cost effective, while LCOH of ~ 30 €/MWh seem to be the typical price fom a heating demand of 0,1 TWh/yr upwards [108]..

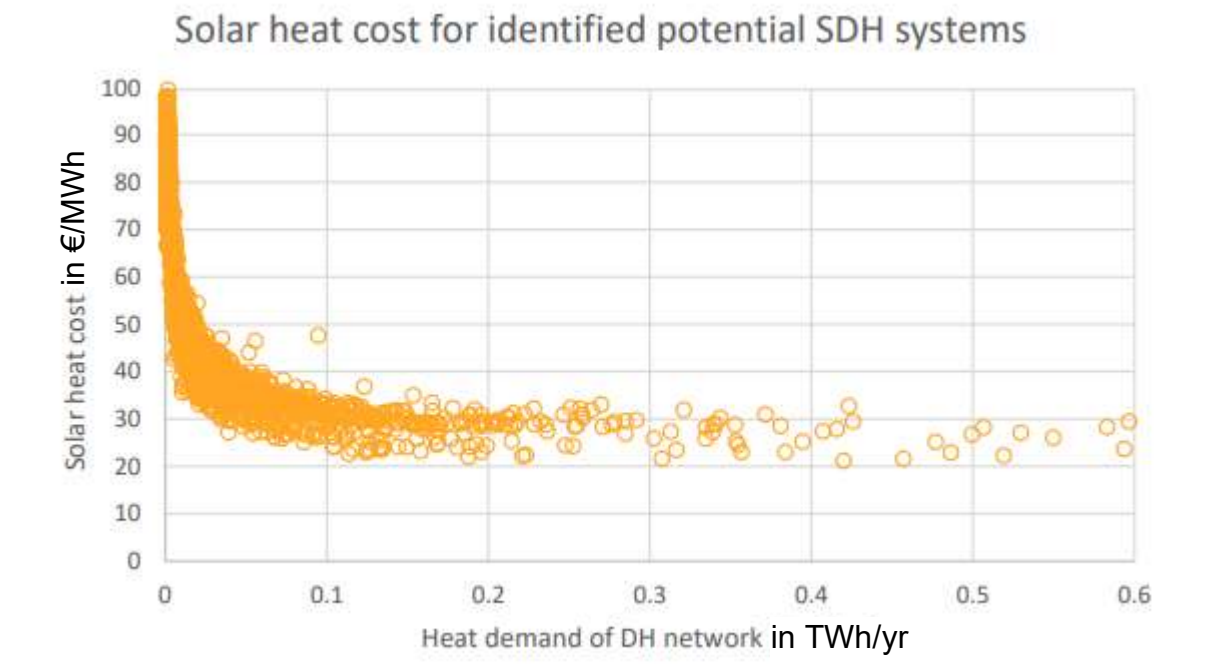


Figure 131 LCOH of a SDH system depending on the thermal energy demand [108]

Another Austrian feasibility study of a SDH is BIG Solar Graz. BIG Solar Graz is a combination between STE, HP, TES, and other waste heat sources. The DH system of Graz provides around 40 % of the thermal energy demand of the city [109], [110]. The peak load of the DH system is 550 MW and the yearly DH demand are 1 200 GWh [111]. The DH feed has a temperature of 120 °C and the return flow is around 60 °C. The highest thermal energy demand (winter) is approximately 20 - 30 times bigger than during the summer. To get the optimum between SF and LCOH a comparison between collector area and storage capacity shown in Figure 132 (in this figure . (dot) are used as thousand-digit-draw) where done. The optimum resulted in a SF of 20 % that can be achieved with a solar aperture area of 450 000 m² (~ 100 football fields) and a TES with 1 800 000 m³ [109], [112].

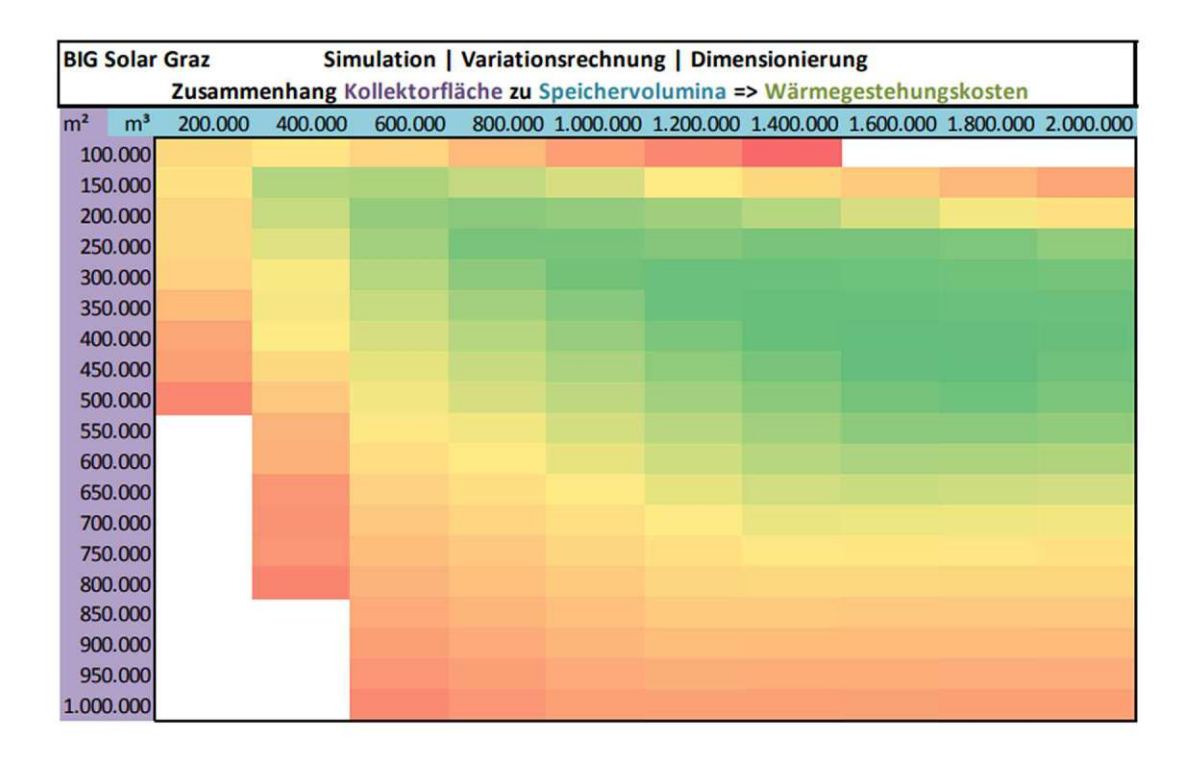


Figure 132 Resulting prices of combinations between solar collector aperture area and storage capacity; green mean cost effective, red bad ratio for cost effectiveness; in this figure . (dot) are used as thousand-digit-draw [112]

The CAPEX cost structure of this project is shown in Table 31 (in this table . (dot) are used as thousand-digit-draw). Based on private equity of 8% and an interest rate of 1,5 % on the loan and a heating price of 35 € / MWh the return-on-investment (ROI) result in 15,5 years [113].

Table 31 CAPEX structure of the BIG Solar Graz project; in this table . (dot) are used as thousand-digit-draw [63]

Gesamtsumme	35	189.000.000 EUR	
Technik)			
Land (Speicher, Kollektoren,		20.000.000 EUR	
Gebäude		1.000.000 EUR	
Verbindungsleitungen		5.000.000 EUR	
Gaskessel inkl. Anbindung	120 MW	8.000.000 EUR	
Re	egelung		
Stromar	nschluss		
Ausdehnung	COLUMN TO THE STATE OF THE STAT		
Solare Übergabe			
Zentrale Technik/Infrastruktur		8.000.000 EUR	
Projektmanagement		10.000.000 EUR	
Absorptions wärme pumpen	96 MW	6.000.000 EUR	
Speicher	1.800.000 m ³	50.000.000 EUR	
Kollektoranlage	450.000 m ²	81.000.000 EUR	

Therefore, LCOH of small SDH systems are around 30 – 40 €/MWh and larger SDH systems show prices of 40 - 55 €/MWh. Increasing solar fractions and larger SDH systems require large storages leading to higher prices. Payback periods are typical very long ~ 10 years [32], [108], [109], [112].

The example of a SHIP system (case study of the textile industry) in chapter 4.3.2 calculated with the RHP shows LCOH of 51 € / MWh including subsidies [105].

4.3.4 Market potential SDH and SHIP systems

DH systems are already well established in Europe, and show a growing trend. Today, most of the thermal energy in DH systems is provided by fossil fuels. SDH systems are a technology to substitute fossil thermal energy generation for DH systems by renewable sources. Role model for SDH systems is Denmark. Figure 133 shows a summary about SDH in Denmark on a 2019 basis [3].



Figure 133 Summary of Danish SDH achievements [3]

2010 the global installed capacity of large-scale STE was low (38 MW), but in 2018 1,55 GW were reached. The growth between 2010 and 2016 of the four main markets (Germany, Denmark, Austria and China) is shown in Figure 134. The decline in 2016 of the newly installed STE capacity in Denmark is a result of the changed promotion scheme [3].

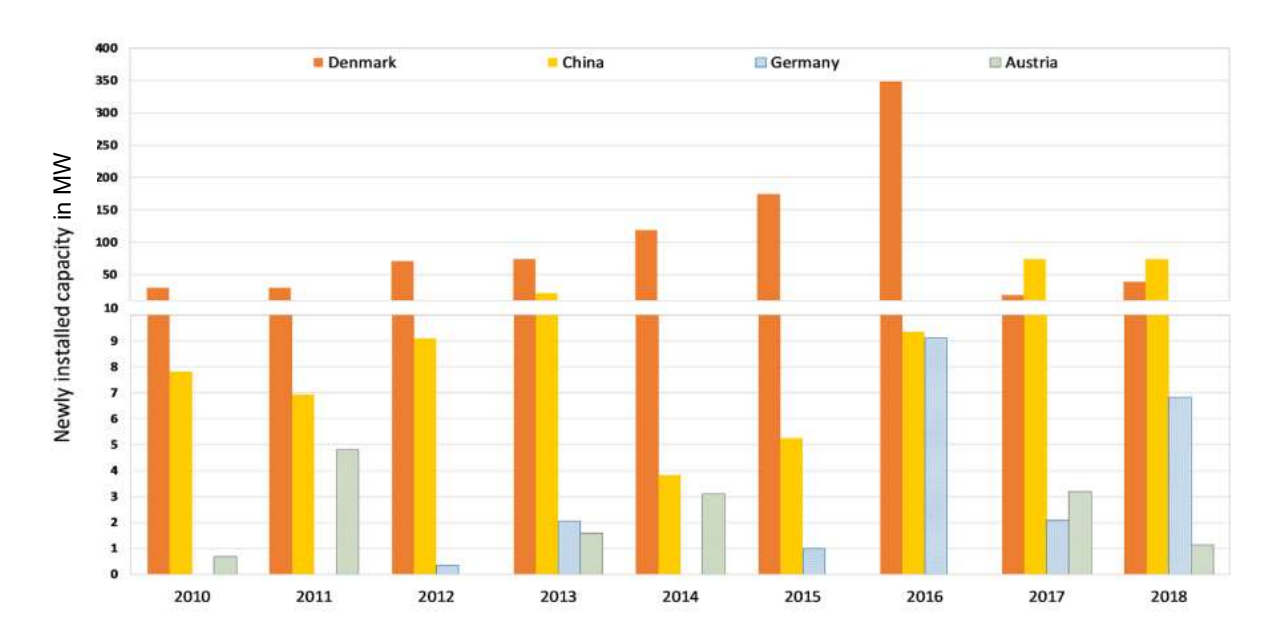


Figure 134 Newly installed large-scale STE capacity between 2010 and 2016 in the countries Denmark, China, Germany and Austria [3]

The trends of SDH systems in the four mentioned countries are shown in Table 32 (in this table . (dot) is used as decimal point and , (comma) as thousand-digit-draw). It is noticeable that in Europe mostly FPC are used, while China relies on different collector types. Europe count on general solutions which offer SF of 20 - 40 %, while China focuses on specialized solutions with SF up top 90 % [3].

Seite | 132

Characteristics of large-scale solar thermal systems.

		Denmark	China	Germany	Austria
Number of plants (2018)	[-]	118	55	37	23
Total installed capacity (2018)	[MW]	969	212	45	27
Installed capacity per 1000 inhabitants	[kW]	167 kW	0.15 kW	0.55 kW	3.08 kW
Total installed collector aperture area (2018)	$[m^2]$	1,384,000	304,000	65,000	39,000
Average collector area	$[m^2]$	11,700	5,500	1,800	1,700
Collector type (main)		FPC	ETC, FPC, PTC	FPC, ETC	FPC
Mounting (main)		Ground mounted	Ground mounted	Ground mounted	Roof mounted
Seasonal heat storage (main)		Water pit storage	Borehole storage	Multifunctional short- and long-term storage	None
Typical solar fraction	[%]	7–20% (diurnal storage), 40–50% (seasonal storage)	Up to 90%	7–20% (diurnal storage), 40–50% (seasonal storage)	10–20%
Applications (main)		SDH including SH and DHW typically for small towns	Industrial processes, SH with fixed heating season, separate DHW systems	SDH including SH and DHW, typically for villages and city quarters	SDH including SH and DHW, typica villages and city quarters
Heat price (typical)		36 €/MWh (systems > 7 MW, diurnal storage); 49 €/MWh (systems > 35 MW, seasonal storage)	Not available	50 €/MWh	Not available

The growth of solar energy-based systems is due to their high CAPEX very much dependent on promotion schemes and given boundary conditions. Figure 135 shows examples for promotion schemes and boundary conditions in the countries Denmark, China, Germany, and Austria. Denmark with the highest installed large-scale STE also meets the most promotion schemes and the best boundary conditions [3].

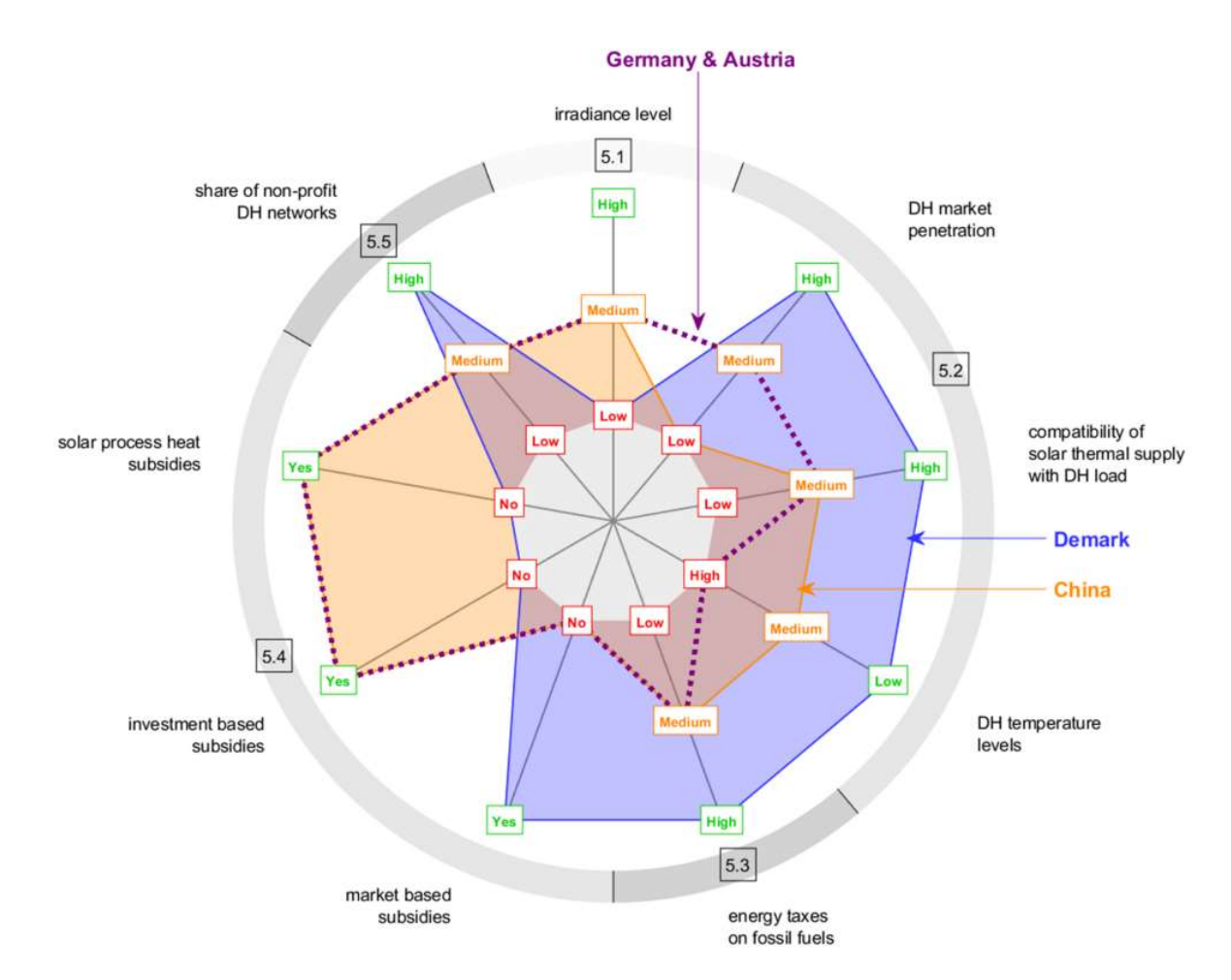


Figure 135 Promotion schemes for solar based systems and boundary conditions in the countries Denmark, China, Germany and Austria along nine axes [3]

Table 33 (in this table . (dot) are used as thousand-digit-draw) shows the number of existing large-scale SDH divided into > 1 MW and > 350 kW in Europe based on 2018. The total power of both categories results in 2,29 GW. The average yearly growth between 2013 and 2018 was 21 % [114].

Table 33 Market data of large-scale SDH systems in Europa (2018); in this table . (dot) are used as thousand-digit-draw [114]

	Anzahl	167	
Anlagen > 1 MW _{th} europaweit in Betrieb	Kapazität [MW _{th}]	1.096	
europaweit iii betrieu	Kollektorfläche ¹ [m ²]	1.579.629	
1 - 250 LW	Anzahl	325	
Anlagen > 350 kW _{th} europaweit in Betrieb	Kapazität [MW,,)	1.196	
europaweit iii betrieb	Kollektorfläche [m²]	1.707.803	
	Anzahl	22	
Hiervon mit erster Inbetriebnahme 2018 ²	Kapazität [MW _{th}]	62,5	
ilibetriebildililie 2010	Kollektorfläche [m²]	89.238	
Mittlerer jährlicher Zubau der vergangenen 5 Jahre	[% pro Jahr]	21	
F	[GWh/a]	700	
Energieproduktion ^{2, 3}	[TJ/a]	2.521	
Vermiedene CO ₂ -Emissionen ²	[tCO ₃ /a]	1.242.714	

Figure 136 shows the solar thermal energy potential in Europe depending on the price limit and the SF of the SDH network. This analysis is based on existing DH systems in 2018, which are suitable for STE (availability of land) and do not have other excess heat options nearby. It is shown that at a SF of 20 % a big part of the SDH potential is reached at LCOH of 35 €/MWh and to not exceed 20 000 GWh/yr. Higher SF in SDH networks result in a bigger potential, while being more expensive [108].

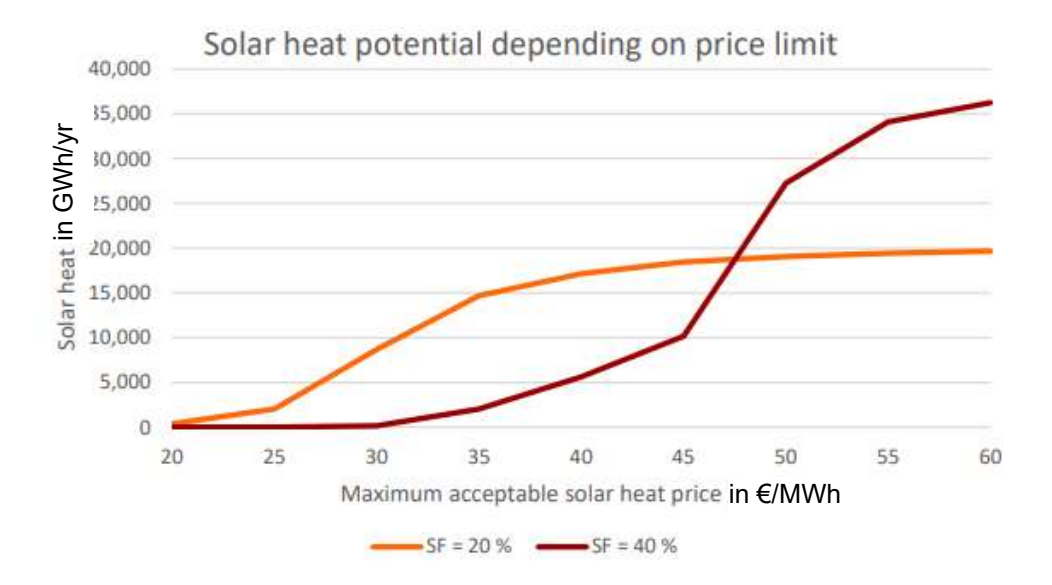


Figure 136 Potential for solar thermal energy in Europe depending on the LCOH and the SF [108]

Figure 137 shows the solar thermal energy potential of different European countries depending on the resulting LCOH of the solar system. If the current thermal energy supply in a country is expensive the market is particularly interesting. This is the case if the SDH potential at LCOH greater than ~40 €/MWh is big. Such countries are for example Spain, Estonia, Czech Republic, or Italy [108].

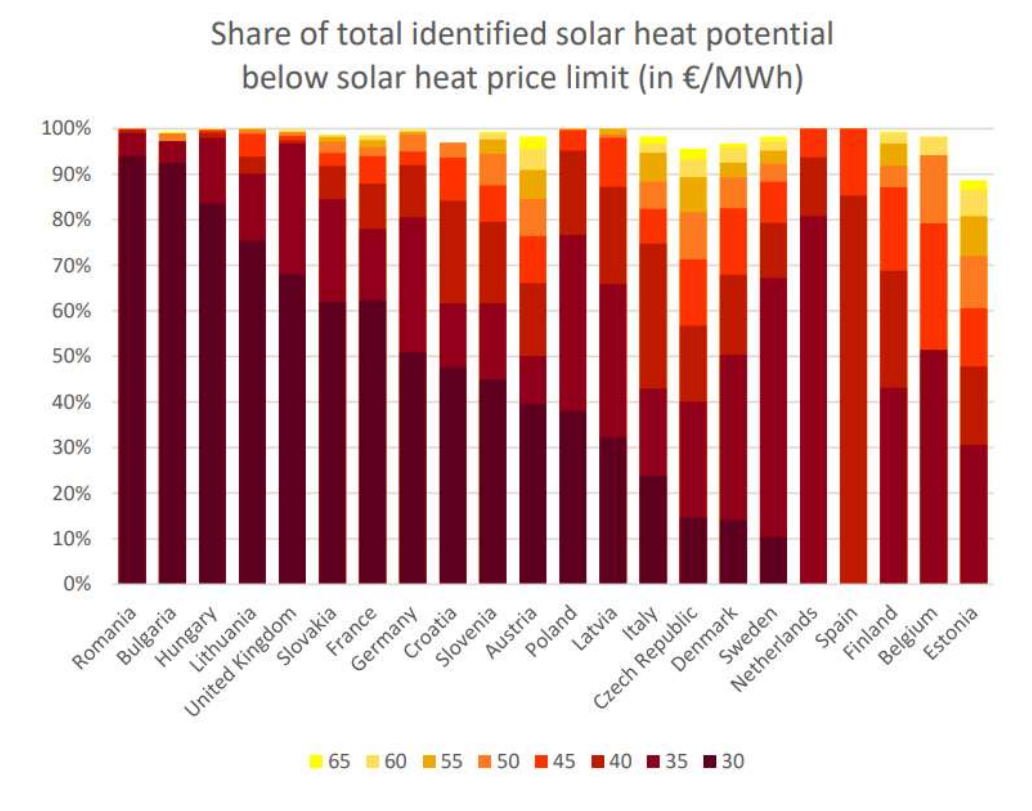


Figure 137 Solar heat potential depending on the LCOH for some European countires [108]

If we assume a SDH economic potential of 100 TWh/yr (very conservative assumption) and a SF of 30 % the solar heat potential in Europe result in 30 TWh/yr. Considering an average solar yield of 500 kWh/(m² yr) and an approximately power per collector aperture area of 0,7 kW/m² the resulting STE power in Europe is 42 GW. Assuming around 70 % of the SDH system are in combination with a HP and the ratio between HP and STE power is 25 % the addressable market potential for HP in SDH systems is 7,35 GW. This result in 10 500 ecop RHP with each having a nominal power of 700 kW [70].

The potential of STE in the industry was analyzed in the International Energy Agency Solar Heating and Cooling (IEA SHC) Task 49. It was found that the global SHIP potential is between 1 500 and 2 200 TWh/year [32].

Figure 138 shows the technical SHIP potential in several European countries. It is shown that the SHIP potential is between 3 - 4 % of the industrial thermal energy demand. According to Figure 46 the process heat demand in Europe is 2 000 TWh/yr (technical potential). Assuming that the European average of SHIP potential is 2,5 % (very conservative) of the process heat demand the addressable process heat is 50 TWh/yr (economic potential). Assuming that 50 % of the 50 TWh/yr are a combination between STE and a HP and the ratio between HP and STE power is again 25 % the market potential for SHIP in Europe result in 8,75 GW or 12 500 ecop RHP [32], [70].

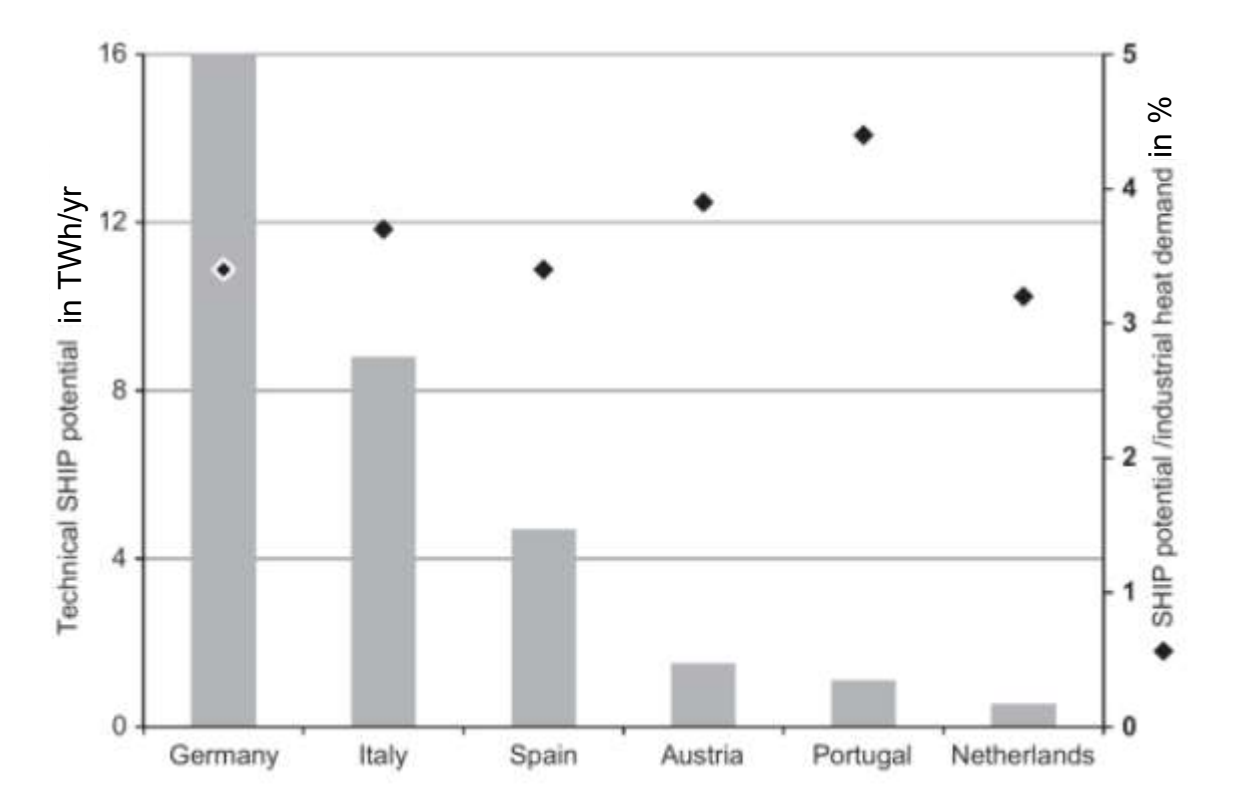


Figure 138 STE potential in several European countries in TWh per year and as fraction of the total industrial thermal energy demand [32]

4.4 Flue gas utilization

In this chapter different methods to treat flue gas of variable combustion processes is examined. The goal is saving primary energy and increasing the efficiency of the overall system.

4.4.1 Steam generator feed preheating with IHP add on

In this section a method to reduce the fossil fuel consumption for steam production by adding an IHP to the system is described. The steam generator is modeled as NG fired steam boiler. In this analysis the steam generator is simplified neglecting water pretreatment, desludging, degassing and other auxiliary systems.

Reusing of the condensed steam (Use case Flue gas-1)

Figure 139 shows on the top a typical setup of a gas boiler. On the bottom of the figure the setup is pictured in a simplified way. In this case it is assumed that the steam circuit is a closed system. Therefore, the condensed process steam can be reused as feed with around 100 °C. In the conventional system the water feed (100 °C) is preheated in an economizer (Eco) by hot flue gas to around 130 °C. At the Eco entry the flue gas is usually 60 – 80 K above the steam output temperature. The flue gas is cooled down to temperatures >140 °C (depending on the primary fuel) to be higher than the acid dew point. In the case of NG combustion, the acid dew point is due to a low sulfur content of NG not a big thing. Nevertheless, the dimensions of the Eco limit the heat transfer. Flue gas temperatures below 130 °C at the Eco outlet can usually not be reached. The remaining thermal energy of the flue gas after the Eco can be used in another downstream Eco to preheat the freshwater feed or to preheat the required air for combustion. Exemplary can a downstream air preheater (LUVO) (condensing Economizer are analyzed in 4.4.2) be used to preheat the needed air for the combustion from 15 – 100 °C. In the gas boiler itself the rest of the needed thermal energy from 130 °C (liquid) to 180 °C saturated steam is supplied [115], [116].

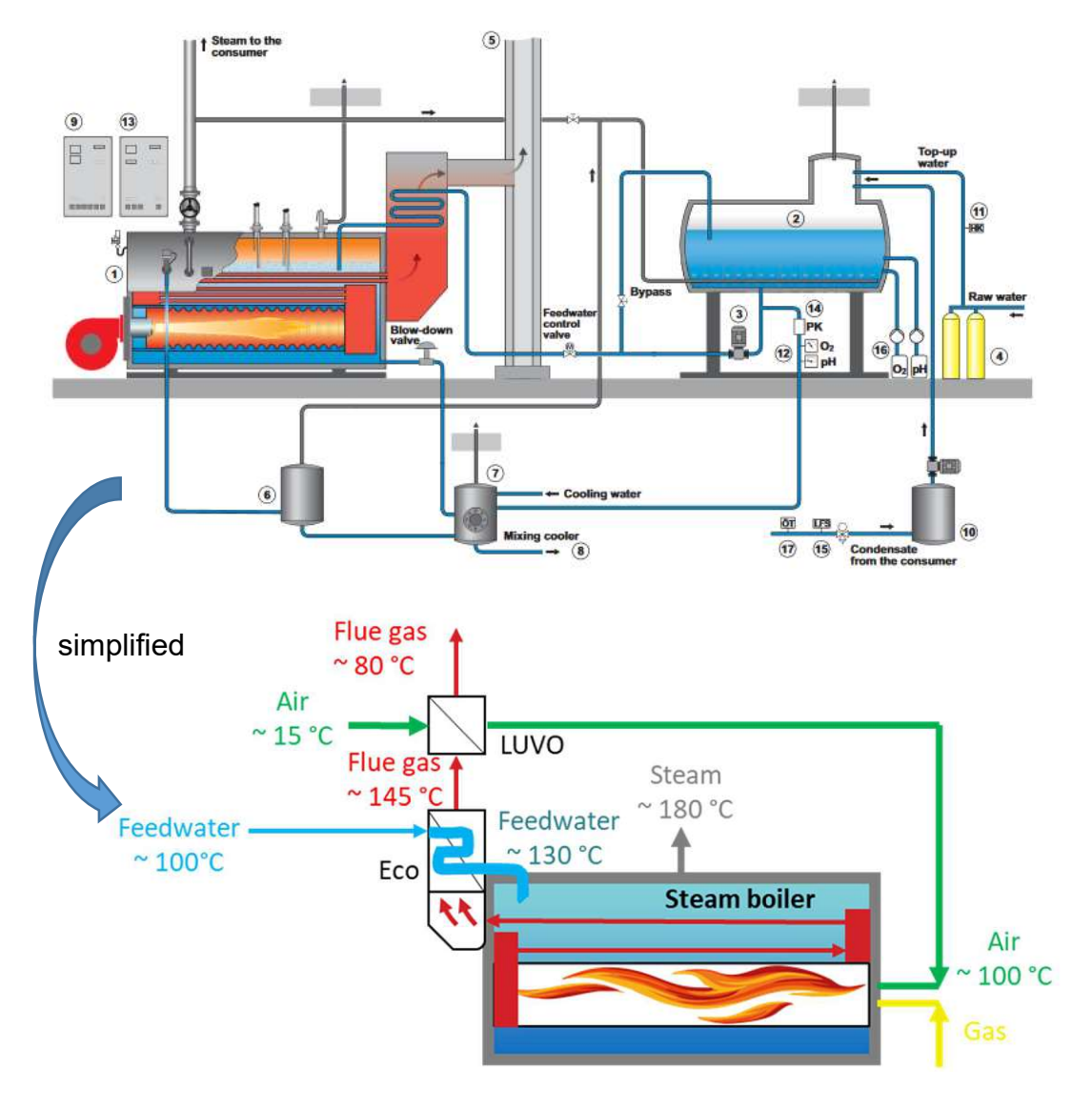


Figure 139 Set up of a conventional gas boiler (top) and its simplified visualization (bottom) based on [70], [115]

Adding a HT-HP to the system can help reducing primary energy. A simplified visualization of the HT-HP add on to the gas boiler circuit is shown in Figure 140. The integration of a HT-HP is used to preheat the freshwater feed from 100 °C to 140 °C before entering the Eco. In this setup the feed reaches higher temperatures in the Eco (~ 160 °C). The increased boiler inlet temperature of the feed directly leads to a lower thermal energy demand in the gas boiler and therefore to fuel savings. In this setup the Eco outlet temperature of the flue gas increases. Therefore, the flue gas should be cooled down in another downstream Eco. The remaining thermal energy in the flue gas is used in a downstream Eco (Eco 2 in Figure 140) to heat the source circuit of the HT-HP. The HT-HP source circuit can also be powered by other excess heat sources or STE [70].

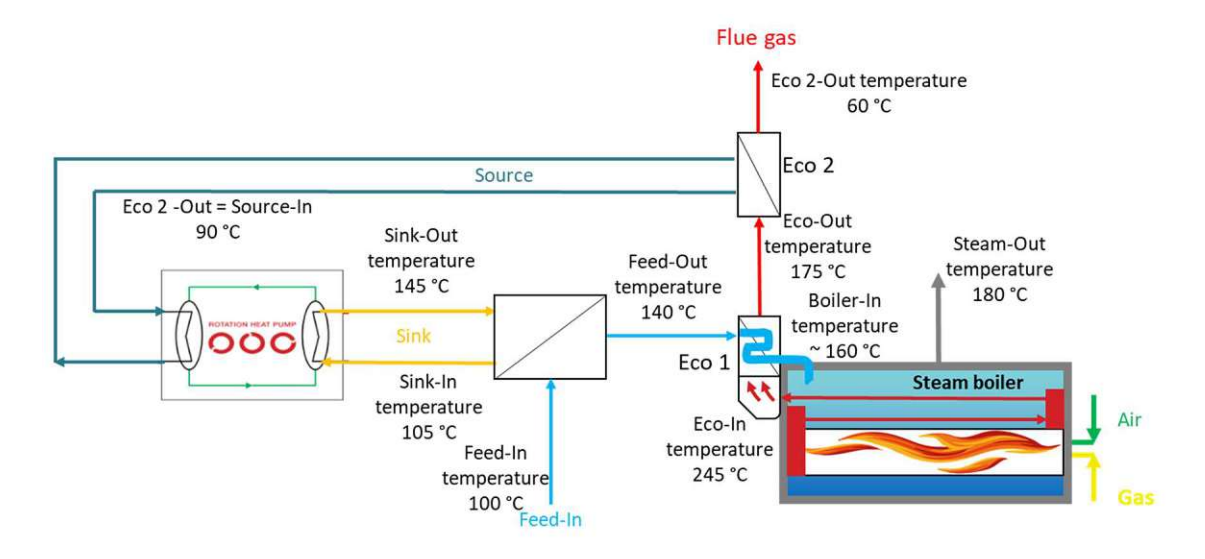


Figure 140 Simplified visualization of the RHP integration for the freshwater feed preheating in the gas boiler circuit [70]

As HT-HP exemplary the ecop RHP can be used which reach in this set up a COP of 3,74 shown in Figure 141. Necessary for this application is that the HP can reach temperatures of > 140 °C [68].

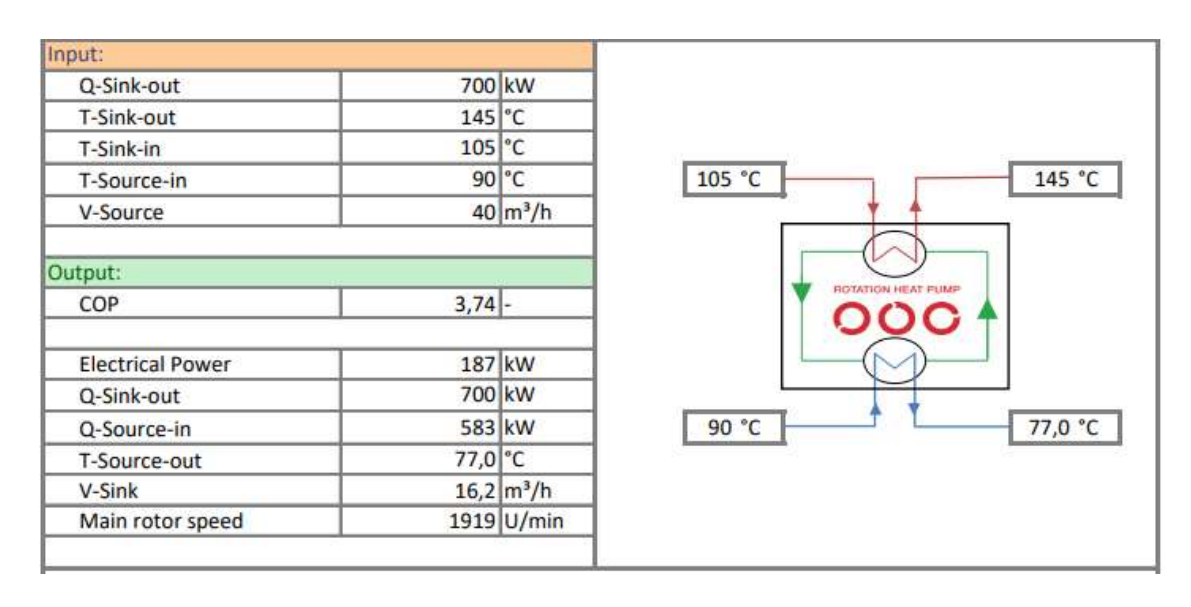


Figure 141 Simulation of the ecop RHP in the gas boiler add on setup (Use case Flue-1) [68]

Economic analysis IHP add on with reusing of the condensed steam (Use case Flue gas-1)

In this section it has been analyzed if the HT-HP add on is economical feasible. For this analysis four key parameter are relevant, which were determined as follows: gas price (25 €/MWh), electricity price (75 €/MWh), CO₂ price 113 €/tco₂), discount rate 3 % and Scope 1 direct emissions of 0,201 tons CO₂ per MWh_{NG} as primary energy carrier (for more details see 3.4). Annually 8000 FLH are assumed for this scenario. Another relevant parameter is the feed temperature at the gas boiler inlet (after Eco), which depends on the HT-HP preheating potential and will be varied between 150 – 170 °C. Higher feed temperatures lead to higher gas savings being more economic. With the given values above for the example of 160 °C gas boiler inlet temperature in total 155 k€ can be saved every year considering a production of 15 t/h saturated steam with 180 °C. 7 k€ result directly from the gas savings and 108 k€ result from the saved CO₂ certificates. The NG savings related to the fossil scenario result in 4,7 % or 798 tCO₂/yr. The required electricity for the RHP (COP of 3,74) are considered in this calculation. The needed thermal power of the HT-HP for the preheating purpose result in 700 kW, what equals one ecop RHP. With costs of 490 k€ of the RHP in this case including auxiliary system the dynamic payback period result in ~ 4,5 years [95], [70], [117]. Figure 142 shows the payback period of the RHP according to the gas boiler inlet temperature, which equals the Eco outlet temperature. It is shown that with increasing gas boiler inlet temperature the payback period decreases, because more gas is saved while the investment is constant [70].

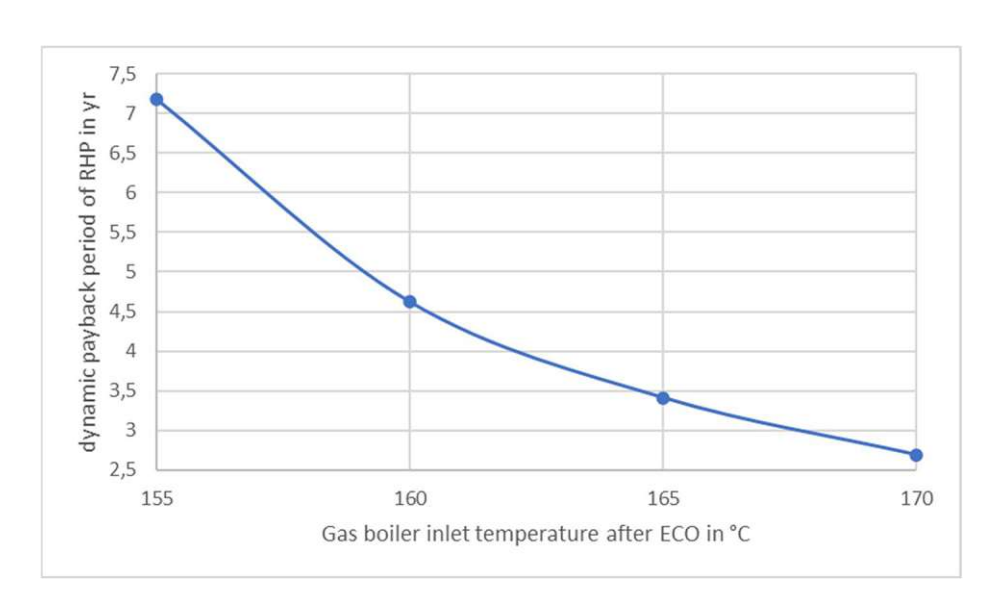


Figure 142 ecop RHP dynamic payback period according to the gas boiler inlet temperature (= Eco outlet temperature) [70]

Fresh water stream with 20 °C - no steam reuse (Use case Flue-2)

In the second example it is assumed that the generated steam is consumed during the industrial process. Furthermore, no external heat sources except the flue gas are used for preheating the freshwater feed. This setup is shown in a simplified way in Figure 143. The freshwater feed with 20 °C is preheated in a downstream Eco (Eco 2 in Figure 143) to around 40 - 50 °C. The preheating potential is depending on the flue gas outlet temperature of the upstream Eco (Eco 1 in Figure 143). The heating between 43 and 100 °C is often done by tapping saturated steam for degassing. In oil boilers this step is necessary, to avoid a cooling down of the flue gas in the Eco 1 below the acid dew point. In general, the freshwater feed needs to be heated to around 100 °C before entering Eco 1 to reach high Eco 1 outlet temperatures of the feed [115].

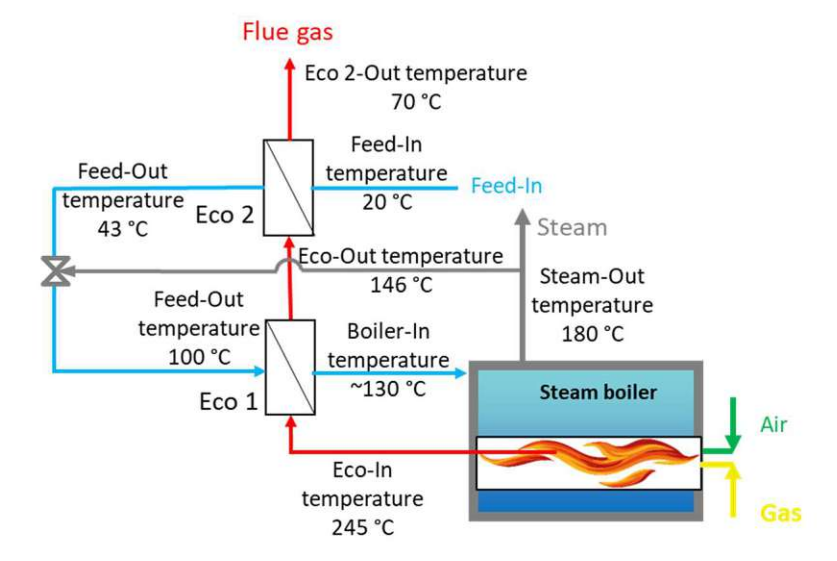


Figure 143 Set up of the steam boiler without external freshwater preheating based on [70], [115]

In comparison to the only fossil scenario (Figure 143) Figure 144 shows the same system with a HT-HP added. The HT-HP is used to lift the temperature from the Eco 2 outlet temperature to 100 °C in the first step and in another step to 140 °C. Depending on the mass flow this can be done in one or several stages. To minimize exergy losses several stages are recommended. Additionally, also waste heat streams can be used for preheating from 40 to 100 °C. Due to the HT-HP feed water preheating to 140 °C the Eco 1 outlet temperature of 160 °C can be reached leading to fossil fuel savings. It is assumed that any case of waste heat or STE can be used as source for the HT-HP [70], [115].

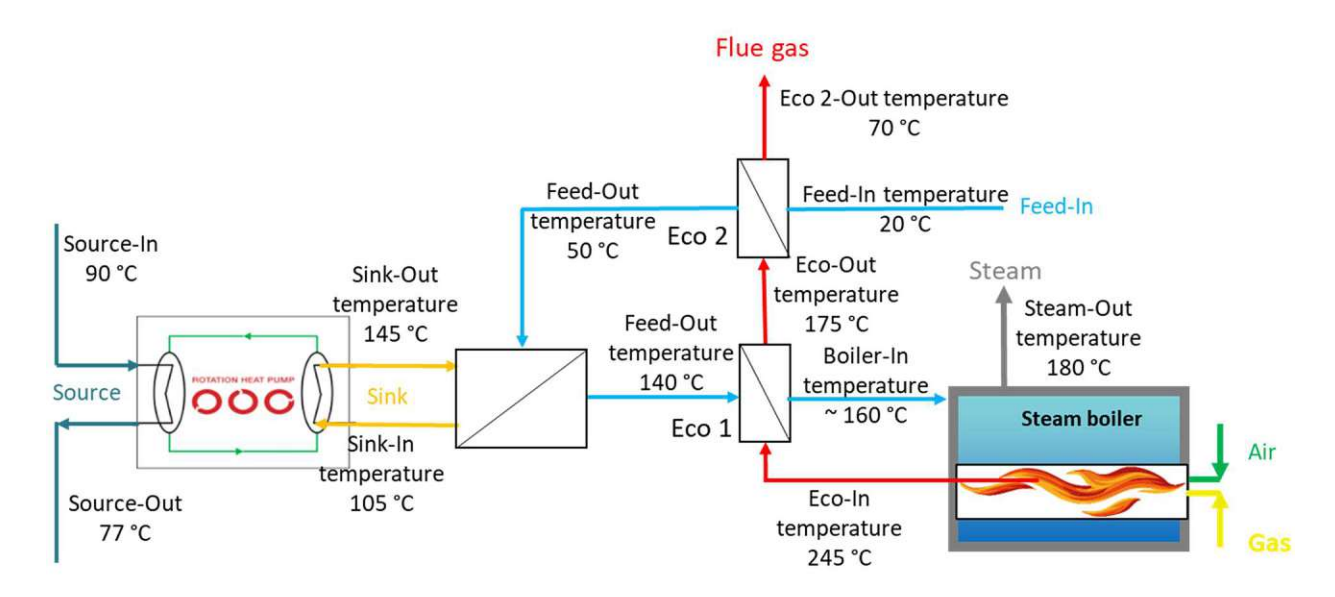


Figure 144 Simplified visualization of the RHP integration in the gas boiler circuit without external freshwater preheating [70], [115]

Considering the same economic parameters as mentioned above the dynamic payback period according to the Eco 1 outlet temperature (150 - 170 °C) is given in Figure 145. For this setup two ecop RHP are needed leading to investment costs of 980k €. The ecop RHP have the same COP than in the previous example (COP 3,74). The dynamic payback period in this setup is lower than in Figure 142, because higher NG savings are realized. The higher NG savings result from the additional preheating task of the HT-HP (50 - 100 °C). In the fossil scenario some steam needs to be generated on top for the feed preheating and degassing. In the case of 160 °C Eco 1 outlet temperature the NG savings related to the fossil scenario result in 14,6 %. 344 k€ are saved with the HT-HP add on every year leading to DPP of 3,02 years. 75 k€ result directly from the gas savings and 269 k€ result from the saved CO₂ certificates [70].

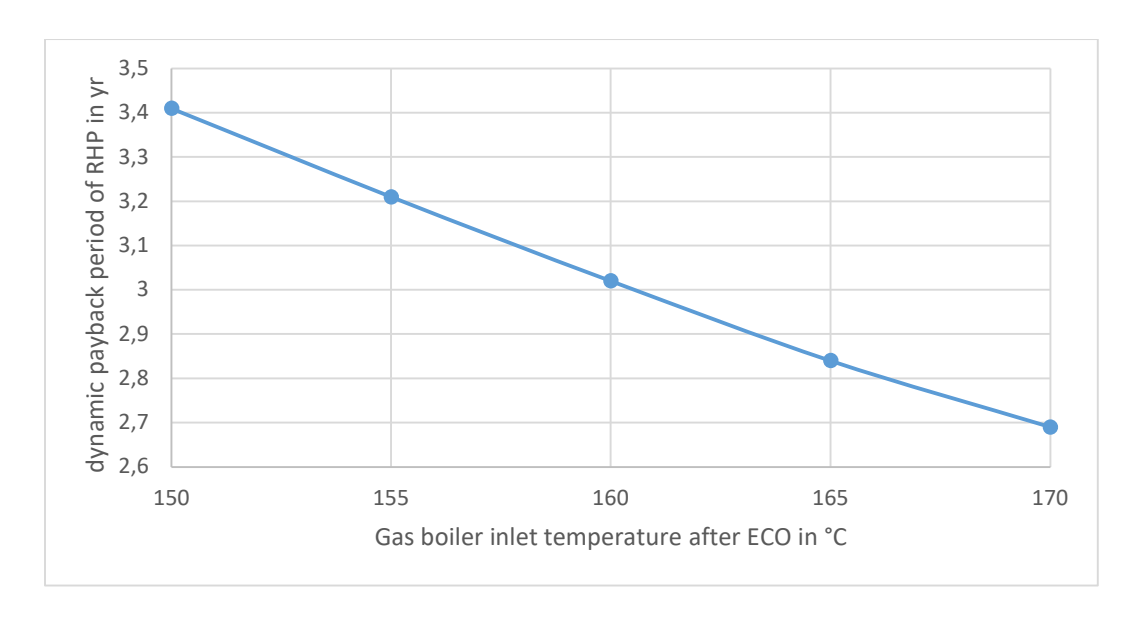


Figure 145 ecop RHP dynamic payback period according to the gas boiler inlet temperature (= Eco 1 outlet temperature) [70]

Potential IHP add on in steam generator

While a lot of research is done for entirely renewable steam production the steam boiler market is still dominated by fossil fuels showed in Figure 146. NG gas boiler have the biggest share of the European steam boiler market with 43,3 %. Fossil steam boilers take up 73,3% of the European steam boiler market [118].

Europe Steam Boiler Market Share, By Fuel, 2022 (Units)

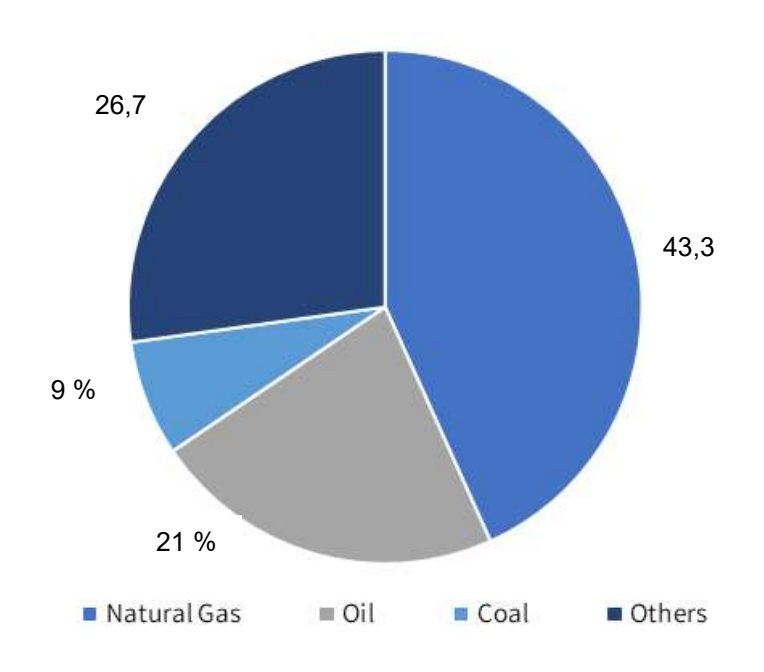


Figure 146 European steam boiler market shares by primary energy (2022) based on [118]

Figure 147 (in this figure . (dot) is used in difference to , (comma)) shows a comparison of the economic efficiency between HP and a NG boiler on the left side. On the right side the related economic parameters like CAPEX, OPEX, et cetera (etc.) are pictured. Gas boiler in this figure is seen as heating unit and not only for steam production. The relevant factors are the electricity to gas price ratio and the needed temperature lift. In general lead lower electricity to gas ratios as well as smaller temperature lifts to advantages of the HP. There are countries (depending on the electricity to gas price ratio) where HP solutions (HP steam generation is investigated in chapter 4.5) are more cost effective and others where the gas boiler is the economic better solution. The cases where gas boilers are the economical better solution are addressed by the HT-HP add on [119], [120].

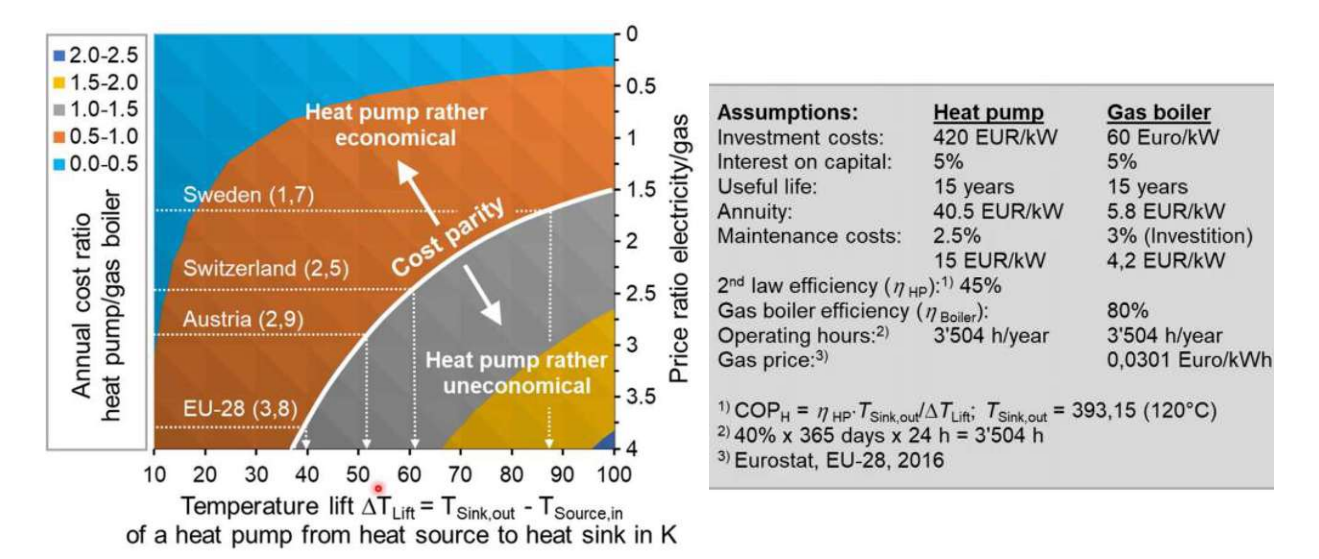


Figure 147 Heat pump integration in comparison to a gas boiler; in this figure . (dot) is used in difference to , (comma) [119], [120]

According to [118] the steam boiler market will grow until 2032 annually by 5,5 %. In 2030 1 138 TWh of primary energy will be needed for steam production in Europe (technical potential). Using the data of [9] show that providing 1 138 TWh of thermal energy needs around 200 GW of thermal power. Assuming that, 20 % are fossil boilers with a HT-HP add on as retrofit or newly built the addressable power are 40 GW (economic potential). Considering a gas to HT-HP power ratio of 8 % on average, due to a mix between the two setups (Flue-1 and Flue-2) the HP potential is 3,2 GW (market potential). Taking into account that one ecop RHP has a thermal power of 0,7 MW the potential of ecop RHP result in 4 571 pieces.

4.4.2 Flue gas condensation (Use case Flue-3)

In this section the focus lies on the flue gas condensation of various fuels. Flue gas condensation is done to decrease the amount of excess heat of combustion processes. If the flue gas is cooled down below the acid dew point different flue gas components like Ammoniac, Chlorides, Sulfur compounds, etc. dissolve in the water making the condensate very corrosive. Therefore, flue gas condensation is usually done if the fuel carries a low amount of these byproducts, such as gas or some kinds of biomass (wood, pellets, wood chips). The flue gas of heavy oil and coal combustion are usually not condensed, because of the high contamination [115], [121].

If the flue gas is cooled below the dew point, the water it contains starts to condense. During the cooling down of the flue gas below the dew point beside sensible heat also the condensing enthalpy (latent energy) is released. The latent energy for cooling down each Kelvin is around 10 times greater than the sensible energy. The acidic water in the flue gas of NG and woody biomass mostly condenses at temperatures around 45 – 70 °C. To condense the gaseous water in the flue gas a cooling circuit with temperatures below the dew point is necessary. Such low temperature fluid streams can be low temperature heating systems, DHW or HP source streams. This section does not focus on the detailed construction of condensing HEX, but the integration of a HP and possible setups [115], [121].

Flue gas condensation can either be done directly in a condensing HEX or indirect in a condensing scrubber. Scrubber are used for cleaning flue gas by absorption of hazardous compounds in a washing fluid. This chapter focuses on condensing HEX, if the flue gas does not need to be cleaned in a scrubber [121], [122], [123].

In the case of gas combustion, the water is generated by Equation (10) [115].

$$CH_4 + 2O_2 = 2(H_2O) + CO_2$$
 (10)

 CH_4 methane

 CO_2 carbon dioxide

The theoretical difference between the calorific value and the heating value of NG are 10 % related to the heating value. That equals 1,5 kg condensable water per Nm³ natural gas. The achievable condensation rate in a condensing HEX is usually between 70 – 100 %, depending on the cooling fluid temperature. The pH (pondus hydrogenii) of the condensate is between 3,5 and 5,2. Hence, the condensing HEX must be made of stainless steel, ceramic, or graphite to ensure an acceptable operating life [115], [121].

The generated energy of the condensing HEX can be calculated according to Equation (11) [115].

$$\dot{Q}_{condensing \ HEX} = \left(\left(T_{in,flue \ gas} - T_{out,flue \ gas} \right) \overline{c}_{p,flue \ gas} + (H_s - H_i) \alpha \right) \dot{B}_{flue \ gas}$$

$$(11)$$

 $Q_{condensing\ HEX}$

extracted thermal power in the condensing HEX in kW

condensing HEX flue gas inlet temperature in K T_{in,flue gas}

condensing HEX flue gas outlet temperature in K Tout, flue gas

mean specific heat capacity of flue gas in kJ / (kg K) $\bar{c}_{p,flue\ gas}$

 H_{s} heating value in kJ/kg H_i caloric value in kJ/kg condensation factor α

 $\dot{B}_{flue\ aas}$ flue gas mass flow in kg/s

Condensing HEX are gladly built if biomass is burned. Biomass can have a water content of up to 60% when it is burned. Therefore, a lot of energy is stored in the emerging water vapor [122].

Figure 148 shows the extractable thermal energy based on the primiary fuel (different coloured lines) and its water content (for wood water content of 15% to 60%). On the abscissa the flue gas temperature is shown. At the point where the line coming from the right curves upwards the water starts to condense. On the ordinate the relative heat recovery on the basis of flue gas with 160 °C, air-fuel ratio of 1,5, relative humidity of 13 % and a reference temperature of 10 °C is shown. The heating value of wood is assmued to be 18,78 MJ/kg. It can be seen that with increasing water content of wood more thermal energy can be extracted. Wood show a greater potential for condensing HEX than NG. Exemplary for the flue gas of a NG combustion the contained water starts to condense at 57 °C. By cooling down the flue gas from 57 to 15 °C 13 % of the NG primiary energy can be extracted [122].

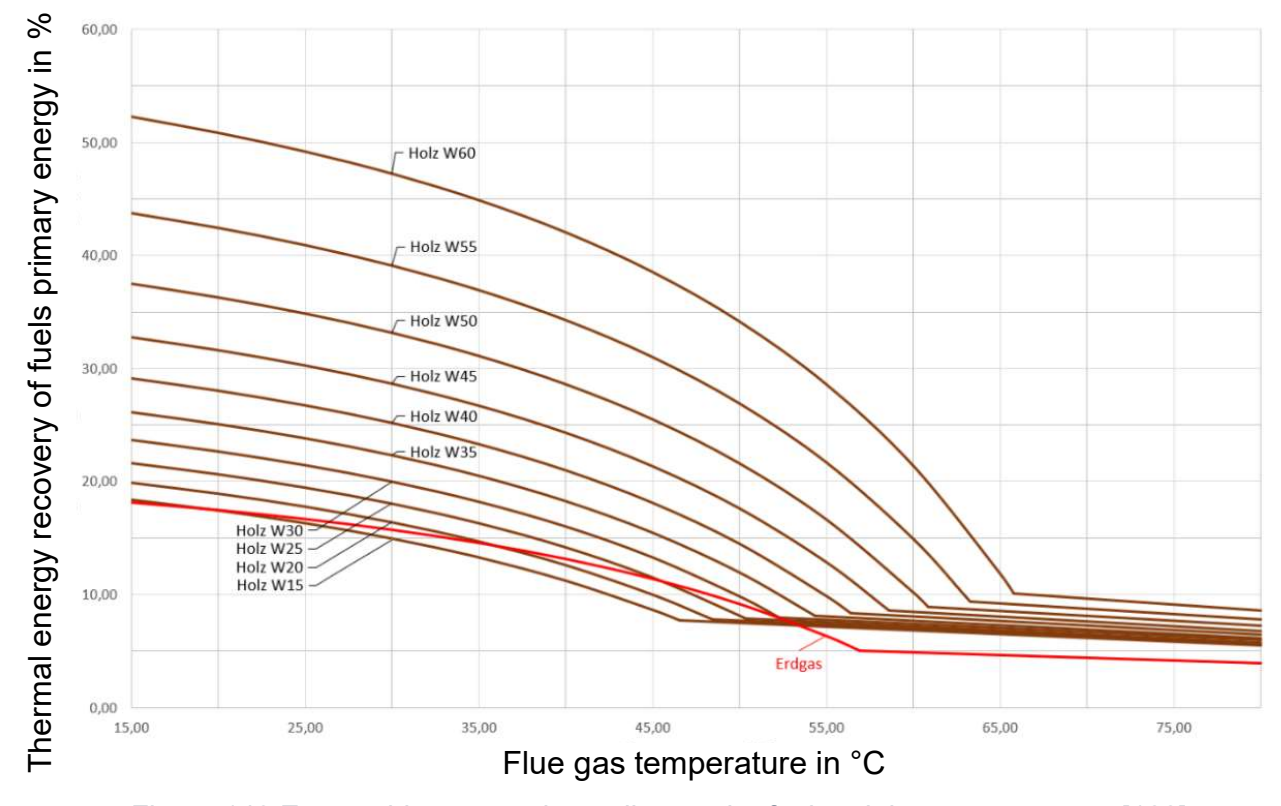


Figure 148 Extractable energy depending on the fuel and the water content [122]

A typical flue gas treatment of a biomass combustion is shown in Figure 149. In the combustion process temperatures of up to 950 °C are reached being used for steam or electricity generation. Afterwards the flue gas with variable temperatures (depending on the usage) is cooled down in an Eco. In a following process step called quenching water can be sprayed to separate dust particles and the relative humidity of the flue gas and the dew point temperature increases. This leads to a more constant condensation rate in the condensing HEX and a better heat transfer. However, continuously wet heat exchanger surfaces corrode less than discontinues wet areas. The sensible and latent heat of the condensing HEX can be used directly for low temperature heating or as source of a HP [121].

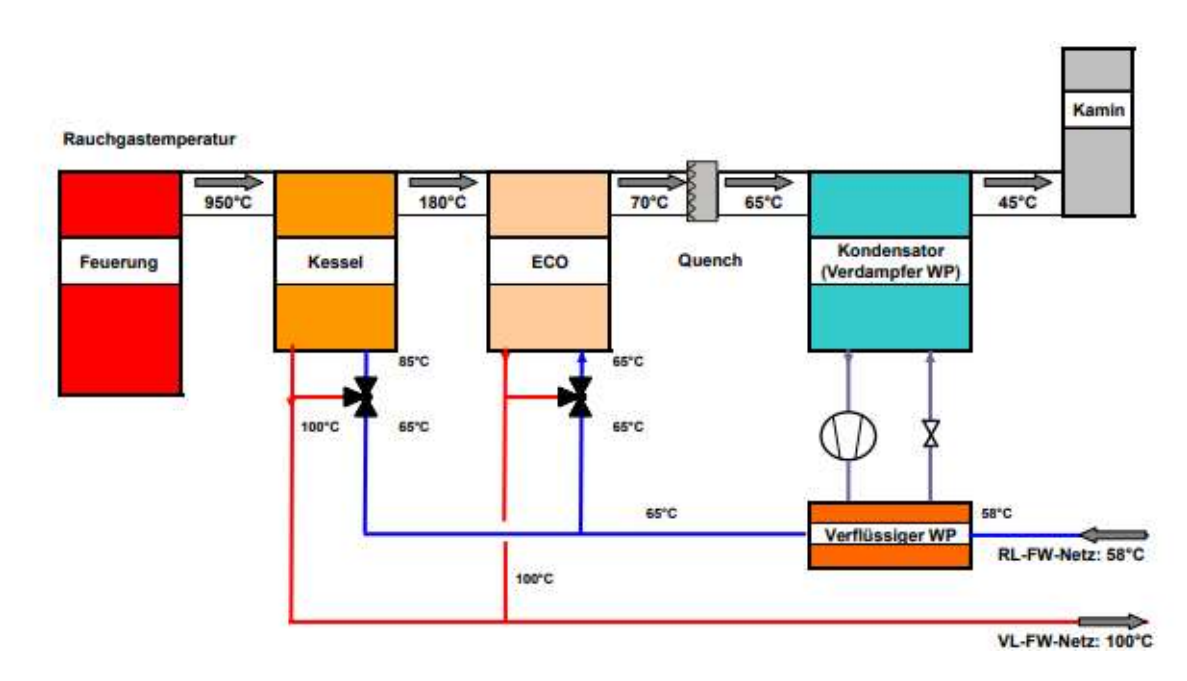


Figure 149 Flue gas treatment in a biomass CHP [123]

To achieve high condensation rates the condensing HEX needs a low temperature cooling circuit. The link between the condensate mass flow and the cooling circuit inlet temperature for a pellet combustion with a dew point of 46 °C is shown in Figure 150. Lower cooling circuit temperatures achieve higher condensation rates. Other fuels usually have higher dew points [124].

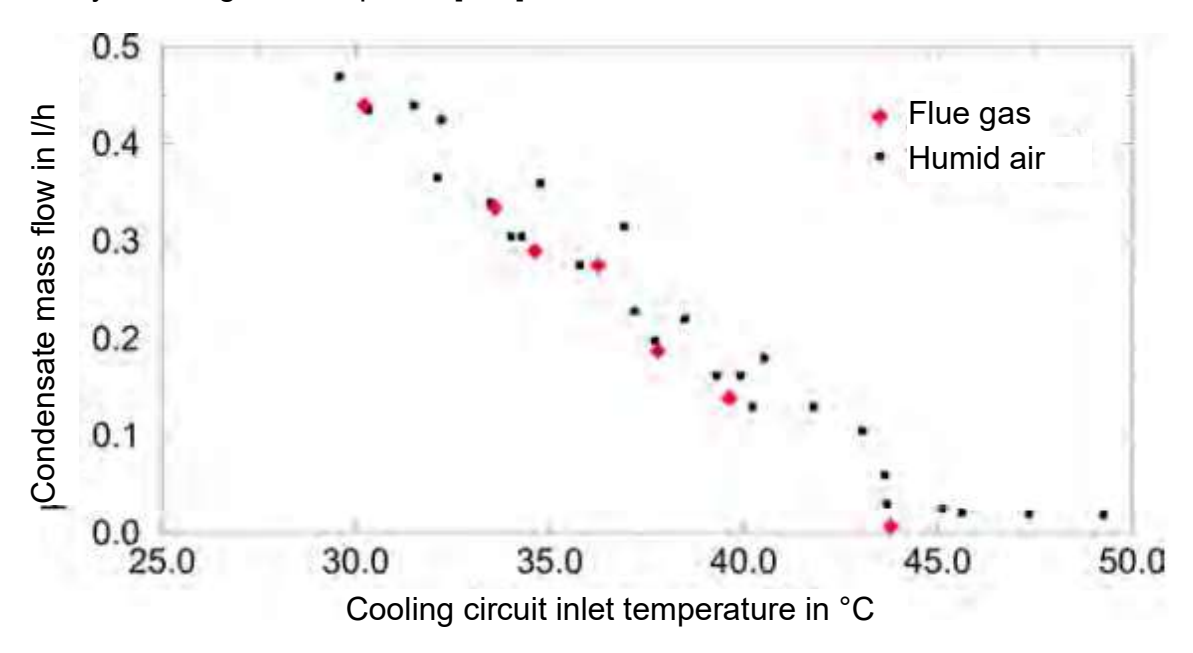


Figure 150 Relation between the cooling circuit temperature and den condensate mass flow [124]

There are two concepts to use the thermal energy of the cooling circuit economically. On the one hand a low temperature network (exemplary space heating, fuel drying or air preheating) can be heated from around 25 - 35 °C to 40 - 50 °C. Figure 151 shows a concept to use the thermal energy of a condensing HEX for air preheating. A part of the DH return with around 60 °C is used to preheat the combustion air (20 – 55 °C) and another air stream for heating purposes (15 – 30 °C). The DH return is cooled down to 30 °C. This stream is afterwards heated up in a condensing HEX ("innovativer Apparat" in Figure 151) from 30 - 60 °C. In a HEX this stream is heated up to 90 °C and afterwards mixed with the remaining DH return. The DH return is then heated up in an Eco to the feed temperature level [124].

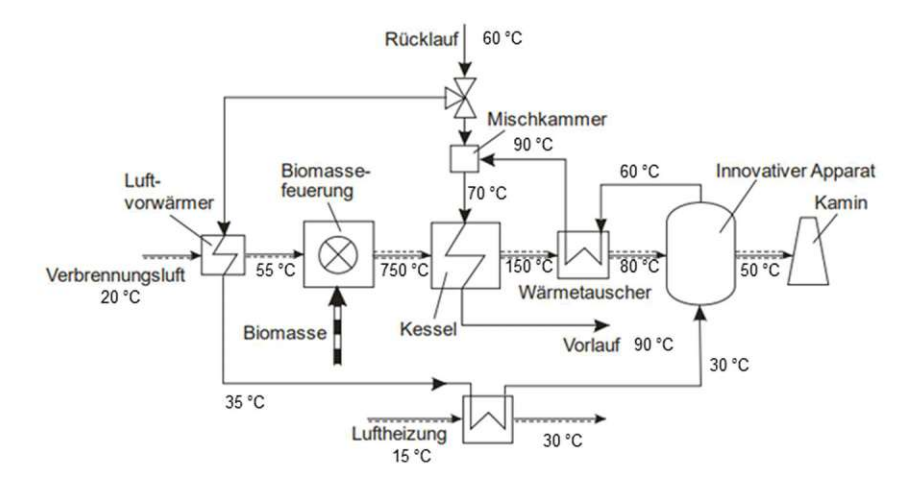
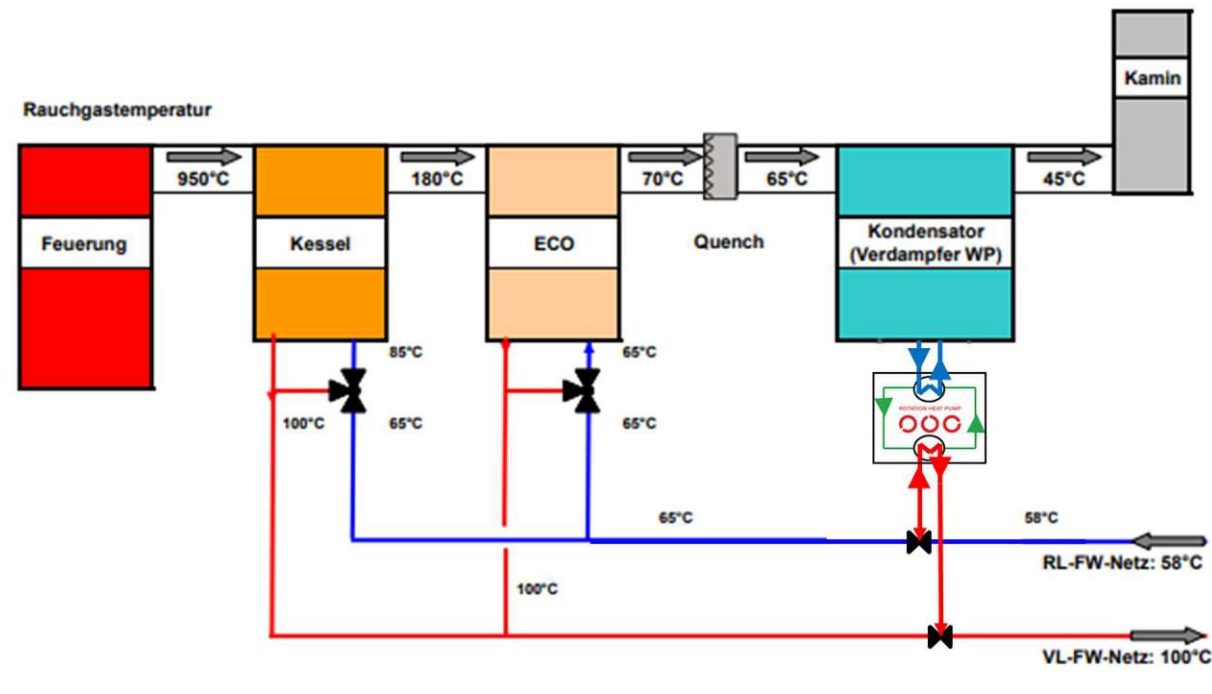


Figure 151 Flue gas condensation used for air preheating [121], [124]

On the other hand, a HP can be used for cooling down the cooling circuit of the condensing HEX using it as source to lift the sink in a serial or parallel way. Figure 152 (top) shows an example for the parallel integration of the ecop RHP into a DH system based on Figure 149. The RHP uses in this configuration the cooling circuit of a condensing HEX as source to lift the DH return to the DH feed temperature. Figure 152 (bottom) shows an exemplary simulation of the ecop RHP in this usage. It is assumed that with quenching a cooling circuit inlet temperature of 28°C achieve high condensation rates. The extracted energy is used to lift the DH return from 58 to 100 °C. It is also possible to integrate the HP sink into process applications (drying, etc.) or to charge a TES for peak loads [121], [123].



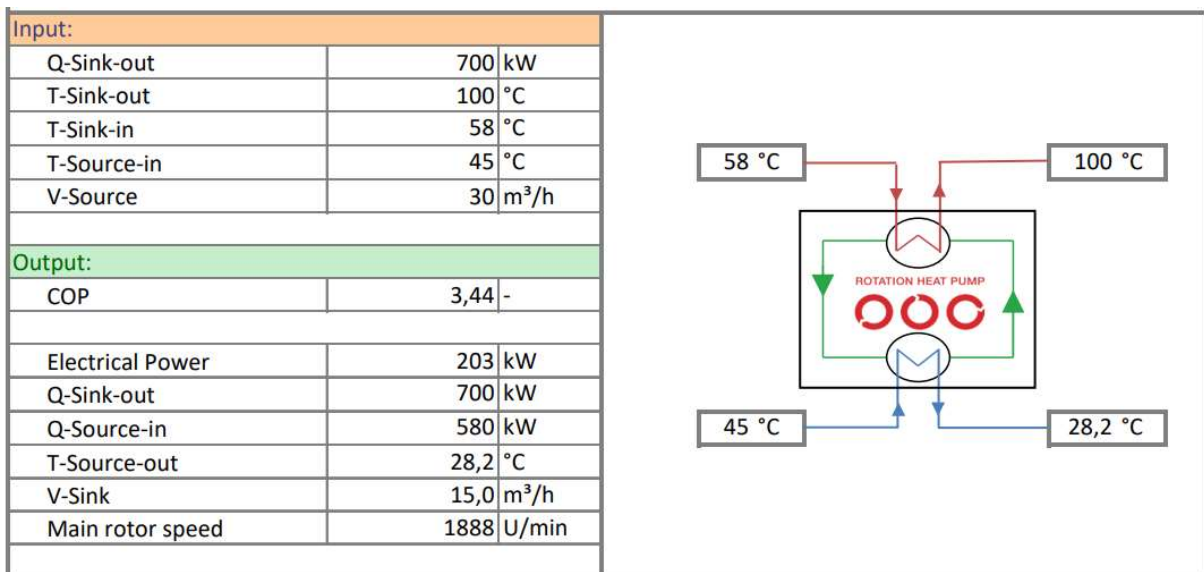
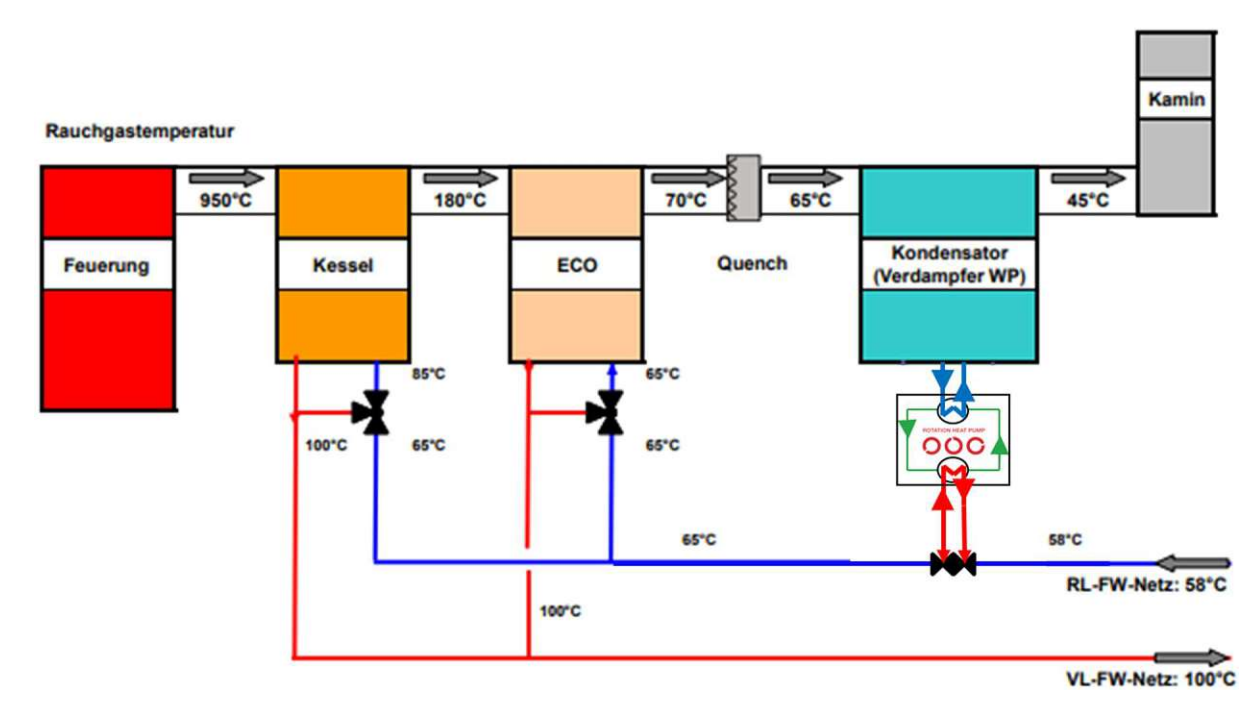


Figure 152 (top) Exemplary visualization of the parallel integration of the ecop RHP in a condensing HEX and (bottom) exemplary simulation of ecop RHP in this setup (Flue-3) based on [68], [123]

In addition to the parallel also a serial setup is possible visualized in Figure 153. In this setup the temperature lift of the HP is smaller and the COP higher. The increased temperature of the DH return leads to an decreased efficiency in the following Eco and HEX, because of a smaller temperature difference [121], [123].



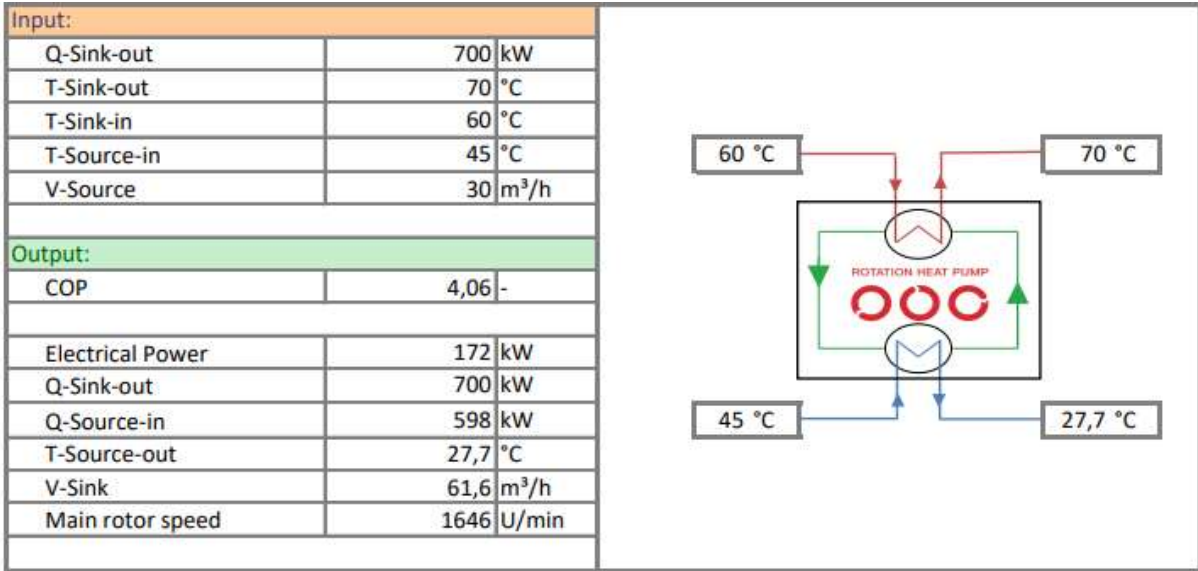


Figure 153 (top) Exemplary visualization of the serial integration of the ecop RHP in a condensing HEX and (bottom) exemplary simulation of ecop RHP in this setup (Flue-3) based on [68], [123]

Usually, it is tricky to manage an integration of the HP source circuit directly as condensing HEX, because of the fixed evaporating temperature of the HP working fluid. Therefore, an intermediate circuit is introduced for condensing and another HEX to transfer the thermal energy to the HP source circuit. This result in additional CAPEX and doubled temperature differences in the HEX. An advantage of the ecop RHP in a condensing HEX is that the ecop working fluid does not need to be vaporized by the source. [121], [123].

Economic efficiency condensing HEX (Use case Flue-3)

In this chapter the economic feasibility of condensing HEX with and without HP are investigated. Condensing HEX can also be built in as retrofit to existing plants.

The payback period of a condensing HEX can be calculated as shown in equation (12) and is usually below one year. The exemplary costs of a condensing HEX with 1 MW power are 105 000 €. The yearly FLH can be assumed with 5000 – 6000 h/yr and the revenue for the extracted heat with 35 €/MWh. With these assumptions the payback period result in around half a year, if the whole energy can be utilized. If a HP is needed around 490 000 €/MW additional CAPEX arise leading to a payback period of less than 3 years. It must be mentioned that in the case of a HP integration the temperature level is higher and can be used for more applications. This fact is not considered in the calculation [3], [115], [70].

$$A_{payback} = \frac{K_{condensing HEX}}{\dot{Q}_{condensing HEX} K_{heat} FLH}$$
 (12)

payback period in yr $A_{payback}$

costs of the condensing HEX in € $K_{condensing\ HEX}$

revenue for extracted thermal energy in €/kWh K_{heat}

FLHyearly full load hours in h/yr

Summarizing it can be said that, a condensing HEX is technical as well as economical feasible in most cases. If a low temperature heating system, that can achieve high condensation rates over the whole year is available, this stream should be used for the flue gas condensation. If such a stream is not available a HP offer the possibility to continuously cool down the source for condensing, while providing high temperatures for other applications. Quenching is possible because it increases the dew point and helps in the dust separation but is not necessary. The biggest hurdle is an efficient integration and control of the HP to reduce the amount of partial load, while enabling high condensation rates. It must be mentioned that a condensing HEX in combination with a HP is only be feasible if the plant is in a MW scale [121], [123].

Potential condensing HEX (Use case Flue-3)

If it comes to the market potential analysis it must be distinguished among different fuels. The European process heat demand of 1952 TWh/a is 90 % supplied by direct combustion processes [4]. According to [9] this would lead to a thermal power of 197 GW (technical potential). If 25 % do not have a condensing HEX, the flue gas is suited for condensing and the operator are willing to invest in a condensing HEX 49,25 GW thermal power can be addressed. Additionally, it is assumed that 80 % of these do not have a low temperature network for condensing or have no need for low temperature

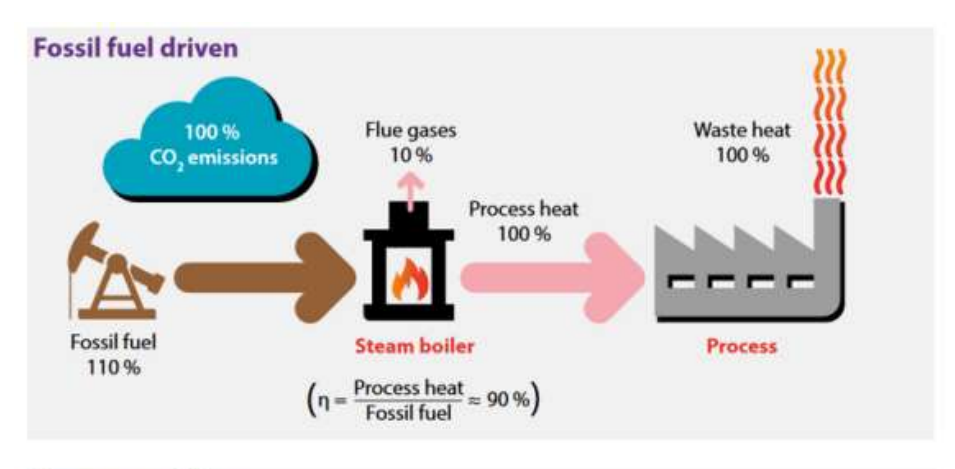
thermal energy. Heat pumps for flue gas condensation can therefore be integrated into combustion processes on the order of 39 GW (economic potential). The market potential arise in 8 443 ecop RHP based on the fact that 15 % of the thermal plant power can be extracted in a condensing HEX [3], [70], [115].

4.5 Steam generation

In the industry steam is often used for heating tasks, because due to the latent heat release better heat transfers are achieved and the temperature control is easier.

This chapter is aiming on steam generating heat pumps (SGHP). In contrast to chapter 4.4 the following use cases get along without combustion processes. Combustion processes for steam generation have high exergy losses due to high temperature differences and are mainly driven by fossil fuels [120].

Figure 154 (in this figure . (dot) is used as decimal point instead of a . (comma)) shows a comparison between fossil driven steam generation and HP driven processes. The advantages of HP driven processes are that waste heat can be recovered leading to primary energy savings. Depending on the electricity mix a CO₂-ev reduction of 100 % is possible, if the electricity is fully renewable [8].



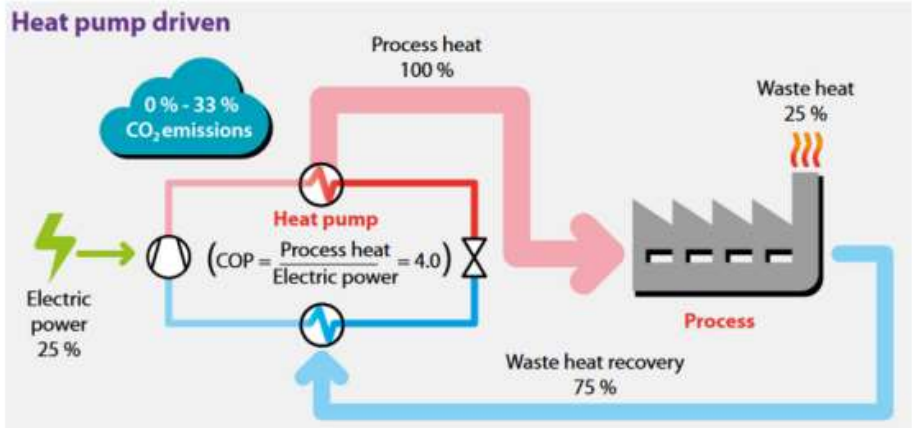


Figure 154 Comparison between conventional combustion-based steam generation and HP driven processes; in this figure . (dot) is used as decimal point instead of a , (comma) [8]

Table 34 (in this table . (dot) is used as decimal point instead of a , (comma)) shows a summary of studies on SGHP all over the world. The table shows that there is not a single SGHP technology, but several different concepts and combinations [120].

Table 34 Research studies of SGHP over the world; in this table . (dot) is used as decimal point instead of a, (comma) [120]

Organization, country	Heating capacity (kW)	Heat source temperature (°C)	Steam temperature (°C) (flow rate kg/h)	Heat pump cycle, compressor	Refrigerant	COP (source/sink temperature °C)	Reference (year)
Korea Institute of Energy Research	300	60	128 (422)	HTHP + flash tank, piston	R245fa	n.a.	Chang et al. (2016) [13]
	100	70	120	HTHP + flash tank, open screw	R245fa	3.05 (70/120)	Wang et al. (2018) [14]
(KIER)	25	60	104 - 123	HTHP + IHX + flash tank + valve	R245fa	~ 3.5 (60/105)	Lee et al. (2017) [15]
Seoul National	6 - 8	60 - 70	115 - 125 (10.8)	HTHP, piston	R245fa	2.95 (60/125) 3.59 (60/115)	Kang et al. (2019) [9]
University, Korea	6 - 12	60 - 80	115 - 125	HTHP + steam reservoir + MVR	R245fa	3.39 (80/125) 2.72 (60/115)	Yoo et al. (2017) [3]
Tokyo Electric Power, Mayekawa, Japan	400	80 - 90	130	HTHP, screw	R601 (pentane)	4.5 (80/130)	Yamazaki and Kubo (1986) [16]
Kobe Steel, Ltd.,	660	35 - 70	165 (890)	HTHP + MVR,	R134a/R245fa (SGH165)	2.5 (70/165)	Kaida et al. (2015) [4]
CRIEPI, and electric companies, Japan	380	25 - 65	120 (20)	screw	R245fa (SGH120)	3.2 (65/120)	Kuromaki (2012) [8]
Mayekawa, Waseda University, Japan	300	80	100 - 180 (thermal oil)	Transcritical HTHP, centrifugal	R600 (butane)	3.5 (80/180) calculated	Kimura et al. (2018) [17]
Shanghai Jiao Tong University, China	285	75 - 85 (evaporation)	111 - 150 (condensation)	VHTHP + flash tank, twin-screw	R718 (water)	6.10 (85/117) 1.96 (85/150)	Wu et al. (2020) [18]
ECN, IBK, Bronswerk, Smurfit- Kappa, Netherlands	160	60	125 (2.4)	HTHP + IHX + subcooler, piston	R600 (butane)	1.9 (60/125)	Wemmers et al. (2017) [19]
Olvondo Technology, TINE dairy, Norway	449	80 - 90	184 (10)	HTHP (reversed Stirling cycle), piston	R704 (helium)	2.1 (85/183)	Tveit (2017) [20]
NTNU, SINTEF, Norway	20	25 - 35	115	HTHP cascade + IHX	R290/R600 (propane/butane)	2.1 (25/115)	Bamigbetan et al. (2019) [21]
AlterECO project, EDF, France	200	35 - 60	80 -140 (condensation)	HTHP + IHX + subcooler, two scroll	ECO3 containing R245fa	2 - 3 (50-60/125) (evap/cond)	Bobelin et al. (2012) [22]
PACO project, Uni Lyon, EDF, France	380	85 - 95	130 -140 (condensation)	HTHP + flash tank, twin-screw	R718 (water)	~5.5 (94/121)	Chamoun et al. (2012) [23, 24]
National Research Council Canada	45	55 - 80	103.5 - 135.5	HTHP + IHX, piston	R113 & R123 (ozone depleting)	2.7 (75/135, R113) 3.6 (60/120, R123)	Linton (1990, 1993) [25, 26]

Steam generation from water is basically an energy upgrading process from lowpressure and low temperature to high-pressure and high temperature. The required energy (2 632,59 kJ/kg) to lift 20 °C and 0,1 MPa (point A) to 125 °C and 0,2 MPa (Point B) is visualized in a p-h (pressure-enthalpy) diagram shown in Figure 155 (in

this figure. (dot) is used as decimal point instead of a, (comma)). A major part of this energy is needed in the two-phase region for evaporation [125].

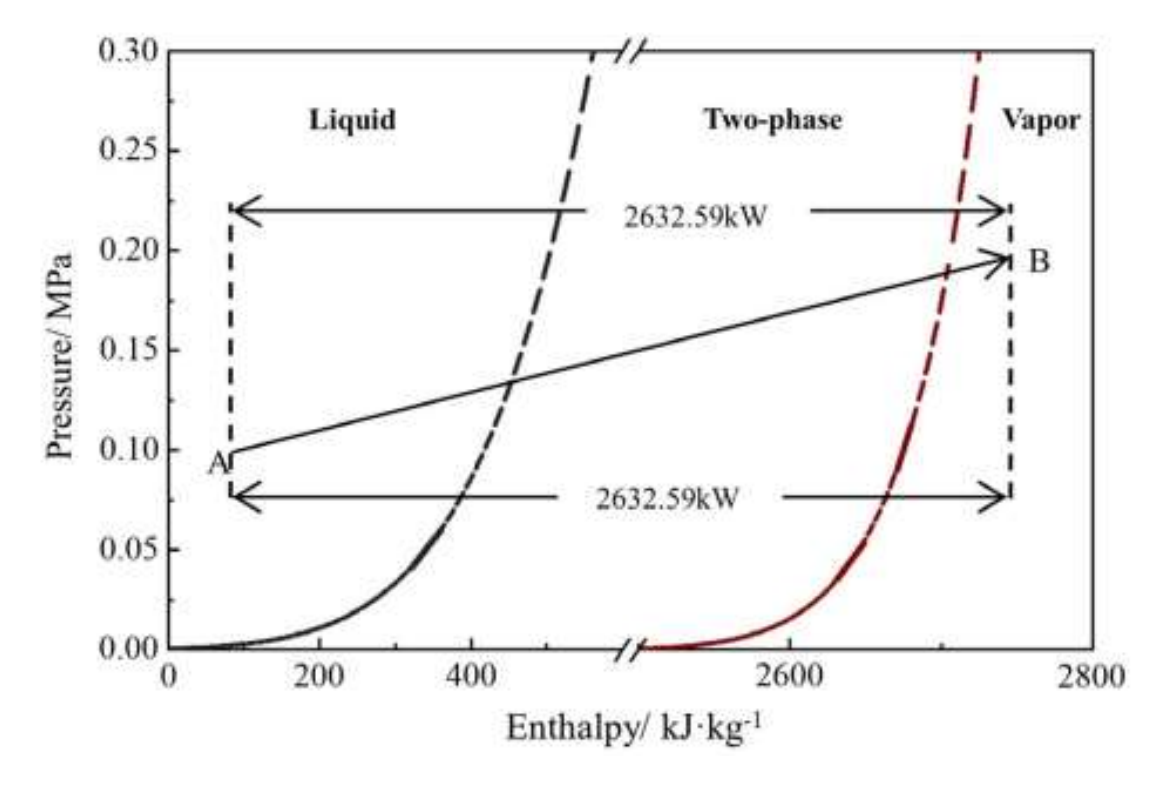


Figure 155 Required energy for steam generation visualized in a p-h diagram, A: 0,1 MPa, 20°C; B: 0,2 MPa, 125 °C; in this figure . (dot) is used in difference to , (comma) as decimal point [125]

Figure 156 (in this figure . (dot) is used as decimal point instead of a , (comma)) shows four different paths to get from A to B. On the left side (a) the direct path is shown which could be approximated by multiple compression and heating stages. If this path is technical realized very high CAPEX and much control effort is needed. Therefore, this application is not practical used. The right side (b) shows three different paths, which are characterized by the three processes compression, heating, and expansion. In process 1 the water is compressed to the final pressure in the liquid state and then evaporated at a high temperature level. This process saves compression energy, because of the higher density in the liquid state, but needs a lot of thermal energy at high temperatures (~ 120°C) for evaporation. In contrast, process 2 evaporates at atmospheric pressure (~ 100 °C) and compresses the saturated steam to the final pressure. Process 3, firstly relaxes the water to 0,05 MPa to evaporate at 85 °C. Afterwards the saturated steam is compressed from 0,05 MPa to the final pressure [125].

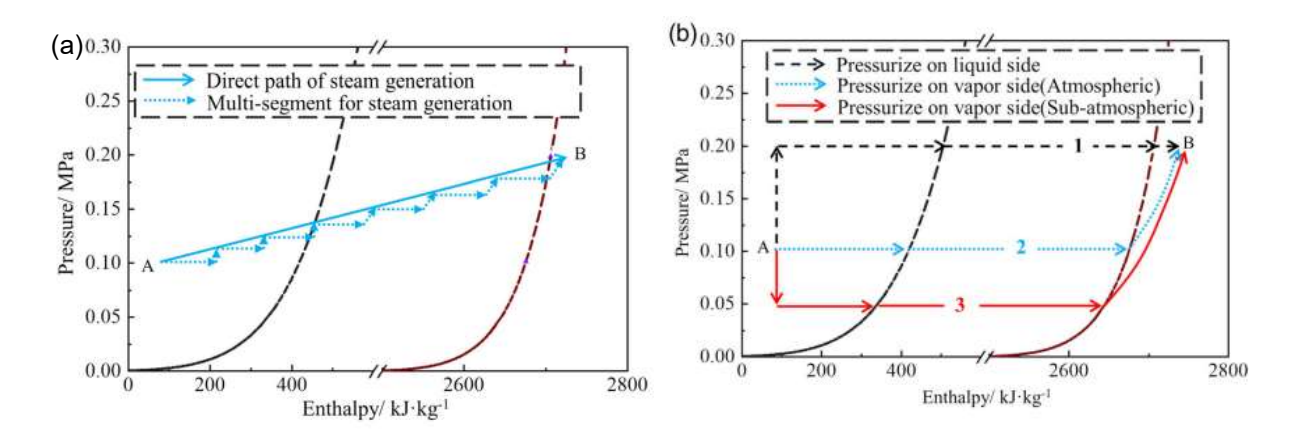


Figure 156 Multiple processes in the p-h diagram to achieve steam generation (getting from point A to B), a) direct path, b) three different paths based on relaxation, heating an compression; in this figure . (dot) is used in difference to , (comma) [125]

It cannot be said in general, which of the following paths for steam generating is for an existing plant the best suited on. The most promising set up, depends on the needed temperatures, pressures and the given infrastructure on site. Figure 157 shows a T-Q diagram (temperature-heat load) and the path 1 and 3 (compare Figure 156) to connect the points A and B. The areas I to III show the exegetic losses of the paths. The exergy losses for path 3 are lower than for path 1 not including the exegetic losses of the compression [125].

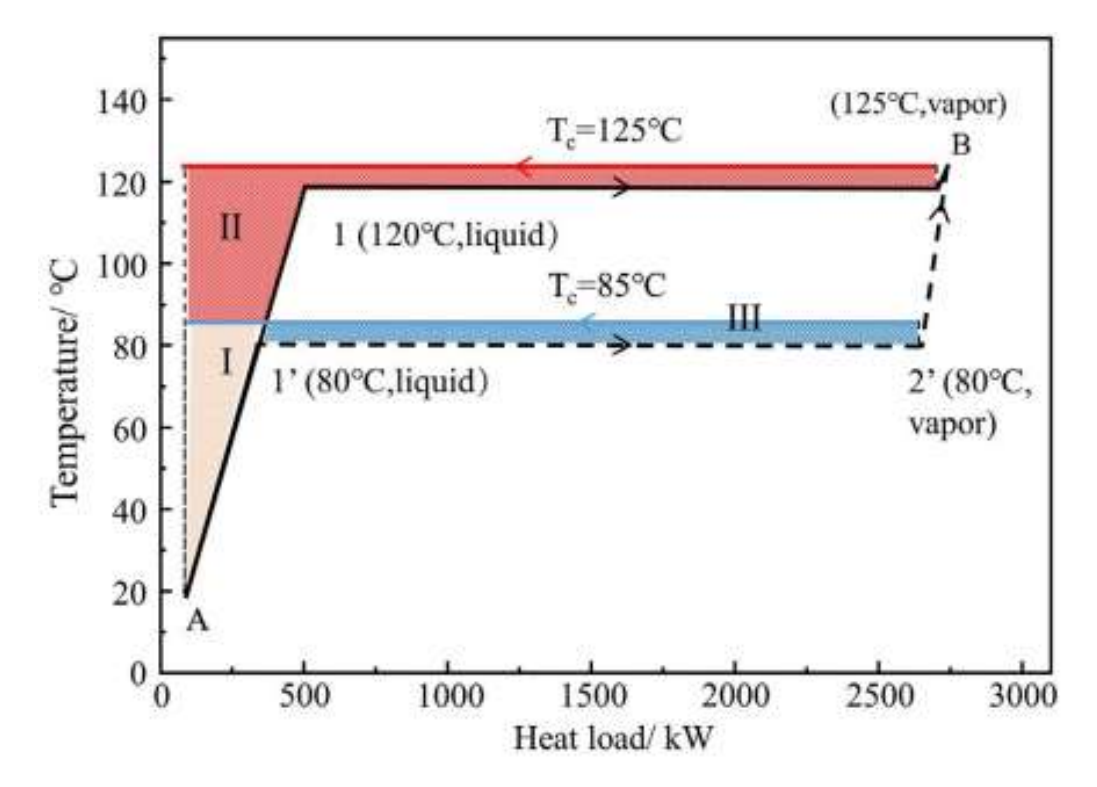
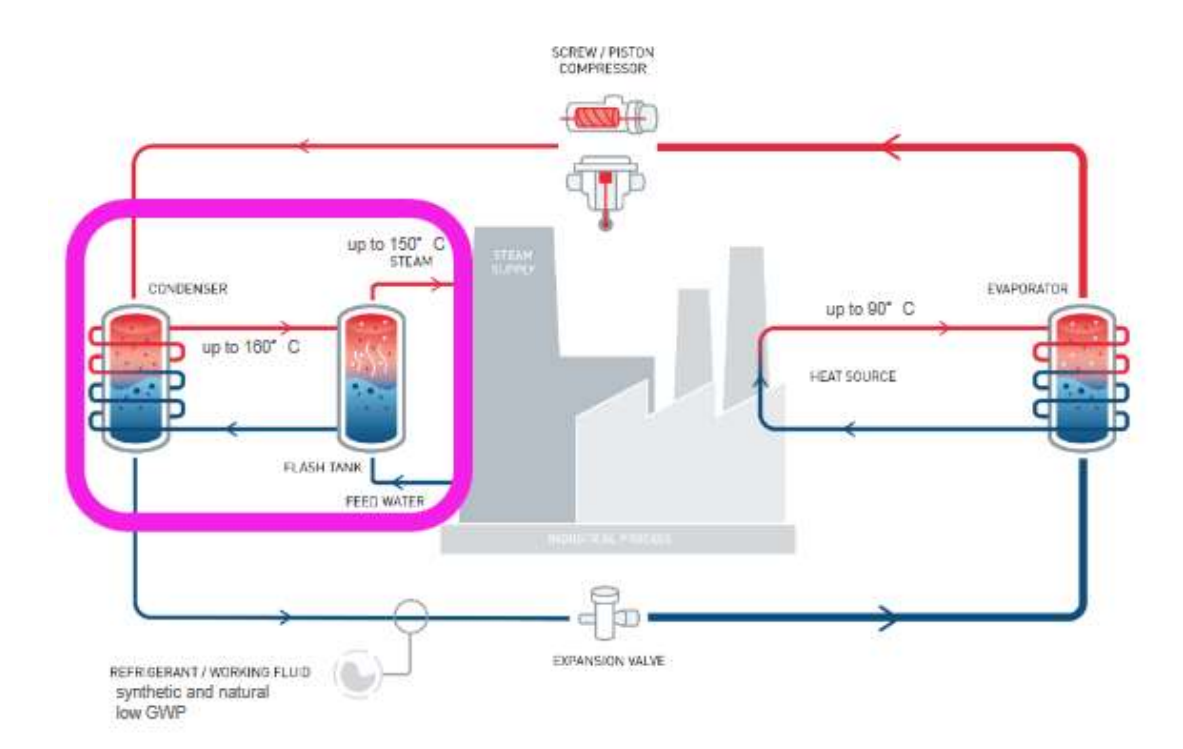


Figure 157 T-Q diagram of the different paths to evaluate the exegetic losses, area I to III symbolize the exergy losses [125]

In the way of the given infrastructure on site it must be distinguished between closedloop and open-loop systems. Closed-loop systems (see Figure 158) use steam as heating medium in a closed circuit. With this setup large amounts of thermal energy can be transferred isothermal in condensing HEX. Closed-loop systems can be driven by a HT-HP using excess heat as source for lifting a sink to the needed temperature level. The sink can either be used in a steam generator to fully evaporate steam (path 1 or 2) or to heat a water circuit, which is expanded in a flash tank to generate steam. Beside that open-loop systems (see Figure 159) use steam directly. High temperature excess heat is used to evaporate water at low pressure. The steam temperature and pressure is then lifted by mechanical vapor compression (MVC) (path 3). Alternative low pressure excess steam can be utilized by mechanical vapor recompression (MVR) and recompressed to higher pressures. There are also combinations between these technologies shown in Figure 160 [8], [126], [127].



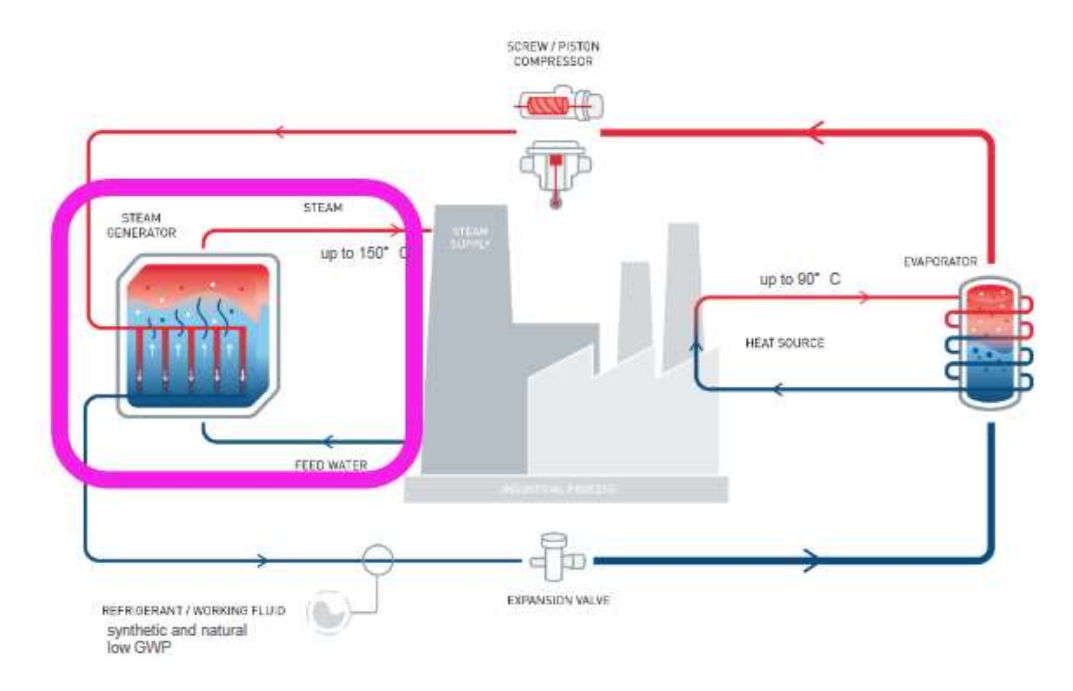


Figure 158 Closed-loop steam generating units; (top) with flash tank, (bottom) with steam generator [8], [126]

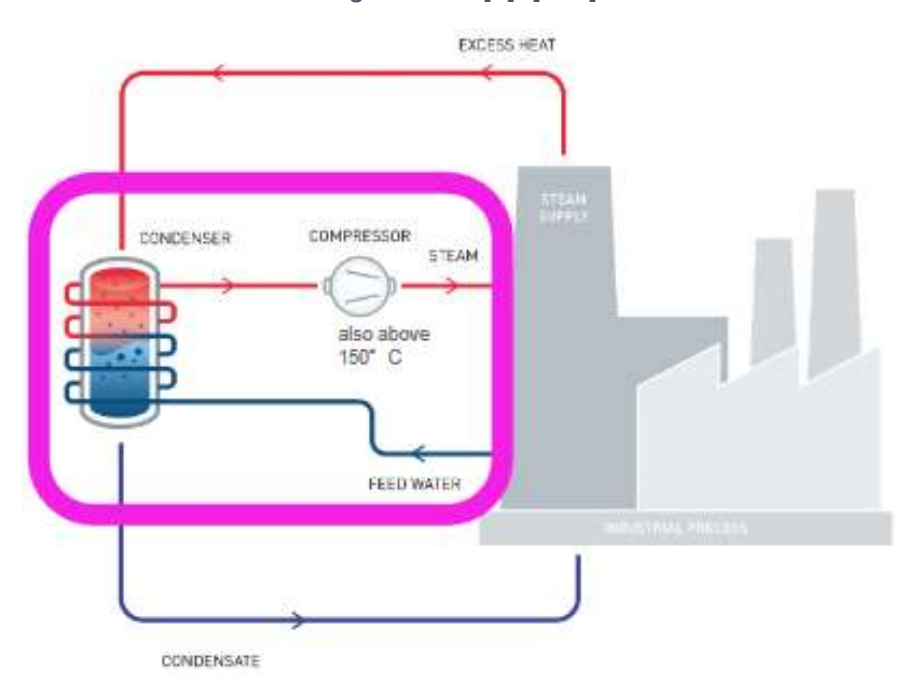


Figure 159 Open-loop steam generating units with MVC [8], [126]

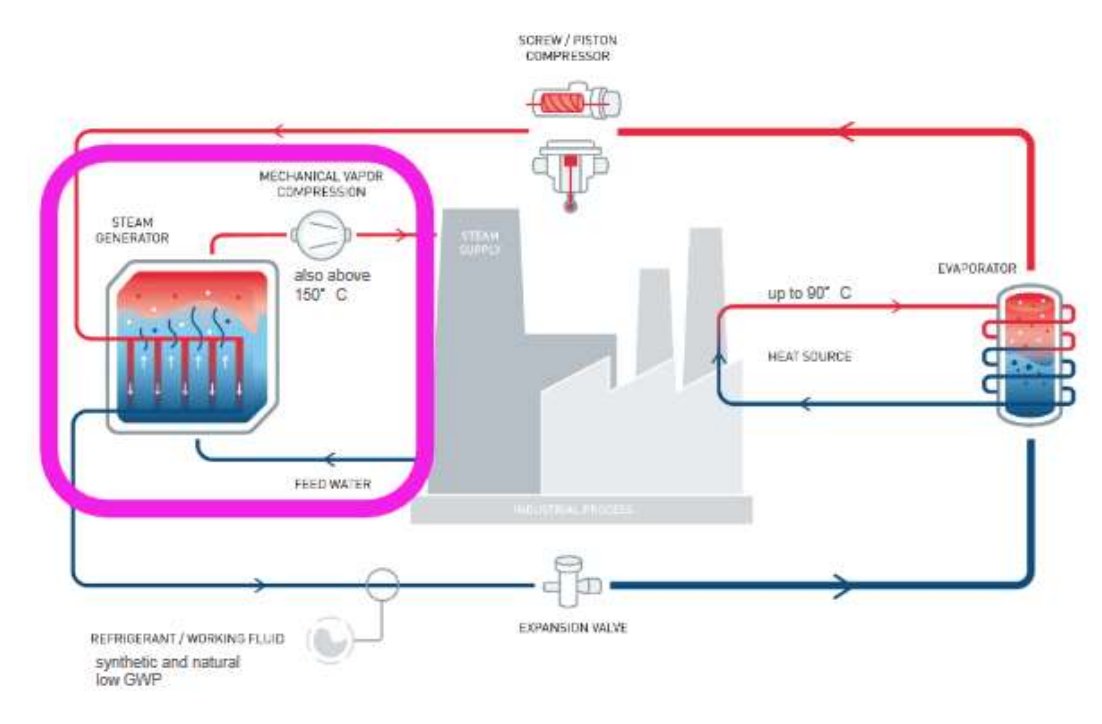
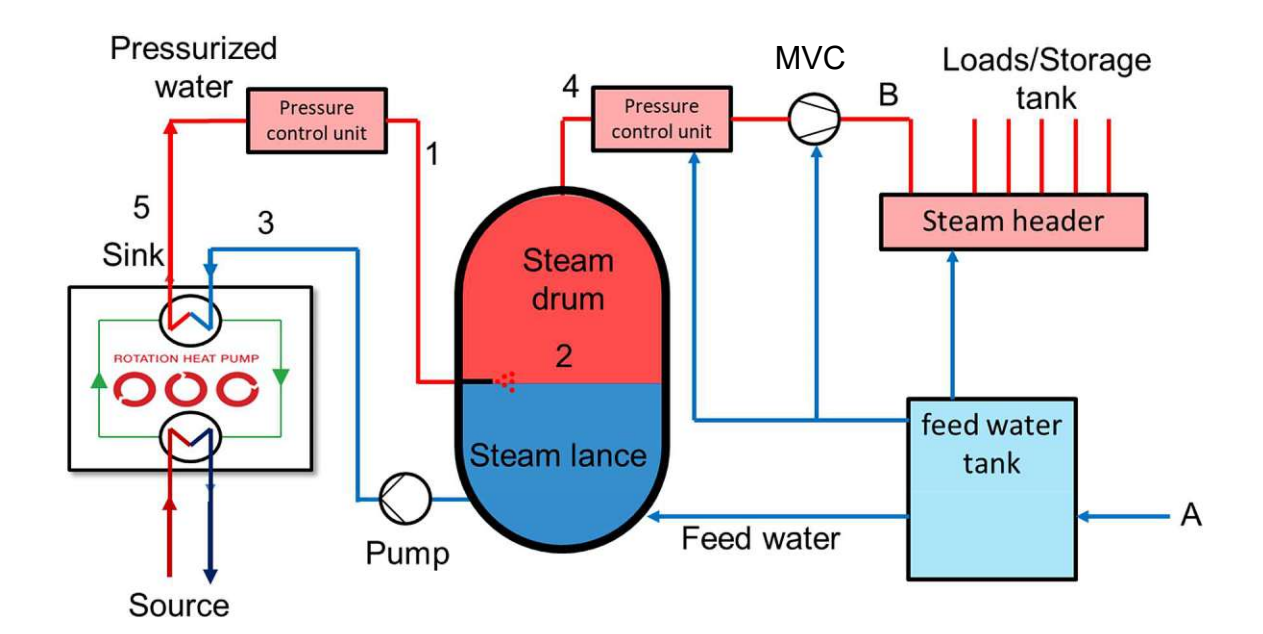


Figure 160 Combined steam generating unit steam generator + MVC [8], [126], [127]

Flash drum (Steam-1)

A flash drum (steam drum) is a unit that can generate water vapor (steam) by relaxing saturated water. The idea of a flash drum is explained by the help of Figure 161 (top). Saturated liquid (1) is fed into the steam drum (2) by passing a throttling valve where it undergoes a reduction in pressure. While entering the steam drum a diffuser reduces the velocity of the incoming liquid and spreads it across the whole cross-section of the vessel. During the pressure relaxation flash evaporation occurs and parts of the saturated liquid flashes into vapor. During the relaxion the saturated water and vapor is cooled to the saturation temperature at the reduced pressure. The separation of the two phases in the vessel is done by gravity and the differences in density. The water vapor is drawn off at the head (4) traveling through a mesh pad which minimizes the entrainment of any liquid droplets in the vapor. In the following pipes water is sprayed into the stream to saturate the steam. The saturated steam is either used directly or compressed and superheated by an MVC (B). The evaporated water is replaced by fresh water (A) and drawn off at the bottom of the steam drum. Afterwards the water stream is compressed by a pump (3) and heated by a HP (5). In the pressure control unit, the pressure is adjusted to prevent evaporation in the pipe until it reenters the steam drum. The bottom of Figure 161 compares a traditional thermal boiler and a HT-HP with flash-tank in a T,s-diagram. Most of the needed energy (for evaporation) is provided by the HP. Only a small part of the needed energy (for lifting the steam temperature) is consumed by the compressor (MVC). The numbers 1 to 5, A and B describe in both figures (top and bottom) the same states [128].



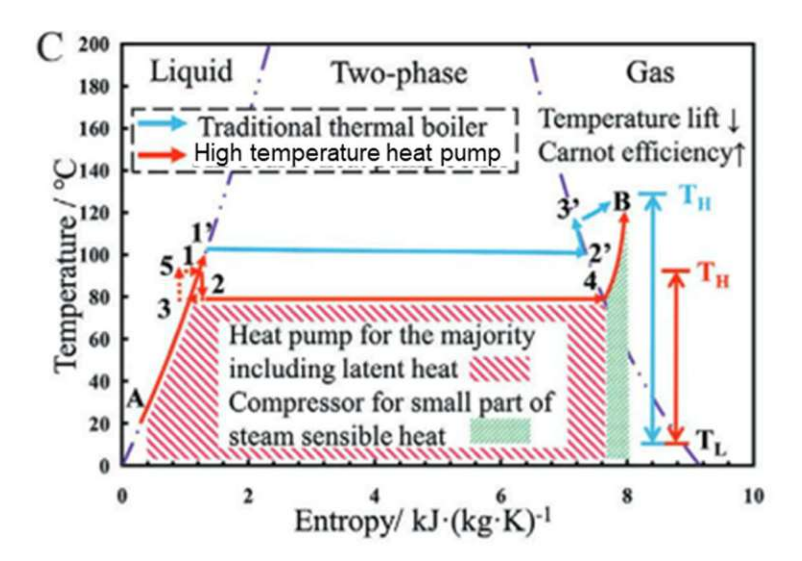


Figure 161 (top) Integration of a HP in a flash drum system, (bottom) T-s diagram of the flash cycle compared to a typical evaporation in a thermal boiler [70], [128]

If a single component liquid flashes by reduction of its pressure the amount of generated steam can be calculated by a simple heat balance around the throttling valve shown in Equation (13) [128].

$$X_{steam} = \frac{H_1 - H_2}{H_4 - H_2} = \frac{c_{p, T_1} (T_{1, sat.} - T_{2, sat.})}{\Delta H_{v, T_2}}$$
(13)

weight ratio of vaporized liquid / total liquid mass X_{steam}

Enthalpy of the saturated (sat.) liquid at the higher pressure in kJ/kg H_1

Enthalpy of the saturated liquid at the lower pressure in kJ/kg H_2

 H_4 Enthalpy of the water vapor at the lower pressure in kJ/kg

Temperature of the saturated liquid at the higher pressure in K $T_{1,sat.}$

$T_{2,sat.}$	Temperature of the saturated liquid at the lower pressure in K
$C_{p,T_{1,sat.}}$	specific heat of the saturated liquid at the higher pressure in kJ/(kg K)
$\Delta H_{v, T_2}$	heat of vaporization of the saturated liquid at the lower pressure in kJ/kg

Depending on the pressure of the saturated liquid and the relaxation in the steam drum different temperatures of the HP are needed. In Figure 161 exemplary a relaxation from 1 bar to 0,5 bar leading to an evaporation temperature of 80 °C is shown. At atmospheric pressure the liquid is saturated at around 100 °C what correspond to the sink temperature of the HP. A simulation of the ecop RHP for this temperature is shown in Figure 162. It is assumed to have a waste heat source of 80 °C leading to a COP of 5,34. In this case an MVC can be used to compress the steam to higher pressures [68], [128].

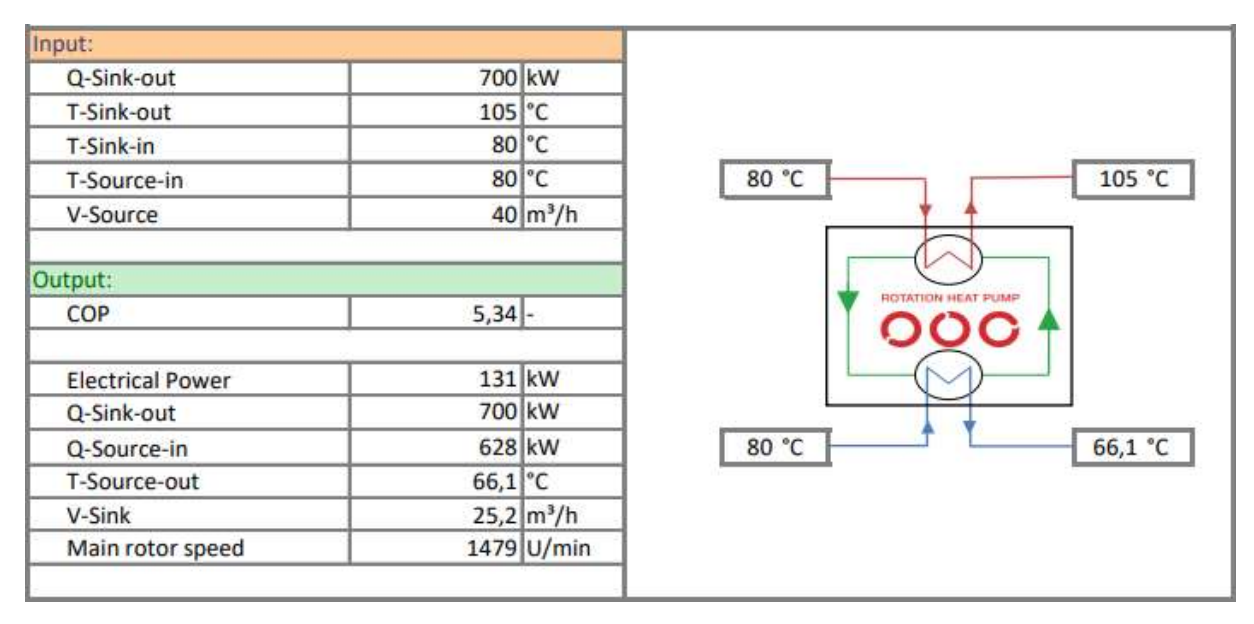


Figure 162 Simulation of the ecop RHP for a flash tank use case (Steam-1) at low temperature [68]

Figure 163 shows a simulation of the ecop RHP to generate steam with 133 °C / 3 bar for direct utilization. The COP in this case result in 3,04. One ecop RHP in this setup can provide 1 t/h saturated steam with 133 °C if the freshwater feed has 40 °C [68], [128].

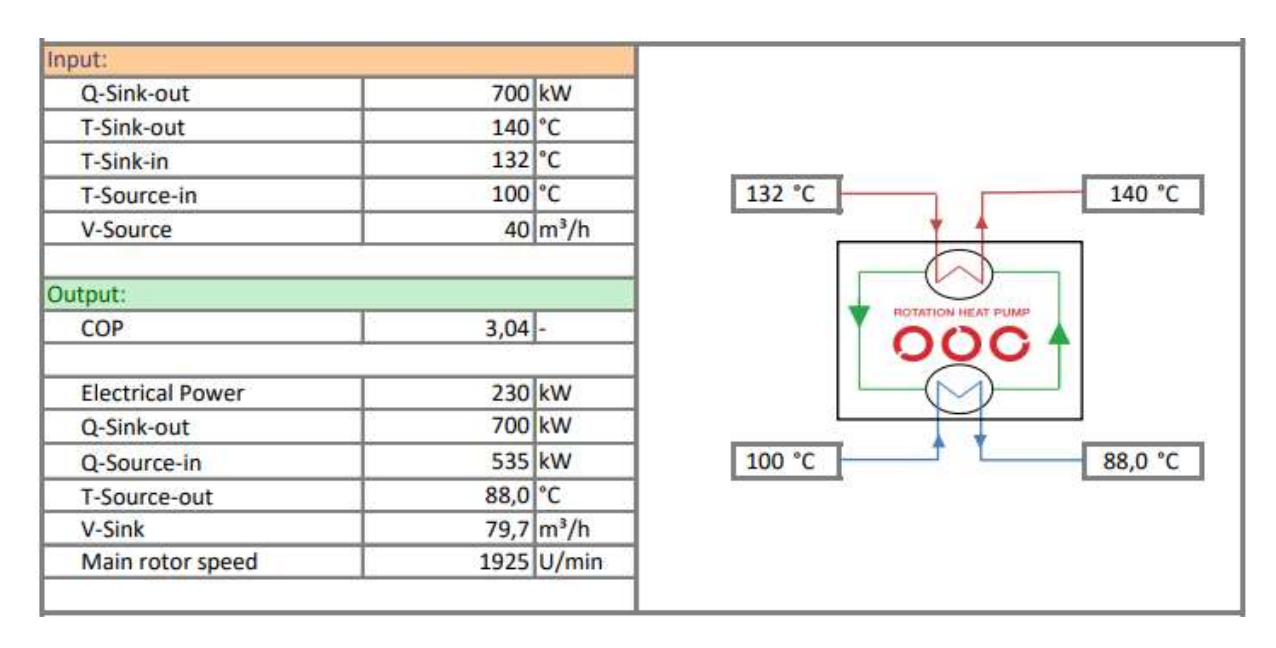


Figure 163 Simulation of the ecop RHP for a flash tank use case (Steam-1) at higher temperatures [68]

Steam generator (Steam-2)

A steam generator is in a simplified way a HEX with a lower pressure and temperature in the inner part being heated by a warmer outer part. The outer part is heated by hot pressurized water from the HT-HP. In the inner part evaporation takes places and the steam is taken off at the head of the HEX. The evaporated part is replaced by fresh water. The separation between the liquid and gaseous phase is done by gravity.

Figure 164 shows a HT-HP driven steam generator circuit to generate saturated steam with 3 bar (135 °C). Fresh water (A = 1 bar (25 °C)) is fed into the steam generator (2). Thermal energy from a closed loop with pressurized water (5 bar) and 150 °C (1) is transferred in the steam generator to evaporate the inner fluid (2) with lower pressure (3 bar) and a boiling point of 133 °C. The evaporated part (4 = B) is taken off at the head of the steam generator. The cooled down pressurized water (6 & 3) is reheated in a HT-HP (5 = 1) before reentering the steam generator. To minimize exegetic losses in the steam generator the fresh water (A) is often preheated by waste heat streams [120].

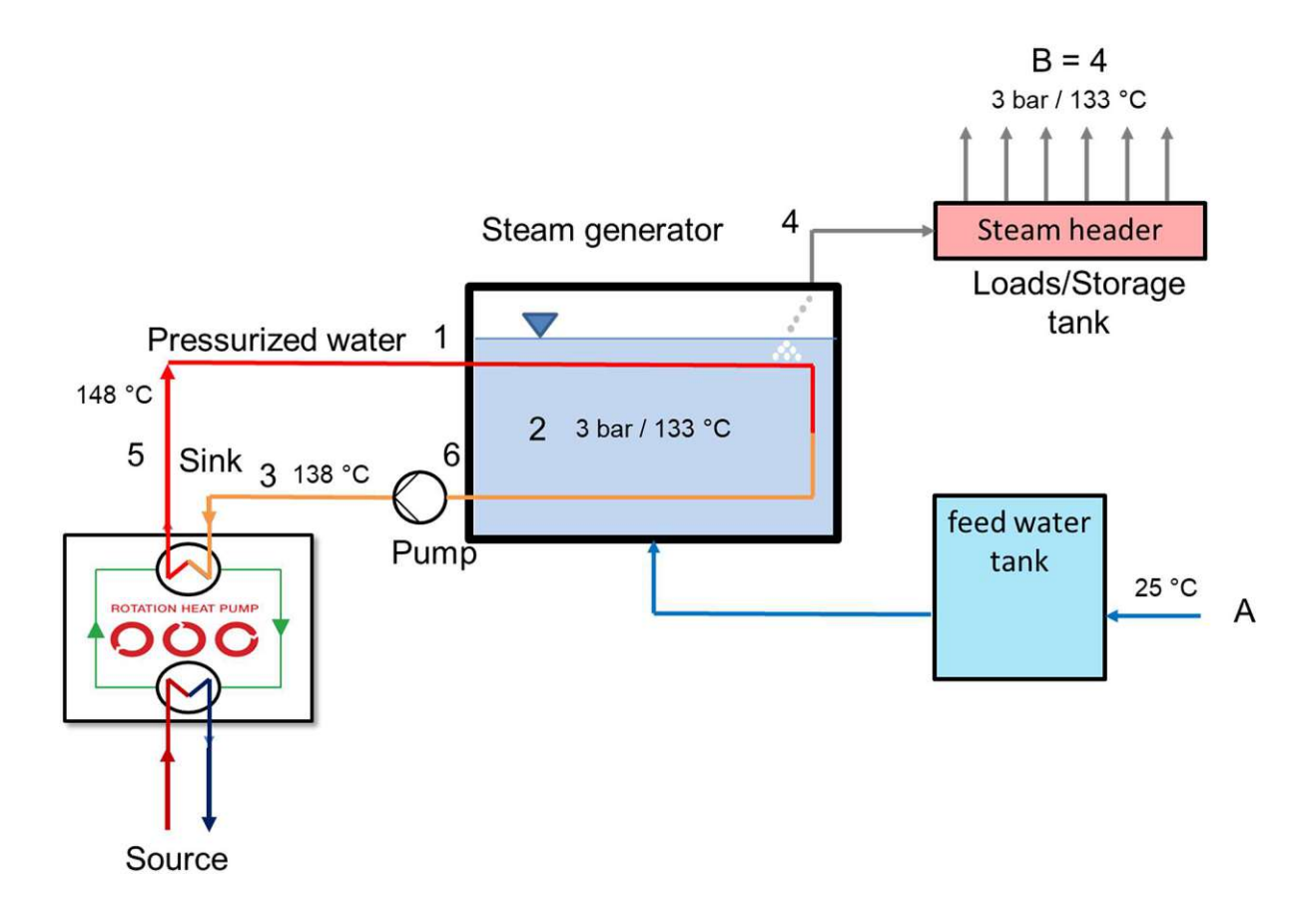


Figure 164 Combination of a HP and a steam generator [70], [120]

The hurdle of this setup is the big amount of thermal energy at high temperatures. Furthermore, is the heat transfer within the steam generator problematic because there are just small temperature differences. The mean temperature difference between the inner and outer part in the steam generator should be between 10 – 15 K [125]. To reach good COP the HP should be able to work almost isothermal with very high mass flows. Conventional HP are not suited for this, because they used to work with a temperature difference between the sink-inlet and sink-outlet [128].

A simulation of the conventional ecop RHP for this use case is shown in Figure 165. It is assumed to have a waste heat source of 100 °C leading to a COP of 2,91. One ecop RHP in this setup can provide 1 t/h saturated steam with 133 °C if the freshwater feed has 40 °C [68], [128].

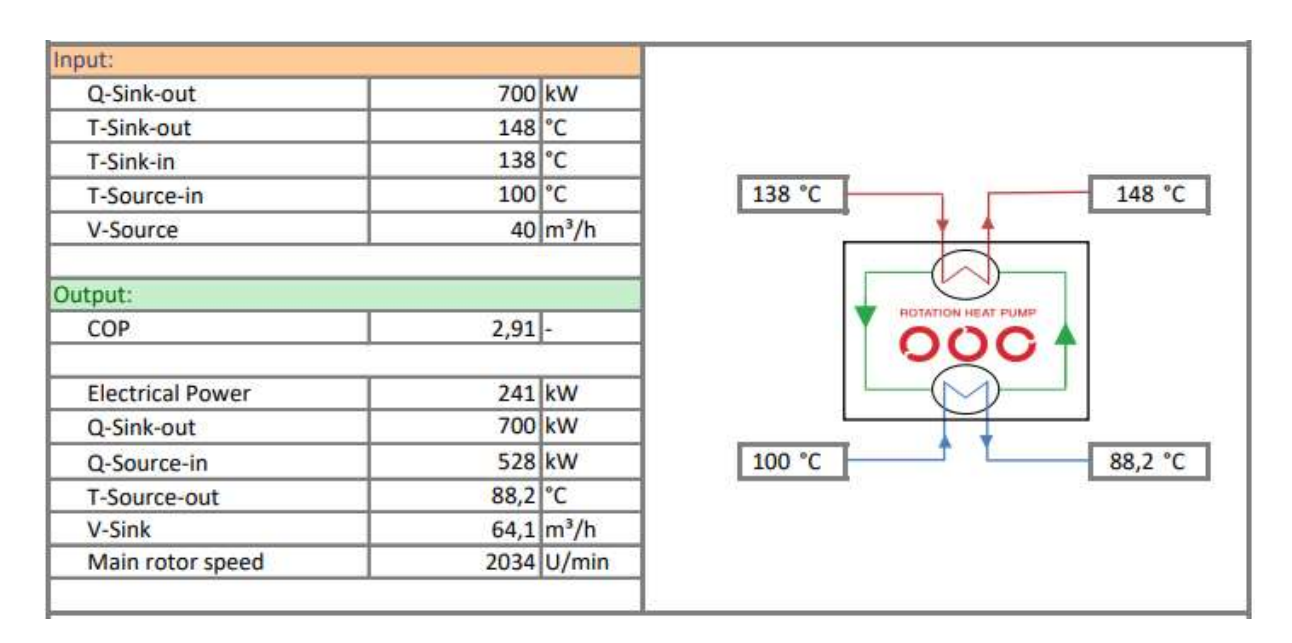
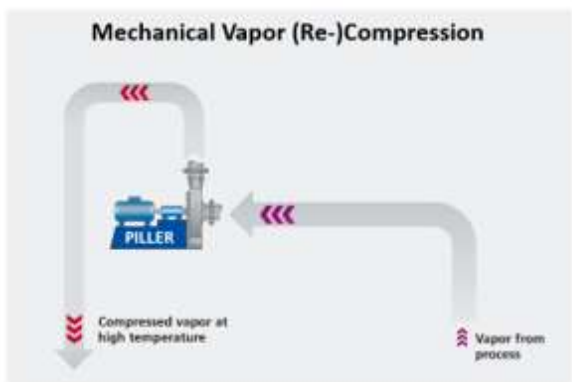


Figure 165 Simulation of the ecop RHP for a steam generator use case [68]

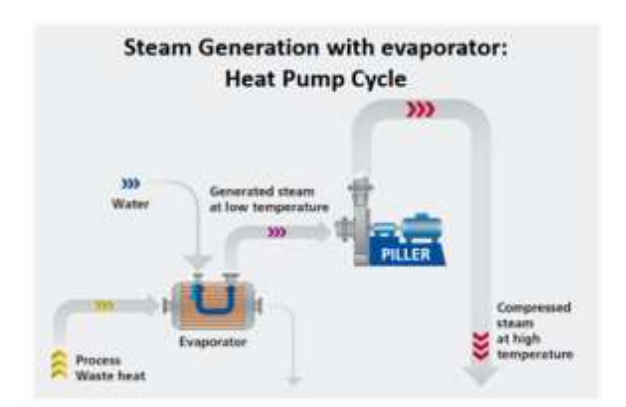
A new concept of the ecop RHP is specialized for providing high amounts of thermal energy isothermal, with great temperature spreads. This concept is specialized for generating steam using a HT-HP and a steam generator. The concept is aiming to reach 60 % of the Carnot efficiency [9], [70].

Mechanical vapor (re-) compression (Steam-3)

Figure 166 shows (left) a mechanical vapor recompression unit and (right) a mechanical vapor compression unit. MVR is a steam recovery unit which is very likely used in open-loop systems. Open-loop means that steam is used directly in the process and not via a HEX. On the left side a steam recovery of relaxed and cooled down process steam with an MVR is shown. The MVR system recollects the relaxed steam and compresses it to reuse it in the process. The MVC unit on the right side works different. Water is evaporated at lower pressures via a steam generator or flash tank and is afterwards mechanically compressed to higher temperatures via an MVC [129].



- Direct compression of steam and other vapors
- · Direct use of compressed vapors for heating or steam generation



- Steam procution directly at the waste heat source
- Steam compression to necessary pressure and Temperature

Figure 166 (left) Recompression via MVR of the vapor in the process, (right) MVC Compression of generated low-pressure steam [129]

Figure 167 shows an industrial example of an MVR system. In this process, parts of the low-pressure steam with 100 °C from a drying process is drawn of and recompressed in an MVR to 150 – 160 °C. The superheated steam is then mixed with low-pressure steam and fed back into the drying process [129].

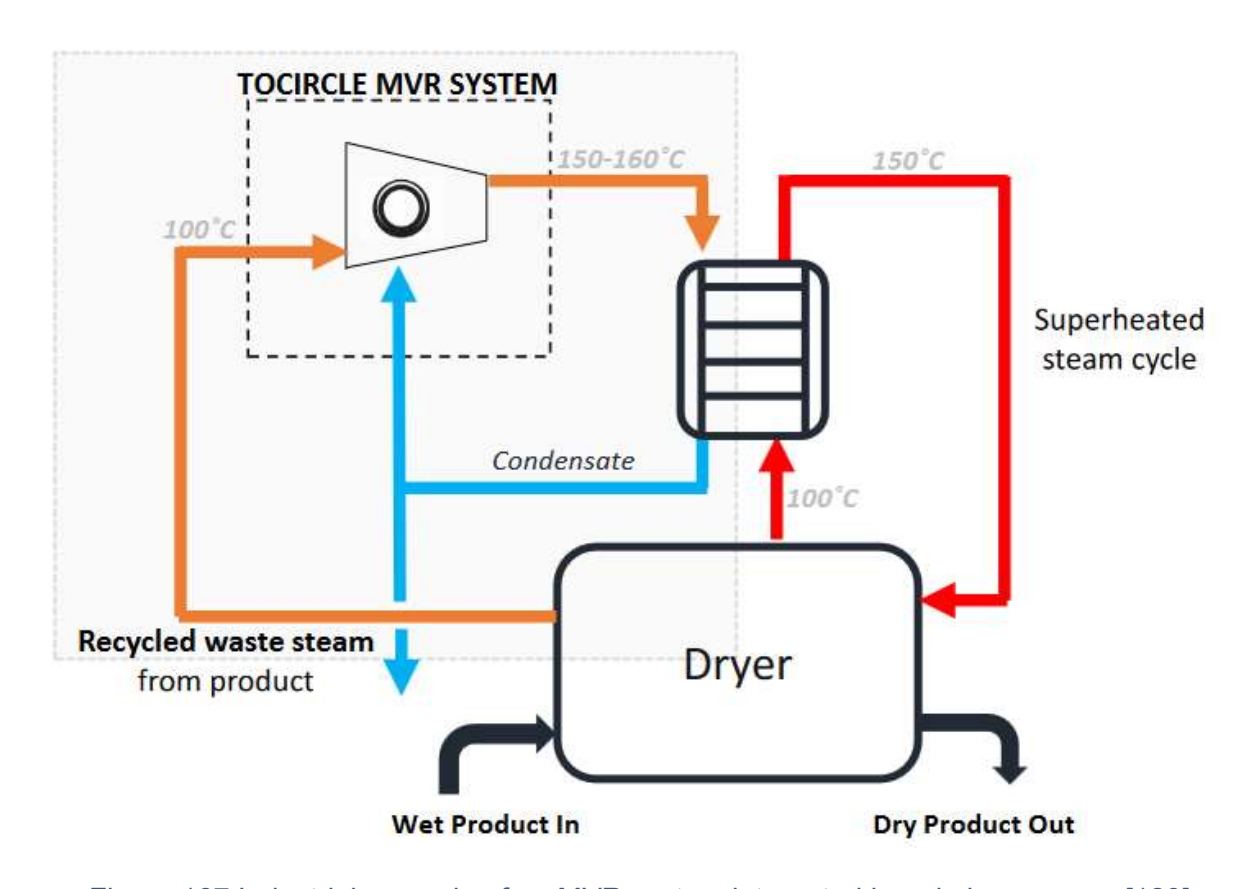


Figure 167 Industrial example of an MVR system integrated in a drying process [129]

Figure 168 (in this figure . (dot) is used as decimal point instead of a , (comma)) shows a MVC example of the manufacturer Epcon. Hot pressurized water is being relaxed in three serial flash tanks generating steam at different pressure levels and temperatures. The lower pressure steam is compressed until the pressure level of all flash stages are equal. In following serial MVC, the steam is compressed to higher pressures. Between stages water is sprayed into the system to saturate the compressed steam. The number of compression stages with given compression ratios defines the end temperature of the steam. In this case the supply of 15 MW thermal energy requires 2,5 MW electricity for compression. The compressed steam is used at three different temperature levels. 5 MW thermal energy are used at 110 °C, 5 MW at 130 °C and 5 MW at 150 °C. The unit to heat the 70 °C outlet stream of the last flash tank to the input temperature (100 °C) of the first tank is not specified in more detail. Exemplary a HT-HP can be used to heat the 70 °C output of the third flash tank unit to the inlet temperature of the first flash tank (100 °C), requiring some kind of source stream [130].

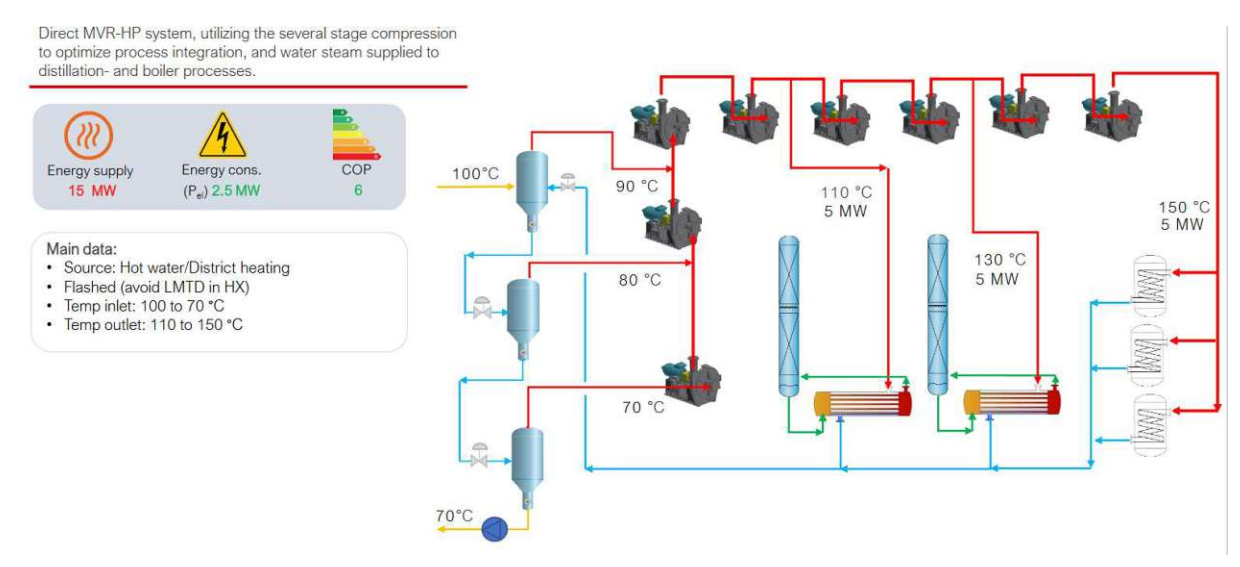


Figure 168 Example for flash tank with MVC driven steam supply; logarithmic mean temperature difference (LMTD), heat exchanger (HX); in this figure. (dot) is used as decimal point instead of a , (comma) [130]

Table 35 (in this figure . (dot) is used as decimal point instead of a , (comma)) summarizes the compression units of an exemplary MVC/R manufacturer depending on the required pressure, temperature and capacity [130].

Table 35 Summary of different MVC/R compression units, PD blowers = positive displacement blowers; in this figure . (dot) is used as decimal point instead of a , (comma) [130]

	\approx	①		℃	(
	Capasity [kg/h]	Max dT [°C] per stage	Footprint [m²] per stage	Max supply temp	Efficiency [%]	Max tip speed [m/s]
PD blowers	150-5000	15-20	≈1.5	130	50	.
Compact MVR-fans	200-5000	8-12	≈1.5	150	75-85	Ž.
MVR-fans	3000- 250000	8-12	>2	150	75-85	315
MVR centrifugal compressor	5000- 55000	15-20	>4	200	75-85	400

Performance data at 100°C saturated steam at Palm

Manufacturers like to specify a COP for MVC/R system what is in a thermodynamic perspective not correct, because COP are defined for thermodynamic cycles. If manufactures define COP for MVC/R system, they compare the heating value of the compressed steam with the electrical input. Therefore, the COP is very much dependent on the pressure level of the steam supply. The needed electricity increases with the needed compression ratio and the compression stages [120].

Combined systems

Depending on the needed temperature and pressure combined systems (HT-HP + MVC) may be the best solution. While MVC/R systems cannot evaporate by itself, HT-HP driven flash tanks and steam generator are limited in the resulting steam temperature and pressure.

The project "Advanced Heat Pump Demonstrator" (AHEAD) is aiming to test a HT-HP and MVC driven steam generation for the industry. The project partner Takeda needs 2,5 t/h steam with 184 °C and 11 bar for its pharmaceutical processes. Figure 169 shows the simplified setup of the process. Waste heat of 35 °C from the Takeda refrigeration system is lifted with a conventional HP to 70 °C. This stream is used as source for a HT-HP to evaporate fresh water at 3 bar (134 °C). In a following MVC



system, the saturated steam is compressed to 11 bar (184 °C). A successful integration leads to a reduction of 90 % of the currently used fossil fuels [131].

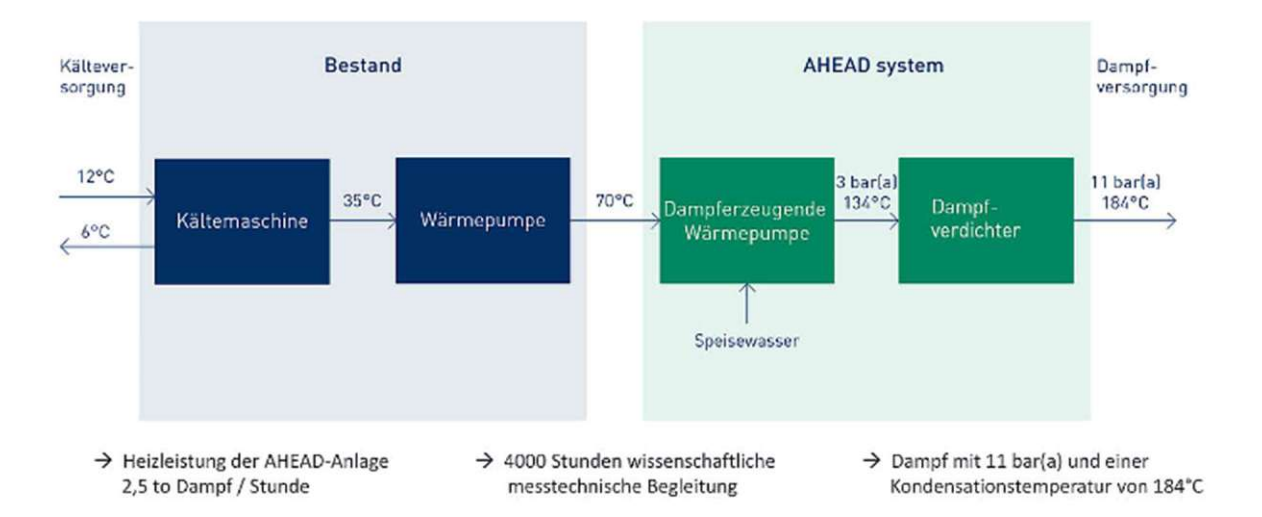


Figure 169 Simplified setup of the HT-HP and MVC driven steam generation in the AHEAD project [131]

Other examples for combined systems are shown in the case studies of the MCV/R manufacturer Epcon. Figure 170 (in this figure . (dot) is used as decimal point instead of a, (comma)) shows a combination between an air source HP for evaporation at low temperatures with a steam generator and a MVC to lift the steam to the needed temperature level (110 and 120 °C). The COP of the overall system result is 3,1 [130].

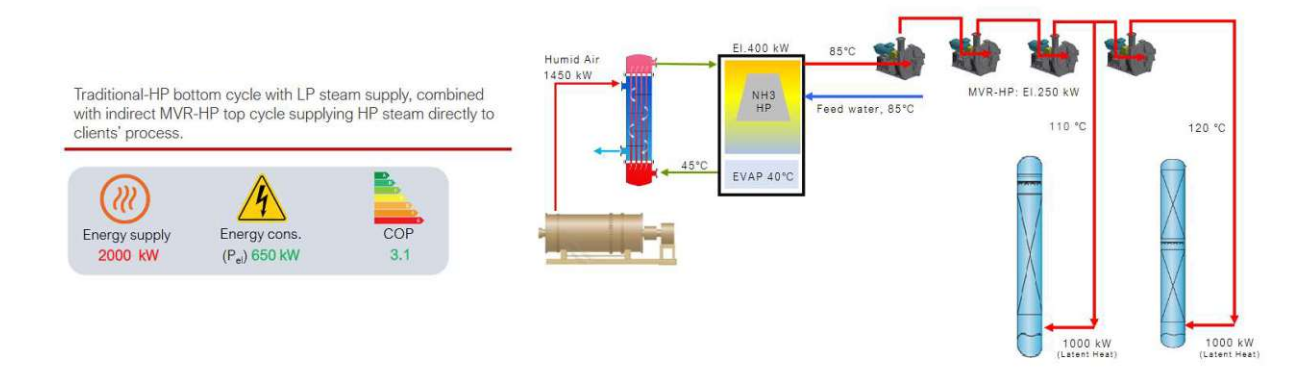


Figure 170 Example for MVR & HP + steam generator driven steam supply; in this figure. (dot) is used as decimal point instead of a, (comma) [130]

The Austrian Institute of Technology (AIT) investigated a combination between geothermal heat and steam generation. In Figure 171 (left) is a combination between geothermal heat used as source for an HP in a steam generator and (right) a direct evaporation with geothermal heat in a steam generator with an MVC unit [127].

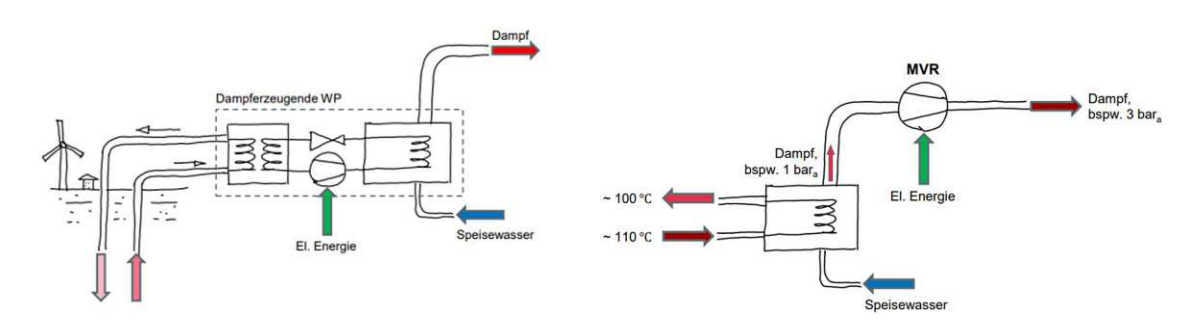


Figure 171 Combination between geothermal heat and a HP for steam generation, (left) HP uses geothermal heat as source for evaporation of feedwater in a steam generator, (right) geothermal heat is used directly in a steam generator for evaporation and an MVR is used for increasing the pressure [127]

The EU funded project BAMBOO focuses on the efficiency improvement of heavy industrial process. As part of this project, it was investigated if waste heat of a steel manufacturer can be utilized by a HP for steam production (Figure 172). During the waste rolling of strips excess heat with 80 °C occur. A closed-loop HP utilizes this waste heat to heat the condensate stream of the pickling line. The heated-up stream is relaxed in a flash tank generating steam. If higher pressures are required MVC systems are used to compress the steam. At the time of the research the HP was not implemented in the facility, but a Demo site based on a m1337mzz piston HP was built and tested successfully by the French company EDF. The system COP is 2,95 and 1,9 in the lab test for delivering 2 and 5 bar saturated steam. The integration led to a reduction of final energy of 69 and 53 %, reduction of primary energy of 46 and 11 % and a reduction of CO₂ emissions of 63 and 47 %, respectively 100% if the electricity is fully renewable. For this comparison a gas burner with an efficiency of 90 % was used. Furthermore, gas and electricity energy primary factors of 1,1 and 2,1, respectively greenhouse gas emission factors of 271 and 275 gCO_{2-ev}/kWh were used [8].

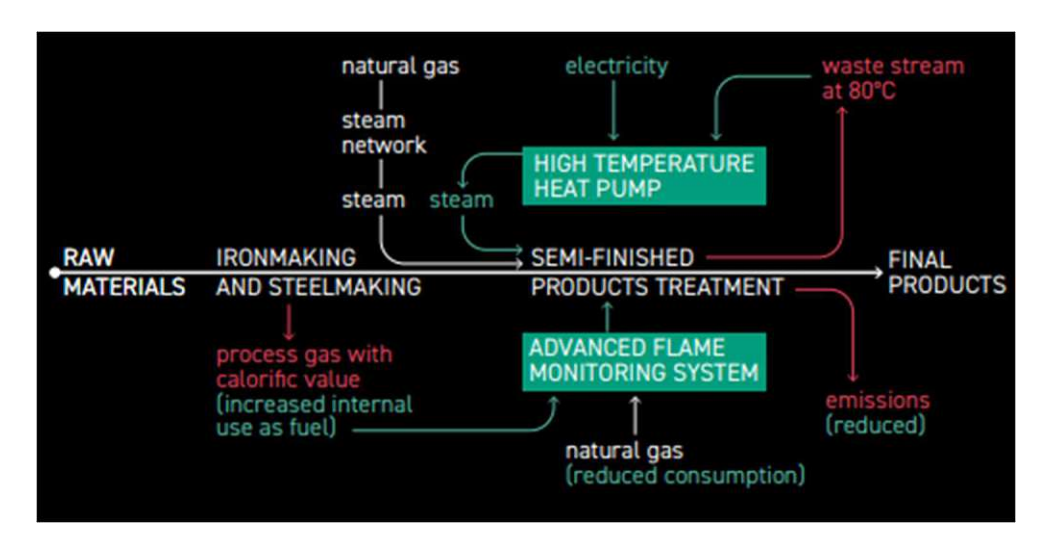


Figure 172 Waste heat utilization for steam generation in a steel plant [8]

Some key findings of the heat pump integration into the steel plant are summarized in the SWOT analysis in Figure 173 [8].

STRENGTHS

- · Making use of waste heat, i.e. increase energy efficiency.
- Possibility for CO₂-neutral electrification, i.e. decarbonized process heat.
- Possible independency from fossil fuels.
- The goal of producing steam with a pressure of 5 bar (152°C) was reached within the BAMB00 project.

WEAKNESSES

- · A new installation of a heat pump requires careful planning.
- · Dynamic operation limited.
- Higher CAPEX.
- More complex equipment and more individual parts, therefore more vulnerable supply chains.

OPPORTUNITIES

- Applicable in other industry sectors (e.g. food & beverage, chemical, pulp and paper).
- Possibly cutting OPEX, esp. regarding emission certificates and energy efficiency.
- · Enables integration of renewables through electrification (Power-to-heat).
- Possible use of various heat sources (geothermal, solar, ambient).
- Simultaneously heating and cooling possible (benefit increases).

THREATS

- · Possible high electricity-to-gas price ratios (including emission certificates) extend the payback period.
- Use of renewable gases may prevent use of more efficient heat pumping technologies (cmp. strengths).

Figure 173 SWOT analysis of the steam generating HP into the steel plant [8]

Economic efficiency steam generation

The study SuPrHeat investigates the hurdles of replacing an existing steam supply system with a HP driven one. In Figure 174 they summarized some major points to keep an eye on if the steam pressure of the supply system is reduced. If a pressure reduction of the steam supply is not an option MVC can be used to increase the steam pressure [132].

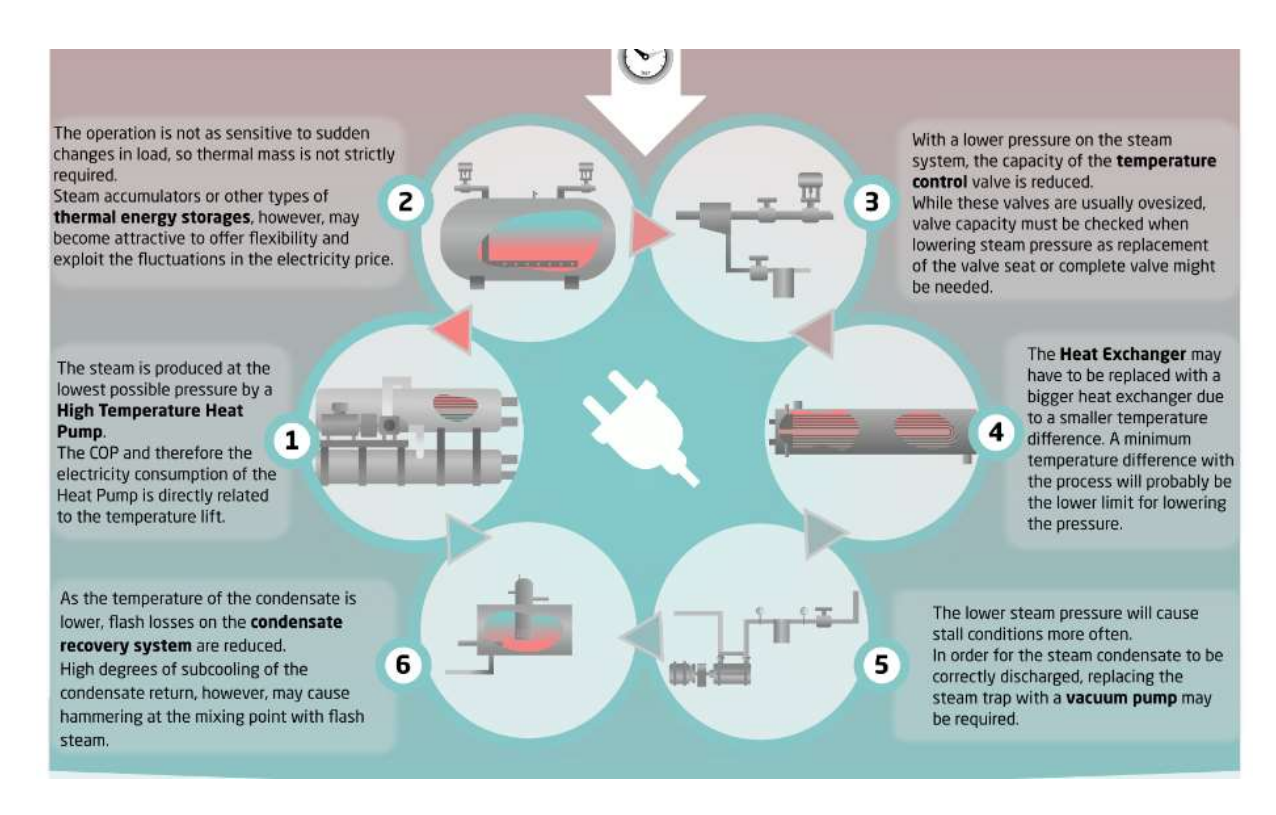


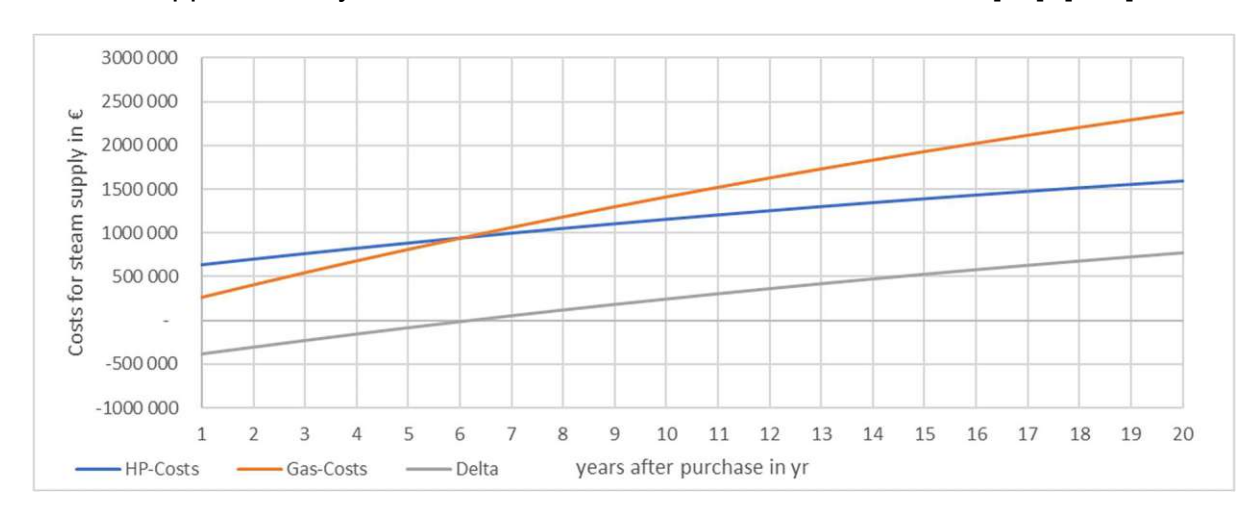
Figure 174 Important points that must be considered if the pressure is being reduced in an existing steam supply [132]

The electrification of the steam generation comes with hurdles to overcome, but with a great potential in CO_{2-ev} savings, if the electricity is renewable generated. Beside the environmental aspect an electrification can also make sense in an economic perspective. As mentioned above is the economic aspect very much dependent on the needed temperatures, pressures, the given infrastructure on site and the supply structure (continuous, batch,). SGHP are better in continuous low temperature and pressure systems in a medium scale. A comparison of costs between a SGHP system with a steam generator, a flash tank and a gas reference scenario based on (Table 36) has been done. The systems are calculated to produce 1 t/h steam with 133 °C (3 bar). The source of the HP is assumed to be available from excess heat [70], [132].

Table 36 Parameters for economic efficiency analysis [70]

Economic analysis	Steam generator	Flash Tank	Gas	Unit
Electricity price	0,075	0,075	0,075	€/kWh
gas price	0,025	0,025	0,025	€/kWh
Electricity/gas price ratio	3	3	3	
approximated HP COP	2,9	3,04	/	
gas boiler combustion efficiency	/	/	0,9	
CO2 price	/	/	113	€/t
CO2 emission factor	/	/	0,201	g/kWh
FLH	4000	4000	4000	h/yr
HP System additional costs	640	640	/	€/kWh

Figure 175 shows the results of the economic analysis for a HP with a flash tank (top) and a steam generator (bottom) compared to the reference scenario with a gas boiler. In blue are the discounted total costs of the HP system including electricity costs and CAPEX. In orange are the total discounted costs of the gas boiler case including CAPEX, gas costs and CO₂ costs. For both HP systems the results are similar and with the given assumptions the dynamic payback period is 6,15 (top) and 6,58 (bottom) years. FLH of 8000 h/yr would shift the dynamic payback period to ~ 3 years. The HP options have higher CAPEX, because the HP is more expensive than the gas boiler. The additional needed plant components (flash tank, pumps, pressure control valve, ...) are for the HP system and gas system very similar. The OPEX of the gas scenario are higher because, of the CO₂ costs. Over a lifetime of > 20 years a significant amount of money can be saved by the HP driven systems. A hurdle to overcome are the higher CAPEX and the resulting DPP of > 3 years. The similar functions for both HP systems result in approximately the same investment costs and similar COP [70], [120].



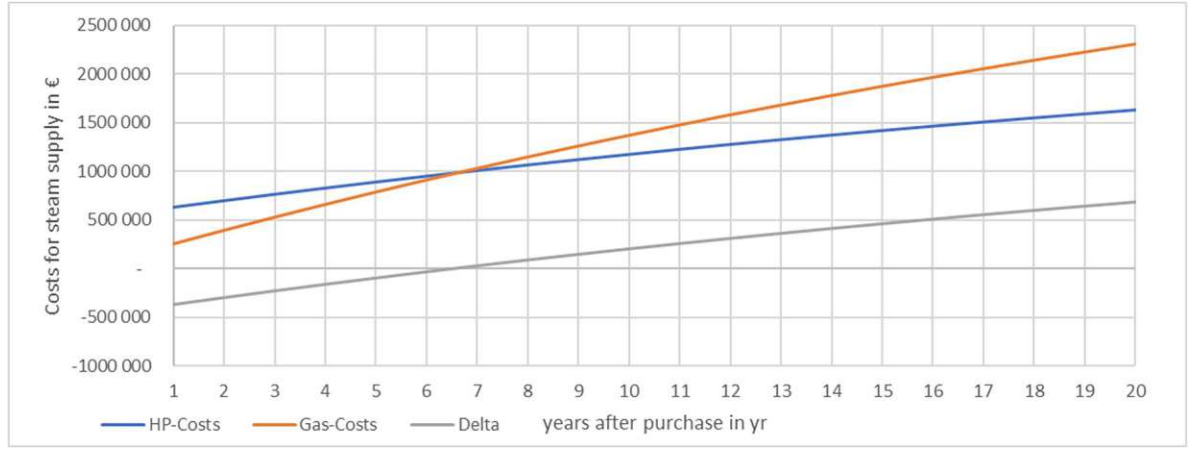


Figure 175 Total costs for steam production (CAPEX + OPEX) for a HP with (top) flash tank, (bottom) steam generator and a reference scenario [70]

A separate calculation for MVC/R system has, because of missing CAPEX data not be done.

Summarizing it can be said that a combination of a HP with a steam generator or flash tank have both advantages and disadvantages. The flash tank system can reach higher COP because of the lower temperature level, but is more complex. The higher complexity results from a more difficult separation between the gaseous and liquid phase in the tank. In the flash tank the steam mass flow is limited by the maximum outlet velocity of the diffuser. The flash tank is the preferred option if the HP can just provide temperatures < 100 °C or an MVC system is available at low costs. Steam generators are simpler and have a little lower CAPEX. The difficulty is to ensure a good heat transfer between the HP circuit and the steam generator. Depending on the heat transfer in the steam generator and the achievable temperature level of the HP the maximum steam temperature is limited. With HP sink temperatures of 150 °C the maximum saturated steam temperature is ~ 133 °C. For higher temperatures either the HP sink temperatures must rise, or MVC systems are necessary. For the HP case a concurrence of the steam demand and the waste heat supply is necessary.

Potential steam generation

A study investigated the process heat < 150 and < 200 °C demand of the four most IHP suited industries paper, chemical, food and refinery. The IHP coverable process heat demand of these four sectors in the range < 150 °C result in 641 PJ/a. The study shows, that around 20 GW thermal power are necessary to provide the needed thermal energy demand. The same literature investigated usual processes in these industries. The results show that 47 % of the processes are based on steam. Considering these assumptions, the European steam generating HP market in these four industries result in 9,4 GW. With a thermal power of 0,7 MW per ecop RHP the steam generating ecop RHP market potential results in 13 429 pieces [4], [9], [133].

Considering that according to [118] the steam boiler market will grow until 2032 annually by 5,5 %, in 2030 1 138 TWh of primary energy will be needed for steam production in Europe. The 9,4 GW in the four industries mentioned above are less than 8 % of the theoretical steam generating potential 2030 in Europe (technical potential) [118].

In a presentation Mr. Arpagaus, professor at Ostschweizer Fachhochschule, shows that the stock of fossil boilers in Europe are more than 18,2 million pieces. The stock of oil and gas boilers in EU28 countries is shown in Figure 176 (in this figure ' (apostrophe) are used as thousand-digit-draw). The largest numbers of fossil boilers are in Germany, UK, Italy, France, and Belgium. More than 3,1 million of them are in an industrial size. If the replacement rate of industrial gas and oil boilers by IHP is only 1 % more than 30 000 units are necessary. The presentation of Mr. Arpagaus as well as the growing steam demand in Europe show that the assumption of 13 429 ecop RHP pieces is very conservative [8], [120].

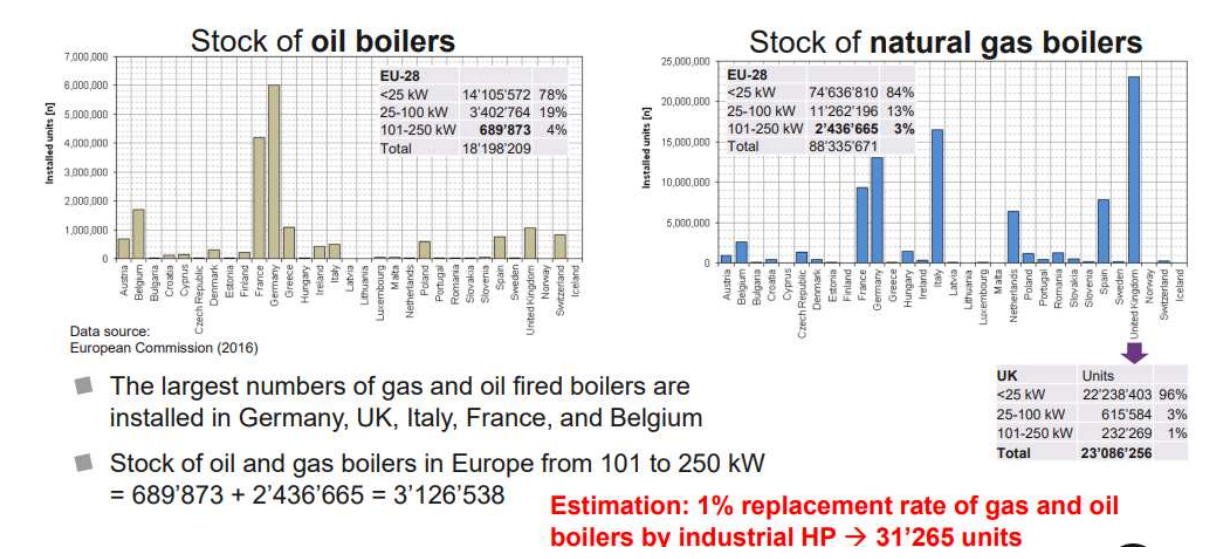


Figure 176 Stock of fossil boilers in European countries; in this figure ' (apostrophe) are used as thousand-digit-draw [120]

5 Summary

5.1 Industrial heat pumps

Around 40 % of the global final energy demand accounts for the industry. 60 % of the energy demand in the industry is thermal energy. A significant amount of the thermal energy is currently provided by burning fossil fuels leading to high CO₂ emissions. 10 % of the global CO₂ emissions accounts for thermal energy in the industry. In order to decarbonize the industries energy supply sustainable technologies for the generation of thermal energy are needed. One of the most promising concepts is Power-to-Heat, with the prerequisite that the electricity is generated by renewable sources. There are different Power-to-Heat technologies for the needed temperature levels in the industry. High temperatures (> 500 °C) and medium temperatures (> 200 °C) can be provided by burning hydrogen, electric heater, or biomass heater (no Power-to-Heat). For temperatures < 200 °C heat pumps are the most effective solution. But heat pumps cannot be used in any < 200 °C application. Conventional heat pumps can reach temperatures up to 90 °C, whereas industrial heat pumps fill the gap to 150 - 200 °C [1], [2], [3], [4].

Current industrial heat pump demonstrator can reach temperatures up to 150 – 165 °C. Annex 58 of the International Energy Agency is aiming on high temperature heat pumps and is collecting information about manufacturers and demonstration sites. More information can be found here [12].

Heat pumps offer the possibility to provide two to seven units of thermal energy with a single unit of power. This ratio is called coefficient of performance. In order to do so heat pumps utilize low temperature excess or environmental heat on the source site to lift the temperature level of the sink site. The possibilities of heat pumps to very efficient provide thermal energy, lower operational expenditures and having low CO₂ev emissions comes with hurdles. These hurdles are the simultaneous need of excess heat supply and process heat demand, high capital expenditures, longer payback periods and a more complex system [1], [6], [8], [9], [10].

The reference industrial heat pump in this thesis is the rotation heat pump (RHP) of the Austrian manufacturer ecop. Their heat pump has a nominal power of 700 kW and can provide temperatures up to 150 °C with a maximum temperature lift between the source inlet and sink outlet temperature of 55 K. The rotation heat pump has per- and polyfluorinated chemicals free, non-flammable and global warming potential <1 noble gases (Helium, Krypton, Argon) as working fluid. The working fluid does not enter the two-phase region during the closed cycle process of the rotation heat pump. Therefore, is the process, unlike conventional heat pumps, not based on the carnot process, but on the joule process. The compression of the working fluid is done by

centrifugal forces of a rotation rotor with high-pressure heat exchanger at the outer part (sink side) and low-pressure heat exchanger (source side) close to the axis. The pressure losses in the closed working fluid circuit are compensated by a fan [23].

5.2 Economic analysis and commodity prices

The economic feasibility in this thesis is based on a total cost of ownership analysis. In the total cost of ownership analysis, all relevant income and expenditures are determined. The investment decision making procedure in this thesis is the dynamic payback period and levelized costs of heat. It has been shown that the payback period is one of the major factors in industries investment decisions and should not exceed two to three years. The interest rate for the dynamic calculations is assumed to be constant 3 % for an investment horizon over the next 20 – 30 years. The presented heat pump solutions are compared with a gas boiler as fossil reference case. A sensitivity analysis showed that the most relevant factors in the economic analysis are the power to gas ratio, the yearly full load hours, and the carbon prices. Due to the very small impact of maintenance and disposal costs these parameters have been neglected. Several predications have been investigated to find good assumptions for the future commodity and electricity price trends [10], [24], [25], [26], [31], [32].

If long payback periods occur also contract models for the supply of thermal energy are possible. Based on full load hours, expected electricity prices and coefficient of performance a specific price of thermal energy can be specified. These contracts usually include more details like heat purchase commitments, maturities, and others [10], [22], [26], [31], [32].

The commodity and power price trends mainly differ according to scenarios. The most relevant scenarios are shortly explained down under. The scenario "central" is based on Europe stopping to import Russian gas. Therefore, the European natural gas price is determined by the global liquified natural gas price. The energy system will strongly decentralize with a significant expansion of renewables. The "Tensions" scenario is based on increasing tensions between Europe and Russia and higher CO₂ prices. Therefore, the early natural gas prices are higher in this scenario. The "Relief" scenario is based on a better relationship between Europe and Russia. Europe decreases the amount of fossil fuels slightly. The renewable expansion target, which were set during the crisis, are kept in place. "GoHydrogen" focuses on a fully decarbonization until 2050 comparable to the international energy agency "Net Zero" scenario [32], [34], [37], [40].

The power to gas ratio, is the ratio between the price for electricity and natural gas. Among the European Union there are big differences in the power to gas ratio. Simplified lead high national CO₂ prices combined with a high share of renewable generated electricity to low power to gas ratios. The most attractive market is Scandinavia, as well as France, Portugal, and Bosnia with ratios between 1 and 2,5. High ratios > 3,5 can be found in Romania, United Kingdom, Hungary, Croatia, and Slovakia. The European average of the power to gas ratio was between 2008 and 2022 in the range of 2,0 and 2,5 tending to slightly increase over time. Forecasters agree that an electricity to gas ratio of about 3 will occur in 2040. After 2040, the scenarios differ and forecast ratios show values between 2,0 and 4,2. This thesis agrees on an European Union average of 3 of the power to gas ratio for an investment horizon of 20 - 30 years, but points to large national differences [32], [34], [37], [40].

In 2021 an average industrial user in Europe paid 40 - 45 €/MWh taxes for electricity and 6 – 6,5 €/MWh taxes for gas. Two-thirds of the revenues from power taxes are then used to subsidize renewable energies. The net effect is that the decarbonization of the electricity supply is subsidized, while disincentivizing the electrification of industry by favoring the use of gas. A review of the taxation framework by favoring the direct use of electricity would accelerate the switch away from fossil fuels [1].

Specific costs for heat pumps in the literature vary between 300 - 1000 €/kW_p, depending on the manufacturer and their scope of services (additional equipment, labor and costs associated with design and installation, ...) [9], [10]. In Europe there are variable national capital and operational expenditures subsidies for heat pumps. A short summary is given in Table 8 [41]. This thesis uses a conservative specific investment cost of 700 €/kWp including subsidies, average costs for ancillary equipment, labour associated with the design and installation, and costs associated with the design and installation.

In Europe, greenhouse gas pricing distinguishes between industries with very high greenhouse gas emissions, which are priced directly via certificates, and all other emitters, which are priced indirectly via taxes. The European emissions trading scheme is a "Cap & Trade" system which was introduced in 2005. It includes > 10,000 plants in the energy sector and energy-intensive industries. Facilities can redeem CO₂ -certificates for released emissions or, if they are not needed, trade them on the market. Detailed information about exceptions and regulations can be found in 3.4. Industries must pay for their Scope 1 emissions, which occur in the plant itself, for example through the conversion of fossil fuels for the generation of thermal energy. Scope 2 and 3 emissions must not be covered with certificates by the industries [42], [43], [44]. For example, the generation of 1 kWh of thermal energy using a modern natural gas boiler emits 202 gCO_{2-ev}/kWh. The combustion technology used is relevant due to the efficiency of different plants. The CO_{2-ev} of other fuels, as well as a calculation tool (Excel) for CO_{2-ev} emissions for thermal energy and electricity production can be found in [49]. Sectors that are excluded from EU-wide certificate trading, like transport, housing, waste, and agriculture are considered nationally through annually increasing CO₂ taxes. However, due to the relevance of these sectors, a certificate trading system is to be introduced by 2027 [45], [51].

All predictions agree that the price of CO_{2-ev} certificates will rise in the future due to the generated shortage of these. Some studies believe that the price will settle at around 113 \$/t, since carbon capture and storage will be economical from this value, while other studies predict CO_{2-ev} prices of above 180 €/t. This thesis will use a carbon certificate price in Europe of 113 €/t, with the assumption that carbon capture and storage will become technological and economical feasible and to weight the early future with more solid price assumptions more than more distant time periods [2], [34], [37].

The values of the most relevant economic parameters are summarized in Table 37 [2], [32], [34], [37], [40].

Table 37 Summary the most relevant gas boiler and HP parameters for later economic calculations [2], [32], [34], [37], [40]

	Variable	Value	Unit
	$\zeta_{gas\ boiler}$	0,9	-
reference scenario	C_{gas}	0,025	€/kWh
	f_{gas}	202	g/kWh
	C _{CO2}	113	€/t
	CAPEX _{gas boiler}	150	€/kW
	Celectricity	0,075	€/kWh
UD accordia	СОР	case	
HP scenario		depending	-
	CAPEX _{HP}	700	€/kW
interest rate	i	3	%
full load hour	FLH	case	h /vr
Tull load flour	ГГП	depending	h/yr

The approach of the thesis is to work out the economic solutions of the technical potential. By including future developments and the future trends of the most important economic parameters like heat pumps capital expenditures, subsidies, CO₂ prices, electricity prices and gas prices, the market potential is determined [40].

5.3 Market potential Europe

In Europe roughly 3000 TWh/yr of thermal energy are used in the industry. Around 600 TWh/yr are < 200 °C what is the long-term temperature target for industrial heat pumps. 200 – 300 TWh/yr are estimated to be suited for industrial heat pumps due to the availability of suited waste heat sources. The greatest potential in this temperature

range is in Germany, Italy, United Kingdom, France, Finland, Spain, and Sweden [8], [9], [52].

The study [11] assumes that the industrial heat pumps market in Europe are 174 TWh. Figure 177 shows industries with a process heat demand below 150 °C. The sectors food and tobacco, paper and chemical have the highest low temperature process heat demand.

Exemplary applications in the food industry are steam production for sterilization, boiling, baking, vaporization, and pasteurization processes. Furthermore, hot water is used during the bottling process (washing and sterilization), and the brewing process (mashing, lautering, wort boiling). But also, in the PET bottle industry process heat between 100 – 150 °C is needed for injection molding of plastic preforms or pellets drying. There are several drying processes, which need < 150 °C such as starch drying, wood drying, paper drying, laundry drying, brick drying (air preheating), drying of animal fodder and others. In the chemical industry steam and hot water is needed for distillation, concentration, boiling and thermoforming processes. The wood sector needs temperatures greater than 100 °C for gluing, essing and drying processes. The textile industry works in the processes of coloring, washing, and bleaching above 100 °C [7], [53].

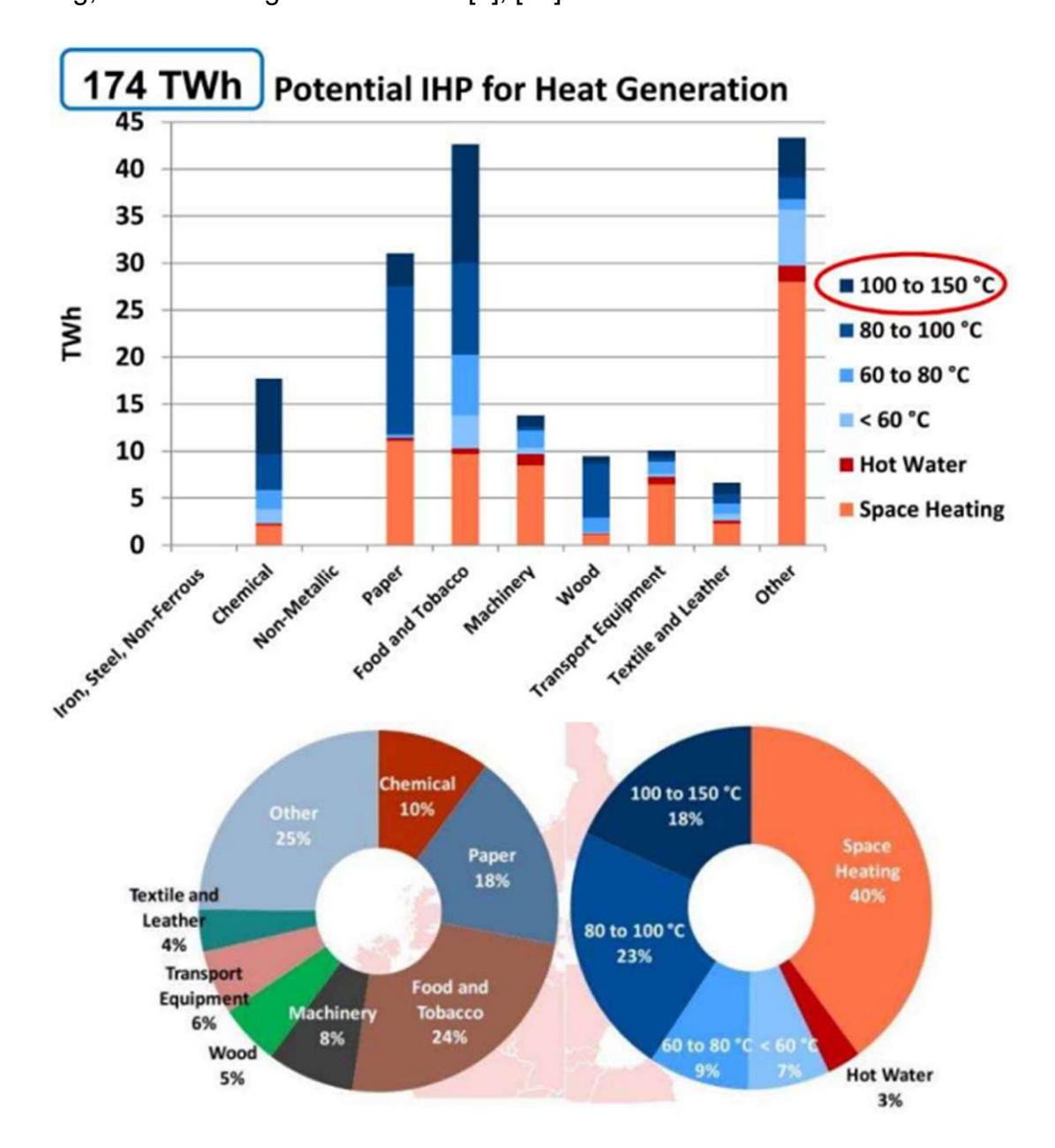


Figure 177 Market potential of IHP in Europe based on industries and temperature levels [11]

The studies [9] and [52] investigated the pulp and paper, chemical, food and beverages and refinery sector as the most promising ones for the use of industrial heat pumps. They estimated the industrial heat pumps suited thermal energy potential among these industries for < 150 °C to ~750 PJ (208 TWh/yr) and < 200 °C to ~1100 PJ (306 TWh/yr). The needed investment to realize the discussed industrial heat pump market with unit costs ranging from 200 – 500 €/kW result in 4,5 – 11,5 billion €. The study names these values as conservative calculations. The investment costs per sector are shown in Table 38 (in this table . (dot) is used as decimal point instead of a , (comma)) [9].

A key message of study [9] is that the investigated industries needs many relatively small units (88 % of total heat pump units) providing around 50 % of the heat capacity. To provide solutions for the whole industry, heat pump manufacturer should provide small standardize machines in high numbers and very big, customized machines depending on the needed use case.

Table 38 Needed investment to realize the IHP demand in the four mentioned sectors with unit costs between 200 – 500 €/kW; in this table . (dot) is used as decimal point instead of a , (comma) [9]

Sector	Cumulative Heating Capacity, Q _{P,HPmarket} (GW)	Lower Bound Investment (G€)	Upper Bound Investment (G€)
Paper	7.9	1.58	3.95
Chemical	9.1	1.82	4.55
Food	5.5	1.10	2.75
Refinery	0.5	0.10	0.25
Total (Σ)	23.0	4.60	11.50

Beside the well-suited sectors discussed above study [6] predicts the fraction of heat pump coverage for process heat < 200 °C in all sectors to reach 40 % in 2050. The fraction of heat pumps out of the < 200 °C total heat technologies in the market between 2010 and 2055 is pictured in Figure 178 [6].

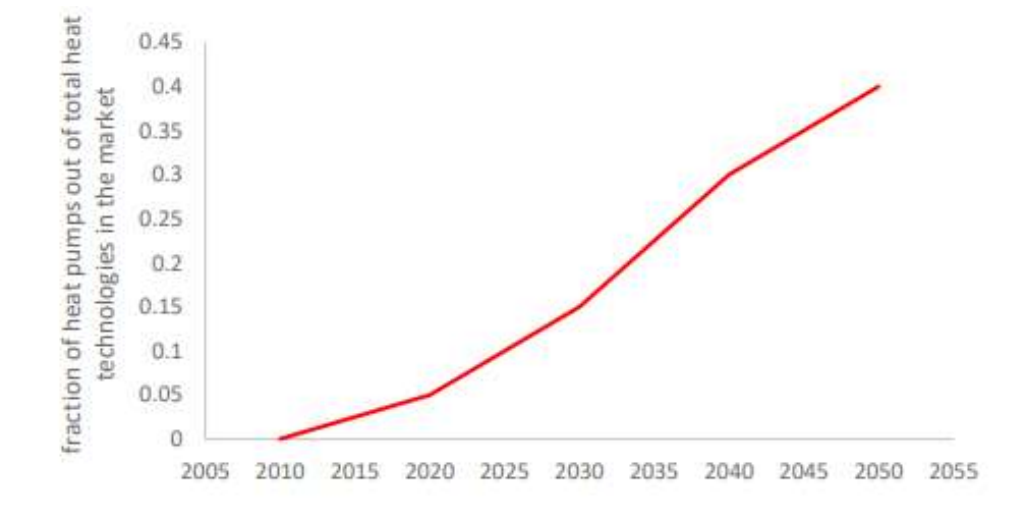


Figure 178 Fraction of heat pump for process heat < 200 °C; in this figure . (dot) is used as decimal point instead of a, (comma) [6]

Beside process heat for industry, district heating is also an interesting sector for the use of heat pumps. District heating is growing massively all over the world. District heating systems of the third and fourth generation are characterized by a lower temperature level and the integration of renewable and waste heat sources into the system [55]. Heat pumps can either be used in combination with renewable sources or to lift low temperature excess heat sources. Possible excess heat sources are data centers, metro tunnels, waste heat in industry, hydrogen generating electrolyser, sewage water treatment facilities and nuclear power plants. Examples for renewable sources are geothermal energy, solar thermal energy, or the burning of waste [56].

The target of district heating and cooling is to connect 350 million buildings globally by 2030, providing 20 % of the space heating needs. The total installed district heating EU28+3 capacity in 2021 where around 300 GW. Roughly 43 % of the district heating thermal energy is supplied by renewable and waste heat sources pictured in Figure 179. The district heating sales in 2021 where around 500 TWh/yr [58].

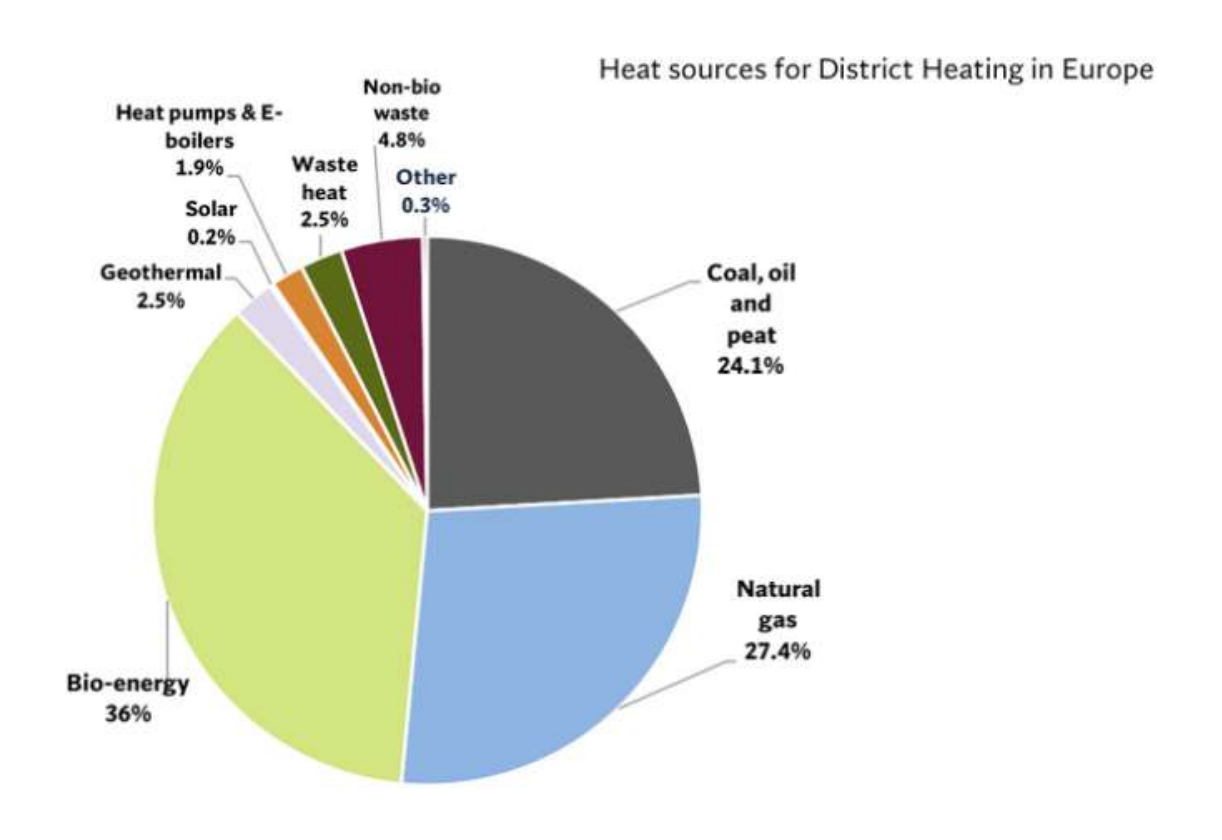


Figure 179 Heat sources for district heating in Europe (2021) [58]

The European capacity of large-scale heat pumps in district heating systems are around 2,43 GW. The key players are Sweden, Finland, and Denmark. According to predictions the amount of heat pumps for district heating in Europe will increase at least by 80 % until 2030 which corresponds to additional 2 GW [58].

This thesis investigated specific fields for the use of heat pumps in the industry and for district heating. The focus was mainly on new high temperature applications and the combination with renewable sources to maximize the CO_{2-ev} savings. In the following sections the different use cases are described briefly.

5.3.1 Geothermal energy

The geothermal heat power of the earth's crust comes from the radioactive decay of long-lived nuclides like ²³⁵U, ²³⁸U, ²³²Th and ⁴⁰K. Geothermal system differentiate between hydrothermal (hot water) and petrothermal (hot stone) storages, open and closed systems, and the depth / temperature level of the geothermal energy source. This thesis focuses on hydrothermal open loop systems in depths between 800 – 3000 m and temperatures between 40 – 150 °C [59], [60].

Figure 180 shows the distribution of geothermal energy in Europe. The color indicates the temperature level, with yellow being cooler and red being warmer. Europe's largest deposits are in Iceland, France, Turkey, Germany, Hungary, Italy, and Serbia [62].

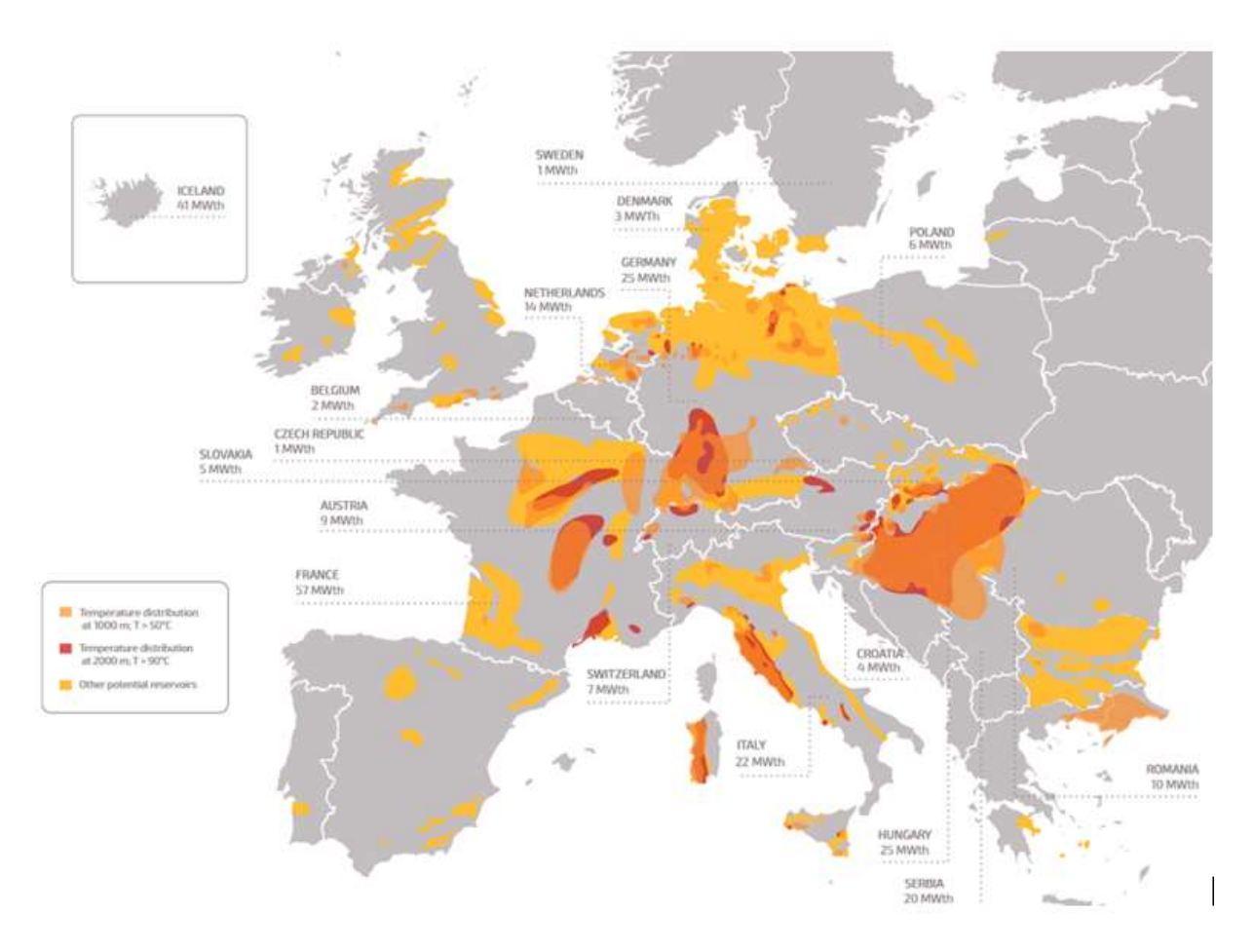


Figure 180 Overview of the geothermal sources in Europe [63]

Geothermal energy at the focused temperature level can be used for process heat or district heating. The generation of electricity in this temperature level is usually economical not feasible. Hot water from hydrothermal sources can be utilized directly or in a serial setup. In the direct setup hot water is used in a heat exchanger to heat the cold side (exemplary a district heat return flow). In the serial setup the geothermal water is used as source in a heat pump. This thesis identified three ways to combine the ecop heat pump with a geothermal source [64], [65], [67].

The first use case (Geo1) is designed to increase the thermal power of a geothermal well and increase the reachable temperatures. Figure 181 shows that the geothermal feed is utilized in a heat exchanger to lift a district heat return from 55 to 75 °C (467 kW). The heat pump is used to extract another 617 kW from the geothermal feed cooling it down to 33 °C by using it as source. The heat pump in this setup can reach temperatures up to 115 °C, and provides 700 kW. Therefore, the thermal power of the geothermal well is increased from 467 to 1 167 kW. The average levelized costs of heat of a GeoDH system are ~ 80 €/MWh. A Geo-1 ecop HP add on would lead to levelized costs of heat between 46,4 and 83,6 €/MWh depending on the full load hours and the electricity price. The HP add on offers the possibility to increase the thermal power and supply temperature of an existing geothermal well [64], [65], [67].

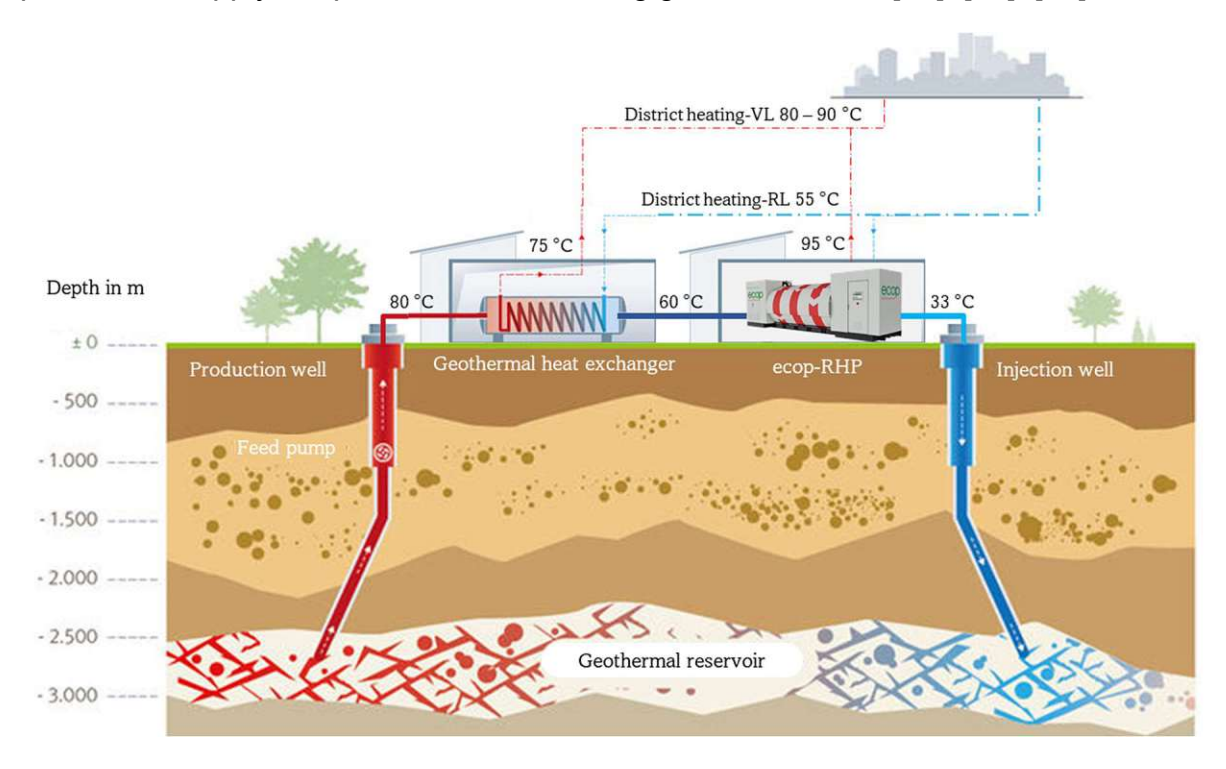


Figure 181 Doubled use of the geothermal energy based on [67]

The second use case (Geo-2) is designed to provide high temperatures for industry or old district heat systems with a heat pump if no suited excess heat sources are available. To generate temperatures of 150 °C with a heat pump source temperatures of 90 - 100 °C are necessary. Often no constant excess heat sources at this temperature level are available. In this case geothermal energy can be used as heat pump source. This use case can also be combined with Geo-1 if two heat pumps utilize the geothermal heat flow in series. The levelized costs of heat of the Geo-2 use case are 104 – 166 €/MWh. Compared to Geo-1 these costs are significant higher, because of the higher temperature level. Other technologies to provide temperatures of 150 °C often come with high CO_{2-ev} emissions. A combination between Geo-1 and Geo-2 can lower the costs [64], [65], [67].

The third use case (Geo-3) focuses on geothermal sources with lower temperatures. These can occur in lower depths with significant lower drilling costs, in old oil wells or in failed geothermal drilling if the expected / needed temperature is not found in reasonable depths. Therefore, Geo-3 can lower the biggest risk of geothermal systems, the risk of failed drilling. In this use case the heat pump uses the geothermal source with 30 – 50 °C as source to lift a sink to a valuable temperature level. If no costs for drilling are necessary, for example if an old oil well is used the levelized costs of heat result in 24 – 86 €/MWh [67].

The HP potential as retrofit to existing GeoDH systems in Europe result in 2,35 GW or 3 357 pieces of the ecop RHP. The resource potential of geothermal power in Europe exceeds 1 770 TWh or 540 GW. The technical potential for the integration of use case 1 - 3 into new geothermal systems result in 378 GW. If only 1 - 2% of these systems are economical feasible the market potential arise in 5400 - 10 800 pieces of ecop RHP [71], [72], [73], [74].

5.3.2 Hydrogen electrolysis

In the future, green hydrogen will be an important renewable energy carrier in the energy intensive industry. Today, hydrogen is mostly produced from fossil sources declared as grown or grey hydrogen. Green hydrogen is produced by electrolysis of water with the help of renewable produced electricity. The predominant electrolyser technologies are alkine electrolyser and polymer exchange membrane electrolyser. During the splitting of water into oxygen and hydrogen, a lot of waste heat is produced. This chapter examines how waste heat generated during the production of green hydrogen can be recovered using a heat pump [57], [76].

The use case (H₂-1) looks deeper in the stack cooling of an electrolysis cell showed exemplary in Figure 182. Due to efficiencies of the electrolysis cell, more energy is consumed than needed for the endothermic splitting of water. For a stationary operation of the electrolysis cell, this thermal energy must be extracted through a cooling circuit. It should be noted that the temperature gradient inside the electrolysis cell should not exceed 10 K to avoid aging and fouling processes. Therefore, the thermal energy of the stack cooling circuit is transferred to a closed-loop heat pump source circuit. The heat pump utilizes the thermal energy to heat a sink for process heat or district heating [57], [78], [79], [80].

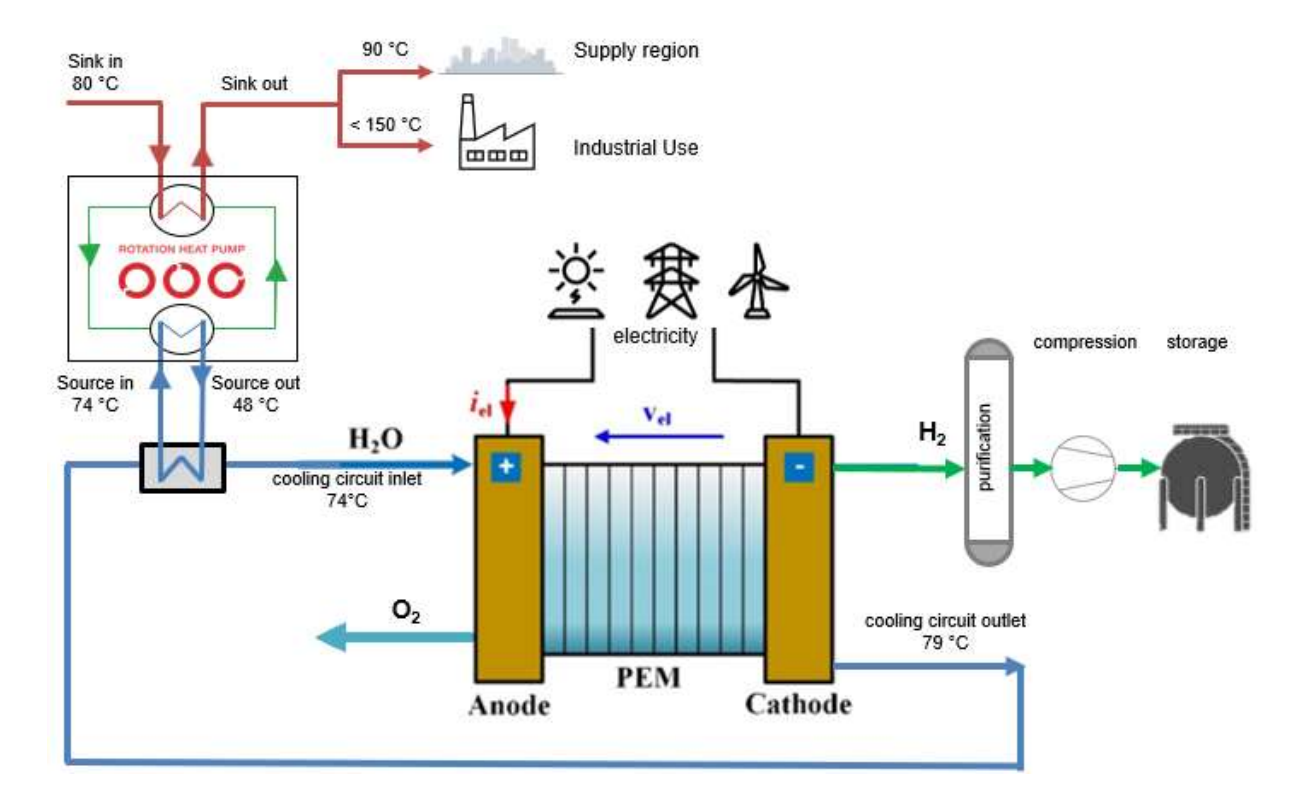


Figure 182 Simplified scheme of an electrolyser stack cooling with a heat pump and further hydrogen processing steps (purification and compression) until storage by [22], [81]

In Lulea (Sweden) a similar project has been determined. They estimated the waste heat potential of a 100 MW PEM electrolyser to 23,2 MW. The waste heat of a AEL would be 31 MW, because of the poorer cell efficiency. They estimated, that the waste heat utilization with a heat pump would be economical feasible and identified the capital expenditures, the discount rate, and the electricity prices as the most sensitive parameters for the cost structure [57].

After the electrolysis the hydrogen is saturated with water vapor. Therefore, the hydrogen needs to be dried for further uses. The drying process usually consist of two steps. First, the hydrogen is cooled down to 20 – 40 °C, where around 90 % of the water condensates. The final drying is done by adsorption of the water vapor to silica gel. Use case H₂-2 is designed to utilize the extracted thermal energy from cooling the hydrogen after the stack from 80 °C to 20 - 40 °C for drying purposes. It has been shown that from the hydrogen generated by a 100 MW electrolyser 400 – 500 kW can be extracted during the first step of drying. Therefore, this use case is limited to large electrolyser [57], [80], [84].

Use case H₂-3 is focusing on the excess heat generated during the compression of hydrogen. Hydrogen is a very light gas, which is why it occupies a very large volume. Therefore, it needs to be either compressed or liquified to be transported and stored. This thesis aims on the excess heat of intercooled mechanical compressor arrangements. On the one hand, large compressors need due to limited efficiencies be cooled, and on the other hand, the hydrogen temperature rises while being compressed. To achieve an approximately isothermal compression (which requires less energy compared to an isentropic compression) the hydrogen must be cooled between each compression stage. The resulting extractable thermal energy for a 100 MW electrolyser as a function of the cathode pressure, the final compression pressure, the initial hydrogen temperature (after gas drying) and the average compression temperature is shown in Table 39 [80], [84], [85], [86], [87], [89], [90].

Table 39 Heat generation during compression to different end pressures depending on the storage facilities *calculated according to Equation (9), parameter estimated by Figure 90 [80], [89], [90]

	Pipeline	cavern storage	hydrogen car refueling station	
initial pressure: cathode pressure	30	30	30	bar
end pressure	80	200	750	bar
initial temperature	28,3	28,3	28,3	°C
compression stages	1	2	3	pcs.
mean temperature after compression	126*	125*	142*	°C
gas temperature after interstage cooling	30	30	30	°C
thermal energy extraction potential	1 264,5	2 518	4 601	kW

Usually, the thermal energy of the compressor cooling circuit is dissipated by a fan to the surrounding. Depending on the temperature level the thermal energy can be utilized by a heat pump or used directly in a heat exchanger. The waste heat utilization can exemplarily look like [68]:

- temperature level of 110 140 °C directly used for process heat or steam generation
- temperature level of 90 110 °C lifted with RHP to 140 °C and used for process heat or steam production
- another RHP in series utilizing the lower temperature level. Cooling down the source to 28 °C and lifting the sink from 80 to 100 °C for district heating.

In all hydrogen use cases the thermal energy is generated anyway and must be extracted in some way. In contrast to release the energy with a fan to the surrounding the thermal energy can be used as source for a heat pump. The electrolyser and the following plants must not be adapted to utilize the waste heat with a heat pump. Therefore, the levelized costs of heat for the thermal energy provided by the heat pump can be set to be the costs for the heat pump itself. These costs are pictured for the ecop RHP in Figure 43 and are between 24 and 86 €/MWh. Since the ecop RHP requires 600 kW on the source side under full load, gas drying and compression applications are limited to larger plants. Stack cooling already provides sufficient thermal waste heat in the scale of 2 - 3 MW electrolyser [70].

The 2030 expected electrolysis capacity in Europe is between 40 - 113 GW dependent on the scenario and study. The biggest capacities are planned to be in Germany, Denmark, Spain, Finland, France, and Netherlands. Studies show that the electrolyser waste heat potential is predicted to be 35 TWh/yr in 2030 and 250 TWh/yr in 2040. Based on the use cases (H₂-1 to H₂-3) the ecop rotation heat pump potential in Europe is 14 864 to 41 991 plants, while the biggest potential is the stack cooling, followed by hydrogen compression [70], [83], [91], [91].

5.3.3 Solar thermal energy

The section solar thermal energy focuses on a combination between solar thermal energy (flat plate collectors, evacuated tube collectors, parabolic through collectors), thermal energy sources and heat pumps. The combination between photovoltaic cells and a heat pump is also reasonable, but will not be investigated in more detail. The thermal energy storage can either be a short-term buffer storage for daily fluctuations or a long-term seasonal storage for seasonal fluctuations. Thermal energy storages are often used in combination with solar thermal energy because the thermal energy supply of renewable sources (solar energy) is often shifted to its demand (highest demand is in winter). Solar thermal energy and heat pumps can either be used parallel, where both charge a thermal energy storage or serial, if one charges the thermal energy storage and the other technology is used for end heating. For example, can solar thermal energy be used to charge a seasonal storage and a heat pump can use the storage as source to lift the sink for district heating or process heat [3], [22], [95], [96], [97], [98], [99], [94].

Use case (Solar-1) presents a concept for cities, towns, and villages to increase the share of renewable / solar thermal energy in district heating systems. Solar district heating (SDH) systems are a combination between solar thermal collectors, thermal energy storages, heat pumps, and peak load boilers. Solar thermal collectors are used to charge a stratified seasonal thermal energy storage. The thermal energy storage is used directly to supply the district heating network if the temperature level is higher than the district heating return. If the temperature in the thermal energy storage decreases the heat pump uses the storage as source to provide the needed temperature level. The heat pump cools down the thermal energy storage increasing the efficiency of the solar collectors. Peak load boilers are used if the peak load cannot be covered or if the thermal energy storage is fully discharged. Best practice example of solar district heating networks can be found in Denmark. Figure 183 shows a simplified process diagram of the solar district heating network in Dronninglung (Denmark). The feed and return temperature are 75 and 40 °C, the solar fraction is 52 % and the levelized costs of heat result in 50 €/MWh without subsidies [3], [100], [101], [102], [103], [104].

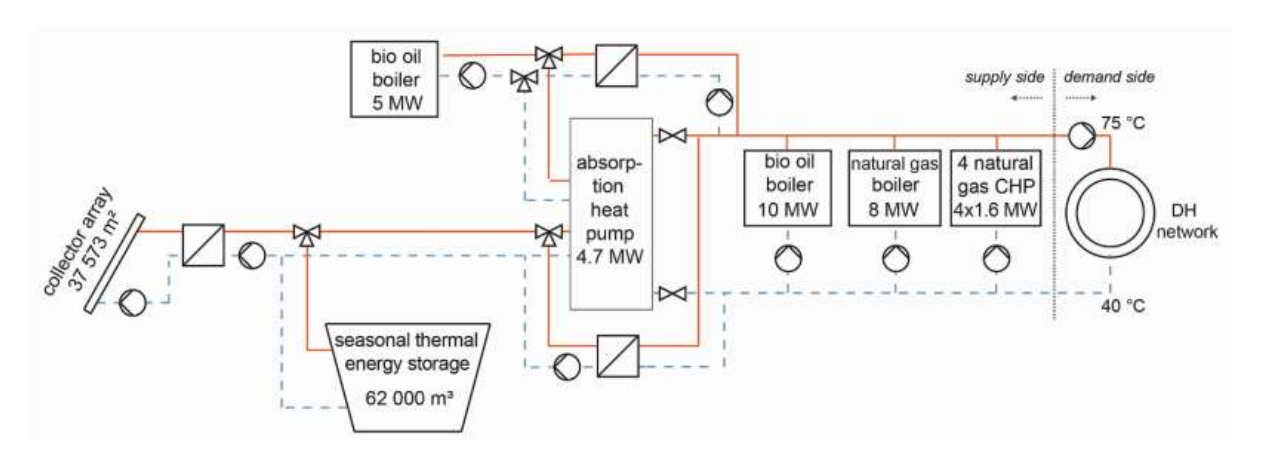


Figure 183 Solar district heating network in Dronninglund (Denmark), the pumps indicate the flow direction [3]

There are many factors that can heavily influence resulting levelized costs of heat of solar district heating systems. The most import are [3], [106], [107]:

- Availability of land as well as the price of land
- District heating temperature level
- Existing infrastructure for heating (gas boilers, biomass combined heat and power plant, ...)
- Difference between maximum and minimal thermal energy demand (winter / summer)
- Necessity of seasonal storage (high capital expenditures)
- Aiming solar fraction
- Prices of other technologies (reference scenario is usually fossil fuels), taxes on fossil fuels are in Nordic countries for example Denmark significantly higher
- The size of the district heating system, because smaller solar district heating systems are already well explored, while bigger solar district heating systems

with several thermal energy sources are more complex and only little experienced.

Solar district heating systems usually have high capital expenditures, but low operational expenditures. Therefore, typical discounted payback periods are between 7 – 12 years. Small scale solar district heating systems and smaller solar fractions (< 30 %) are usually cheaper, because of smaller storages. Small scale solar district heating systems have levelized costs of heat between 30 – 40 €/MWh, while bigger systems range from $40 - 55 \in /MWh$ [3], [32], [106], [107], [108], [109], [112], [113].

The use case (Solar-2) aims on providing thermal energy for industries by a combination of renewable sources and heat recovery. These systems are called solar heat for industrial processes. Solar heat for industrial processes is like solar district heating with the difference that storages are usually dimensioned smaller and the temperature level is higher. This thesis shows an example of solar heat for processes in a textile industry. The process is based on solar thermal energy charging a stratified storage and a heat pump providing the necessary temperature level. Furthermore, photovoltaic cells are used to cover the electricity demand of the heat pump. The analyzed feasibility study showed that the renewable concept achieves lower prices (51 €/MWh including subsidies) than the fossil reference scenario. The discounted payback period result in 7,2 years [70], [105].

The role model for solar district heating is Denmark, where it has been shown that the concept work and is economical feasible. The expansion of solar district heating systems is very much depended on promotion schemes and boundary conditions. Austria and Germany try to establish attractive promotion schemes and boundary conditions to follow the Danish example. Especially countries with high costs for heating, while having a high solar yield are attractive markets. Such countries are Spain, Estonia, Czech Republic, and Italy. Studies predict a solar district heat potential of > 100 TWh/yr in Europe. Considering some conservative assumptions the market potential of heat pumps in solar district heating systems result in 7,35 GW or 10 500 ecop RHP [32], [108], [114].

Solar heat for industrial processes is not yet well established. The major hurdles are the availability of land, the complexity and long payback periods. The international energy agency found a global potential for solar process heat of 1 500 – 2 200 TWh/yr or 3 – 4 % of the industrial thermal energy demand. The conservative assumption of 2,5 % solar process heat in Europe lead to a heat pump market potential of 8,75 GW or 12 500 ecop RHP [32], [70].

5.3.4 Flue gas utilization

Flue gas is one of the major excess heat sources in industry. Flue gases of fossil combustion processes are often not cooled below 140 °C. If the flue gas is cooled down below the acid dew point different flue gas components like Ammoniac, Chlorides, Sulfur compounds, etc. dissolve in the water making the condensate very corrosive [70], [115], [116], [119], [120].

Use case (Flue-1 and Flue-2) is aiming on the fossil small to medium scale steam generation. Fossil steam generator (natural gas, oil, ...) are using an economizer to reduce the needed thermal energy in the boiler itself. In the economizer thermal energy from the flue gas is transferred to the freshwater feed. In this section a high temperature heat pump is added to an existing fossil steam generator setup to preheat the freshwater feed before entering the economizer. A simplified visualization of the high temperature heat pump add on to the gas boiler circuit is shown in Figure 184 (Flue-1). The integration of a high temperature heat pump is used to preheat the freshwater feed from 100 °C to 140 °C before entering the economizer. In this setup the feed reaches higher temperatures in the economizer (~ 160 °C). The increased boiler inlet temperature of the feed directly leads to a lower thermal energy demand in the gas boiler and therefore to fuel savings [70], [115], [116], [119], [120].

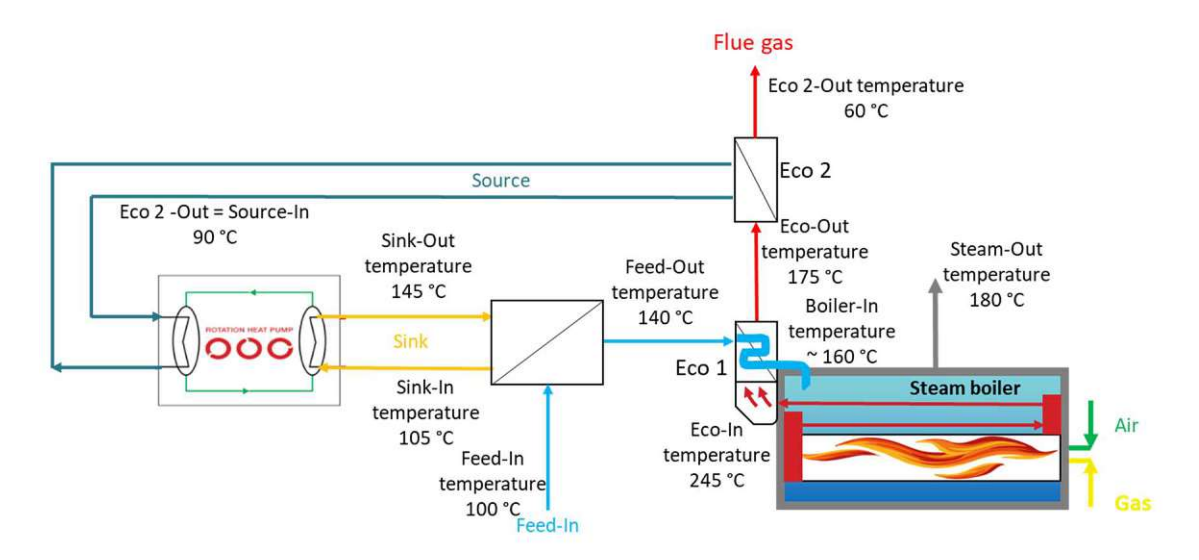


Figure 184 Simplified visualization of a high temperature heat pump integration for the freshwater feed preheating in the gas boiler circuit [70]

The use cases Flue-1 and Flue-2 differentiate in the temperature of the freshwater feed. Use case Flue-1 is considering that the steam condensate (~100 °C) can be reused as freshwater feed. Use case (Flue-2) assumes that the steam is consumed and the freshwater feed has a temperature of 20 °C [70], [115], [116], [119], [120].

The dynamic payback period is very much depended on gas, electricity, and CO₂ prices. Another very sensitive parameter is the reachable economizer outlet temperature (= boiler inlet temperature). The dynamic payback period for the use case Flue-2 is pictured in Figure 185. In the case of 160 °C economizer outlet temperature the natural gas savings related to the fossil scenario result in 14,6 %. 344 k€ are saved every year with 75 k€ resulting directly from the gas savings and 269 k€ from the saved CO₂ certificates [70]

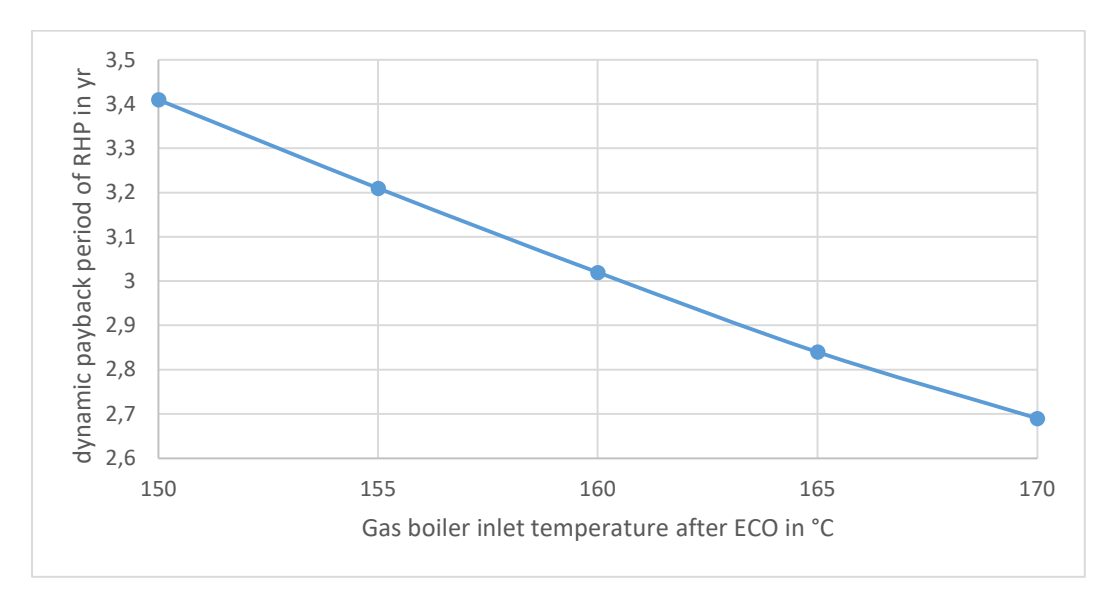


Figure 185 ecop RHP dynamic payback period according to the gas boiler inlet temperature (= economizer outlet temperature) [70]

The generation of steam is dominated by fossil fuels. According to [118] the steam boiler market will grow until 2032 annually by 5,5 %. In 2030 1 138 TWh of primary energy or 200 GW will be needed for steam production in Europe. Assuming that 20 % will use Flue-1 or Flue-2 as retrofit or in a newly built steam boiler the addressable power are 40 GW. Considering a gas to high temperature heat pump power ratio of 8 % on average the heat pump market potential is 3,2 GW or 4 571 pieces ecop RHP [70], [70], [115], [115], [116], [119, 120].

The use case (Flue-3) focuses on the condensation of the gaseous water in the flue gas produced during the combustion process or contained in the fuel. Usually, the flue gas is only condensed if the proportion of corrosive dissolved components (ammoniac, chlorides, sulfur compounds) in the condensate is low. This is the case for exemplary woody biomass or natural gas. The flue gas condenses when the temperature falls below the dew point, which is usually in the range of 45 - 70 °C for these fuels. The flue gas condensation takes place in a condensing heat exchanger, with a low temperature flow on the cooling side. This can be, for example, a space heating circuit or the source of a heat pump. If a permanently available low temperature source is available, it makes sense to use it for the condensing heat exchanger. If this is not the

case or if there is no demand for the low temperature thermal energy, a heat pump can be used. In this case, the heat pump cools down the source below the dew point temperature and extracts the condensation energy from the flue gas and is thus reheated. The heat pump can use the source power to heat any sink accordingly. The dynamic payback time depends on the achievable temperature level and prices for the thermal energy and can vary between half a year and three years. The potential in the European industry is huge. It is assumed that around 5 910 MW are wasted from suitable flue gas stream. 8 443 ecop RHP could be used to utilize this excess heat [3], [70], [115], [121], [122], [123], [124].

5.3.5 Steam generation

Today, process steam comes largely from fossil fuel steam generators. However, there are already renewable approaches with heat pumps. If the electrical energy used in the heat pump comes from renewable sources, CO₂ savings of 100% can be achieved. There are three main types of steam generating heat pump concepts. The generation of pressurized water at high temperatures in a heat pump for the use in a steam generator or in a flash tank. Or the compression of steam at low pressures to higher pressures with specialized compressors [8], [120], [125], [126], [127].

The use case (Steam-1) deals with flash tanks for steam generation. Here, pressurized saturated hot water is generated in the heat pump and expanded in a steam drum. Due to the reduction of the pressure, flash evaporation occurs. The resulting steam is extracted via the header. The remaining hot water is mixed with fresh water, compressed, and reheated in the heat pump. Figure 186 shows a heat pump driven flash evaporation with a mechanical vapor compression (orange) and a traditional thermal boiler (blue) in a temperature-entropy diagram [128].

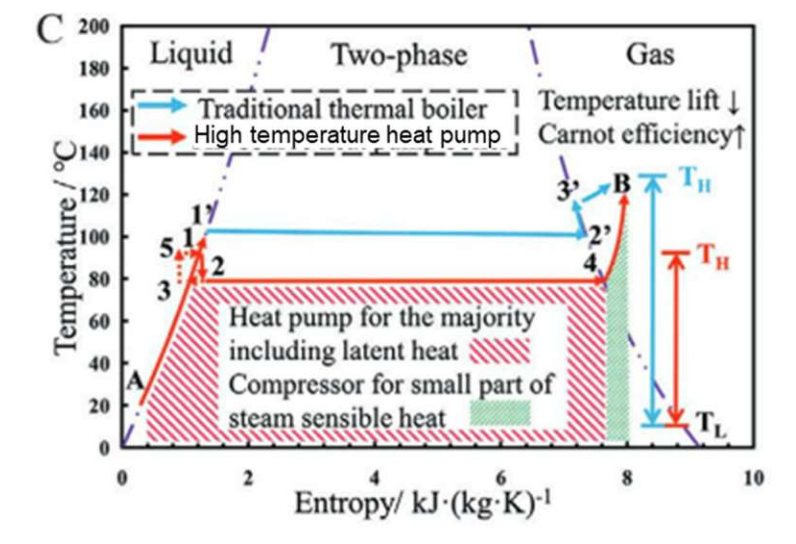


Figure 186 T-s diagram of the flash cycle compared to a typical evaporation in a thermal boiler [70], [128]

Use case Steam-2 deals with the generation of steam using a heat pump and a steam generator. A steam generator is in a simplified way a heat exchanger with a lower pressure and temperature in the inner part being heated by a warmer outer part. The outer part is heated by hot pressurized water from the high temperature heat pump. In the inner part evaporation takes places and the steam is taken off at the head of the heat exchanger. The evaporated part is replaced by fresh water. The separation between the liquid and gaseous phase is done by gravity. An exemplary setup is shown in Figure 187 [120], [128].

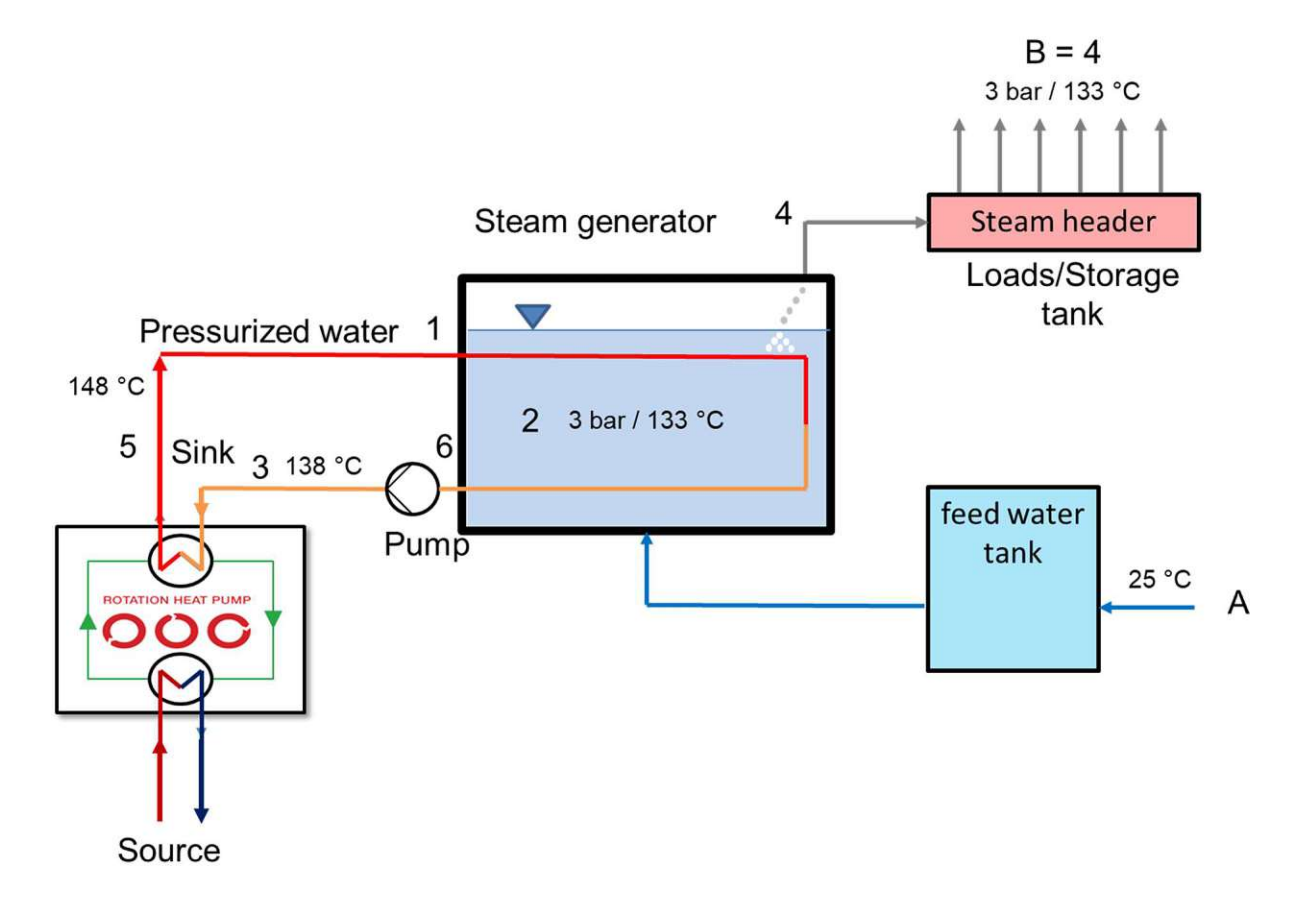
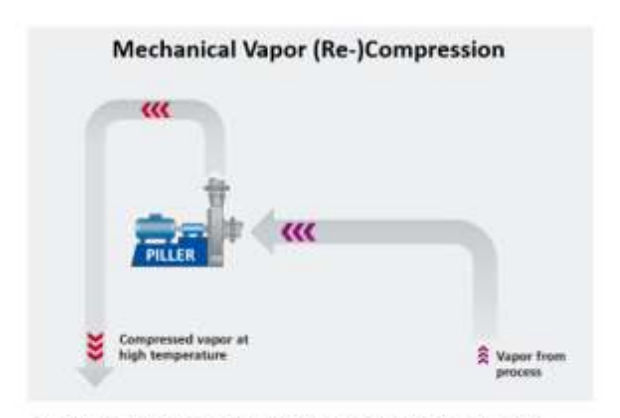
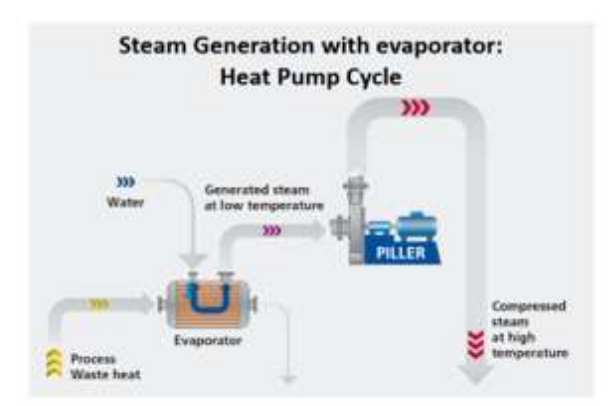


Figure 187 Combination of ecop rotation heat pump and a steam generator, exemplary temperature levels are shown in the figure [70], [120]

Use case Steam 3 deals with the mechanical compression of low-pressure steam using specialized compressors. Depending on the application, capacity, temperature and pressure, different compressors are used for this purpose. A distinction is made between mechanical vapor compression and mechanical vapor recompression units pictured in Figure 188. Mechanical vapor compression units are used to compress steam from a steam generator or flash tank to higher pressures and temperatures in several stages (right). Mechanical vapor recompression units (left) are used to recycle low-pressure steam from open-loop processes. Low-pressure steam (exemplary from a drying process) is drawn of from the system and mechanically compressed to higher pressures and temperatures and fed back into the process [120], [129], [130].



- · Direct compression of steam and other vapors
- · Direct use of compressed vapors for heating or steam generation



- · Steam procution directly at the waste heat source
- · Steam compression to necessary pressure and Temperature

Figure 188 (left) mechanical vapor recompression, (right) mechanical vapor compression of generated low-pressure steam [129]

The flash tank system can reach higher coefficient of performance because of the lower temperature level, but is the more complex system, because it must be achieved a good separation between the steam and liquid phase. In the flash tank the steam mass flow is limited by the maximum outlet velocity of the diffuser in the steam drum. The flash tank is the preferred option if the heat pump can just provide temperatures < 100 °C or a mechanical vapor compression system is available at low costs. Steam generators are simpler and have a little lower capital expenditures. The difficulty is to ensure a good heat transfer between the heat pump circuit and the steam generator. Depending on this heat transfer and the achievable temperature level of the heat pump the maximum steam temperature is limited. With heat pump sink temperatures of 150 °C the maximum saturated steam temperature is ~ 133 °C. For higher temperatures either the heat pump sink temperatures must rise, or mechanical vapor compression systems are necessary.

In an economic efficiency calculation, the heat pump-based systems with a flash tank and a steam generator were compared with a gas boiler as reference system. The boundary conditions and economic parameters were used according to the previous analyses. The full load hours were varied between 4000 and 8000 hours per year. It has been shown that the dynamic payback time of both heat pump systems are very similar. The flash tank variant achieves better coefficient of performance and therefore shorter payback times due to the lower temperature level. The dynamic payback time is about 6 years for 4000 and 3 years for 8000 full load hours a year. With both systems considerable costs can be saved during a life cycle of 20 years [70], [120], [132].

The study [9] investigated the potential of thermal energy that can be provided by heat pumps in Europe in the four sectors paper, chemical, food and refinery. The potential resulted in 641 PJ or 20 GW of thermal power. 47% of these processes are based on steam. The potential of steam-generating heat pumps in these four sectors is therefore 9,4 GW or 13 429 ecop RHP units. Further studies show that the steam boiler market will grow to 1 138 TWh by 2030. The stock of oil and gas boilers in the EU28 countries is about 3,1 million units. Based on these comparisons, it can be estimated that the caclulated 13 429 ecop RHP units are a conservative estimation for the market potential [4], [8], [9], [118], [120], [133].

5.4 Summary heat pump COP and EU market potential

In this section the necessity and justification, the coefficient of performance and the market potential of the analyzed market segments is summarized.

- Geothermal energy (4.1): Geothermal energy is a renewable energy sources that opens the possibility to supply thermal energy with a heat pump if no waste heat sources are available. The heat pump can increase the thermal power output of a geothermal energy well or increase its temperature level.
- ➤ Hydrogen Electrolysis (4.2): Green hydrogen will become an important energy carrier in the European Union towards its path to "net zero emissions". The major technology to provide green hydrogen is electrolysis generating a lot of waste heat. This waste heat can be utilized by a heat pump and lifted to valuable temperature levels.
- Solar thermal heat (4.3): Solar thermal energy can provide thermal energy for industries and district heating, but is subject of large seasonal fluctuations. Systems that can store solar oversupply and make it available at later times typically require a heat pump.
- Flue gas utilization (4.4): Flue gas is still one of the major excess heat sources leaving the plant usually at temperatures greater than 100 °C.
- Steam production (4.5): Much of the European process heat is needed as process steam. All conventional steam supplies are based on fossil fuels and need to be replaced by a renewable technology in the future.

Table 40 shows as summary of the calculated coefficient of performance (COP) of the ecop rotation heat pump for all presented use cases. The calculated COP are in the range of 2,91 – 5,97. The temperature levels are only examples for the presented market segments.

Table 40 Summary of the ecop rotation heat pump COP calculations of the different use cases

Name	Use Case	Customer	Sink In in °C	Sink Out in °C	Source In in °C	Source Out in °C	СОР
Increase geothermal heating capacity	Geo-1	Industry / District heating	55	95	60	33	4,41
Rise geothermal temperature level	Geo-2	Industry / District heating	90	140	90	53	3,58
Utilize low temperature geothermal energy	Geo-3	Industry / District heating	55	80	40	14,6	3,56
Hydrogen stack cooling	H ₂ -1	Industry / District heating	80	120	74	48	3,84
Hydrogen stack cooling	H ₂ -1	Industry / District heating	60	100	74	57,7	5,97
Hydrogen drying	H ₂ -2	Industry / District heating	80	100	80	28	3,56
Hydrogen compression	H ₂ -3	Industry / District heating	100	140	100	81,7	4,63
Hydrogen compression	H ₂ -3	Industry / District heating	80	100	80	28	3,56
Solar district heating	Solar-1	District heating	40	75	40	5,3	3,72
Solar district heating	Solar-1	District heating	80	115	75	25	3,16
Solar district heating	Solar-1	District heating	70	115	75	61,4	4,7
Solar district heating	Solar-1	District heating	70	115	61,4	48,1	3,72
Solar district heating	Solar-1	District heating	52	80	50	10	3,67
Solar district heating	Solar-1	District heating	40	80	45	7,6	3,77
Solar heat for industrial processes	Solar-2	Industry	100	140	90	76,8	3,99
Steam generator feed preheating	Flue-1	Industry (Steam)	105	145	90	77	3,74
Steam generator feed preheating	Flue-2	Industry (Steam)	105	145	90	77	3,74
Condensing heat exchanger	Flue-3	Industry / District heating	60	70	45	27,7	4,06
Condensing heat exchanger	Flue-3	Industry / District heating	58	100	45	28,2	3,44
Flash drum (low temperature)	Steam-1	Industry (Steam)	80	105	80	66,1	5,34
Flash drum (high temperature)	Steam-1	Industry (Steam)	132	140	100	88	3,04
Steam generator	Steam-2	Industry (Steam)	138	148	100	88,2	2,91

Table 41 gives a summary of the EU28 market potential in thermal power and pieces of ecop rotation heat pumps having each a thermal power of 700 kW. The calculation is simplified in the matter that the source input equals the thermal power output of 700 kW. The targeted thermal power is in the range of 51,1 – 73,9 GW that equals 73 064 - 105 591 ecop RHP. The greatest potential is the H₂-stack cooling, followed by the heat pump-based steam generation. Other great potential lies in the combination with solar or geothermal systems. Some of these potentials may overlap to some extent, but this does not refute the basic statement of the table that there is an enormous potential for high temperature heat pumps.

Table 41 Summary of the market potential (EU28) of the investigated market segments; decimal places are not pictured in this table; District heating = DH

Name	Reference Case	Customer	Thermal power potential in MW	pieces of ecop RHP each 0,7 MW	Potential horizon
Retrofit of GeoDH stock	Geo-1,2,3	Industry / District heating	2 350	3 357	2020
GeoDH potential	Geo-1,2,3	Industry / District heating	3 780 - 7 560	5 400 - 10 800	general
GeoDH failed drilling	Geo-3	Industry / District heating	no estimations	no estimations	general
H ₂ stack cooling	H ₂ -1	Industry / District heating	9 280 - 26 216	13 257- 37 451	2030
H₂ gas drying	H ₂ -2	Industry / District heating	160 - 452	228 - 646	2030
H ₂ compression cooling	H ₂ -3	Industry / District heating	965 - 2726	1 379 - 3 894	2030
Solar district heating (SDH)	Solar-1	Industry / District heating	7 350	10 500	general
Solar heat for industrial processes (SHIP)	Solar-2	Industry	8 750	12 500	general
Steam generator feed preheating	Flue-1 + 2	Industry (Steam)	3 200	4 571	2030
Condensing heat exchanger	Flue-3	Industry (Steam)	5 910	8 443	2020

Heat pump based steam generation	Steam-1, 2, 3	Industry (Steam)	9 400	13 429	2030
		sum	51 145 - 73 914	73 064 - 105 591	

The named market potential is larger than the one identified in other studies for following reasons:

- Most of the other studies name the potential in certain industries in contrast to the whole market.
- Other studies focus on the utilization of available excess heat sources in given industries, which is why they focus on suited industries like chemical, paper, food and refinery. In contrast to that this thesis includes source streams of renewable sources such as geothermal or solar thermal heat.
- Previous studies for this topic focused on the existing European industry in 2016 – 2020 and do not include future developments. This thesis focuses in terms of economic factors as well as the potential on a horizon till 2030. Exemplary the greatest analyzed potential of H₂-stack cooling is nowadays almost not existing.
- > Furthermore, this thesis includes not only the thermal energy demand of industry, but also district heating and its future development.

Study [9] stated in 2020 the potential of high temperature heat pumps < 150 °C and < 200 °C in the four industries food, chemical, paper and refinery to 20 and 23 GW. They only considered processes were simultaneous available suitable waste heat sources where available. Study [11] predicted the potential of industrial heat pump coverable thermal energy in Europe to 178 TWh/yr. The results of other related studies are summarized in Table 42.

Table 42 Summary of different studies aiming on identifying the industrial heat pump potential in EU28 [40]

Region	Art des Potenzials	Potenzial in TWh/a	Temp bereich	Anmerkung	Quelle
	Technisch	476			
EU28	Ökonomisch	75	-	2,3% des industriellen Endenergieverbrauchs; 15,75% des technischen Potenzials;	S. Wolf, M.
	Technisch	62,8	<100°C	34,4% des theoretischen Potenzials	Blesl, 2016 [9]
Deutsch -land	Ökonomisch	10,3	3	3,4 % des industriellen Wärmebedarfs; 16,4% des technischen Potenzials;	
	Theoretisch	182,8	<500°C	WP Technologie mit Wasser als Arbeitsfluid bis zu 500°C	S. Wolf, Diss., 2017, [8]
EU28	Technisch	739 (inkl. Nutzung für Fern- wärme)	<165°C	Industrie 237 TWh/a, Fernwärme 502 TWh/a; Wichtigste Sektoren: Molkerei, Papier & Zellstoff, Fleisch, Getränke	S. Wolf, 2 nd DryF EEAB WS, Mannhein 12/2018
EU28	Technisch	32,2	100°C - 150°C	Wichtigste Sektoren: Nahrungsmittel & Tabak (8,2%), Chemie (23,9%), Papier & Zellstoff (10,9%)	Arpagaus et al., 2018 [10]
EU28	Technisch	28,37	100°C - 200°C	1,5% des industriellen Wärme- bedarfs; Deutschland, Frank- reich, Italien, Spanien und GB > 60% des Gesamtpotenzials; Wichtigste Sektoren: Nicht- metallische Minerale, Papier und Zellstoff, Nahrungsmittel & Tabak and Nicht-Eisen Metalle.	G. Kosmodakis, 2019 [4]

5.5 Outlook

The thesis has shown that there are many renewable concepts that can replace conventional / fossil systems. Some of these systems are based on storage solutions with heat pumps due to fluctuating environmental influences or fluctuating operating conditions. Needs of the heat pump are large temperature lifts at a reasonable coefficient of performance and a flexible operation. It has been shown that the heat pump of the Austrian manufacturer ecop Technology GmbH, meets these requirements and thus has a very wide applicability and thus potential. The examined concepts are under the given basic conditions and with the ecop rotation heat pump as reference plant all economical. Economic hurdles are the high capital expenditures and the resulting long payback periods. This can be remedied by government subsidies, as they already exist in some cases, or by a contracting model, where the responsibility for the provision of thermal energy lies with the heat pump supplier/operator. Technical hurdles are fluctuating operating conditions and complex overall systems. Remedies for this can be provided by possible follow-up work. These can analyze the most interesting use cases under a technical focus and take a closer look at possible demonstration projects or best practice examples in the industry.

VI List of References

- [1] Ambienta: Electrifying Industrial Heat: A Trillion Euro Opportunity Hiding in Plain Sight. Ambienta Sustainability Lens: 02/2023.
- [2] Unterluggauer, F. Helminger and I. Beck, J. Solis-Gallego: Decarbonisation Pathways for the Finishing Line in a Steel Plant and Their Implications for Heat Recovery Measures. Energies: Band 16, Seite 852, 2023.
- [3] D. Tschopp, Z. Tian, M. Berberich, J. Fan, B. Perers und S. Furbo: Largescale solar thermal systems in leading countries: A review and comparative study of Denmark, China, Germany and Austria. Applied Energy Band 270, 2020.
- TNO, DTI, NTB, SINTEF, AIT, DTU, RISE, UPValencia: Strengthening [4] Industrial Heat Pump Innovation. Decarbonizing Industrial Heat, 2022.
- [5] J. Schäfer and S. Energy: HT-heat pumps: Heading towards the decarbonization of industry. EHPA, 2023.
- [6] Voswinkel, F.; Gouy, A.: Heat pumps in the industry. IEA, 12/2022.
- [7] IEA: The future of heat pumps. World energy outlook special report, 12/22.
- F. Hubmann, C. Gachot und L. Zeilerbauer: Industrial Heat Pumps and [8] Steam-Generation - Capabilities and Challanges of Heat Pumps in industrial processes. AIT, EDF, EI-JKU, European Union, 2022.
- [9] A. Marina, S. Soelstra, H. Zondag und A. Wemmers: An estimation of the European industrial heat pump market potential. Renewable and Sustainable Energy Reviews: Band 139, 2020.
- C. Arpagaus: Potential for High-Temperature Heat Pumps and Market [10] Analysis. Easter Switzerland University of Applied Sciences, 2022.
- [11] C. Arpagaus: Hochtemperatur Wärmepumpen. Buchs: NTB (Interstaatliche Hochschule für Technik Buchs), 2020.
- RISE: Website: [12] Heatpumpingtechnologies www.heatpumpingtechnologies.org [Online], https://heatpumpingtechnologies.org/annex58/task1/ , 2022. Zugriff am 29.12.2022.
- C. Arpagaus: Chillventa CONGRESS. High temperature HP: Nürnberg, [13] 2018.
- [14] Kobelco: Website: www.heatpumpingtechnologies.org [Online], https://heatpumpingtechnologies.org/annex58/wp-

- content/uploads/sites/70/2022/07/technologykobelcosgh165.pdf Zugriff am 29.12.2022.
- [15] AS: Hybrid Energy www.hybridenergy.no [Online], Zugriff https://www.hybridenergy.no/reference-plants/ 2022. am 29.12.2022.
- [16] Combitherm GmbH: www.combitherm.de [Online], https://www.combitherm.de/de/produkte-undloesungen/hochtemperaturwaermepumpen/, 2022. Zugriff am 29.12.2022.
- [17] CO. LTD: www.mayekawa.com MAYEKAWA MFG. [Online], https://mayekawa.com/products/heat_pumps/, 2022. Zugriff am 29.12.2022.
- Sustainable Process heat GmbH: Webiste: www.spheat.de, [18] https://spheat.de/2022/02/15/zwei-auftraege-fuer-die-lieferung-im-jahr-2022-unterzeichnet-2/, 2022. Zugriff am 28.12.2022.
- [19] OCHSNER Energietechnik GmbH: www.ochsner-energietechnik.com, https://ochsner-energietechnik.com/hochtemperatur-[Online], waermepumpen/. Zugriff am 28.12.2022
- [20] engie refrigeration GmbH: Website: www.engie-refrigeration.de, [Online], https://www.engie-refrigeration.de/de/referenzen/dekarbonisierung-vongewaechshaeusern-mit-thermeco2-hochtemperatur-waermepumpen, 2022. Zugriff am 28.12.2022.
- [21] engie refrigeration GmbH: www.engie-refrigeration.de , [Online]. Available: https://www.engie-refrigeration.de/de/waerme/thermeco2-<u>hochtemperaturwaermepumpen</u>, 2022. Zugriff am 28.12.2022.
- [22] ecop Technology GmbH: ECOP Pitchdeck 07/2022, [internal], Wien, 2022.
- [23] ecop Technology GmbH: Technsiche Beschreibung Rotation Heat Pump K7.2.4., Wien, 2022.
- Müller. A; Walter F.: Praktischer Leitfaden für [24] Wirtschaftlichkeitsberechnungen. Bern: RAVEL, 08.1992.
- [25] Geißdörfer: Total Cost of Ownership (TCO) und Life Cycle Costing (LCC). Münster: LIT Verlag, 2009.
- G. S. Karl, W. Schmitz: Kraft-Wärme-Kopplung, Berlin Heidelberg: Springer, [26] 2005.
- U. Götze: Investitionsrechnung. Berlin: Springer, 7. Auflage, 2014. [27]
- [28] S. Krischun: Total Cost of Ownership: Bedeutung für das internationale Beschaffungsmanagement. Hamburg: Diplomica Verlag, 2010.
- [29] sevDesk GmbH: Website: www.sevdesk.at. [Online], https://sevdesk.at/lexikon/investitionsrechnung/#:~:text=Die%20dynamisch e%20Investitionsrechnung%20umfasst%20die,um%20aussagef%C3%A4hi

- gere%20Berechnungen%20zu%20erhalten , 15 04 2020. Zugriff am 14.03.2021.
- [30] Ρ. Website: http://www.docju.de/ Η. Jurscha: [Online], http://www.docju.de/themen/mathe/aequivalenzprinzip.pdf Zugriff am 30.03.2023.
- [31] 1&1 IONOS SE: www.ionos.de [Online], https://www.ionos.de/startupguide/unternehmensfuehrung/kapitalwertmetho de/, 20.03.2019. Zugriff am 30.03.2021.
- B. V. Mathiesen and K. Hansen: The role of Solar thermal in Future Energy [32] Systems. Aalborg Universitet: Aalborg, 2017.
- [33] Technische Universität Wien: Electricity markets. Introduction to Industrial Energy Systems and Digital Methods, 2023.
- [34] H. Zhou, A. Schmitt and J. Steppat: EU Energy Outlook 2060 – How will the Europen electricity market develop over the next 37 years?. Germany, 2023.
- [35] H. Martin: A Limit Order Book Model for the german intraday market. ETH Zürich, 2017.
- Clean Energy Wire CLEW: Website: www.cleanenergywire.org , [Online], [36] https://www.cleanenergywire.org/factsheets/setting-power-price-meritorder-effect, 2020. Zugriff am 22.05.2023.
- [37] IEA: The future of heat pumps. World energy outlook special report, 12/22.
- [38] Commission: European ec.europa.eu [Online], https://ec.europa.eu/eurostat/cache/infographs/energy_prices/enprices.html ?geos=EU27 2020,EA,BE,BG,CZ,DK,DE,EE,IE,EL,ES,FR,HR,IT,CY,LV,L T,LU,HU,MT,NL,AT,PL,PT,RO,SI,SK,FI,SE,IS,LI,NO,ME,MK,AL,RS,TR,BA ,XK,MD,UA,GE&product=6000&consumer=HOUSEHOLD&consoms=41 2022. Zugriff am 23.05.2023.
- E. Rightor, P. Scheihing, A. Hoffmeister and R. Papar: Industrial Heat [39] Pumps: Electrifying industry's process heat supply. ACEEE, 2022.
- [40] M. Koller, A. Schneeberger and V. Wilk: Marktpotential für Hochtemperatur-Wärmepumpen in Europa. 16. Symposium Energieinnovation: Graz, 2020.
- Euroheat & Power: Large Heat pumps in district heating & cooling systems. [41] Euroheat & Power: ep@euroheat.org, 12/2022.
- Umweltbundesamt: [42] Website: www.umweltbundesamt.de [Online], https://www.umweltbundesamt.de/themen/eu-kommission-schlaegtumfassende-reform-des, 18.10.2021. Zugriff am 23.03.2023.
- [43] Frederic: Website: [Online], www.euractiv.com https://www.euractiv.com/section/emissions-trading-

- scheme/interview/analyst-eu-carbon-price-on-track-to-reach-e90-by-2030/ 19.07.2021. Zugriff am 27.03.2023.
- [44] R. Pietzcker, S. Osorio and R. Rodrigues: Lightening EU ETS targets in line with the European Green Deal: Impacts on the decarbonization of the EU power sector. Applied Energy: Band 293, 2021.
- [45] Energie: Website: www.positionen.wienenergie.at [Online], https://positionen.wienenergie.at/grafiken/eu-co2-preise/ 30.09.2022. Zugriff am 28.03.2023.
- [46] Kramer: Website: www.plant-values.de, [Online], https://plantvalues.de/3-schritte-zu-einer-co2-bilanz-im-unternehmen/8085/ 2021. Zugriff am 28.03.2023.
- [47] S. Smedley: Website: www.climateeverything.com [Online], https://climateeverything.com/climateinfographics/scope123emissions 2021. Zugriff am 28.03.2023.
- [48] A. Vollmer: Border Carbon Adjustment in the EU: Indirect Emissions in the CBAM. 2022.
- [49] Bayrisches Landesamt für Umwelt: Website: www.umweltpakt.bayern.de, [Online], https://www.umweltpakt.bayern.de/energie klima/fachwissen/217/berechne <u>n-sie-ihre-treibhausgasemissionen-mit-co2-rechner</u> 2023. Zugriff am 28.03.2023.
- V. Quaschning and B. Siegel: Website: www.volker-quaschning.de, [Online], [50] https://www.volker-quaschning.de/datserv/CO2-spez/index.php , 11.2022. Zugriff am 28.03.2023.
- [51] Wien Energie: Website: www.positionen.wienenergie.at [Online]. https://positionen.wienenergie.at/wissenshub/energiedashboard/emissionsreduktion-im-non-ets-bereich/ 2021. Zugriff am 23.03.2023.
- [52] M. Rehfeldt, C. Rohde and T. Fleiter: A bottom-up estimation of heating and cooling demand in the European industry. Industrial summer study proceedings, 2016.
- [53] G. Kosmadakis: Estimating the potential of industrial (high-temperature) heat pumps for exploiting waste heat in EU industries. Applied Thermal Engineering Band 156, 2019, Seite 287 - 298.
- [54] **IEA** 35: R. Rieberer: Heat Pump Programme Annex Anwendungsmöglichkeiten für industrielle Wärmepumpen. Nachhaltigwirtschaften: 2015.

- [55] J. E. Thorsen, H. Lund und B. V. Mathiesen: Progression of District Heating - 1st to 4th generation, Aalborg: Aalborg University, 2018.
- Website: [56] C. Delmastro: www.iea.org [Online], https://www.iea.org/reports/district-heating, 09/2022. Zugriff am 05.06.2023.
- F. Jonsson und A. Miljanovic: UTILIZATION OF WASTE HEAT FROM [57] HYDROGEN PRODUCTION. Mälardalen University: Mälardalen, 2022.
- Euroheat & Power: DHC Market Outlook Insights & Trends, 2023. [58]
- [59] **OMV** AG: Website: [Online], www.omv.com www.omv.com/de/innovationen/lowcarbon/geothermie?msclkid=4c3f91c070d91ebace0cf26060274198&utm s ource=bing&utm medium=cpc&utm campaign=(AT)%20SEA%20Geother mie&utm term=geothermie&utm content=(AT)%20SEA%20Geothermie%2 0%7C%20Geothermie, 2022. Zugriff am 19.12.2022.
- [60] IEA, GFZ, KIT, UFZ, UMSICHT: Roadmap Tiefe Geothermie für Deutschland. Bochum: Frauenhofer Institut für Energieinfrastruktur und Geothermie – IEG und Helmholtz Zentrum Potsdam Deutsches GeoForschungsZentrum GFZ, 2022.
- [61] Rödl & Partner: Website. www.roedl.com [Online], https://www.roedl.com/insights/renewable-energy/2018-02/key-europes-<u>district-heating-lies-deep-under-ground</u>, 2018. Zugriff am 01.02.2023.
- EU Science Hub: Earth's geothermal hotspots: new dataset launched. EU [62] Science Hub: 2019.
- [63] European Technology & Innovation Platform on Deep Geothermal (ETIP-DG): Vision for deep Geothermal.ETIP-DG, 2018.
- Bundesverband Geothermie: Tiefe Geothermie-Projekte in Deutschland [64] 2021/22. Bundesverband Geothermie: Berlin, 2021.
- European Geothermal Energy Council (EGEC): EGEC Geothermal Market [65] Report 2021 - Key Findings. EGEC: 2022.
- [66] TU-Wien, ENERGIE AG OÖ Wärme GmbH, ecop Technologies GmbH, agotec GmbH, Energieanalyse.DK, e-think: Potentiale, Wirtschaftlichkeit und Systemlösungen für Power-to-Heat. BMVIT: Wien, 2017.
- [67] wien.gv.at-Redaktion: Website: www.wien.gv.at [Online], https://www.wien.gv.at/umwelt-klimaschutz/geothermie-anlage-aspern.html , 2022. Zugriff am 02.03.2023.
- [68] ecop Technology GmbH: Firmeninternes Berechnungstools. Wien: ecop Technology GmbH, 2022.

- [69] Joanneum Research, Geoteam, Energie AG Oberösterreich Wärme: Potenzial der Tiefengeothermie für die Fernwärme- und Stromproduktion in Österreich. Wien, 2014.
- ecop Technology GmbH: internal work, Wien, 2022/2023. [70]
- [71] S. Ortner, M. Pehnt, S.Blömer, A. Auberger, J. Steinbach, J. Deurer, E. Popovski, O. Lösch, N. Langreder, N. Thamling, M. Sahnoun, D. Rau: Abschlussbericht des wirtschaftlichen Potenzials für eine effiziente Wärmeund Kälteversorgung. Umweltbundesamt: Deutschland, 2021.
- Institut: [72] Frauenhofer www.tiefengeothermie.de, [Online], https://www.tiefegeothermie.de/news/mikro-bohrturbine-soll-dasfuendigkeitsrisikoverringern#:~:text=Nach%20Angaben%20des%20Fraunhofer%20Instituts, heute%20bei%20etwa%2030%20Prozent... 04 01 2022. Zugriff am 18.01.2023.
- [73] Landesforschungszentrum Geothermie, Handlungsleitfaden Tiefe Geothermie, Stuttgard: Ministerium für Umwelt. Klima und Energiewirtschaft: 2017.
- [74] C. Danese: Potential and Costs of Geothermal Energy with particular interest on district heating. Bozen: Technische Universität Wien, 2016.
- [75] S. I.: Geothermie. Spinger Verlag: 2021.
- [76] Siemens Energy: Website: www.4echile.cl, [Online], https://4echile.cl/wpcontent/uploads/2020/10/20200930-SE-NEB-PEM-Electrolyzer-and-Applications EW.pdf, 2020. Zugriff am 16.12.2022.
- D. Stolten und B. Emonts: Hydrogen Science and Engineering. Weinheim: [77] Wiley-VCH, 2016.
- Z. Wang, X. Wang, Z. Chen, Z. Liao, C. Xu und X. Du: Energy and exergy [78] analysis of a proton exchange membrane water. Renewable Energy: Band 180, Nr. Elsevier, Seiten 1333-1343, 2021.
- [79] W. Tiktak: Heat Management of PEM Electrolysis. Delft: TU Delft, 2019.
- G. Tjarks: PEM-Elektrolyse-Systeme zur Anwendung. Jülich: Jülich [08] Forschungszentrum, 2017.
- energieplus: [81] Steinbeis Innovationszentrum Website: www.neueweststadt.de, [Online], https://neue-weststadt.de/en/energiekonzept/, 2023. Zugriff am 03.07.2023.
- S. Reuter and R. Schmidt: Assessment of the future waste heat potential [82] from electrolysers and its utilization in district heating. NEFI-Conference, Linz, 2022.

- [83] Statista GmbH. Website: www.statista.com, [Online], https://de.statista.com/, 2022. Zugriff am 22.12.18.
- [84] U.S. Secretary of Commerce: NIST Chemistry WebBook: U.S. Secretary of Website: www.webbook.nist.gov, Commerce: [Online], https://webbook.nist.gov/chemistry/, 2022. Zugriff am 30.01.2023.
- [85] D. Stolten und B. Emonts: Hydrogen Science and Engineering: Materials, Processes, Systems and Technology. Wiley Verlag, 2016.
- [86] J. Gochermann: Halbzeit der Energiewende?. Dülmen: Springer Verlag. ISBN 978-3-662-63476-9, 2021.
- [87] J. Töpler und J. Lehmann: Wasserstoff und Brennstoffzelle. Esslingen: Springer Verlag, ISBN 978-3-662-53359-8, 2017.
- [88] G. Sdanghi, G. Maranzana, A. Celzard und V. Fierro: Review of the current technologies and performances of hydrogen. Renewable and Sustainable Energy Reviews, 2019, Band 102, Seiten 150 - 170.
- [89] D. Krieg: Konzept und Kosten eines Pipelinesystems zur Versorgung des deutschen Straßenverkehrs mit Wasserstoff. Energie & Umwelt, Jürlich, Forschungszentrum Jürlich GmbH, 2021.
- [90] Hyfindr: Website: www.hyfindr.com/hydrogen- [Online], https://hyfindr.com/hydrogen- cooling-system/, 2022. Zugriff am 10.01.2023.
- [91] AIT, EURAC Research: Website: www.iea-dhc.org, [Online], https://www.iea-dhc.org/the-research/annexes/annex-xiii/annex-xiii-project-02, 2020. Zurgiff am 04.07.2023.
- [92] M. Battaglia, R. Haberl, E. Bamberger and M. Haller: Increased selfconsumption and grid flexibility of PV and heat. Energy Procedia, 2017, Band 135, Seiten 358-366.
- [93] D. Rosell: Website: www.solarthemalworld.at, [Online], https://solarthermalworld.org/news/heat-pumps-competition-orcomplement-in-district-heating/, 13.09.2022. Zugriff am 16.01.2023.
- [94] M. Hartl and A. Heinz: IEA Solares Heizen und Kühlen: Task 44 Solar- und Wärmepumpensysteme. BMVIT: Wien, 2014.
- Technology GmbH: [95] Website: www.ecop.at, [Online], https://www.ecop.at/de/produkt/, 2.2022. Zugriff am 06.12.2022.
- M. Hartl: IEA Solares Heizen und Kühlen Task 44: Solar- und [96] Wärmepumpensysteme. Nachhaltig Wirtschaften, 2014, Band 36.
- [97] Wilk, V.; Windholz, B.; Hartl, M.; Fleckl, T.; AIT; AEE; TU-Wien: EnPro -Erneuerbare Prozesswärme (Planungsleitfaden). Klima- und Energiefonds der österreichischen Budesregierung: Wien, 2017.

- [98] solrico; Oropeza, M.: solar heat for cities: the sustainablke solution for district heating (Task 55). IEA: Germany, 2019.
- [99] D. Mangold and L. Deschaintre: Task 45: Large Systems - Seasonal thermal energy storage - report on state of the art and necessary further R+D. ISA: Germany, 2015.
- [100] P. Leoni and J. E. Nielsen: Task 55 Towards the Integration of Large SHC Systems into DHC Networks. IEA: Austria, 2020.
- [101] V. Unterberger, M. Berberich, S. Putz, J. Byström and M. Gölles IEA SHC Task 68: Efficient Solar District Heating Systems: Website: www.bestresearch.eu, [Online], https://www.bestresearch.eu/files/publications/G%C3%B6lles/ISEC Poster.pdf, 04/2022.Zugriff am 01.02.2023.
- J. Ploteny and C. Holter: Solare Nahwärme bis BIG SOLAR. austria solar + [102] klima energie fonds, 2020.
- STAWAG: Solare Nahwärme für Aachen-Walhmeim. Aachen-Walheim, [103] 2022.
- M. Maximini, Enerko: Unterschiedliche Betriebsarten SolNa Walheim. [104] Enerko: Düren, 2023.
- Alexe, S (greeniXcloud); Stoessel, H. P., Becke, W. (AEE Intec): [105] Solargestütztes ZERO EMISSION PROCESS DESIGN - Textilindustrie am Beispiel Südost-Österreich. Klima + Energiefonds, 2022/23.
- [106] P. Reiter, H. Poier and C. Holter: BIG Solar Graz: Solar District Heating in Graz – 500,000 m2 for 20% Solar Fraction. Energy Procedia, 2016, and 91, Seiten 578-584.
- [107] E. B. and M. Oropeza: solar heat for cities - the sustainable solution for district heating. IEA: 2019.
- PlanEnergi, D. Trier, F. Bava, C. Skov and S. Sorensen: Task 52: Solar [108] district heating trends and possibilities - CHARACTERISTICS OF GROUND-MOUNTED SYSTEMS **FOR SCREENING** OF LAND USE REQUIREMENTS AND FEASIBILITY. IEA: Denmark, 2018.
- H. Poier, C. Holter, P. Reiter and R. Söll: www.aee.at, [Online], [109] https://www.aee.at/81-zeitschrift/zeitschriften/2016-01/908-big-solar-graz 500000-m-solarkollektoren-fuer-20-solaranteil-bei-grazer-fernwaerme, 01/2016. Zugriff am 02.02.2023
- BMK: www.energy-innovation-austria.az, [Online], [110] https://www.energyinnovation-austria.at/article/big-solar/, 01/2016. Zurgiff am 02.02.2023.
- C. Holter: Website: www.irena.org/, [Online], https://www.irena.org/ [111] /media/Files/IRENA/Agency/Events/2020/Apr/Technology-specific-focus-

- Challenges-Christian-Holter.pdf?la=en&hash=EAA625BF93CD57D0F847A0DFBD5963C79CB1 E0FC, 20.04.2020. Zugriff am 02.02.2023.
- [112] M. Schubert: www.aee-intec.at, [Online], https://www.aeeintec.at/0uploads/dateien1244.pdf, 2017. Zugriff am 22.02.2023.
- [113] S.O.L.I.D. Gelellschaft für Solarinstallation und Design GmbH: Machbarkeitsstudie BIG SOLAR: 20% solarer Deckungsanteil eines Fernwärmenetzes - Beispiel Graz. Graz, 2015.
- [114] Pauschinger, T.; Geiger, P.; Winterscheid, C.: Solare Wärmenetze -Marktstatus 2018 für Deutschland und Europa. Steinbeis Innovation GmbH: 2018.
- [115] Viessmann: Technical guide steam boilers. Viessmann, 2011.
- A. Niederhauser: Ermittlung des Säuretaupunktes im Rauchgas des Kraftwerkes der voestalpine Stahl GmbH. Linz: TU Graz, 2018.
- Siegel, B.; Quatschning, V.: Website: www.volker-quaschning.de, [Online], [117] https://www.volker-quaschning.de/datserv/CO2-spez/index.php. 11.2022. Zugriff am 23.03.2023.
- A. Gupta and S. Chaudhary: Europe Steam Boiler Market Size By Capacity, [118] By Fuel (Natural Gas, Oil, Coal), By Technology (Condensing, Non-Condensing), By Application (Commercial, Industrial), COVID-19 Impact Analysis, Forecasts 2023 – 2032. Global market insights, 03/2023.
- [119] A. Aydemir and C. Rohde: Steam Boilers and the European Ecodesign process. Karlsruhe, Frauenhofer Institut for Systems and Innovation Research, 2015.
- [120] F. Bless, C. Arpagaus und S. Bertsch: Theorretical investigation of hightemperature heat pump cycles for steam generation. 13th IEA Heat Pump Conferenc:, Band 1, Switzerland, 2021.
- [121] C. Doczekal: Rauchgaskondensation bei Biomassekessel unter Zuhilfenahme von Wärmepumpe und Regelenergie. FH Burgenland, Pinkafeld, 2018.
- Website: [122] stepsahead: www.stepsahead.at, [Online], https://stepsahead.at/wpcontent/uploads/2020/01/Absorptionsk%C3%A4Itemaschinen-f%C3%BCr-Biomasse-Feuerungen.pdf, 2019. Zugriff am 11.04.2023.
- T. Fleckl: Neue Energien 2020. AIT: Wien, 2020. [123]
- [124] H. Walter, M. Haider und D. Huber: Rauchgaskondensation aus Biomassekesseln mit einer multifunktionalen Tauund Feinstaubabscheidung. BMVIT: Wien, 2011.

- [125] H. Yan, R. Wang, S. Du, B. Hu and Z. Xu: Analysis and Perspective on Heat Pump for Industrial Steam Generation. Advanced Energy & Sustainability Research, Band 2021, Nummer 2, 2021.
- [126] G. Drexler-Schmid: Decarbonizing of industrial processes and digitalitaion. AIT: Wien, 2022.
- [127] J. Riedl, S. Dusek und V. Wilk: Website: www.nefi.at, https://nefi.at/files/media/Bilder/News/NEFI%20Technologie%20Talk%20D ekarbonisierung%20der%20W%C3%A4rme-%20und%20K%C3%A4Iteversorgung%20mit%20Geothermie%20und%20i ndustrieller%20Abw%C3%A4rme/05 Riedl Hochtemperatur-W%C3%A4rmepumpen.pdf, 2022. Zugriff am 10.05.2023.
- [128] H. Yan, B. Hu and R. Wang. Air-Source Heat Pump for Distributed Steam Generation: A New and Sustainable Solution to Replace Coal-Fired Boilers in China. Advanced Sustainable Systems, Band 4, 2020.
- [129] G. www.sweet-decarb.ch, Schumm: [Online], https://www.sweetdecarb.ch/fileadmin/downloads/Presentations File/OST-Webinar on Steam Generating Heat Pumps 1st March 2023 -Piller.pdf, 2022. Zugriff am 16.05.2023.
- [130] Epcon: Website: www.sweet-decarb.ch, [Online], https://www.sweetdecarb.ch/fileadmin/downloads/Presentations File/OST-Webinar on Steam Generating Heat Pumps 1st March 2023 -EPCON.pdf, 2023. Zugriff am 08.05.2023.
- [131] AIT: Website: www.ait.ac.at, [Online], https://www.ait.ac.at/newsevents/singleview/detail/7544?cHash=bbf0aea7c142c89fcc916755d1ad65cd, 2023. Zugriff am 08.05.2023.
- [132] DTI. DTU: Website: www.suprheat.dk, [Online], https://suprheat.dk/media/1204/from-boiler-based-to-heat-pump-basedindustrial-steam-systems.pdf, 2022. Zugriff am 24.04.23.
- A. Marina und S. Soelstra: Website: www.data.mendeley.com, [Online], [133] https://data.mendeley.com/datasets/gyxjmvzbx8/1, 2020. Zugriff 16.05.2023.
- D. Ansari, J. Grinschgl and J. M. Pepe: Stiftung Wissenschaft Berlin, [Online], [134] https://www.swp-berlin.org/en/publication/elektrolyseure-fuer-diewasserstoffrevolution, 2022. Zugriff am 22.12.18.
- [135] I. Stober, K. Bucher: Geothermie. Springer Verlag, 2021.
- [136] AIT, AEE, IET: EnPro Erneuerbare Prozesswärme. Industriemagazin Verlag, Wien, 2017.

- [137] G. Moravi: BIG Solar Graz, [Online], https://docplayer.org/109452188-Bigsolar-graz-grossspeicher-einbindung-in-fernwaermesysteme.html, 25.01.2018. Zugriff am 02.02.2023.
- [138] European Comission: Website: climate.ec.europa.eu, [Online], https://climate.ec.europa.eu/eu-action/eu-emissions-trading-system-euets/revision-phase-4-2021-2030 en, 2021. Zugriff am 23.03.2023.
- Bundesministerium für Finanzen: Website: www.ris.bka.gv.at, [Online], [139] https://www.ris.bka.gv.at/GeltendeFassung.wxe?Abfrage=Bundesnormen& Gesetzesnummer=20011818, 23.03.23. Zugriff am 23.03.2023.
- Spoelstra: An estimation of the EU industrial heat pump market potential. [140] TNO: Netherlands, 2022.
- [141] A. Beck, A. D.-S. G. Sevault, M. Schöny and H. Kauko: Optimal Selection of Thermal Energy Storage Technology for Fossil-Free Steam Production in the Processing Industry. Applied Sciences, Band 11, Number 1063, 2021.
- E. Haslinger: Geothermie und Energiesysteme. AIT: Wien, 2023. [142]
- F. Bless, C. Arpagaus, S. Bertsch and J. Schiffmann. Theoretical analysis of [143] steam generation methods- Energy, CO2 emission, and cost analysis. Energy, Band 129, Seiten 114-121, 2017.
- [144] Visable GmbH: Website: www.wlw.de, [Online], https://www.wlw.de/de/inside-business/praxiswissen/strategischereinkauf/tco, 2019. Zugriff am 06.05.2021.
- [145] H. Krcmar: Informationsmanagement. Berlin: Springer, 4. Auflage, 2005.
- [146] B. Denkeena: Total Cost and Benefit of Ownership. GITO-Verlag, Hannover, 2009.
- [147] B. Denkena: Linking total costs and benefits of ownership (TCBO) and process chain simulation for integrated assessment of manufactoring technologies and processes. GWP, Hannover, 2011.